

**Development of a pressurised transmural
decellularisation method for application in tissue
engineering trachea**

A thesis submitted to University College London for the degree of

Doctor of Engineering

by

Leanne Partington

September 2014

Department of Biochemical Engineering

University College London

UCL Engineering Doctorate in Biochemical Engineering

Thesis declaration

I, Leanne Partington, confirm that the work presented in this thesis is my own. Where information has been derived from other sources, I confirm that this has been indicated in the thesis.

Signature:

Name: Leanne Partington

Date: 15th September 2014

Abstract

Tracheal abnormalities, congenital or acquired, represent a currently unmet clinical need. Tissue engineering has recently advanced and has been used to engineer hollow organs, including tracheae, for clinical use on a compassionate basis. However the current clinically used method for tracheal decellularisation has received mixed success and requires development to achieve GMP translation, quality manufacturing standards and ultimately routine clinical use. This thesis first examined the current clinically used detergent-enzymatic method (DEM) of decellularisation, a highly manual process that takes twenty-eight days to complete. Although the method achieved full decellularisation of non-cartilaginous regions of the tracheae, it failed to reduce the donor nuclear material sufficiently and resulted in the loss of key biochemical components, glycosaminoglycans (GAG) and collagen Type II, and the loss of biomechanical strength. A novel method for rapid, effective and non-detrimental tracheal decellularisation was required. Pressurised transmural flow was hypothesised to meet those requirements. A dual chamber bioreactor system was designed, fabricated and optimised to enable pressurised transmural decellularisation (PTD) to be investigated. Optimal PTD process parameters were ascertained and shown to produce tracheal scaffolds that achieved full decellularisation of the non-cartilaginous regions of the tracheae, a reduction of donor nuclear material (95%) which met the currently recommended levels of residual donor DNA for tissue engineered products, as well as maintaining GAG, collagen and biomechanical strength at comparable levels to the native tracheae. Additional to this, the new PTD process achieved this effective and non-detrimental decellularisation of tracheae in five working days with a ten-fold cost of goods reduction. With further development, the PTD method could become a fully automatable and closed process which could progress tissue engineered tracheae towards becoming a validated and regulated advanced therapy medicinal product (ATMP) and enable the advancement of tissue-engineered tracheae into regular clinical use.

Acknowledgements

I would like to take the opportunity to thank everyone who has contributed to my engineering doctorate and helped support me throughout the past five years.

I would like to thank and express my upmost gratitude to my primary UCL supervisor Dr. Ivan Wall for his continued support and guidance throughout the EngD, I am particularly grateful for his diligence, patience and good humour. I would also like to thank my primary industrial supervisor Dr. Mark Lowdell, with whom I spent the latter years of my EngD, for his abundant expertise as well as his guidance and support. Additionally a huge thank you to my secondary UCL supervisor Prof. Chris Mason, who always made time to give me advice, and to my secondary industrial supervisor Prof. Martin Birchall, whose knowledge, energy and kindness has been inspirational throughout.

I would like to thank all of the Biochemical Engineering departmental staff for their assistance and training throughout my EngD. In particular: Dr. Martina Micheletti for her expertise and input with the bioreactor concept; Alan Craig for his expertise, manufacturing skill and superb creation of the tracheal decellularisation bioreactor; Ludmila Ruban and Dhushy Stanislaus for their expertise and assistance at the UCL Biochemical Engineering labs. I would also like to thank Erich Herrmann and his staff in the Biochemical Engineering Workshop, particularly Graeme Smith, for their continued support and assistance in the design and manufacture of other bespoke bioreactor concepts and prototypes.

From the Royal Free London I would like to thank: Janet North, the BioBank laboratory manager, and her staff for their assistance; Maryam Sekhavat and Fiona O'Brien for their GMP training; and John Yaxley and Kathryn Knapp for their support and help.

From the Eastman Dental Institute I would like to thank: Dr. Nicola Mordan for her kindness in hosting me for several months and for her expertise in TEM; Jonathan Knowles, George Georgiou and Graham Palmer for their assistance with the DMA testing.

From Northwick Park Institute for Medical Research I would like to thank: Dr. Tahera Ansari for her expertise and knowledge in tracheal decellularisation; and Farhana Surti for her patience and sharing her expertise in paraffin embedding and staining.

I would also like to extend my thanks and gratitude to my colleague Carla Carvalho at the Royal Free London whose sparkling Portuguese personality made me smile throughout and with whom I shared one of the proudest moments of my life in delivering a tissue-engineered trachea for clinical use. I would also like to thank my fellow EngD students, in particular the other members of the now infamous “RegenMed Five”, John Thwaites, Owen Bain, Yvonne Pang and Iwan Roberts. Thank you all for the laughs, the support and the unforgettable memories.

I would like to thank the UK Stem Cell Foundation, especially Lil Shortland, the EPSRC and the Royal Free London NHS Foundation Trust for funding my EngD project.

Thank you lastly to Alex Perry who started my EngD journey as my girlfriend and ended it as my wife. I know I will never be able to fully express my appreciation for your love, understanding and support.

Contents

Abstract.....	- 3 -
Acknowledgements.....	- 4 -
List of Figures.....	- 13 -
List of Tables.....	- 23 -
Abbreviations	- 25 -
1 Introduction.....	- 28 -
1.1 Structure and function of the human airway	- 28 -
1.1.1 Structure and function of the human respiratory tract.....	- 28 -
1.1.2 Structure and function of the human trachea.....	- 29 -
1.1.3 Pathophysiology of the trachea	- 33 -
1.1.4 Methods for addressing pathology and the limitations of current therapies	- 36 -
1.2 Tissue engineering	- 37 -
1.2.1 What is tissue engineering?	- 37 -
1.2.2 How can tissue engineering and regenerative medicine be used? - 38 -	
1.2.3 Scaffold use in tracheal tissue engineering	- 39 -
1.2.4 Biological scaffolds.....	- 40 -
1.3 Tracheal transplantation for chronic airway indications.....	- 44 -

1.3.1	Current situation	- 44 -
1.3.2	Proof of concept in patient	- 45 -
1.3.3	Health care cost concerns	- 47 -
1.3.4	Potential techniques to achieve scale-up	- 48 -
2	Materials and Methods	- 51 -
2.1	Procurement and preparation of porcine tracheae for experimentation .	- 51 -
2.2	Preparation of porcine tracheal scaffolds by detergent-enzymatic method (DEM) decellularisation.....	- 51 -
2.3	Preparation, embedding and sectioning of tissue in paraffin	- 52 -
2.4	Preparation, embedding and sectioning of tissue in optimum cutting temperature (OCT) compound	- 53 -
2.5	Preparation and embedding of tissue in LR white resin	- 54 -
2.6	Sectioning and analysis by transmission electron microscopy (TEM) ..	- 55 -
2.7	Haematoxylin and eosin staining of tracheal tissue sections	- 55 -
2.8	Analysis of cell clearance and survival following decellularisation-	56 -
2.9	Alcian blue staining for GAG analysis	- 56 -
2.10	Fluorescence labelling for analysis of residual DNA	- 57 -
2.11	IHC primary antibody optimisation for analysis of ECM components .	- 57 -
2.12	IHC for analysis of ECM components	- 58 -
2.13	Quantitative analysis of DNA content	- 59 -
2.14	Quantitative analysis of GAG content	- 59 -

2.15	Quantitative analysis of total collagen content	- 60 -
2.16	Tensile testing of tracheae tissue and scaffolds	- 60 -
2.17	Radial compression force testing of tracheae tissue and scaffolds .	- 61 -
3	Detergent-enzymatic method of decellularisation	- 62 -
3.1	Introduction	- 62 -
3.2	Aims and hypotheses	- 66 -
3.2.1	Aims	- 66 -
3.2.2	Hypotheses	- 66 -
3.3	Materials and methods	- 67 -
3.3.1	Sectioning of LR White embedded matrices for histology .	- 67 -
3.3.2	Histological analysis of LR White embedded matrices by toluidine blue staining	- 67 -
3.3.3	Histological analysis of LR White embedded matrices by haematoxylin and eosin (H&E) staining	- 67 -
3.3.4	Quantitative analysis of protein content	- 68 -
3.3.5	Quantitative analysis of soluble collagen content	- 68 -
3.3.6	Dynamic mechanical analysis (DMA) compression testing of tracheae tissue	- 69 -
3.4	Results	- 70 -
3.4.1	Macroscopic overview of the trachea pre and post detergent- enzymatic method of decellularisation.....	- 70 -

3.4.2	Histological analysis of DEM of decellularisation by toluidine blue staining	- 72 -
3.4.3	Histological analysis of DEM of decellularisation by H&E staining	- 73 -
3.4.4	Analysis of DNA removal by detergent-enzymatic method of decellularisation	- 79 -
3.4.5	Analysis of protein concentration throughout and following the detergent-enzymatic method of decellularisation	- 82 -
3.4.6	Analysis of key ECM proteins (laminin and fibronectin) throughout and following the detergent-enzymatic method of decellularisation	- 82 -
3.4.7	Analysis of collagen throughout and following the detergent-enzymatic method of decellularisation.....	- 84 -
3.4.8	Analysis of glycosaminoglycans throughout and following the detergent-enzymatic method of decellularisation	- 87 -
3.4.9	Tensile testing of scaffolds throughout and following the detergent-enzymatic method of decellularisation	- 89 -
3.4.10	DMA compression testing of scaffolds throughout and following the detergent-enzymatic method of decellularisation.....	- 93 -
3.5	Discussion	- 94 -
3.6	Conclusions	- 103 -
4	Design and engineering of a pressurised transmural bioreactor	- 104 -

4.1	Introduction	- 104 -
4.2	Aims and hypotheses	- 107 -
4.3	Materials, methods and results	- 108 -
4.3.1	Pressurised transmural bioreactor design v1.0	- 108 -
4.3.2	Manufacture of the pressurised transmural bioreactor v1.0-	109
	-	
4.3.3	Visual analysis of the mixing of internal and external flows in the pressurised transmural bioreactor v1.0.....	- 113 -
4.3.4	Transmural flow testing in bioreactor design v1.0.....	- 116 -
4.3.5	Pressurised transmural bioreactor design v1.1	- 119 -
4.3.6	Pressurised transmural bioreactor design v1.2	- 121 -
4.3.7	Pressurised transmural bioreactor design v1.3	- 123 -
4.3.8	Pressurised transmural bioreactor design v1.4	- 126 -
4.3.9	Pressurised transmural bioreactor design v1.5	- 130 -
4.3.10	Pressurised transmural bioreactor design v1.6	- 131 -
4.4	Discussion	- 133 -
4.5	Conclusion	- 136 -
5	Pressurised transmural decellularisation	- 137 -
5.1	Introduction	- 137 -
5.2	Aims and hypotheses	- 141 -
5.3	Materials and methods	- 142 -

5.3.1	Preparation of the pressurised transmural decellularisation (PTD) decellularisation solution and waste reservoirs.....	- 142 -
5.3.2	Preparation of the pressurised transmural decellularisation (PTD) decellularisation solutions.....	- 144 -
5.3.3	Bioreactor versions for pressurised transmural decellularisation-	146 -
5.3.4	Preparation of porcine tracheal scaffolds by pressurised transmural decellularisation	- 158 -
5.3.5	Pressurised transmural decellularisation experiment failures	- 164 -
5.3.6	Cost comparison of the DEM and PTD methods	- 165 -
5.4	Results.....	- 166 -
5.4.1	Pressurised transmural decellularisation 1 to 3 (PTD 1 - 3)-	166 -
		-
5.4.2	Pressurised transmural decellularisation 5 to 8 (PTD 5 - 8)-	170 -
		-
5.4.3	Pressurised transmural decellularisation 9 and 10 (PTD 9 & 10)	- 174 -
	Pressurised transmural decellularisation 13 to 15 (PTD 13 - 15) .-	177 -
5.4.4	Pressurised transmural decellularisation (PTD 11, 18 and 20) ..	- 180 -

5.4.5	Pressurised transmural decellularisation experiment failures	- 195 -
5.4.6	Cost comparison of the DEM and PTD methods	- 196 -
5.5	Discussion	- 198 -
5.6	Conclusion	- 205 -
6	Discussion	- 206 -
6.1	Current process.....	- 206 -
6.1.1	Unmet clinical need.....	- 206 -
6.1.2	Process developments.....	- 207 -
6.1.3	Limitations of the current process	- 209 -
6.1.4	Future work	- 211 -
6.2	Future projects.....	- 212 -
7	Conclusions	- 215 -

List of figures

Figure 1.1: The respiratory system (Canadian_Lung_Association 2015).	- 29 -
Figure 1.2: Light microscopy images of the trachea structure highlighting its various structures.	- 32 -
Figure 1.3: High magnification micrograph of the respiratory epithelium. The respiratory epithelium consists of; pseudostratified ciliated columnar epithelium (EP); basal bodies (BB); goblet cells (GC); nuclei (N); cilia (C) and the basement membrane (Bm).	- 33 -
Figure 2.1: Overview of the detergent and enzymatic method (DEM) decellularisation.	- 52 -
Figure 3.1: Macroscopic view of the trachea upon arrival from the abattoir (A), after preparation (B), after PBS rinses (C) and after cycle 25 of chemical enzymatic decellularisation (D) (Partington, Mordan et al. 2013). Permission to reproduce this figure has been granted by Elsevier.	- 71 -
Figure 3.2: Toluidine staining of the epithelial layer (A), mucosal glands (B), cartilage (C), and adventitia (D) of native trachea and the lamina propria of native trachea (E) and of trachea that has undergone 25 cycle of the DEM of decellularisation (F).	- 73 -
Figure 3.3: Histological staining by H&E of the trachea as native tissue (A) and after cycle 25 (B). Scale bar = 500 mm (Partington, Mordan et al. 2013).	- 75 -
Figure 3.4: Histological staining by H&E of the tracheal epithelial layer (A), mucosal gland (B) cartilage ring (C) and adventitia (D) as native tissue (0), after cycle 10 (1), after cycle 20 (2) and after cycle 25 (3). Scale bar = 10 mm (Partington, Mordan et al. 2013). Permission to reproduce this figure has been granted by Elsevier.....	- 77 -
Figure 3.5: Cell clearance (by histological analysis of H&E) of the mucosa, sub-mucosa and adventitia sub-regions of the trachea as native tissue, after cycle 10, after cycle 20 and after cycle 25 (Partington, Mordan et al. 2013). Permission to reproduce this figure has been granted by Elsevier.	- 78 -
Figure 3.6: Chondrocyte clearance and apoptosis from the cartilage ring of the trachea as native tissue, after cycle 10, after cycle 20 and after cycle 25 (Partington, Mordan et al. 2013). Permission to reproduce this figure has been granted by Elsevier.....	- 78 -

Figure 3.7: DNA quantification in tracheal tissue during decellularisation demonstrated a similar reduction in the decellularised ($P < 0.005$) and non-decellularised groups ($P < 0.005$) compared to the native trachea despite no DNase treatment in the non-decellularised group (Partington, Mordan et al. 2013). Permission to reproduce this figure has been granted by Elsevier..... - 79 -

Figure 3.8: Fluorescent labeling of nuclear material with DAPI in the native trachea (A) and in scaffolds produced by DEM after cycle 10 (B), cycle 20 (C) and cycle 25 (D). Scale bar = 100 μm - 81 -

Figure 3.9: Protein quantification demonstrated no change in the decellularised (DC) and non-decellularised (NDC) groups, at any time point, compared to the native trachea (Partington, Mordan et al. 2013). Permission to reproduce this figure has been granted by Elsevier. - 82 -

Figure 3.10: Immunofluorescence labelling of the two key ECM components laminin and fibronectin demonstrated they were conserved after the DEM decellularisation process. Laminin staining (A-C) in the native tracheae (A, B, B') demonstrated the staining to be localised to the lamina propria (lp), with the mucosal glands (mg) and basement membrane (bm) clearly stained, and connective tissue (ct). No laminin staining was observed in the cartilage (ca). In the DEM scaffold, the same structures were positively stained (C, C'). Fibronectin staining (D - F) in the native tracheae (D, E, E') and the DEM scaffold (F, F') demonstrated similar expression patterns and was present in the lamina propria (lp), connective tissue (ct), adventitia (ad) as well as at a low level in the cartilage (ca). Co-staining with DAPI indicated that genetic material remained post DEM decellularisation, mainly observed in mucosal glands (C'') or bound to matrix fibrils in the lamina propria (F''). Scale bar: (A and D) = 200 μm ; (B, C, E, F) = 50 μm (Partington, Mordan et al. 2013). Permission to reproduce this figure has been granted by Elsevier. - 83 -

Figure 3.11: Quantitative analysis of total collagen content indicated that decellularisation (DC) did not significantly alter the total collagen content (A). Quantitative analysis of soluble collagen content indicated that decellularisation (DC) reduced the amount of soluble collagen compared with time-matched PBS stored tissue (NDC) ($P < 0.01$) and native tissue ($P < 0.01$ and $P < 0.05$) (B). Values are mean \pm SD; N = 5 (Partington, Mordan et al. 2013). Permission to reproduce this figure has been granted by Elsevier. - 85 -

Figure 3.12: Immunofluorescence labelling of type II collagen within the cartilage matrix using two different antibodies (A–F) suggested that, compared with native trachea (A and D), the DEM scaffolds (C and F), but not PBS-stored trachea (NDC) (B and E), experienced a decline in collagen content. Scale bar for (A–F) = 100 μ m (Partington, Mordan et al. 2013). Permission to reproduce this figure has been granted by Elsevier..... - 86 -

Figure 3.13: TEM images showed that the ultrastructure of the collagen bundles were similar in both the native trachea (A) and DEM-produced scaffolds (B), with parallel bundles of collagen fibres, of a similar diameter, appearing in both examples. Image at 40,000x magnification (Partington, Mordan et al. 2013). Permission to reproduce this figure has been granted by Elsevier..... - 87 -

Figure 3.14 Quantitative sGAG analysis demonstrated a significant incremental loss of sGAG from both the time-matched PBS controls (NDC) and the DEM decellularised scaffolds (DC) compared with the native tissue, which appeared to only be slightly accelerated by the DEM treatment (Partington, Mordan et al. 2013). Permission to reproduce this figure has been granted by Elsevier..... - 88 -

Figure 3.15: Alcian blue staining for qualitative GAG analysis demonstrated a significant loss of sGAG from the time-matched PBS controls (B, E) and the DEM decellularised scaffolds (C, F) compared with the native tissue (A, D), which appeared to be greatly accelerated by the DEM treatment (Partington, Mordan et al. 2013). Permission to reproduce this figure has been granted by Elsevier. - 89 -

Figure 3.16: Young’s modulus of the tensile testing demonstrated a significant loss of stiffness in the DEM decellularised scaffolds (DC) only after 25 cycles ($P < 0.05$) compared to the native tracheae. However the effect of the DEM treatment overall had a significant effect, reducing the stiffness of the DEM scaffolds, compared to the time-matched PBS controls (NDC) ($P < 0.005$) (Partington, Mordan et al. 2013). Permission to reproduce this figure has been granted by Elsevier..... - 90 -

Figure 3.17: The ultimate tensile stress of the tensile testing demonstrated a significant loss of strength in the DEM decellularised scaffolds (DC) only after 25 cycles ($P < 0.05$) compared to the native tracheae. However the effect of the DEM treatment overall had a significant effect, reducing the strength of the DEM scaffolds, compared to the time-matched PBS controls (NDC) ($P < 0.005$) (Partington, Mordan et al. 2013). Permission to reproduce this figure has been granted by Elsevier..... - 91 -

Figure 3.18: The ultimate tensile strain of the tensile testing demonstrated no significant differences between the native tracheae, the time-matched PBS controls (NDC) and the DEM scaffolds (DC) (Partington, Mordan et al. 2013). Permission to reproduce this figure has been granted by Elsevier. - 92 -

Figure 3.19: The compressive modulus of the DMA compression testing demonstrated no significant differences between the native tracheae, the time-matched PBS controls (NDC) and the DEM scaffolds (DC) (Partington, Mordan et al. 2013). Permission to reproduce this figure has been granted by Elsevier. - 93 -

Figure 4.1 Schematic of the initial dual chambered pressurised transmural decellularisation bioreactor design v1.0. The concept envisaged the decellularisation solution to be pumped under pressure into the external chamber of the tracheal bioreactor and whilst pumping wash solution through the internal chamber of the tracheal bioreactor. The pressure differential would permit transmural flow of the decellularisation through the tracheal wall which decellularises the trachea over the course of the flow. The aim was to achieve abluminal to luminal transmural flow due to the larger density of cells on the luminal side of the trachea in the lamina propria. - 109 -

Figure 4.2: Prototype parts of the SAC connectors to ensure the SACs were suitable for the attachment of porcine trachea. - 110 -

Figure 4.3: Images of bioreactor components and assembly. Manufactured from polycarbonate, the bioreactor can be sterilised by autoclaving. The internal and external ports were machined to produce BSP $\frac{1}{8}$ or G $\frac{1}{8}$ female threads allowing a range of adapters to be fitted. The trachea was secured to the size adjustable connectors (SACs) using sutures outside of the bioreactor. The O-ring and the O-ring compressor were slotted onto the SAC and the SAC fastener was threaded onto the SAC but not tightened. The internal assembly was then passed into the bioreactor tube. The external chamber of the bioreactor was sealed through compression of the O-ring by the O-ring compressor as the SAC fastener was tightened. One SAC assembly was prevented from rotating inside the bioreactor tube whilst tightened by the addition of a screw. The other SAC assembly was prevented from rotating by slightly angling the SAC assembly as tightened. This allowed the bioreactor to be assembled and sealed without twisting the trachea *in situ*. - 111 -

Figure 4.4: Attachment of the trachea to the SAC using sutures was aided by utilisation of a laboratory support stand (A) and clamps to hold the SAC and trachea in position (B). - 112 -

Figure 4.5: Sequential assembly of the SACs with the trachea in position. After attachment of the trachea to both SACs (A) the O-rings were positioned onto the SACs (B), then the O-ring compressor, with the screw in position on the left-hand side (C), and finally the SAC fasteners (D). - 112 -

Figure 4.6: The assembled SACs, with the trachea in position, was passed through the bioreactor (A). The screw was slotted into a slit in the bioreactor wall and assisted with the tightening of the top SAC. The bottom SAC was then tightened, taking care not to twist the trachea (B). - 113 -

Figure 4.7: Stills were captured from mixing experiments on the internal and external chamber. The internal chamber experiment demonstrated laminar flow that took 18.03 seconds to fully mix post injection of the dye at a pump speed of 3 rpm (A – E). The external chamber experiment demonstrated turbulent flow that took 70 seconds to fully mix post injection of the dye at a pump speed of 20 rpm (F – J and F' - J')..... - 115 -

Figure 4.8: The mixing time for the specified pump speeds tested indicated there was a linear relationship between the two factors. $N = 1$ - 116 -

Figure 4.9: Stills from the initial transmural experiments demonstrate the trachea in position (A), the effect of external over-pressurisation (B) causing internal collapse of the trachealis muscle and the effect of internal over-pressurisation (C) causing external strain of the trachealis muscle. - 119 -

Figure 4.10: 6 mm hose barb to G¹/₄ male thread (A) and T-connector with 6 mm hose barbs to G¹/₈ male thread (B). - 120 -

Figure 4.11: 6.4 mm hose barb to male luer (A), male luer to G¹/₈ male thread (B), male luer to male luer (C), 6.4 mm hose barb to female luer (D), female luer to G¹/₈ male thread (E), female luer to female luer (F), male luer to female luer rotating connector (G). - 121 -

Figure 4.12: 0 - 6 bar pressure gauge connected to a 3 way t-connector (3 G¹/₄ female threads) and G¹/₄ male thread to 6 mm hose barbs (A). 0 -1.6 bar pressure gauge connected to a G¹/₈ female thread to male luer and a 3 way t-connector (2 female and 1 male luer) (B). A male luer to female luer pressure transducer (C). - 121 -

Figure 4.13: The pumps used in early experiments were the Watson Marlow 503U (A) and 505S (not shown) peristaltic pumps which both utilized a two sprung rollers pump-head. The tubing was 6.4 mm ID silicone tubing. Due to tubing creep, common with the two sprung roller type of pump-head over long experiments, the tubing frequently became entangled in the pump head (B) and in doing so shredded the tubing (B') causing leakage of the decellularisation solution. As this tended to occur overnight, it meant the experiment frequently had to be abandoned. Another style of peristaltic pump with top tube loading and a four cartridge roller (C) along with 6.4 mm ID Bioprene tubing was adopted which mitigated tube creep and established reliability to the pump system which allowed the development of the bioreactor system to progress. After development of the pressurised transmural method, the system was transferred to the Harvard Apparatus OCRA controller and so the use of their peristaltic pump (D) was briefly used which was controlled via the Bio_1 software (D inset). - 123 -

Figure 4.14: The use of ratchet tubing clamps (A) did not allow for fine enough control when creating a back pressure to achieve transmural flow. Replacement with the Hoffman clamps (B) allowed for fine control to transmural flow via back pressure but did not provide long-term stable pressure over multiple days of use. Replacement by one-way check valves (C) set at manufacture to the desired cracking pressure allowed for long term stable transmural flow over multiple days without the need for user intervention..... - 125 -

Figure 4.15: Readings from the ORCA controller from the pressure transducers positioned pre and post the internal chamber (IC), or tracheal lumen, demonstrated the average pre-IC pressure was 4.79 ± 0.17 psi and the average post-IC pressure was 4.00 ± 0.16 psi with an average difference of 0.79 psi between the two pressure transducers..... - 126 -

Figure 4.16: Early experiments were performed in a 37°C CO₂ to maintain the experiment at 37°C (A). This potentially caused instrument failure of the incubator. Therefore the experiment was moved to a laboratory bench where a water bath was used to heat the decellularisation solution (B). Temperature probes from Harvard Apparatus (C) and Biorep (D) were used to monitor the solution temperature in the internal chamber..... - 128 -

Figure 4.17: Readings from the ORCA controller from the temperature probes positioned pre and post the internal chamber (IC), or tracheal lumen, demonstrated the average pre-IC temperature was $33.59 \pm 0.66^{\circ}\text{C}$ and the average post-IC temperature was $33.10 \pm 1.31^{\circ}\text{C}$ with an average difference of 0.84°C between the two temperatures probes. - 130 -

Figure 4.18: Horizontal orientation (A) of the pressurised transmural bioreactor resulted in a build-up of air above the port inlet and outlets. Rotation of the pressurised transmural bioreactor to a vertical orientation (B) prevented any such build-up and allowed total transmural flow through all areas the tracheae. - 131 -

Figure 4.19: GMP grade wire mesh (A) was rolled and trimmed, as appropriate, to produce stents (B) which were then inserted into the lumen of the trachea during tracheal attachment to the SACs (C) as part of the bioreactor assembly. - 132 -

Figure 4.20: Pressurised transmural decellularisation without a stent would cause the trachea to twist and kink (A) which could weaken the tracheal scaffold at that pressure point. The addition of a stent prevented such contortion (B). - 132 -

Figure 5.1: Solution reservoir set-up for bioreactor version 2.0 which compromised a 600 mL transfer bag with two male luer lock (MLL) port to spike lines..... - 142 -

Figure 5.2: Waste reservoir set-up for bioreactor version 2.0 which compromised an adapted 500 mL Duran bottle with two added glass 6.4 mm hose barbs ports. Silicone tubing with the other end connected to a hose barb to female luer lock (FLL) were added to the bottom served as the waste line..... - 143 -

Figure 5.3: Solution reservoir set-up for the bioreactor versions 2.1, 2.2 and 2.3 which compromised a 600 mL transfer bag with a spike to two spike ports adapter and three MLL port to spike lines. - 144 -

Figure 5.4: Bioreactor system assembly components for bioreactor version 2.0 to 2.3. - 147 -

Figure 5.5: Bioreactor version 2.0. With this version the decellularisation solution was recirculated through the internal chamber/lumen of the trachea and the transmural flow was collected in the waste reservoir. - 148 -

Figure 5.6: Bioreactor version 2.1 with the two differing set-ups from the size adjustable connectors (SACs) for PTD 5 or PTD 6 and 7. With these set-ups the decellularisation solution was recirculated through the internal chamber/lumen of the

trachea and the transmural flow was collected in the same reservoir and recirculated.	- 151 -
Figure 5.7: Bioreactor version 2.2. With this set-up the decellularisation solution was recirculated through the internal chamber/lumen of the trachea and the transmural flow was collected in the same reservoir and recirculated. The pressure and temperature was measured and recorded online.	- 154 -
Figure 5.8: Bioreactor version 2.3. With this set-up the decellularisation solution was recirculated through the internal chamber/lumen of the trachea and the transmural flow was collected in the same reservoir and recirculated. The external chamber was pre-filled and minimal manipulation was required to drain the internal and external chambers. The pressure and temperature was measured and recorded online....	- 157 -
Figure 5.9: Bioreactor version 2.0 in use with the PTD 3.....	- 167 -
Figure 5.10: Differences in remaining DNA in the “decellularised” (DC) regions of the trachea compared to the “non-decellularised” (NDC) regions of the trachea due to uneven transmural flow.....	- 168 -
Figure 5.11: Readings from the pressure gauges before (PG2) the and after (PG3) the internal chamber.....	- 170 -
Figure 5.12: Histological analysis of the mucous glands (A) and cartilage rings (B) of the trachea (PTD 2 results shown) stained with H&E revealed the presence of nuclei in both regions indicating these regions were not adequately decellularised....	- 170 -
Figure 5.13: Bioreactor version 2.1 in use with the PTD 5.....	- 171 -
Figure 5.14: Histological analysis of the mucous glands (A) and trachealis muscle (B) of experiment PTD 6 stained with H&E revealed the presence of nuclei in these regions indicating an inadequate level of cell clearance compared to the analysis of the mucous glands (C) and trachealis muscle (D) of experiment PTD 8 which indicated a good level of cell clearance.	- 172 -
Figure 5.15: Compression testing in the PTD 5 - 8 experiments indicated weakened scaffolds comparable to tracheae that had undergone a freeze-thaw step for PTD 5 and 6 when a lower detergent concentration was used and increased weakening in the scaffold beyond that observed in freeze-thawed tracheae for PTD 7 and 8 when a higher detergent concentration was used.	- 173 -
Figure 5.16: Formation of salt crystals on the ablumen of the tracheae during the second DNase step of PTD8.	- 174 -

Figure 5.17: Bioreactor v2.2 whilst performing experiment PTD 10. - 175 -

Figure 5.18: Histological analysis of the cell clearance in PTD 9 revealed good removal of cells from the trachea by the decellularisation process in all regions of the trachea, for example the mucous glands (A) and the trachealis muscle (B) with a few nuclei remaining in the cartilage rings. However for PTD 10 cells were observed to be present after decellularisation in the mucous glands (C) and the trachealis muscle (D) as well as the cartilage rings. - 176 -

Figure 5.19: Compression testing in the PTD 9 & 10 experiments indicated weakened scaffolds beyond the tracheae that had undergone a freeze-thaw step.- 177 -

Figure 5.20: Bioreactor v2.3 which had extra ports included to allow for easy fill and drain of the decellularisation solutions. - 178 -

Figure 5.21: Histological analysis of PTD 14 indicated removal of cells from the mucous gland (A) and the trachealis muscle (D) however there were some remaining nuclei in the lamina propria (B) and some apoptotic cells visible in the cartilage rings (C). - 179 -

Figure 5.22: Compression testing of PTD 13 – 15 indicated a comparable loss in strength in the decellularised scaffolds as tracheae that had undergone a freeze-thaw step and approximately 50% of the compressive strength of native tracheae..... - 180 -

Figure 5.23: The ORCA controller was able to record the online temperature of the decellularisation solutions from the readings off the temperature probes positioned before and after (pre and post) the internal chamber (IC) or tracheal lumen. Both temperatures were stably maintained over the course of the decellularisation with an average difference of 0.84°C detected across the lumen with the solution cooling as it travelled down the fluidic path from the solution reservoir..... - 181 -

Figure 5.24: The ORCA controller was able to record the online pressure of the decellularisation solutions from the readings from the pressure transducers positioned before and after (pre and post) the internal chamber (IC) or tracheal lumen. Both pressures were stably maintained over the course of the decellularisation with an average difference of 0.79 psi detected across the lumen with the pressure of the solution diminishing as it travelled further down the fluidic path from the peristaltic pump. - 182 -

Figure 5.25. Comparing the native trachea (A) with the PTD 20 tracheal scaffold (B), the gross morphological appearance of the scaffold is retained appearing denuded with the cartilage rings maintaining an open structure and a visible epithelial layer lining the lumen. - 183 -

Figure 5.26: Low power (x4) microscopic evaluation of native trachea (A) and PTD demonstrated overall retention of the microscopic structure of the tracheae in the decellularised scaffold and overall clearance of cells. - 184 -

Figure 5.27: High power (x60) microscopic evaluation comparing native trachea and PTD 11, PTD 18 and PTD 20 demonstrated retention of the microscopic structure of the tracheae in the decellularised scaffold and total clearance of cells in the mucosa and mucosal glands regions of the decellularised scaffold. - 185 -

Figure 5.28: High power (x60) microscopic evaluation comparing native trachea and PTD 11, PTD 18 and PTD 20 demonstrated retention of the microscopic structure of the tracheae in the decellularised scaffold and total clearance of cells in the adventitia region of the decellularised scaffold. However chondrocytes were observed in the cartilage rings of the decellularised scaffold. - 186 -

Figure 5.29: Low power (x10) microscopic evaluation comparing native trachea and PTD 11, PTD 18 and PTD 20 demonstrated retention of the microscopic structure of the tracheae in the decellularised scaffold and total clearance of cells in the trachealis muscle region of the decellularised scaffold. - 187 -

Figure 5.30: Quantification of the cell clearance observed in the mucosa, sub-mucosa, adventitia and trachealis muscle regions of the trachea demonstrated total cell clearance was achieved in these non-cartilaginous regions. - 188 -

Figure 5.31: Quantification of the cell clearance observed in the cartilage rings regions of the trachea demonstrated no cell clearance was achieved however over 50% of the cells appeared to have undergone apoptosis. - 189 -

Figure 5.32: Quantitative DNA analysis demonstrated a significant decrease in the DNA concentration in the PTD scaffold (38.53 ± 9.84 ng/mg) compared to native trachea (695.87 ± 159.02 ng/mg) and scaffolds produced with the DEM of decellularisation (264.7 ± 69.92 ng/mg). - 190 -

Figure 5.33: Quantitative analysis of the total collagen content of the native tissue versus DEM and PTD scaffolds indicated native levels of collagen were retained in the PTD scaffolds (97.97% retained) whereas loss of collagen content was identified in the DEM scaffolds (76.99% retained) ($P < 0.005$). - 191 -

Figure 5.34: Quantitative analysis of the GAG content of the native tissue versus DEM and PTD scaffolds indicated comparable levels of GAGs were retained in the PTD scaffolds (87.09% retained) whereas loss of GAGs were identified in the DEM scaffolds (55.76% retained) ($P < 0.005$). - 192 -

Figure 5.35: Measurement of the tensile modulus indicated comparable tensile modulus was retained between the native tracheae and the PTD scaffolds (91.39%) however tensile modulus decreased in the DEM scaffolds (73.71%) compared to native tracheae ($P < 0.05$). - 193 -

Figure 5.36: Measurement of the ultimate tensile stress indicated a loss of the ultimate tensile stress capacity of the PTD scaffolds (64.25%) ($P < 0.05$) and the DEM scaffolds (75.19%) ($P < 0.01$) compared to native tracheae. - 194 -

Figure 5.37: Measurement of the ultimate tensile strain indicated a loss of the ultimate tensile strain capacity of in the PTD scaffolds (56.85%) ($P < 0.005$) compared to native tracheae whilst comparative strain was observed in the DEM scaffolds (90.61%). - 194 -

Figure 5.38: Measurement of the compression testing indicated the force required to occlude the lumen to 50% was statistically comparable between the native tracheae and the PTD scaffolds (85.45%). - 195 -

Figure 5.39: Reagent CoG for the DEM and PTD methods indicated a >10 fold reduction in the CoG for the PTD compared to the DEM. - 197 -

List of tables

Table 1.1. Pathophysiology of the trachea.	- 34 -
Table 3.1: Table of average pig tracheae sizes, with comparison for human tracheae (Iivanov 2007).	- 71 -
Table 3.2: Cell clearance by DEM decellularisation literature comparison (Conconi, De Coppi et al. 2005, Jungebluth, Go et al. 2009, Partington, Mordan et al. 2013) *Likely to be a typographical error and actually 2980/mm ² , 1520/mm ² and 150/mm ² respectively.	- 96 -
Table 4.1: Experimental detail and results from the initial attempts to achieve transmural flow. For post-EC clamp closure, the number of notches related to the extent of closure of the ratchet clamp. Incrementally increasing the notch the clamp was closed to, increased the level of closure.	- 118 -
Table 5.1: Summary of the experiments for the pressurised transmural decellularisation.	- 159 -
Table 5.2: Transmural flow rates of the decellularisation solutions for PTD 1-3.-	168
-	

Abbreviations

ANOVA - analysis of variance

ATMP(s) - advanced therapy medicinal product(s)

bFGF - basic fibroblast growth factor

BSA - bovine serum albumin

BSPP - British standard pipe parallel

CaCl₂ - calcium chloride

CoG - cost of goods

CO₂ - carbon dioxide

CQA - critical quality attributes

cm - centimetre

CSSD - Central Sterile Services Department

DAPI - 4',6-diamidino-2-phenylindole

DEM - detergent-enzymatic method

DC - decellularised

DPX - distyrene plasticizer xylene mountant

dH₂O - water

DMA - dynamic mechanical analysis

dsDNA - double-stranded deoxyribonucleic acid

DNA - deoxyribonucleic acid

DoE - design of experiments

EC - external chamber

ECM - extracellular matrix

EMA - European Medicines Agency

FDA - Food and Drug Administration

FISH - fluorescent in situ hybridization

FLL - female luer lock

GAG(s) - glycosaminoglycan(s)

GCP - good clinical practice

GMP - good manufacturing practice

H&E - haematoxylin and eosin

HBSS - Hank's balanced salt solution

HCl - hydrochloric acid

HSC - haematopoietic stem cells
HTA - human tissue act
HUV - human umbilical vein
IC - internal chamber
ID - inner diameter
IHC - immunohistochemistry
IMS - industrial methylated spirits
kU - Kunitz units
LR - London resin
MA - marketing authorisation
MSC - mesenchymal stem cells
mL - millilitre
MLL - male luer lock
MHC - major histocompatibility complex
MHRA - Medicines and Healthcare products Regulatory Agency
mg - milligram
 μm - micrometre
mm - millimetre
 MgCl_2 - magnesium chloride
N - Newtons
NaCl - sodium chloride
NBF - neutral buffered formalin
NDC - non-decellularised
ng - nanogram
NHS - National Health Service
NHSBT - National Health Service Blood and Transplant
 O_2 - oxygen
OCT - optimum cutting temperature
OD - outer diameter
PBS - phosphate buffered saline
PCC - pseudostratified ciliated columnar
PDS - polydioxanone
PEEK - polyetheretherketone
PG - pressure gauge

PTD - pressurised transmural decellularisation
PTFE - polytetrafluoroethylene
psi - pounds per square inch
QbD - quality by design
RNA - ribonucleic acid
rpm - revolutions per minute
RT - room temperature
RT-PCR - reverse transcriptase - polymerase chain reaction
SAC - size adjustable connectors
SD - standard deviation
SDS - sodium dodecyl sulphate
sGAG - sulphated glycosaminoglycans
SOP(s) - standard operating procedure(s)
TBS - tris buffered saline
TEM - transmission electron microscopy
TFF - tangential flow filtration
TPP - target product profile
UW - University of Wisconsin Solution (Viaspan)
VAD - vacuum-assisted decellularisation
VEGF - vascular endothelial growth factor

1 Introduction

1.1 Structure and function of the human airway

1.1.1 Structure and function of the human respiratory tract

The pulmonary airway in humans, otherwise known as the respiratory system or respiratory tract, starts at the mouth and nose and ends at the alveolus (air sac) of the lung where gas-exchange occurs with blood pumped through the pulmonary artery to the pulmonary vein (Figure 1.1). The primary function of the pulmonary respiratory system is to supply oxygen (O₂) to and remove carbon dioxide (CO₂) from the cells and tissues of the body (Martin 1988). The main function of the respiratory tract is to ensure the air that arrives in the lungs is of the correct temperature, humidity and purity. Therefore the respiratory tract must act as a purifying biological barrier and so remove almost all of the particulates and noxious biological and chemical agents from the air (Martin 1988).

After the nostrils and mouth the air is drawn into the pharynx (the throat) and onto the larynx (the voice box). At the laryngopharynx, air is prevented from entering the oesophagus by the hypopharyngeal sphincter and the larynx protects the trachea by preventing food from entering the respiratory tract. The larynx joins the trachea at the cricoid cartilage which is the only complete cartilaginous ring of either organ. Below the larynx is the trachea which completes the respiratory passage until the air passes into the bronchi and the lungs (Martin 1988).

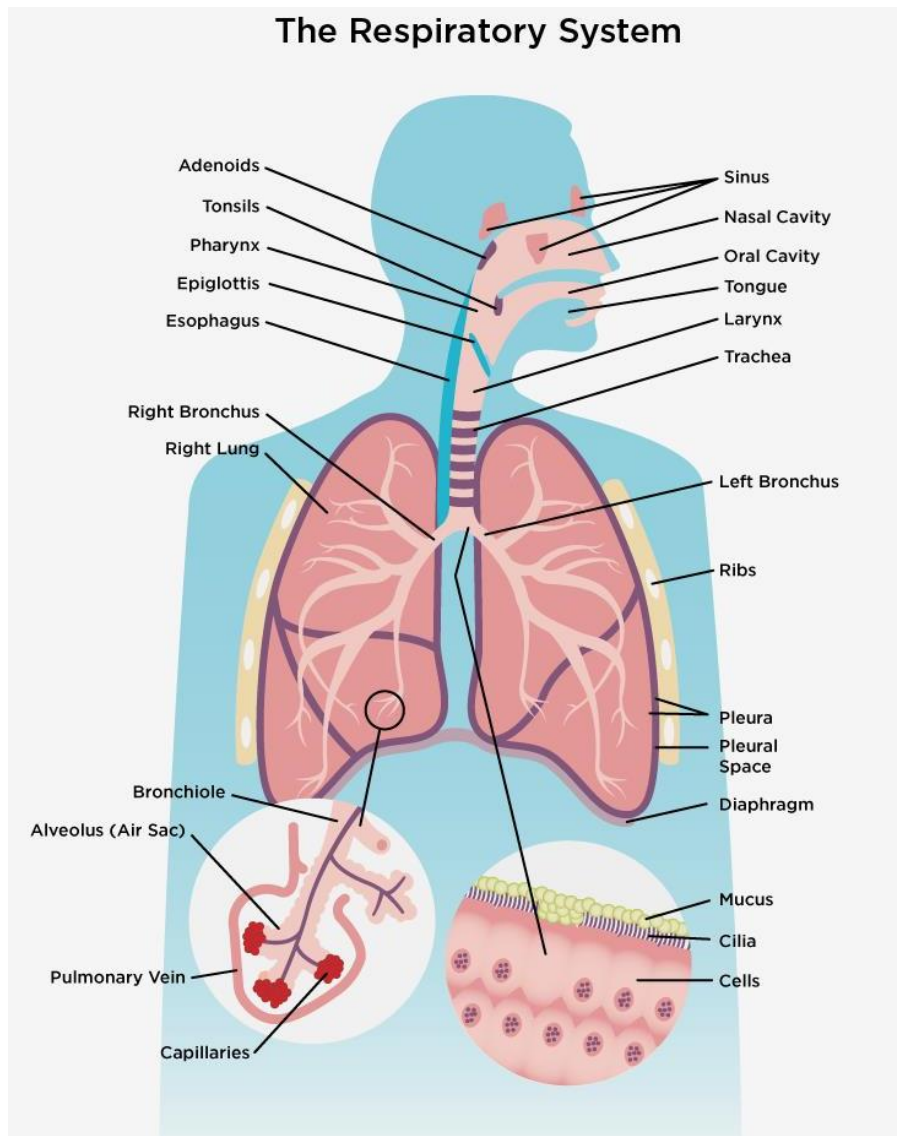


Figure 1.1: The respiratory system (Canadian_Lung_Association 2015). Permission to reproduce this figure has been granted by the Canadian Lung Association.

1.1.2 Structure and function of the human trachea

In the embryo, the cartilage, connective tissue and muscles of the trachea differentiate from the splanchnic mesenchyme that surrounds the laryngotracheal tube (foregut) and the epithelium and glands of the trachea differentiate from the endodermal lining of the foregut (Legasto, Haller et al. 2004). In adults, the trachea is an average of 11 cm in length, with a range of 10 - 13 cm, and is on average 2.3 cm in diameter laterally and 1.8 cm antero-posteriorly (Iivanov 2007). In children antero-posterior diameter is the greater of the two (Cameron 1999). *In situ* the actual tracheal dimensions of an individual fluctuate continuously as a result of postural

movements and movements of the larynx and diaphragm (Martin 1988). The trachea starts at the lower margin of the cricoid cartilage and continues to the carina where it then divides into the two branches of the main bronchi. (Cameron 1999). The blood supply of the trachea is complex with the cervical (upper section) being mostly supplied by the inferior thyroid artery, the thoracic (mid-section) being supplied by the innominate (brachiocephalic) and subclavian arteries and the distal (lower section) being supplied by the bronchial arteries (Visosky 2004). The trachea is comprised of 16-22 incomplete C-shaped cartilage rings (Baiguera, Birchall et al.) which are embedded into its fibrous and smooth muscular walls (Martin 1988) to create rigidity and hold open the tubular structure whilst allowing flexibility vertically between the cartilage rings. The cartilage rings are formed from hyaline cartilage (Caceci 2008). The cartilage is formed by chondroblasts which secrete the extracellular matrix components. The extracellular matrix is composed of tropocollagen type II, the basic structural unit of collagen which polymerises extracellularly into collagen fibres, and ground substance, which predominately consists of the GAGs, hyaluronan, chondroitin sulphate and keratan sulphate. In the developing foetus and human, the chondroblasts become isolated in lacunae, small cavities, as they produce and increase the amount of matrix between themselves. During this period the chondroblasts also differentiate into chondrocytes. In living cartilage the chondrocytes occupy the lacunae (Slomianka 2009) but as chondrocytes undergo cell death, termed chondroptosis by Roach in 2004 (Roach, Aigner et al. 2004), they appear to shrink and retract within their lacunae. Also, as the chondrocytes undergo apoptosis, the cell and nucleus can appear darker as the cell condenses and the nucleus condenses and convolutes (Ford, Robinson et al. 2003, Roach, Aigner et al. 2004). There are two means by which growth occurs in cartilage, either interstitial or appositional growth. Interstitial growth occurs predominately in immature cartilage through the mitosis of chondroblasts that results in isogenous groups of cells. The cells in these isogenous groups produce small amounts of matrix so that the cells in the group become marginally separated from each other. Appositional growth occurs in immature and mature cartilage through the differentiation of mesenchymal stem cells from the inner chondrogenic layer of the perichondrium into chondroblasts which then produce extracellular matrix (Slomianka 2009). The matrix near the isogeneous groups is termed territorial matrix and is more basophilic due to the higher levels of sulphated proteoglycans secreted

by chondrocytes. Haematoxylin and Eosin (H&E) staining shows territorial matrix stains darker than the remainder of the matrix, known as interterritorial matrix (Slomianka 2009). The posterior wall of the trachea is constructed from fibrous and muscular tissue (Martin 1988).

Lining the trachea lumen is the respiratory epithelium. Its function is to provide an effective biological barrier from any particulates or noxious biological or chemical agents that may be inhaled. Particulate sizes of 30 μm or larger are trapped by the epithelial lining from the nose to the trachea, particulates of 10 μm to 3 μm are trapped by the lining in the bronchial tree and particulates of 3 μm to 1 μm can reach as far as the alveoli, where they are then trapped by the epithelial lining (Martin 1988). Tracheal respiratory epithelium is known as the pseudostratified ciliated columnar (PCC) epithelium (Chute 2008) (Figure 1.2 and Figure 1.3). It consists of ciliated columnar cells, secretory goblet (mucous) cells, brush cells, small granule cells and basal cells that are situated above a basement membrane (Kolchanov, Ignatieva et al. 2002). There are approximately five ciliated cells to each goblet cell (Martin 1988). The epithelium is called pseudostratified because the columns of cells are tightly packed together with the nuclei towards one end to the extent that there appears to be several layers of cells, which is characteristic of stratified epithelium (Caprio 2005) (Figure 1.3). Below the epithelial layer there is the lamina propria layer, which is formed of loose connective tissue. The lamina propria contains elastic connective tissue fibres, collagen fibres, smooth muscle cells, cells of the immune system, nerves and blood vessels. The high levels of collagen and elastin in the lamina propria aid the elastic recoil of the trachea. Together the epithelial and lamina propria layers form what is termed the mucosa layer.

Below the mucosa layer is the sub-mucosa layer which is comprised of a gland layer and a cartilage layer. Submucosal glands in the gland layer also produce mucous which is carried to the lumen by numerous interconnecting mucous ducts and tubules (Engelhardt, Schlossberg et al. 1995, Caprio 2005, Chute 2008). These glands, ducts and tubules help regulate the mucous secretions to the lumen surface (Engelhardt, Schlossberg et al. 1995). The mucous that is continuously produced by the goblet cells and the mucous glands forms an aqueous mucous secretion that is a mechanical barrier that lines the respiratory epithelium, and therefore the respiratory tract, to a thickness of 10 to 20 μm . The aqueous mucous secretion consists of a top gel layer

of hydrated mucous and a lower less viscous sol layer (Martin 1988). There are typically 250 cilia per ciliated cell in the PCC epithelium, each approximately 6 μm in length and 0.2 μm in diameter. These cilia beat approximately 1,300 times per minute, in a coordinated way, in the sol layer so that the tips of the cilia hit the bottom of the gel layer (Caceci 2008). This moves the mucous, and the particulates that have been trapped by the mucous, away from the lungs to the epiglottis, where the mucous can be swallowed or expectorated (Caceci 2008, Chute 2008). It does this at a rate of 7 to 20 mm per minute which means a whole new layer of mucous can cover the trachea in a time period of 30 minutes to an hour (Martin 1988) and in so doing aids keeping the airway clear (Caceci 2008, Chute 2008).

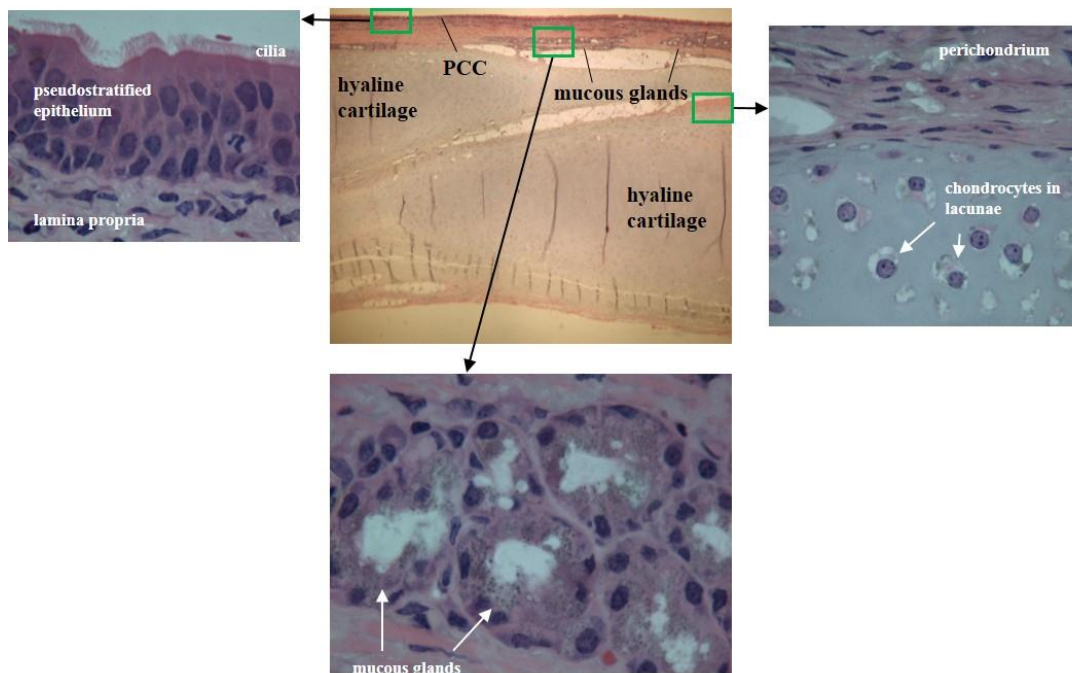


Figure 1.2: Light microscopy images of the trachea structure highlighting its various structures.

This process is known as mucociliary clearance and it is a highly regulated process. Even small fluctuations in the volume of the sol or gel layer can impede or sometimes inhibit mucociliary clearance, such as observed in the pathophysiology of cystic fibrosis. The mucous layer in the respiratory tract also acts a waterproof barrier to prevent excessive uptake or transudation of water. However it is water evaporating into the inspired air that humidifies it, therefore very dry air can cause

mucosal dehydration, which increases the mucous' viscosity and impedes its ability to be cleared by the cilia. This is of importance as bacteria and viruses trapped in the mucous will then have more time to penetrate the underlying cells and cause a respiratory infection (Martin 1988). The brush cells in the respiratory epithelium are columnar cells that produce microvilli. These cells function as sensory cells as their basal surface is synaptically in contact with afferent neurons, which are known as sensory or receptor neurons. The small granule cells are called as such because their cytoplasm contains many membrane-bound dense granules. These cells release polypeptide hormones and catecholamine that are presumed to act in regulating the diameter of the tracheal lumen and tracheal vasculature (Kolchanov, Ignatieva et al. 2002). Basal cells are thought to be multipotent stem cells which are able to differentiate into the ciliated and goblet cells. Current evidence suggests that these cells reside in the protected niche of the mucosa ducts and glands. These cells are thought to be involved in the homeostasis of the respiratory epithelial layer and are able to migrate to and repopulate denuded areas (Rock, Randell et al. 2010). Outside of the cartilage is the adventitia layer which forms the outer surface of the trachea (Martin 1988).

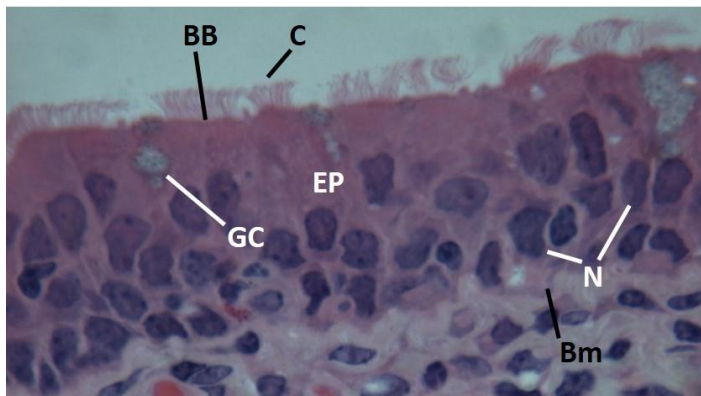


Figure 1.3: High magnification micrograph of the respiratory epithelium. The respiratory epithelium consists of; pseudostratified ciliated columnar epithelium (EP); basal bodies (BB); goblet cells (GC); nuclei (N); cilia (C) and the basement membrane (Bm).

1.1.3 Pathophysiology of the trachea

The pathology of the trachea in humans can occur by several different means (Table 1.1). Congenital tracheal anomalies can occur as agenesis, atresia, stenosis, webs and

tracheomalacia. Tracheal agenesis describes failure of the trachea to develop and atresia describes cases where the trachea is present but not fully formed. These cases are almost always fatal (Iivanov 2007, Kay 2007), with most patients dying within hours of birth and long-term survival cases are rare. In one case a patient survived to 6 years and 10 months (Soh, Kawahawa et al. 1999). Thankfully, these are both rare conditions (Iivanov 2007, Kay 2007). Congenital tracheal webs and stenoses are another form of malfunction of the trachea. It is thought that they result from the unequal separating of the foregut when it develops into the oesophagus and trachea during foetal growth (Legasto, Haller et al. 2004). A tracheal web is when a thin layer of tissue has grown across and narrows the tracheal lumen, but does not completely block the lumen. Importantly there is no abnormality of the cartilage structure with this condition, unlike tracheal stenosis. The position in the trachea and the degree of occlusion of the tracheal lumen is proportional to the degree to symptoms presented by the patient. When over 75% of the lumen is obstructed, the patient suffers from dyspnoea (Kay 2007).

Pathophysiology of tracheal disease		Characteristics
Congenital	Acquired	
Agenesis/atresia	Not applicable	Absence or under formed trachea. Respiration requires surgical intervention.
Web	Not applicable	Thin layer of tissues span lumen (<75% obstruction is asymptomatic). No damage to cartilage.
Stenosis		Funnel like narrowing of tracheal cartilage.
Tracheobronchomalacia		Airway becomes flaccid and dilated. Lack of rigid support from cartilage rings.
Not applicable	Neoplasms	Progressive obstruction of the airway. Asymptomatic until near-total luminal obstruction.

Table 1.1. Pathophysiology of the trachea.

Congenital tracheal stenosis is a fairly rare condition which refers to a narrowing of the trachea, caused either by an abnormality of the trachea itself or as a result of the trachea being compressed by an external force, for example, a cardiovascular

abnormality. In the majority of cases however it presents as a funnel-like narrowing caused by the presence of abnormal complete cartilaginous tracheal rings, instead of the normal C-shaped cartilaginous rings (Phipps, Raymond et al. 2006). There are various degrees of severity ranging from only a single affected tracheal ring to almost the entire length of the trachea being affected, (Kay 2007). Most forms of congenital stenosis are life-threatening with only the mild forms being an exception (Phipps, Raymond et al. 2006). Congenital tracheomalacia is a rare condition which occurs when the cartilage rings have not developed properly. In these cases, instead of providing rigid support to the trachea the walls of the trachea are flaccid to the extent that the posterior wall can move towards and sometimes even touch the anterior wall during heavy breathing (Kay 2007).

In adults, pathology of the trachea includes tracheal neoplasms, strictures and tracheomalacia caused by infection and inflammation, trauma and post-intubation injuries (Iivanov 2007). Tracheal neoplasms (tumours) are a rare condition and represent less than 1% of all malignant cancers and less than 0.1% of all cancer deaths each year (Visosky 2004, Daley 2009). 80% of tracheal primary tumours are malignant with 66% of these being either adenoid cystic carcinoma or squamous cell carcinoma (Daley 2009). The remaining one third of all tracheal tumours are of a varied type of either benign or malignant tumours. Tumours from surrounding tissue such as the larynx, thyroid, lung and oesophagus can also cause secondary tracheal tumours (Daley 2009). Most tracheal tumours are slow growing with benign neoplasms presenting as smooth rounded tissue masses that are generally less than 2 cm long. Malignant tumours generally present as tumours that proliferate outwardly on the exterior surface of the trachea and can cause ulcers (Daley 2009). Tracheal tumours cause progressive airway obstruction, but acute respiratory difficulty may not arise until the airway is almost entirely blocked. For this reason correct diagnosis is usually delayed and the condition commonly fatal (Daley 2009). Tracheal strictures and stenoses caused by infection, inflammation, trauma or post-intubation injuries can cause chronic and progressive constrictive airway defects in the cartilage rings which can restrict the passage of air. As discussed previously this can ultimately lead to respiratory difficulties which can potentially be fatal. Tracheobronchomalacia can also occur from chronic airway inflammation or infection such as a result of smoking, chronic bronchitis, emphysema, tuberculosis

and cystic fibrosis, and results in large segments of the airway becoming flaccid and dilated (Marom, Goodman et al. 2001).

1.1.4 Methods for addressing pathology and the limitations of current therapies

For congenital tracheal agenesis and atresia, a newborn can only survive if an alternative route for respiration exists by way of a tracheo- or bronchoesophageal fistula (Kay 2007). Suspicion of the condition prenatally gives the patient the best chance of survival as ventilation can begin immediately following birth (Panthagani, Santos et al. 2009). Corrective surgical techniques are available but the success rate is low, deeming these conditions to be non-correctable (Kay 2007). The inability to successfully engineer a *de novo* trachea from biological or artificial materials has hindered medical progress in this disease condition however the advancement of tissue engineering could provide a solution (Panthagani, Santos et al. 2009). For congenital tracheal webs, most are successfully treated by breaking up the web and thereby widening the lumen using either a laser or cutting instrument. Only much thickened webs need to be treated with open surgery where resection of the trachea is employed (Kay 2007). For congenital tracheal stenoses, surgery is the most successful form of treatment. For short to mid length stenoses, slide tracheoplasty is the preferred method as the trachea is shortened less than the trachea is with resection. For long segment tracheal stenosis, slide tracheoplasty has been used with some success but in many cases patch tracheoplasty with autologous material is required (Phipps, Raymond et al. 2006). For cases of congenital tracheomalacia, surgery is rarely needed. This is because, as the patient grows, the trachea cartilage is strengthened so that by the age of 2 years old the condition dissipates without intervention (Kay 2007). Tracheal tumours are treated most successfully by surgical resection of the trachea (Daley 2009).

Where the diseased area is too large for resection, there is the possibility of transplantation and this can greatly improve the quality of life. Autografts are possible if only short segment replacement is required and these segments are adequately vascularised (Grillo 2002). Fresh allografts would also be possible, however a major limitation is the need for the allografts to be re-vascularised and their use would require the patient to receive immunosuppressive therapy for the

remainder of their lives to prevent major histocompatibility complex (MHC) rejection (Grillo 2002). Considering these post-operative complications, one could argue it may not be justifiable to treat tracheal disease with transplantation as the surgical procedure is more life-threatening than the disease (Grillo 2002). Indeed, leading clinicians in this field consider tracheal transplant to be a debatable option given that current surgical procedures are limited. However, with the clinical emergence of tissue engineering it could become a viable treatment method although current tissue engineering and stem cell research would need to become more advanced to produce a dependable tracheal substitute (Birchall and Macchiarini 2008, Badylak, Weiss et al. 2012).

1.2 Tissue engineering

1.2.1 What is tissue engineering?

Tissue engineering emerged in the early 1980s as a discipline that draws on biological, medical and engineering components. Although much has been learnt and changed over the last thirty years, the central goal remains the same: to be able to develop replacements for damaged, failing or lost organs and tissues (Langer and Vacanti 1993, Simpson and Bowlin 2006). Early examples of cartilage tissue engineering were demonstrated by Green in 1977, in which chondrocytes subjected to different treatments, e.g. sub-cultured or grafted onto a decalcified bone structure, were assessed for their ability to form collagen following an allograft (Green 1977). The low antigenicity of chondrocytes means that allogeneic chondrocytes can be used and can survive in the host for some time without rejection (Tan, Steiner et al. 2006). Although Green's attempts were not entirely successful, the principles that were developed paved the way for further work (Green 1977, Meyer-Blaser, Handschel et al. 2009).

Current tissue engineering strategies commonly incorporate three elements. These are:-

- 1) Cells - to provide tissue specific functions.
- 2) Scaffolds – to provide tissue architecture and regulate aspects of the local cell population.
- 3) Growth factors - to regulate cell functions, e.g. proliferation and differentiation (Simpson and Bowlin 2006, Morrison 2009).

1.2.2 How can tissue engineering and regenerative medicine be used?

For the commercially viable transplantation of tracheas there is a need to generate an “off-the-shelf” replacement tissue for clinicians. The replacement organs or tissues should have the correct form and shape of the original tissue, it should be able to fulfil the function of the original tissue, it should facilitate the regeneration of the tissue and should be able to be easily implanted and attached to the surrounding tissue once the defect has been removed (Hollister 2009). It is important, generally due to the pressing medical need, that these can be prepared for use by clinicians with little preparation time or intervention needed. The optimal requirements or critical quality attributes (CQA) for replacement tracheae include: removal of foreign (donor) immunogenic cellular material: removal of immunogenic nuclear material, predominately DNA, to less than 50 ng/mg (dry weight) of dsDNA (Badylak, Weiss et al. 2012, Keane, Londono et al. 2012); comparable tensile strength to the native trachea; no toxicity; no immunogenicity; long-term stability once implanted into the patient; and, if transplanted into children, growth potential. Theoretically, with tissue engineering it could be possible that scaffolds for tracheae with the above characteristics can be generated in advance, in an off-the-shelf manner, without any intervention required from the potential recipient. However other important characteristics of the trachea include it being vascularised and seeded with patient’s cells to generate a respiratory epithelial lining in the lumen and chondrocytes to support cartilage growth and replacement. These latter requirements present a major challenge for generating off-the-shelf tracheas which can currently only be generated with intervention and involvement from the patient prior to transplantation (Macchiarini, Jungebluth et al. 2008, Delaere, Vranckx et al. 2010).

Recent advances in tissue engineering and regenerative medicine have facilitated the construction of replacement tracheas which has allowed patients with tracheal pathology to be not only treated, but possibly cured through transplantation of these tissue engineered tracheas (Macchiarini, Jungebluth et al. 2008, Delaere, Vranckx et al. 2010). In order to achieve this there has been a drive across many other disciplines to ensure that there is equipment and technology ready to support these advances in the tissue engineering and regenerative medicine fields. An example of this was the need to develop a double-chamber rotating bioreactor which enabled the growth of the different cell types on the tissue-engineered tracheae or other hollow

organs. (Asnaghi, Jungebluth et al. 2009). This bioreactor has been licenced to and commercialised by Harvard Apparatus Regenerative Medicine (HARegenMed 2013), which also has other tissue engineering bioreactor systems commercially available (HARegenMed 2013).

1.2.3 Scaffold use in tracheal tissue engineering

Tracheal prosthesis employing silicone (Neville, Bolanowski et al. 1990) and hydroxy apatite and carbon fibre (Takahama, Onishi et al. 1989) have been historically tolerated with limited pre-clinical and clinical success. There has therefore been a shift to produce scaffolds that are more physiologically relevant and can incorporate and encourage native cell growth similar to the extra-cellular matrix (ECM). The ECM provides tissue specific structural elements to which cells can adhere (Simpson and Bowlin 2006). To be able to engineer tissues and organs, there is a need for clinically usable scaffold material that is not only the correct form or shape of the desired structure, but to which the cells can adhere and, if necessary, differentiate, proliferate and re-organise (Hollister 2009). This purports that any substitute scaffold will need to be more than a simple inert framework that is generic for all applications and will need to consider tissue-specific issues such as scaffold composition, architecture and porosity (Simpson and Bowlin 2006). To evaluate potential scaffolds, it must be possible to characterise how the cells interact with the scaffold material and it is preferable that the performance of the scaffold with the cells *in situ* can be evaluated *in vitro* as well as *in vivo* through the use of molecular, cellular and histological methods (Hollister 2009). It is also important that the mechanical properties of the resulting scaffold match the mechanical properties of the tissue it is to replace, although it is unclear as to what extent this is necessary (Funamoto, Nam et al. 2010). This is a challenge as there are many ways to define the mechanical properties of tissue in question in terms of models such as linear elasticity, non-linear elasticity, viscoelasticity and poroelasticity. This complexity is increased by the fact that the same tissue can be defined by different versions of these models and there is no consensus on which model should be used (Hollister 2009). There is also the issue that even if the mechanical properties of the tissue can be matched *in vitro*, once implanted the mechanical properties may alter *in vivo* which could affect the function of the engineered tissue (Hollister 2009). Beyond the mechanical properties there is also the issue of the mass transport properties of the

scaffold for nutrient supply and metabolic waste removal, which takes into account the scaffold's diffusivity and permeability (Hutmacher 2000). All of these different properties need to be taken into account when designing the scaffold to determine the scaffold's required critical quality attributes and ultimately the target product profile (TPP).

Scaffolds can either be synthetic or biological scaffolds, the latter of which are typically allogeneically or xenogeneically derived from a donor. For synthetic scaffolds, although different novel materials and structures have been adapted and used as scaffolds at research level, the clinical application of synthetic scaffolds has been very limited (Hollister 2009, Jungebluth, Alici et al. 2011) because of the complex issues involved in scaffold choice and design. Ultimately, for the scaffold generation process to become clinically relevant, it must be possible to scale-up production whilst adhering to quality manufacturing principles (Williams, Thomas et al. 2012) towards robustly generating potentially hundreds of scaffolds per year with minimal CQA variation (Hollister 2009). The focus of this engineering doctoral project was on biological scaffolds.

1.2.4 Biological scaffolds

Biological scaffolds can be generated by obtaining the desired tissue or organ from either a human donor (allogenic) or an animal donor (xenogenic). For these biological scaffolds to be functional and not elicit an immune response in the recipient, the donor's cells need to be removed from the tissue or organ. This process is known as tissue decellularisation. The remaining ECM of structural and functional proteins has the advantages that it should have the desired structure and mechanical behaviour. However the process of decellularisation can have some unwanted side effects on the biochemical composition and ultrastructure of the ECM. As the cells contribute to holding the ECM in place, their removal can weaken the ECM scaffold. Also detergents and enzymes involved in the decellularisation process can damage the ECM by removing or modifying certain proteins e.g. GAGs (Gilbert, Sellaro et al. 2006) and undesirable alteration in the structure of the ECM could also hinder cell growth during recellularisation (Gratzer, Harrison et al. 2006). In addition to this, the chemical(s) used to remove the donor's cells may have a toxic effect upon the viability of the newly seeded cells, or to the recipient upon transplantation, if it is not possible to adequately remove traces of it from the ECM (Gilbert, Sellaro et al.

2006). An immune response and tissue rejection in the recipient could also be an issue if all traces of the donor cells are not removed (Balasundari, Gupta et al. 2007, Macchiarini, Jungebluth et al. 2008).

Several methods have already been explored with regard to the decellularisation of biological tissues and organs for use as biological scaffolds; these include various chemical treatments (including detergents, acids, hypotonic and hypertonic solutions), enzymatic treatments, ultra-high pressure treatments, cryopreservation treatments and immunological treatments. Various methods, which have been notably applied to tracheal decellularisation, along with the advantages and disadvantages of each will be discussed below.

One method, a perfusion method, for decellularising tracheas was outlined in a US Patent application form, developed by Ott (Ott, Matthiesen et al. 2008), for the decellularisation of a rat lung and trachea. This method relied on two to twelve hours of perfusion with 1% SDS followed by a fifteen minute perfusion with distilled water and then a fifteen to thirty minute perfusion with 1% Triton-X. The authors stated that SEM micrographs were used to confirm the ECM structure was intact and the respiratory epithelium had been removed leaving a rough luminal basal membrane (Ott 2009). Whilst published results for this perfusion method have been used to demonstrate decellularisation of a rat heart, data is yet to be published on the lung or the tracheal decellularisation or in porcine models (Ott, Matthiesen et al. 2008).

Another, perhaps less conventional, method was explored by Delaere and colleagues (Delaere, Vranckx et al. 2010, Delaere, Vranckx et al. 2014). This method, which has treated five patients to date, involved the implantation of a donor trachea into the forearm of the recipient. During the three to nine months that the tracheae were in the recipients' forearms, the respiratory epithelium and trachea were revascularised and autografts of recipient buccal mucosa were introduced prior to orthotopic transplantation when it replaced the recipients' defective section of trachea. Immunosuppressive medication was administered for seven and a half to nine months to prevent rejection. Post-immunosuppression, the authors stated that the tracheae were decellularised by the recipients' own immune systems, without the tracheae being rejected, because they had been and were continuing to be

repopulated with the patients' buccal mucosal cells and vascular network. This manner of decellularising the trachea is interesting as it employs the use of the patient's own immune system to decellularise the trachea (Delaere, Vranckx et al. 2010, Delaere, Vranckx et al. 2014). In one highlighted case, the authors presented evidence to demonstrate that after four months of implantation in the forearm, donor cells were present in the respiratory epithelium. This suggests that donor cells were surviving due to the fact that immunosuppressive medication was administered to the recipient. At the time of the orthotopic transplantation, data revealed there were no donor cells present in the respiratory epithelium which meant donor cell removal would have occurred when the immunosuppressive medication was withdrawn. This time period was based on the time it took for a donor skin graft to become necrotic and slough off and was therefore the necessary length of time (Delaere, Vranckx et al. 2010). Although this procedure overcomes the challenge of revascularisation, at up to a year in length, it is a very long and costly procedure with a high risk of infection as the patient would be on immunosuppressants and the forearm opened frequently to verify progress. Other potential limitations of the process include an anatomically incorrect squamous epithelial cell layer being formed due to the use of buccal mucosa and the fact that several of the tissue engineered tracheae have required stenting suggesting a loss of biomechanical properties. Unless the process can be radically improved upon, this could render the procedure unsuitable for routine clinical use (Delaere, Vranckx et al. 2010, Delaere, Vranckx et al. 2014).

Another method by Conconi (Conconi, De Coppi et al. 2005), adapted from Meezan (Meezan, Hjelle et al. 1975) as a way to decellularise trachea involved the following treatment: loose fascia was removed from the donor trachea; the trachea was then treated with eighteen to twenty-two cycles of incubation in distilled water treatment for seventy-two hours followed by 4% sodium deoxycholate for four hours at room temperature and 20kU per mL DNase I for three hours at room temperature. Each cycle of water, sodium deoxycholate and DNase I took four days to complete. Due to the number of steps involved in this method, automation or anything beyond small scale scale-up is likely to be a bioprocessing challenge. It would be advantageous if the incubation times or cycle number could be reliably reduced, but ideally the number of steps involved in each wash would be minimal. Immunohistochemistry (IHC) was performed on sections taken after 25 cycles and demonstrated that the

epithelial cells and glands had been removed by the decellularisation process. There were still a few chondrocytes detected within the cartilage rings, although these were mostly disrupted, with indistinct cell borders and most had lost their nuclei. However given the isolation and low immunogenicity of chondrocytes it is unlikely that their presence would raise an immunological response in the recipient, though this issue is yet to be resolved. MHC staining demonstrated that MHC class I expression had been completely removed after 25 cycles but there was still some localised MHC class II expression detected in several areas in the cartilage rings (Conconi, De Coppi et al. 2005, Macchiarini, Jungebluth et al. 2008). Originally the overall process of decellularising the trachea took between 72 and 88 days, although in further work performed on porcine models (Jungebluth, Go et al. 2009), the authors claimed to have been able to successfully reduce the distilled water treatment to 48 hours and the number of sodium deoxycholate and DNase I cycles needed to 17. These reductions served to reduce the overall preparation time to approximately 35 days, with the limiting step then becoming the expansion of the recipient's cells. However, from the immunostained sections shown in the paper it is ambiguous as to whether all of the MHC class I and II expression has been completely removed and to whether the number of nuclei has been significantly reduced after seventeen cycles as claimed in the paper (Jungebluth, Go et al. 2009).

Whichever method is ultimately used for the generation of tracheal bioscaffolds will need to demonstrate that it can achieve the required CQA in terms of histology for cell and DNA removal (Sasaki, Funamoto et al. 2009, Hashimoto, Funamoto et al. 2010), the presence of GAGs (Sasaki, Funamoto et al. 2009, Hashimoto, Funamoto et al. 2010) and collagen content, which are important as they contribute to the mechanical properties of the trachea. Also it will be important to ensure the re-seeded cells can redeposit GAGs and proteoglycans to engineer a trachea that possesses acceptable compressive and tensile properties (Elder, Eleswarapu et al. 2009, Funamoto, Nam et al. 2010). Most importantly the chosen method must be able to comply with good clinical practice (GCP) or good manufacturing practice (GMP) and will need to be scalable in order to produce the required quantities needed to fulfil the current unmet clinical need.

1.3 Tracheal transplantation for chronic airway indications

1.3.1 Current situation

Short segment tracheal defects, which are defined as less than half the length (five to six cm) of the trachea in adults and less than a third of the length of the trachea in children, can be repaired by resection of the trachea with end-to-end anastomoses or slide tracheoplasty (Macchiarini, Jungebluth et al. 2008, Delaere, Vranckx et al. 2010). Long segment tracheal defects can be treated by a variety of treatments. For stenosis, a stent or multiple stents can be positioned in the trachea to reinforce the tracheal structure and maintain an open airway. Alternatively a tracheostomy, which involves the formation of a stoma (artificial opening) in the trachea, can be performed, and followed by intubation with an endotracheal tube or cannula through which the patient can breathe or speak (Delaere 2009). Although such palliative treatments permit long-term survival, when breathing and speaking patients generally experience significant discomfort (Delaere 2009). An improved treatment would employ the use of a tracheal replacement for long segment and recurrent short segment defects (Delaere 2009). Autografts have been used to repair trachea defects, however due to limited donor sites and the specific structure of the trachea, this method is not optimal (Rinker 2009). A more physiological appropriate solution is the use of allograft tracheae from heart-beating and non-heart-beating donors, but this poses major challenges (NHSBT 2009). As the trachea is immunologically active (Birchall and Macchiarini 2008), current allotransplantation relies on major histocompatibility complex (MHC) matching of the donor and the recipient in order to reduce the amount of immunosuppressive medication required to prevent graft versus host disease and graft rejection. This requires the patient to wait until a matched donor is found for the allotransplantation to proceed. In the Delaere and colleagues tracheal allotransplantation the procedure was delayed by nine months whilst a suitable donor was found for the patient (Delaere, Vranckx et al. 2010). In conventional allotransplantation, immunosuppressive medication therapy would then be administered to the patient for the remainder for the patient's life to prevent rejection and ensure graft survival. Due to the differences in drug metabolism from patient to patient, therapeutic drug monitoring is then required on an individual basis to achieve the desired therapeutic effect whilst minimising toxicity to the patient (Kahan, Keown et al. 2002). Even so the toxic side effects caused by the

immunosuppressive medication can be severe (Delaere 2009). These can include high blood pressure, diabetes, high cholesterol, osteoporosis, susceptibility to infections and cancer. Overall, the medication can reduce life expectancy by an average of 10 years (Hathaway, Winsett et al. 2003, Highfield 2008). This risk of cancer is especially relevant for patients whose tracheal defect was originally caused by neoplasms. The overall effect of this can result in an improved quality of life afforded by the transplant being diminished by the immunosuppressive drug side effects (Hathaway, Winsett et al. 2003). In the Delaere allotransplantation, the immunosuppressive medication regime lasted only seven and a half months, whilst the trachea was adapted in the patient's forearm to prevent rejection by the patient's immune system, which is an acceptable length of time given the overall benefits (Delaere, Vranckx et al. 2010). However, in typical tracheal transplants, where the defects are not life-threatening and the primary objective is to improve the patient's quality of life, allotransplantation is unlikely to be justified due to the nature of the side effects (Delaere 2009). This results in an unmet medical need for patients who suffer with high morbidity as a result chronic airway defects.

1.3.2 Proof of concept in patient

In 2008 Dr Macchiarini and colleagues performed a ground breaking clinical transplantation of a tissue-engineered airway into a thirty year old woman, Claudia Castillo, with end-stage bronchomalacia as a result of infection with tuberculosis. The procedure, as previously described (section 1.2.4 Biological scaffolds), involved a trachea from a deceased donor being decellularised using detergents and enzymes over a period of six weeks resulting in an ECM scaffold. Mesenchymal stem cells and bronchial epithelial cells were then taken from Castillo and expanded in the laboratory, during which time the mesenchymal stem cells were differentiated into chondrocytes. The bronchial epithelial cells were seeded onto the lumen of the decellularised scaffold and the chondrocytes were applied to the outside of the decellularised scaffold. After four days of incubating the scaffold and the attached cells in a bioreactor designed specifically for that purpose, the newly tissue engineered trachea was cut to the appropriate size and was transplanted into Castillo without any need for immunosuppressive medication. At four days post-operatively, the graft was virtually impossible to distinguish from the adjoining tracheobronchial epithelium (Macchiarini, Jungebluth et al. 2008). Within 10 days of the transplant

operation Castillo was able to leave the hospital and as a result her life was transformed. Pre-operatively Castillo experienced a high level of morbidity. She was essentially bed-bound and unable to breathe adequately enough to perform simple duties. Post-operatively, she was able to work full time and look after her children (Bristol_University 2008, Macchiarini, Jungebluth et al. 2008). At one month post-operatively, the graft was identical to the adjacent epithelium and elicited local bleeding when a biopsy was taken, which means revascularisation had occurred within the graft to support cell growth and survival (Macchiarini, Jungebluth et al. 2008).

The major success of this clinical procedure with this outcome was achieved without the needed for immunosuppressive medication, so there were no undesirable side effects, mild or serious, which could diminish Castillo's future quality of life. Follow up reports indicated that five years on from the operation, Castillo was in good health, the trachea remained open with a functional respiratory epithelium and showed no sign of developing anti-donor antibodies, which could be indicative of potential rejection, or stem cell related teratoma. However a progressive stenosis and partial loss of mechanical integrity had developed which required repeated treatments and stenting (Baiguera, Birchall et al. 2010, Gonfiotti, Jaus et al. 2014). A similar case was reported for a two year follow-up of a tissue engineered tracheal replacement in a child. The results detail that although after two years post operatively the boy had a functional airway and was living a normal active life, medical intervention including stenting had been required until the respiratory epithelium and biomechanical strength was restored (Elliott, De Coppi et al. 2012). Given that the alternative to these highly experimental procedures was for the patients to remain with a high level of morbidity, the outcomes for these patients, despite the need for post-operative medical intervention, represents landmarks in transplant history.

Despite the success with this type of tissue engineered trachea transplantation, the transplanted tissue-engineered trachea was avascular and there was a risk of unpredictable healing which could cause stenosis (Macchiarini, Jungebluth et al. 2008, Delaere, Vranckx et al. 2010). There are many groups researching methods to aid revascularisation of an ECM scaffold which are briefly highlighted below. Delaere and colleagues attached a donor trachea to the recipient's blood supply by

wrapping trachea in fascia, which was attached to the radial artery and two radial veins. The donor trachea was then implanted into the recipient's arm for nine months. By doing this they used the patient's own body as a bioreactor to ensure revascularisation of the trachea (Delaere, Vranckx et al. 2010). Muioli and colleagues reported that the addition of haematopoietic stem cells (HSC) or bone marrow aspirate onto the ECM scaffold could help with vascularisation (Muioli, Clark et al. 2008). Tan and colleagues reported that the addition of vascular endothelial growth factor (VEGF) to a continuous flow of medium to which the scaffold was exposed increased angiogenesis on the scaffold (Tan, Steiner et al. 2007). Lastly, Kapickis and colleagues explored the idea of implanting a vascular bundle into the avascular tissue to encourage revascularisation (Kapickis, Sassu et al. 2009). The methods proposed here, along with others, will need to be evaluated if it becomes apparent that revascularisation is necessary for tissue engineered tracheal transplantation.

1.3.3 Health care cost concerns

Currently there are approximately 270 patients in the United Kingdom that would benefit from a tracheal transplantation (Boseley 2008). Tracheal transplantation is theoretically an unproblematic procedure, however the high number of surgical and prosthetic tracheal alternatives that have been attempted throughout the last century implies that there is a lack of ideal tracheal replacements (Birchall and Macchiarini 2008). As a result, tracheal transplantations are somewhat of a rare event. The consequence of this being the unknown mortality and morbidity associated with the procedure (Birchall and Macchiarini 2008). Due to the lack of cost analysis for tracheal transplantation, data extrapolated from National Health Service for all day operations on head and neck cancers were used as models of tracheal transplants and human lung transplants for the corresponding immunosuppression requirements. These estimate the cost of tracheal allotransplantation in 2008 at £37,000 (Guy's Hospital London tariff), inclusive of preparation, patient follow-up and associated drug costs for the first six months. After this, the continuing yearly cost of immunosuppression is estimated to be approximately £5,100 (Birchall and Macchiarini 2008). However if the trachea were to be tissue engineered prior to transplantation then the cost of preparing the transplant would rise. However, given there would be no need for immunosuppressive medication, there would be an initial

cost saving of £2,550 for the first six months of post-operative care for the patient and then a continuing cost saving of £5,100 per annum, over the initial five years this saving amounts to approximately £27,500 (Birchall and Macchiarini 2008). Comparing this to the long-term cost of admitting a patient as symptomatic as Castillo pre-operatively into intensive care twice a week, which Macchiarini was quoted as saying cost £3000 per day, then the treatment cost will be swiftly recouped with an overall cost saving being made by the health care provider. Factoring into this the human cost of improved quality of life, the treatment costs are modest given the likely benefit to the patients (Birchall and Macchiarini 2008) and the removal of their reliance on the health care system.

1.3.4 Potential techniques to achieve scale-up

Following on from the pioneering clinical work performed by Macchiarini and colleagues in 2008, whereby a tissue-engineered trachea was transplanted into a thirty year old woman with end-stage bronchomalacia (Macchiarini, Jungebluth et al. 2008), this research project aims to build upon that achievement. To that end, the aim of this project is to develop a method for the rapid, effective and non-detrimental decellularisation of the trachea that is amenable to automation and scale-out. This would represent progress towards the generation of a process for ‘off-the-shelf’ tissue-engineered trachea that can be easily accessed by clinicians to meet the medical need of patients with serious clinical airway disorders. Challenges to be investigated are the process of tracheal decellularisation, with the particular need for developing a robust technique which gives reproducible results and ideally can be fully or semi-automated. Also to be investigated are the analysis techniques to ensure the ECM and cartilage rings of the trachea remain structurally intact whilst being appropriately decellularised. These include light and electron microscopy techniques and immunohistochemistry methods, qualitative assessment of remaining ECM components and biomechanical testing of the scaffolds. With regards to recellularisation, although Macchiarini, as a follow-on from the clinical transplantation of a tissue-engineered airway (Macchiarini, Jungebluth et al. 2008), sprayed mesenchymal stem cells (MSC) directly onto the tracheal scaffold for the last two patients to be treated, indicating the cells can differentiate instinctively *in vivo* possibly due to the presence of protein residues on decellularised tracheal ECM, this could possibly result in undesirable differentiation of cells and the data is yet to

be published. Therefore, methods for the efficient expansion, differentiation and seeding the recipient's cells onto the scaffold will also need to be investigated as well as the use of adult stem cells and progenitor cells.

To achieve tissue engineered trachea on a commercial level, other considerations will need to be taken into account. These include the procurement of the donor scaffolds ensuring compliance with the Human Tissue Act (HTA) regulations on organ donation, guidance on the appropriateness of the donated trachea, primarily regarding the age and health of the donor and consideration to the means of transporting the donated trachea to the site where the decellularisation occurs. The method of procuring the patient's cells would also entail the same considerations as the tracheal procurement. As mentioned previously, the process of decellularisation would need to comply with GMP, would need to have clearly defined CQA, TPP and release criteria and would ideally involve automation. The culture system for the expansion of the patient's cells would again need to adhere to GMP, would ideally involve automation and the use of chemically defined media and associated solutions or, if this is not possible, evidence would be required to prove due diligence in the procurement of the cell culture media and/or solutions. The assembly of the tissue engineered trachea would have to optimise the time for culturing the cells on the ECM, it would also ideally incorporate automation of the procedure, the use of chemically-defined media, and compliance with GMP with clearly defined release criteria. Delivery to the site of transplantation would then need to resolve the logistics of packaging criteria, especially concerning the temperature control, the vibration control and a method of monitoring to ensure the ranges of neither have been exceeded. For the actual clinical application of the tissue engineered trachea, considerations include its on-site storage and the maximum shelf-life prior to transplantation (Kemp 2010). Again, as tissue engineered tracheae would be classed as ATMP, their use in the United Kingdom would be regulated by the Medicines and Healthcare products Regulatory Agency (MHRA) and the European Medicines Agency (EMA) (Daniels 2010).

To achieve true scale-up rather than just scale-out, the employment of synthetic scaffolds and non-immunogenic embryonic stem cells will most likely be necessary. Until suitable reproducible artificial scaffolds can be created, and are proven as such in pre-clinical trials, then it is unlikely that true scale-up can be achieved. Similarly

until pre-clinical and clinical trials have proven that embryonic stems cells can be used in a non-immunogenic manner, true scale-up will be difficult to achieve because of the ongoing need for individual patient involvement.

2 Materials and Methods

2.1 Procurement and preparation of porcine tracheae for experimentation

Porcine tracheae, from male pigs with an average weight of 90 kg, were obtained from Animal Organs for Research (based at Cheale Meats Ltd. abattoir, Brentwood, UK). Porcine plucks, which consist of the heart, liver, windpipe, and lungs of the slaughtered pig, were trimmed by Matthew Cheale onsite to obtain the trachea from the larynx to the carina. They were packaged into plastic bags, which were surrounded by wet ice, in a polystyrene box and transported by motorcycle courier to the laboratory. Upon arrival they were further trimmed to remove the cricoid cartilage from the upper region and the bronchi branches from the lower region of the trachea. The loose visceral fascia was also trimmed from the organ. The tracheae were either used fresh or stored (frozen) for future use as required.

2.2 Preparation of porcine tracheal scaffolds by detergent-enzymatic method (DEM) decellularisation

To achieve DEM decellularisation the tracheae were treated as previously reported (Conconi, De Coppi et al. 2005, Macchiarini, Jungebluth et al. 2008, Jungebluth, Go et al. 2009) with some modifications: a tenfold reduction in the concentration of DNase I to reduce assay costs; the omission of the 48/72 hour distilled water incubation step from every cycle due to misinterpretation of the published methodology; and the inclusion of an overnight (18 hour) phosphate buffered saline (PBS) incubation step (Figure 2.1). Process steps were performed in 50 mL centrifugation tubes with a solution volume of up to 50 mL.

Fresh tracheae were washed 3 x 15 minutes in 1 x phosphate buffered saline (PBS) (Sigma, Poole, UK) containing 100 units/mL of penicillin, 100 µg/mL of streptomycin, and 250 ng/mL of amphotericin B solution (Life Technologies, Paisley, UK) whilst rotating at 33 revolutions per minute (rpm) at room temperature (RT). The tracheae were cut into approximately 5 x 30 mm length sections. The tracheae were then subjected to the decellularisation protocol. Initially the tracheae were incubated statically in distilled water for 72 hours at 4°C followed by: 25 cycles of a chemical detergent step of 4% sodium deoxycholate (Sigma, Poole, UK)

in distilled water for 4 hours at RT on a roller mixer at 33 rpm; an enzymatic step of 2kU/mL DNase I (Sigma, Poole, UK) in 1M sodium chloride (NaCl) (Sigma, Poole, UK) for 3 hours at RT on a roller mixer at 33 rpm; and a wash step of 1 x PBS containing 100 units/mL of penicillin, 100 µg/mL of streptomycin, and 250 ng/mL of amphotericin B solution 16 hours statically at 4°C. In between steps the tissues were washed 3 x 5 minutes in PBS containing 100 units/mL of penicillin, 100 µg/mL of streptomycin, and 250 ng/mL of amphotericin B solution. Samples (a single 30 mm section) were taken for testing at cycles 10, 20 and 25 at which point the sections were stored in PBS containing 100 units/mL of penicillin, 100 µg/mL of streptomycin, and 250 ng/mL of amphotericin B solution at 4°C for no more than 3 days. Non-decellularised control (NDC) tracheae were stored statically in PBS containing 100 units/mL of penicillin, 100 µg/mL of streptomycin, and 250 ng/mL of amphotericin B solution at 4°C for matched periods of time.

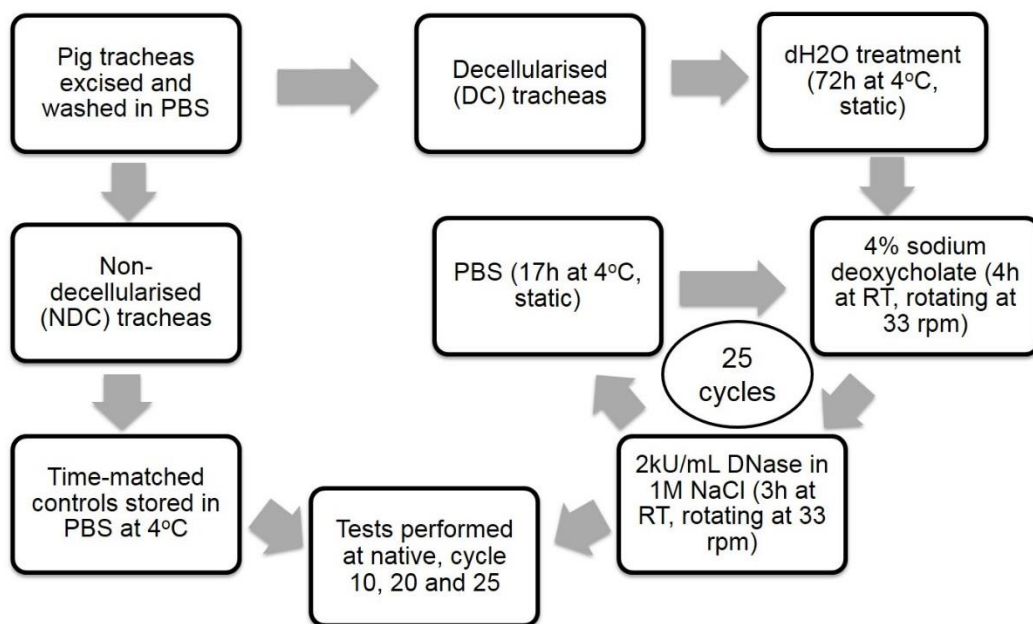


Figure 2.1: Overview of the detergent and enzymatic method (DEM) decellularisation.

2.3 Preparation, embedding and sectioning of tissue in paraffin

Tracheal tissues cut to 3-4 mm in depth in the transverse and sagittal planes were fixed in 10% neutral buffered formalin (NBF) solution in approximately 20 times the tissue volume for a minimum of 48 hours. The tissues were placed in appropriately labelled and sized processing cassettes and fixed in place with a lid. The processing

cassettes were placed back into 10% NBF until processed. The tissues were automatically processed using the VIP 3000 Tissue Processor (Sakura, Thatcham, UK) to dehydrate the tissue to remove the fixative and water, clear the tissue to prepare it for impregnation and finally impregnate the tissue with embedding medium. Briefly the tissues were immersed in 10% NBF for 2 hours at RT, 70% industrial methylated spirits (IMS) for 1 hour at RT, 90% IMS for 1 hour at RT, 3 x 100% IMS for 1 hour at RT, 50% IMS:50% toluene for 1 hour at RT, toluene for 30 minutes at RT, toluene for 1 hour at RT, toluene for 30 minutes at RT, paraffin wax for 30 minutes at 60°C, paraffin wax for 1.5 hour at 60°C, paraffin wax for 1.5 hour at 60°C. When the processor was finished the processed cassette was transferred to the Tissue Tek III embedding centre and placed into the thermal console drawer at 60°C, where it could be stored for up to 4 hours before embedding. When ready to embed, a suitable sized embedding mould was selected and the base of the mould covered in molten wax, the tissue was removed from the cassette and embedded into the mould and molten wax, ensuring the required surface was face down in the mould. The cassette (without the lid) was placed atop the mould and the mould was filled with more molten wax. The mould was moved to the cryo-console at -5°C to solidify the wax. After approximately 30 minutes, when the wax had hardened, the blocks were removed from the moulds and chilled on ice. The process of sectioning began by roughly trimming of the tissue block on the rotary Shandon Finesse AS325 microtome (Thermo Scientific, Loughborough, UK) until a complete section of tissue was obtained. The blocks were then cooled again on ice for a further 1 hour. Sections of 5 µm thick were the obtained from the block and floated, in a 40°C water bath (Thermo Scientific, Loughborough, UK), onto the surface of the water and allowed to flatten out. The desired sections were separated and, using a pre-labelled slide, gently lifted out of the water. The slides were placed onto a 60°C hot plate overnight to dry the sections onto the slides before staining.

2.4 Preparation, embedding and sectioning of tissue in optimum cutting temperature (OCT) compound

To analyse specific components of the tissues, the tissues were prepared for immunohistochemistry (IHC) and immunofluorescence labelling. Tracheal tissues were cut to 3-4 mm in depth in the transverse and sagittal planes and were then immersed in 20% sucrose solution (Sigma-Aldrich, Poole, UK) for 24 hours at 4°C

to preserve the tissue structure. The sections were then briefly rinsed in PBS to remove external sucrose solution. Cryomolds were half filled with optimum cutting temperature compound (OCT compound) (VWR, Leuven, Belgium). The tissue was positioned carefully, ensuring the side of interest was facing the bottom of the cryomold, in the OCT compound. The cryomold was then filled with OCT compound until the tissue was fully submerged, ensuring there were no bubbles near the tissue as this would cause problems when sectioning. The cryomolds were then placed in liquid nitrogen to allow uniform freezing of the OCT compound and tissue to a solid white block. The frozen samples were removed from the cryomolds stored at -80°C until sectioned. When sectioning was required, the samples were transferred to Thermo Scientific Cryotome FE Cryostat (Thermo Scientific, Loughborough, UK) and mounted onto an appropriately sized cryocassette using OCT compound. The cryocassette was then attached to the cryocassette clamp and OCT compound embedded sample positioned just above and behind the blade. The sample was trimmed to remove overlying OCT compound until all regions of the tissue were fully exposed. With the anti-roll bar in position, sections of 6 µm thickness were then taken, using a new area of the blade, and picked up onto a positively charged adhesion microscope slide (Thermo Scientific Menzel-Gläser, Loughborough, UK). The sections were air-dried onto the slides at 60°C for approximately 4 hours before use then used immediately or stored at -20°C until required.

2.5 Preparation and embedding of tissue in LR white resin

To analyse the tissues, the tissues were prepared for transmission electron microscopy (TEM) by embedding the tissue in London Resin (LR) White. This embedding technique also enabled histological analysis of the tissues by haematoxylin and eosin staining. The tissues were pre-fixed in 3% glutaraldehyde (Agar Scientific, Stansted, UK) in 0.1M sodium cacodylate (Agar Scientific, Stansted, UK) (pH 7.4) at room temperature for 30 minutes or overnight. The tissue samples were then sliced with a sharp razor blade into approximately 1-2 mm thick sections. These sections were then fixed in 3% glutaraldehyde in 0.1M sodium cacodylate (pH 7.4) at 4°C for 3 hours. The sections were then dehydrated in a graded series of alcohols: 20% ethanol for 15 minutes; 50% ethanol for 15 minutes; 70% ethanol for 15 minutes; and 3 x 90% ethanol for 10 minutes, all performed at RT. The sections were then infiltrated with LR white resin hard grade (Agar

Scientific, Stansted, UK) as follows: 1:1 of LR white: 90% ethanol for 30 minutes at RT; pure LR white for 30 minutes at RT; pure LR white at 4°C overnight; pure LR white for 30 minutes at RT. The sections were then embedded into the LR white resin by placing the sections into foil containers, in the desired orientation, and covering with 50 mL LR white containing 75 µL of LR white accelerator (Agar Scientific, Stansted, UK). Pre-cut parafilm was gently placed on the surface of the resin to exclude the air. The sections were then incubated at -20°C for 1 hour followed by 24 hours at 4°C to polymerise the LR white. The parafilm was then removed from the resin blocks for final curing at room temperature for at least two days.

2.6 Sectioning and analysis by transmission electron microscopy (TEM)

Ultrathin sections (90–100 nm) of the LR White embedded tissue sections were cut for TEM analysis with an ultramicrotome (Reichert UltracutE, Cambridge Instruments, Cambridge, UK) using a diamond knife (Diatome AG, Biel, Switzerland). The sections were mounted onto Formvar/Carbon coated 200 mesh gold grids (Agar Scientific) and stained with 0.1% (w/v) uranyl acetate in absolute alcohol for 5 minutes followed by Reynold's lead citrate for 5 minutes. The sections were then examined by TEM using a JEOL 100CX II transmission electron microscope (JEOL UK, UK) operating at 80 kV. The images were recorded on Kodak EM 4638 film (TAAB, UK) then scanned to provide a digital image. The sectioning and imaging of the trachea and the decellularised scaffolds for TEM was performed by Nicola Mordan (UCL Eastman Dental Institute).

2.7 Haematoxylin and eosin staining of tracheal tissue sections

Tissue sections were stained with haematoxylin and eosin, the most common general purpose stain, to differentiate the full cellular detail of tracheal tissue sections. Nuclei of cells stain blue, cartilage and mucin stain light blue/purple and other tissue components such as cytoplasm, connective tissue, red blood cells and muscle stain from pink to orange to red.

The tissue sections on microscope slides from the paraffin embedding process were 'taken to water' to remove the paraffin wax and rehydrate the tissue sections. This process involved immersing the slides in xylene for 5 minutes, xylene for 2 minutes, absolute industrial methylated spirits (IMS) for 2 minutes, 95% IMS for 2 minutes,

70% IMS for 2 minutes and tap/distilled water for 2 minutes. The sections were then stained with Gill's III haematoxylin for 1.5 minutes, washed in tap water for 5 minutes, differentiated in acid-alcohol (1% HCl in 70% IMS) for 3 seconds, the differentiation stopped in tap water for 4 minutes and stained with 0.5% aqueous eosin for 5 minutes and rinsed in tap water for 20 seconds. The sections were then dehydrated in 70% IMS for 5 seconds, 95% IMS for 5 seconds, absolute IMS for 5 seconds, cleared in xylene for 2 minutes and held in xylene for at least 2 minutes, remaining in the xylene until the sections were mounted with DPX and covered with coverslips. The slides were allowed to dry then examined under a microscope (Nikon Eclipse Ti, Kingston, UK) and imaged digitally (Nikon BR Elements, Kingston, UK).

2.8 Analysis of cell clearance and survival following decellularisation

A representative 100x or 60x magnification image from each trachea from the specific tissue region being analysed was obtained. The nuclei, stained blue by the haematoxylin, were counted to investigate the clearance of cells from the different regions of the tracheae before, during and after the decellularisation process. Chondrocytes were also analysed further to distinguish cells that appeared healthy, whether the nuclei remained; and those that were undergoing chondrocyte apoptosis, which was characterised by condensed nuclei and cell shrinkage resulting in unstained regions in the lacunae. The cell counting was performed by Vivienne Vu (UCL Biochemical Engineering MEng student). Rules were applied to the counting process to ensure consistency throughout the analysis. Statistical analysis was performed on the cell clearance and cell survival studies following decellularisation treatment. GraphPad Prism v5.03 (GraphPad Software, La Jolla, USA) using one-way ANOVA and Dunnett's multiple comparison test.

2.9 Alcian blue staining for GAG analysis

Tissue sections were stained with alcian blue to differentiate acidic mucopolysaccharides or GAGs, found in the cartilage and mucosal glands of the trachea, which stain blue, nuclei of cells which stain red/pink and the cytoplasm of the cells which stain a pale pink.

The tissue sections on microscope slides from the paraffin embedding process were 'taken to water' to remove the paraffin wax and rehydrate the tissue sections. This process involved immersing the slides in xylene for 5 minutes, xylene for 2 minutes, absolute industrial methylated spirits (IMS) for 2 minutes, 95% IMS for 2 minutes, 70% IMS for 2 minutes and tap/distilled water for 2 minutes. The sections were then stained with 1% alcian blue in 3% acetic acid (pH 2.5) for 5 minutes, washed in tap water for 2 minutes and stained with 0.1% nuclear fast red in 5% aluminium sulphate for 1 minute and rinsed in tap water for 20 seconds. The sections were then dehydrated in 70% IMS for 5 seconds, 95% IMS for 5 seconds, absolute IMS for 5 seconds, cleared in xylene for 2 minutes and held in xylene for at least 2 minutes, remaining in the xylene until the sections were mounted with DPX and covered with coverslips. The slides were allowed to dry then examined under a microscope (Nikon Eclipse Ti, Kingston, UK) and imaged digitally (Nikon BR Elements, Kingston, UK).

2.10 Fluorescence labelling for analysis of residual DNA

Localisation analysis of residual DNA in the tissue was performed using the fluorescent stain 4',6-diamidino-2-phenylindole (DAPI) (Sigma-Aldrich, Poole, UK). The analysis was performed on OCT embedded tissue sections fixed to microscope slides. If the slide/sections had been frozen, they were brought to room temperature, and fixed with a fixative (acetone) then washed three times with Tris-buffered saline (TBS) with 0.025% Triton X-100 for 5 min. The sections were then stained with DAPI for 30 minutes at room temperature in the dark. The sections were briefly rinsed with TBS then mounted and cover-slipped using fluorescence mounting medium (Dako, Ely, UK). Imaging was performed on the Nikon Eclipse TE2000-U with NIS-Elements BR software (Nikon). ImageJ software (NIH) or NIS-Elements BR software was used to annotate the images.

2.11 IHC primary antibody optimisation for analysis of ECM components

Primary antibody optimisation was performed as described for the immunohistochemical (IHC) analysis below, with the following exceptions. The fixative was; ice cold acetone for 10 minutes at -20°C, ice cold methanol for 10 minutes at -20°C, cooled ethanol for 10 minutes at RT, or 4% paraformaldehyde for

10 minutes at RT to establish which provided optimal fixation and permeabilisation for each primary antibody. The primary antibody concentration was investigated at 1:50, 1:100, 1:200 and 1:500 dilutions to determine the lowest concentration with the optimal staining.

2.12 IHC for analysis of ECM components

Immunohistochemical (IHC) analysis was performed on the OCT embedded tissue sections when fixed to microscope slides. If the slide/sections had been frozen, they were brought to room temperature, and fixed with ice cold acetone for 10 minutes at -20°C then washed three times with Tris-buffered saline (TBS) with 0.025% Triton X-100 for 5 minutes. The sections were then blocked, to reduce non-specific staining, with 10% normal serum with 1% bovine serum albumin (BSA) in TBS for 2 hours. All blocking incubation steps were performed at RT on an orbital shaker. The sections were then incubated overnight at 4°C with a primary antibody reactive to pig tissue, either: mouse monoclonal anti-collagen II (ab3092, Abcam, Cambridge, UK); rabbit polyclonal anti-collagen II (ab300, Abcam, Cambridge, UK); sheep polyclonal anti-fibronectin (ab23516, Abcam, Cambridge, UK); or rabbit polyclonal anti-laminin (ab11575, Abcam, Cambridge, UK), all at 1:100 dilution in 1% BSA in TBS. The sections were then washed two times in TBS with 0.025% Triton X-100 for 5 minutes. The sections were then incubated for 1 hour at RT in the dark with the secondary antibodies conjugated with a specific Alexafluor, all at 1:200 dilution in 1% BSA in TBS. The secondary antibodies were either Alexa Fluor® 488 goat anti-mouse IgG (H+L) (A-11001, Invitrogen, Paisley, UK) for the anti-collagen II (ab3092) primary antibody, Alexa Fluor® 488 goat anti-rabbit IgG (H+L) (A-11008, Invitrogen, Paisley, UK) for the anti-laminin and anti-collagen II (ab300) primary antibody, or Alexa Fluor 555 donkey anti-sheep IgG (A-21436, Invitrogen, Paisley, UK), for the anti-fibronectin primary antibody. Following the secondary antibody incubation, the sections were washed two times with TBS for 5 minutes before counterstaining with DAPI for 30 minutes at room temperature in the dark. The sections were briefly rinsed with TBS then mounted and cover-slipped using fluorescence mounting medium (Dako, Ely, UK). For the negative controls, the primary antibody was omitted. IHC imaging was performed on the Nikon Eclipse TE2000-U with NIS-Elements BR software (Nikon). ImageJ software (NIH) or NIS-Elements BR software was used to annotate the images.

2.13 Quantitative analysis of DNA content

For the quantitative DNA analysis, approximately 25 mg of tissue, frozen at -80°C since harvest, was taken and minced using razor blades. The DNA was extracted from the tissue using the DNeasy Blood & Tissue Kit (Qiagen, Crawley, UK) according to the manufacturer's instructions. Briefly, the tissue was digested and the cells lysed overnight at 56°C whilst shaking in proteinase K solution. The DNA is then selectively bound to the DNeasy membrane of a spin column, washed and then eluted into a buffer. The quantity of DNA extracted from the tissue was assessed using the NanoDrop (ND1000; NanoDrop Products, Wilmington, USA). For each DNA quantitative test, the concentration of DNA was normalized to the tissue weight and the mean \pm SD was determined. Two-way ANOVA was used to find any statistically significant differences between native and decellularised trachea, as well as the corresponding control tissue.

2.14 Quantitative analysis of GAG content

For the quantitative total sulphated GAG (sGAG) analysis, approximately 50 mg of tissue, frozen at -80°C since harvest, was taken and minced using razor blades. The GAG was extracted from the tissue using the Blyscan sGAG Assay (Biocolor Ltd, Carrickfergus, UK), according to the manufacturer's instructions. Briefly, the tissue was digested and the cells lysed overnight at 65°C in papain solution (Sigma, Poole, UK). The lysate was then diluted appropriately, typically 1:100 in deionised water. The sGAG were then selectively bound and formed a complex with 1,9-dimethyl-methylene blue in the dye reagent, which precipitated out of the solution. Following centrifugation, the bound sGAG-dye complex pelleted and the supernatant was removed. The sGAG-dye complex was then dissociated and the absorbance read at 656nm using the Tecan Sunrise (Tecan) or the Tecan Safire2™ (Tecan) and compared to a 0 - 50 μ g/mL standard curve. For each GAG quantitative test, the concentration of GAG was normalized to the lysate dilution and the tissue weight and the mean \pm SD was determined. Two-way ANOVA was used to find any statistically significant differences between native and decellularised trachea, as well as the corresponding control tissue.

2.15 Quantitative analysis of total collagen content

For the quantitative total collagen analysis, approximately 25 mg of tissue, frozen at -80°C since harvest, was taken and minced using razor blades. The total collagen was extracted from the tissue using the Quickzyme Total Collagen Assay (2BScientific, Upper Heyford, UK), according to the manufacturer's instructions. The method was based on the detection of hydroxyproline which is present in mammalian collagen and elastin and was modified from a previously described method for quantifying hydroxyproline. Briefly, the tissue was completely hydrolysed overnight at 95°C in 6M hydrochloric acid (HCl) (Sigma, Poole, UK). The lysate was then diluted appropriately, typically 1:75 in 4M HCl. The hydroxyproline was oxidised to a modified form of hydroxyproline (likely to be pyrrole in the presence of toluene) and then reacted with a chemical (likely to be p-dimethylaminobenzaldehyde) to form a chromogen. The absorbance of the chromogen was read at 570nm using the Tecan Sunrise (Tecan) or the Tecan Safire2™ (Tecan) and compared to a 0 - 300 µg/mL standard curve. For each total collagen quantitative test, the concentration of total collagen was normalized to the tissue weight and the mean ± SD was determined. Two-way ANOVA was used to find any statistically significant differences between native and decellularized trachea, as well as the corresponding control tissue.

2.16 Tensile testing of tracheae tissue and scaffolds

Tensile testing was used to evaluate the uniaxial ultimate tensile strength (stress at failure), the Young's (tensile) modulus and tensile extension (strain at failure) of the tracheal cartilage rings, in the transverse plane for native, decellularised (DC) and corresponding PBS control (NDC) tracheas from various stages in the decellularisation process. The Instron 5565 (Instron, High Wycombe, UK) was used to mechanically interrogate and record, using Bluehill 2 software (Instron, High Wycombe, UK), in real time the tensile properties of each sample. For the cartilage ring tensile testing, a section of cartilage ring was punched out of the tracheal tissue using a 10 x 2 mm dumbbell shaped punch in a specimen cutting press (Model S1) (Wallace Instruments, Cambridge, UK). The thickness of the sample was measured using digital callipers and recorded. The sample was then clamped into the specimen grips. The uniaxial tension was increased at a constant rate of 100 mm min⁻¹ until rupture of the cartilage or ECM, which was confirmed through observation of tears

in the cartilage and assessment of the stress–strain curves. The three parameters were determined from the tensile stress–strain curves. All were plotted as the mean \pm SD for each analysis. Two-way ANOVA was used to compare decellularised scaffolds findings with native tracheae and corresponding control (NDC) findings over the decellularisation process.

2.17 Radial compression force testing of tracheae tissue and scaffolds

Radial compression force testing was used to evaluate the resistance to collapse of sections of tracheae as an indication of circumferential strength of the tracheae, the cartilage rings and ability of a bioengineered tracheae to maintain an open airway *in vivo* (Jones, Rueggeberg et al. 2014). For the testing, 3 cm sections were cut from the tracheal length for native, freeze-thawed (by various methods) tracheae, and decellularised (DC) tracheae. The Instron 5565 (Instron, High Wycombe, UK) was used to mechanically interrogate the compressive properties of each sample. As the compression software was not available with the current Bluehill 2 software, the lowering of the upper grip was manually controlled and the readings were manually recorded from the Bluehill 2 software package. Small flat plastic plates, with graspable handles, were placed into the upper and lower grips of the Instron 5565 (Instron, High Wycombe, UK). The 3 cm tracheal section was placed onto the lower grip and the upper plate manually lowered until just touching the top to the tracheal section. The extension and load reading on the Bluehill 2 software were reset. Using the fine adjust control on the Instron 5565 control pad, the upper grip was manually lowered at a steady rate until the lumen of the trachea was fully occluded. Load (N) readings were recorded every 0.5 mm of compression. The circumferential strength was determined by plotting the compression (mm) versus the load (N), calculating the straight line equation for the linear portion and the radial compressive load (N) at 50% occlusion. The results were plotted as the mean \pm SD for each analysis. Two-way ANOVA was used to compare native tracheae findings with decellularised scaffold findings at various stages of the decellularisation process.

3 Detergent-enzymatic method of decellularisation

3.1 Introduction

Since the high profile first tissue engineered tracheal transplant in 2008 (Macchiarini, Jungebluth et al. 2008), the method for preparing the decellularised human trachea construct remains unchanged. This clinical gold standard decellularisation method is an adaptation of a detergent-enzymatic method (DEM), which investigated the potential of decellularised porcine tracheal scaffolds repopulated with autologous cells for transplantation purposes (Conconi, De Coppi et al. 2005). The DEM had itself been derived from a method which described a detergent based method that solubilised the cell membranes and intracellular components of tissue but left the basement membranes intact. Thereby inferring that the ECM, with this treatment, could remain intact and indistinguishable by ultrastructure from native tissue (Meezan, Hjelle et al. 1975). Meezan had also recognised the issue of agglutination of the cell debris, primarily the nuclear material, around the tissue when treated with the detergent and therefore demonstrated that prior washes with distilled water and treatment with the enzyme DNase could lessen the extent of agglutination (Meezan, Hjelle et al. 1975).

Whereas Meezan had been treating isolated organ subfractions (Meezan, Hjelle et al. 1975), Conconi intended to decellularise a whole pig trachea and therefore altered Meezan's method by increasing the incubation times and changing the order of the DNase and detergent steps. The new method now comprised a distilled water wash step, followed by a detergent treatment step and lastly an enzymatic DNase treatment step (Conconi, De Coppi et al. 2005). Crucially Conconi also recognised that this single treatment would be insufficient for adequate decellularisation of a whole trachea and therefore multiple cycles of the treatment were performed, with each cycle taking 79 hours or 4 working days to complete. Through experimentation, Conconi determined that although 18 cycles (which would take 72 working days to complete) didn't completely decellularise the porcine trachea, it reduced the immunogenicity of the trachea sufficiently and that 22 cycles (which would take 88 working days to complete) completely decellularised the porcine trachea but resulted in loss of structural integrity of the trachea (Conconi, De Coppi et al. 2005). Conconi used the Herberhold method, which takes the alternative approach of chemically

conserving trachea tissue for transplant purposes, as the control method. The Herberhold method is a process that requires a minimum of 80 days to complete (Herberhold, Franz et al. 1980). Conconi successfully demonstrated clearance of cells, along with MHCs class I and II, from the epithelial layer and sub-mucosal gland regions, but conceded that after 18 cycles, chondrocytes were still visible in the cartilage ring region. Conconi established that if the number of cycles were increased from 18 to 22 then full decellularisation could be achieved but that structural integrity of the trachea was compromised. However, as the cartilage matrix is an immunologically privileged region of tissue, with limited infiltration of immune cells due to lack of vasculature, it was regarded as satisfactory to merely remove the immunogenic material from the non-cartilaginous regions of the trachea, rather than compromise structural integrity. Conconi also demonstrated that improved seeding of chondrocytes and tracheal epithelial cells could be achieved over the Herberhold method treated control tracheas (Conconi, De Coppi et al. 2005), which was deemed critical prior to *in vivo* transplantation.

In translating the DEM for clinical practice (Macchiarini, Jungebluth et al. 2008), it was determined that 18 cycles of the treatment was not sufficient to remove all traces of donor MHC in human trachea and it was necessary to increase the process to 25 treatment cycles (Macchiarini, Jungebluth et al. 2008), which would take 100 working days to complete. The impact of these additional cycles, if any, on the structural integrity of the human tracheal scaffold was not discussed in the paper.

Following publication of the clinically tested DEM (Macchiarini, Jungebluth et al. 2008), follow-up work investigating the structural and morphological effects of the DEM on pig tracheae (Jungebluth, Go et al. 2009) and the requirement for seeding of the recipient's cells on DEM tracheal scaffolds *in vivo* (Go, Jungebluth et al. 2010) were published. Both of these papers contained a revised DEM of 17 treatment cycles where the distilled water step had been reduced from 72 hours to 48 hours (Jungebluth, Go et al. 2009, Go, Jungebluth et al. 2010), with the authors reporting the revised DEM would take 35 ± 1 days to complete for pig tracheae scaffolds (Jungebluth, Go et al. 2009). These latter papers confirmed the cell clearance from all regions of the trachea, except the cartilage rings, (Jungebluth, Go et al. 2009) and removal of MHCs class I and II (Jungebluth, Go et al. 2009, Go, Jungebluth et al. 2010) described by Conconi (Conconi, De Coppi et al. 2005). They further described

the mechanical characteristics of whole tracheae by testing for longitudinal uniaxial tensile strain (Jungebluth, Go et al. 2009), quantifying Conconi's observed loss in biomechanical strength beyond 17 cycles of DEM decellularisation (Conconi, De Coppi et al. 2005). Jungebluth also described heterotopic allogeneic and xenogeneic transplantation, observing that DEM decellularisation greatly reduced the inflammatory response from the host and prevented rejection of the implanted tissue (Jungebluth, Go et al. 2009). Go further described successful seeding of the DEM scaffolds with cells and detailed how orthotopic allogeneic transplantation and maintenance of the longitudinal mechanical strength is only possible if both MSC-derived chondrocytes and epithelial cells are seeded onto the scaffolds to prevent stenosis of the scaffold or bacterial/fungal contamination of the graft (Go, Jungebluth et al. 2010).

When clinically translated to focus on optimisation of the decellularisation of human trachea (Baiguera, Jungebluth et al. 2010), the water washes were reduced to brief rinse steps before and during the detergent-enzyme cycles. The protocol suggested that between each detergent-enzymatic cycle there was an overnight PBS hold/wash step. This change was implemented so that 25 cycles of DEM would typically take 30 days, which would be expected if the lengthy water washes were replaced with overnight static PBS hold/wash steps. Furthermore, the authors stated it could be shortened to a 17 day process without altering the ultimate number of cycles of the DEM. This suggests the authors completed up to two cycles in one day, which would suggest the PBS wash between these two cycles would be considerably shorter or skipped altogether, with an 8 hour PBS wash step every other cycle if skipped, or 4 hour PBS wash steps between each cycle. The latter would entail laboratory staff working shifts to staff the laboratory 24 hours a day. Baiguera demonstrated that the DEM decellularisation protocol could be translated from porcine to human trachea, substantiating the Macchiarini paper (Macchiarini, Jungebluth et al. 2008), to obtain a similar reduction in cell and DNA clearance whilst maintaining longitudinal tensile strength. Evidence of the DEM scaffolds' angiogenesis potential from retained pro-angiogenic molecules, such as bFGF, that were retained on the decellularised scaffolds was also demonstrated (Baiguera, Jungebluth et al. 2010).

By 2012, nine paediatric and adult patients had received tracheae that had been decellularised by the DEM method and recellularised with the patient's own cells

either in a bioreactor or intraoperatively on a compassionate basis ((Badylak, Weiss et al. 2012)). However, although no graft-related mortality had occurred 12 - 42 months post-implantation, partial collapse had been observed in three of the patients. The reasons for the collapse of these grafts were unknown and were considered unpredictable. These collapses suggest that the current DEM-based tissue engineering process could be compromising the structural properties of the scaffolds or provoking a phenotypic predominance of M1 macrophages which could hinder tissue remodelling (Keane, Londono et al. 2012). As a result the authors indicated that improvements would be necessary to the decellularisation process and the biomechanical stabilisation as well as the recellularisation and implantation processes (Badylak, Weiss et al. 2012) before the processes could be employed to manufacture tissue engineered tracheae for routine clinical use.

3.2 Aims and hypotheses

3.2.1 Aims

- To evaluate the methodology of the detergent-enzymatic method (DEM) of decellularisation.
- To evaluate and expand product validation and potential critical quality attributes for decellularised tracheal scaffolds.
- To determine what effect the decellularisation process has on key structural components needed for: the recellularisation process, such as the basement membrane components laminin and fibronectin; and maintaining cartilage and scaffold strength to resist collapse, such as collagen and GAGs.

3.2.2 Hypotheses

- As cells interact with their extracellular matrix, it is hypothesised that removal of cells during DEM will negatively impact on ECM components crucial to tracheal function resulting in reduced biomechanical properties.

3.3 Materials and methods

3.3.1 Sectioning of LR White embedded matrices for histology

Taking into account the desired orientation of the final tissue sections (sagittal or transverse), the resin embedded tissues were excised from the resin. The embedded tissue blocks were placed in a microtome (Ultracut E, Reichert-Jung, Depew, USA) sample holder and excess resin was trimmed from the face of the block with a sharp razor blade until the tissue was exposed. Glass knives were made (2178 Knifemaker II, LKB, Bromma, Sweden) and used to obtain a smooth flat surface of the embedded samples for sectioning. A new glass knife was used to obtain 2 μM sections of the samples. Cut sections were carefully placed onto a drop of distilled water on a microscope slide. The sections were semi-fixed to the slide by placing the slide onto a heating block (Dishwarmer 2, Photax, USA) for 24 hours. The slides were then stored in a slide container at RT until required (Partington, Mordan et al. 2013).

3.3.2 Histological analysis of LR White embedded matrices by toluidine blue staining

Toluidine blue, otherwise known as toloum chloride, is an acidophilic metachromatic. Filtered toluidine blue was gently dropped onto the section and then immediately but gently washed off with distilled water. The sections were observed under an optical microscope (BX50, Olympus, UK) and imaged (Coolsnap-Pro *cf* color, Media Cybernetics, Bethesda, USA).

3.3.3 Histological analysis of LR White embedded matrices by haematoxylin and eosin (H&E) staining

The slides were immersed in Mayer's haematoxylin for 1 hour at room temperature. The sections were then blued by being immersed in gently running tap-warm water for 20 minutes. The slides were then immersed in 5% eosin for 1 hour at room temperature. The sections were then rinsed very gently in static tap water. The sections were dried on the heating block for a few minutes then mounted in DPX Mountant (BDH Chemicals Ltd., Poole, UK). The sections were then observed under an optical microscope (BX50, Olympus, UK) and imaged (Coolsnap-Pro *cf* color,

Media Cybernetics, Bethesda, USA). Five representative sections for each treatment stage were stained (Partington, Mordan et al. 2013).

3.3.4 Quantitative analysis of protein content

The quantitative protein assay used was the microplate procedure for the Pierce BCA Protein Assay Kit which utilises bicinchoninic acid (BCA) to detect the total amount of protein in a sample. The principle of the assay was based upon the ability of protein, in an alkaline solution, to reduce copper (II) ions or cupric ions (Cu^{2+}) to copper (I) ion or cuprous ion (Cu^+). The Cu^+ ions form a purple coloured complex with BCA which could be quantitated with a spectrophotometer. Briefly, dilutions for a standard curve of BSA were prepared. The working reagent was prepared by combining Reagent A, containing the BCA, and Reagent B, containing cupric sulphate. The test samples were prepared using the tissue lysis component of the Qiagen DNeasy Blood and Tissue Kit. The working reagent was added to the BSA standards and the test samples in a 96 well plate, and then incubated at 37°C for 30 minutes. The plate was then cooled to room temperature and the absorbance measured at 562 nm using the Tecan Safire2™ (Tecan) and compared to a 20 - 2000 $\mu\text{g}/\text{mL}$ standard curve. For each total protein quantitative test, the concentration of protein was normalized to the tissue weight and the mean \pm SD was determined. Two-way ANOVA was used to find any statistically significant differences between native and decellularised trachea, as well as the corresponding non-decellularised control (NDC) (PBS treated) tissue (Partington, Mordan et al. 2013).

3.3.5 Quantitative analysis of soluble collagen content

The quantitative assay used to determine soluble collagen was the Biocolor Sircol™ Soluble Collagen Assay Kit, (Biocolor Ltd, Carrickfergus, UK) which was used according to the manufacturer's instructions. The kit can be used to analyse cold acid and pepsin soluble collagen Types I to V that are produced in soft tissues and cartilages of the body, but is not suitable for covalently cross-linked collagen. The assay is a colorimetric assay which utilises the binding of Sirius Red in picric acid to the (Gly-X-Y) tri-peptide of the triple helix structure of collagen. Briefly, approximately 50 mg of tissue, frozen at -80°C since harvest, was taken and minced using razor blades. The tissue was digested overnight at 4°C in pepsin (0.1 mg/ mL) (Sigma, Poole, UK) in 0.5M acetic acid (Sigma, Poole, UK). The acid solution was

then neutralised. The sample was centrifuged to pellet any non-digested tissue and from the supernatant fraction the collagen was isolated and concentrated. The sample was then diluted appropriately; typically 1:20 in 0.5M acetic acid. The soluble collagen was then selectively bound and formed a complex with the Sirius Red in the dye reagent, which precipitated out of the solution. Following centrifugation, the bound soluble collagen-dye complex pelleted and the supernatant was removed. The soluble collagen-dye complex was then dissociated in an alkaline solution and the absorbance read at 555 nm using the Tecan Sunrise (Tecan) or the Tecan Safire2™ (Tecan) and compared to a 0 - 50 µg/mL standard curve. For each soluble collagen quantitative test, the concentration of soluble collagen was normalized to the lysate dilution, the tissue weight and the mean \pm SD were determined. Two-way ANOVA was used to find any statistically significant differences between native and decellularised trachea, as well as the corresponding non-decellularised control (NDC) (PBS treated) tissue (Partington, Mordan et al. 2013).

3.3.6 Dynamic mechanical analysis (DMA) compression testing of tracheae tissue

Dynamic Mechanical Analysis (DMA) compression testing was used to evaluate the compressive properties of the cartilage rings in the tracheal wall. The PerkinElmer DMA 7E (PerkinElmer, Seer Green, UK) was used to mechanically interrogate and record, using the DMA 7E software (PerkinElmer, Seer Green, UK), in real time the tensile properties of each sample. For the tracheal wall testing, 5 mm x 5 mm (W x L) sections were punched out of a section of trachea tissue using a specimen cutting press (Model S1) (Wallace Instruments, Cambridge, UK). The adventitia and lamina propria were removed and the height of the tracheal wall section then measured before compression testing using callipers. The specimen was placed into position in the instrument and the measurements inputted into the software. The force was applied at 200 mN/minute up to 6000 mN and the results recorded in real time by the software. The Young's (compressive) modulus (MPa) was determined for each analysis. All were plotted as the mean \pm SD for each analysis. Two-way ANOVA was used to compare the decellularised (DC) scaffold findings with native and the corresponding non-decellularised control (NDC) (PBS treated) trachea findings over the decellularisation process (Partington, Mordan et al. 2013).

3.4 Results

3.4.1 Macroscopic overview of the trachea pre and post detergent-enzymatic method of decellularisation

When the tracheae were delivered from Animal Organs for Research (a subsidiary of Cheale Meats) they had been roughly trimmed from the pluck, but still had the larynx and bronchi attached in addition to surplus tissue which could include the tongue, oesophagus, aorta and lung (Figure 3.1 A). The tracheae were further trimmed to produce tracheae that were 10 to 15 cm in length (Figure 3.1 B), but on average were approximately 12 cm in length with an average inner diameter (ID) of 1.35 cm antero-posteriorly and 1.65 cm laterally and an average external diameter of 2.23 cm antero-posteriorly and 2.43 cm laterally (Table 3.1). The PBS washes removed the majority of the surface blood before proceeding to the DEM (Figure 3.1 C). After 25 cycles of the DEM, the tracheae sections appeared decoloured, as expected of decellularised tissue. Importantly, the DEM-treated tracheae: retained the macroscopic structure of the trachea; the cartilage rings were still visible and detectable by touch; the mucosa layer in the lumen was still present with the ribbed internal surface of the posterior wall still visible; and the lumen of the trachea was retained and held open by the cartilage rings and resisted collapse under light pressure (Figure 3.1 D) (Partington, Mordan et al. 2013).

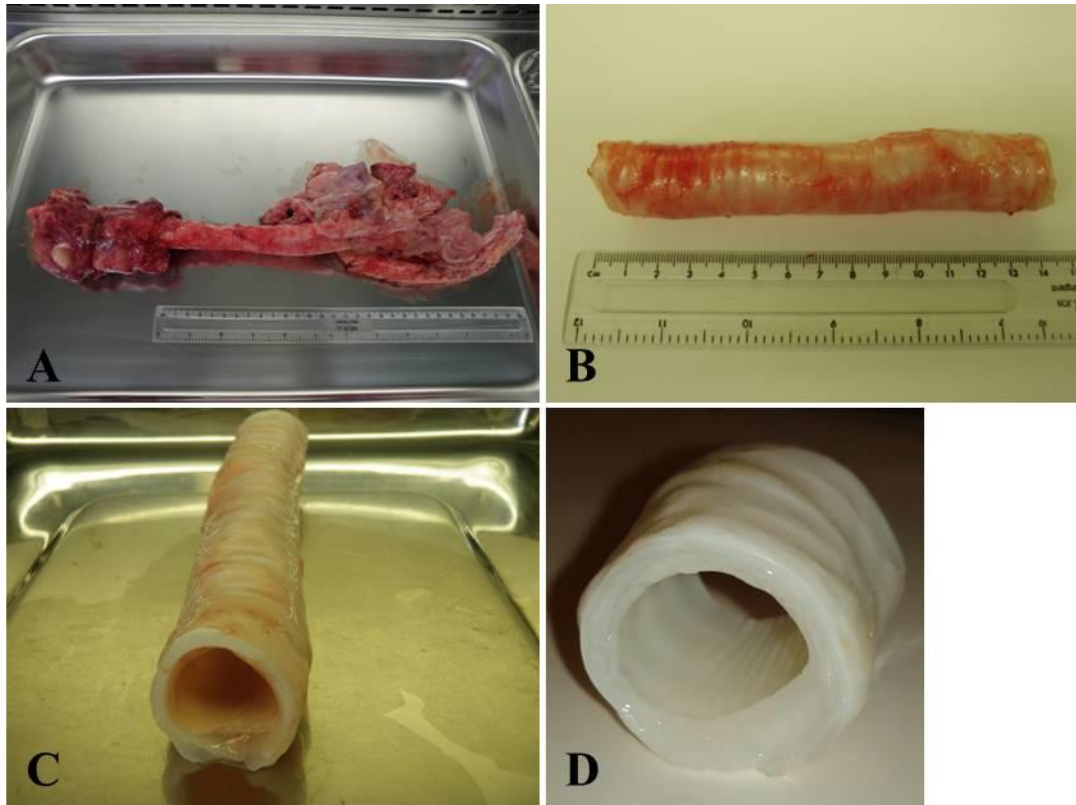


Figure 3.1: Macroscopic view of the trachea upon arrival from the abattoir (A), after preparation (B), after PBS rinses (C) and after cycle 25 of chemical enzymatic decellularisation (D) (Partington, Mordan et al. 2013). Permission to reproduce this figure has been granted by Elsevier.

Porcine Trachea	Length (cm)	Antero-posteriorly		Laterally	
		Internal Diameter (cm)	External Diameter (cm)	Internal Diameter (cm)	External Diameter (cm)
1	12	1.1	2.2	1.5	2.3
2	12.2	1.5	2.3	1.9	2.5
3	12	1.5	2.2	1.7	2.5
4	12.5	1.3	2.2	1.5	2.4
Average Pig	12.18	1.35	2.23	1.65	2.43

Average Human	11.5		1.8		2.3
----------------------	-------------	--	------------	--	------------

Table 3.1: Table of average pig tracheae sizes, with comparison for human tracheae (Iivanov 2007).

3.4.2 Histological analysis of DEM of decellularisation by toluidine blue staining

Native, defined as untreated tracheae harvested from healthy animals, and DEM decellularised tracheal sections were stained with toluidine blue to differentiate the different components of the tissue and determine whether the cells had been eliminated from the trachea during the decellularisation process to produce the tracheal scaffolds. In the native trachea sections, although the cartilage was distinguishable as purple due to the effects of weak metachromasy (Figure 3.2 C & E), the remainder of the tracheal tissue was orthochromatic and was only stained blue. Subtle differences in the intensity of the blue staining made the nuclei, and therefore cells, distinguishable in the epithelial layer (Figure 3.2 A) and the mucosa glands (Figure 3.2 B), but it was difficult to distinguish the nuclei which could lead to errors when cell counting to determine clearance. It was even more difficult to distinguish the nuclei in the lamina propria or adventitia (Figure 3.2 D & E) with the surrounding collagen and elastin bundles. Therefore, although the DEM processed trachea had been stained with toluidine blue (Figure 3.2 F), it was decided that due to the unsuitability of the stain for tracheal tissue, toluidine blue would not be an appropriate stain for this purpose and the stained sections were not used for cell clearance analysis.

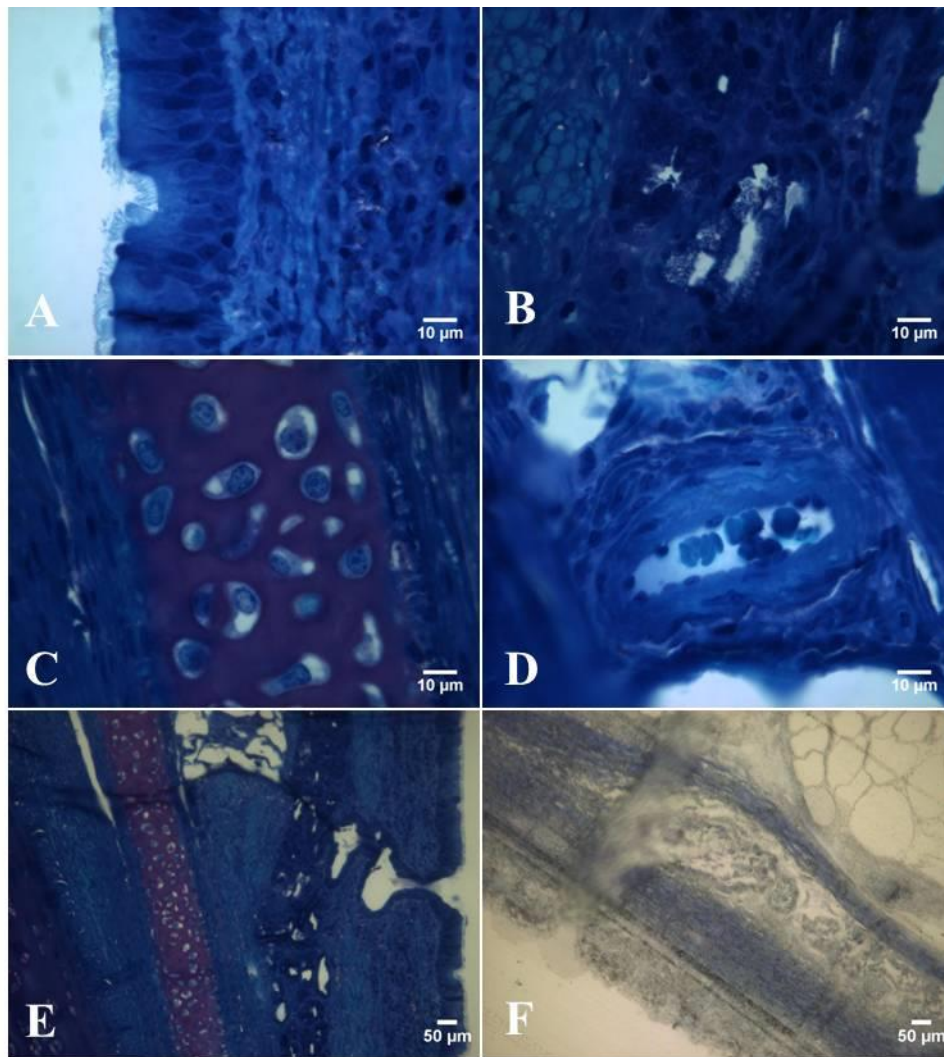


Figure 3.2: Toluidine staining of the epithelial layer (A), mucosal glands (B), cartilage (C), and adventitia (D) of native trachea and the lamina propria of native trachea (E) and of trachea that has undergone 25 cycle of the DEM of decellularisation (F).

3.4.3 Histological analysis of DEM of decellularisation by H&E staining

Native and DEM decellularised tracheal sections were stained with H&E to determine whether this stain improved clarity, over and above toluidine blue, for distinguishing cells in these sections and would therefore allow for easier determination of cell clearance throughout the DEM of decellularisation process. As expected, the stained native tracheal sections (Figure 3.3 A, Figure 3.4 A0, Figure 3.4 B0, Figure 3.4 C0 and Figure 3.4 D0) demonstrated typical H&E staining. The nuclei were stained blue by the haematoxylin, with the remainder of the tissue components stained a range of pinks and reds by eosin. For example, elastin bundles

and red blood cells were stained red, collagen and cell cytoplasm were stained shades of pink. This ultimately resulted in tissue sections where it was easy to identify nuclei and therefore cells within the tissue. This method allowed unambiguous observation of any clearance of the cells throughout the decellularisation process (Partington, Mordan et al. 2013). Therefore H&E was used as the stain to analyse cell clearance by decellularisation and also assess tissue morphology throughout the decellularisation process. The results show the staining of native tracheae and decellularised scaffolds at cycle 10 (Figure 3.4 A-D,1), 20 (Figure 3.4 A-D,2) and 25 (Figure 3.3 B; Figure 3.4 A-D,3). The analysis for cell clearance was focussed on the four major sub-regions of the trachea: the epithelial region of the lamina propria; the sub-mucosal gland of the lamina propria; the cartilage ring; and the adventitia. By focussing on the cell clearance in these particular regions, it was hoped that an overall representative view of the cell clearance across the trachea would be achieved. Total clearance of the cells was achieved by cycle 10 of the DEM for the epithelial layer, sub-mucosa gland and adventitia of the trachea (Figure 3.4 A,1, B,1, and D,1; Figure 3.5). Total cell clearance was not achieved in the cartilage ring, but significant cell clearance was observed by cycle 10 ($p < 0.05$) (Figure 3.4 C,1; Figure 3.6) which was further cleared by cycle 25 ($p < 0.01$) (Figure 3.4 C,3; Figure 3.6). Apoptosis of the chondrocytes, which could be determined by the morphology of the chondrocyte according to published criteria (Roach, Aigner et al. 2004), was detected from cycle 10 onwards ($p < 0.05$) and represented over 90% of all residual cells detectable in the cartilage rings from cycle 20 onwards (Figure 3.4 C,2 and C,3; Figure 3.6).

With regard to the microscopic morphological analysis of the trachea as it progressed through the DEM of decellularisation, the overall ECM structure was preserved (Figure 3.3 A and B) after 25 cycles of the DEM, with the ECM of the lamina propria, the sub-mucosa glands, the cartilage rings and the adventitia remaining identifiable. At 100x magnification it was possible to observe that the majority of the pseudostratified columnar epithelium was removed. It was also possible to observe potential damage to the elastin fibres, stained red, as they appeared to become disrupted as the DEM progressed (Figure 3.4 A,3). The sub-mucosal glands generally appeared undamaged throughout the DEM (Figure 3.4 B,1 and B,3) but occasionally appeared to lose their internal structure (Figure 3.4 B,2). The cartilage

rings appeared undamaged (Figure 3.4 C,3) and the adventitia retained enough structure to observe decellularised blood vessels (Figure 3.4 D,1) during the initial part of the DEM, but became slightly more disrupted as the DEM progressed (Figure 3.4 D,2 and D,3) (Partington, Mordan et al. 2013).

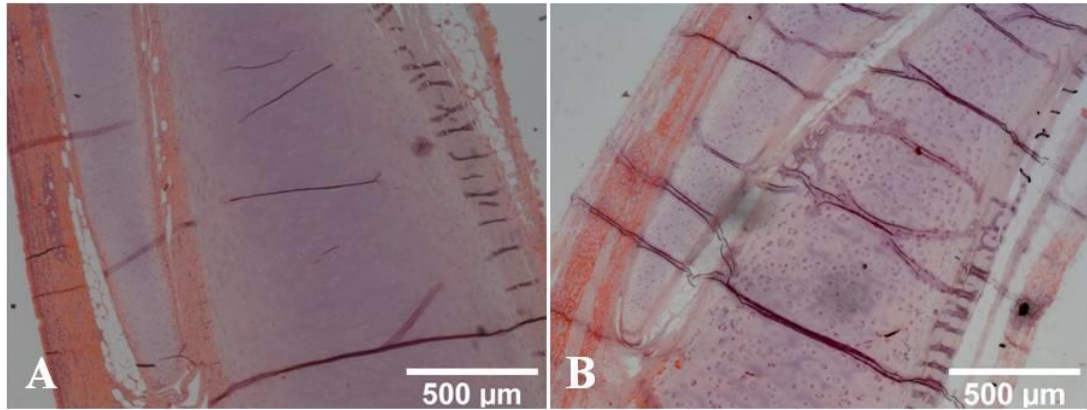
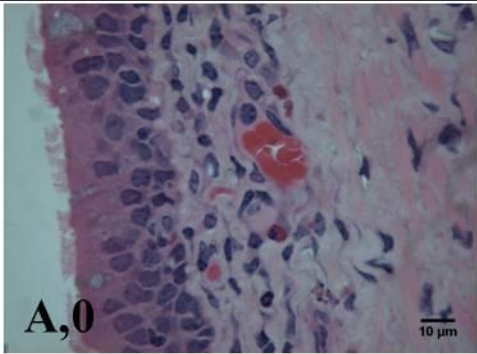
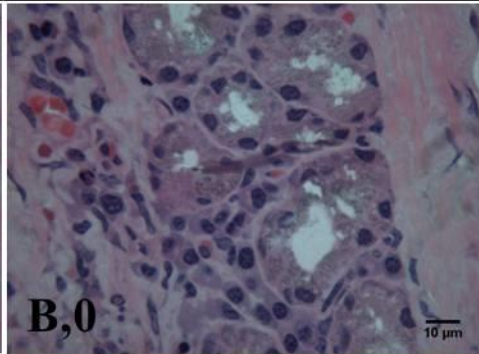
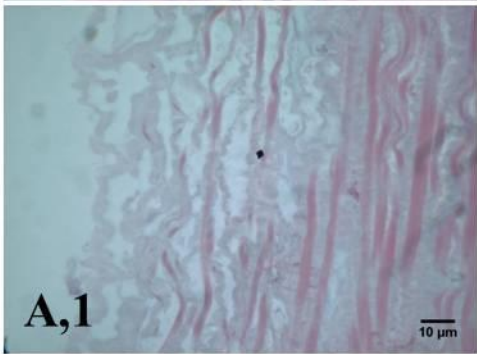
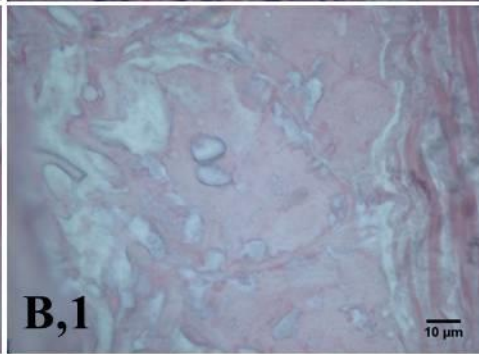
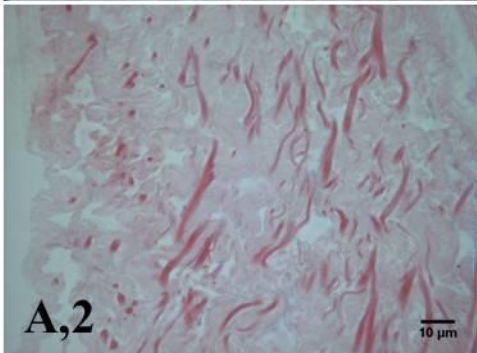
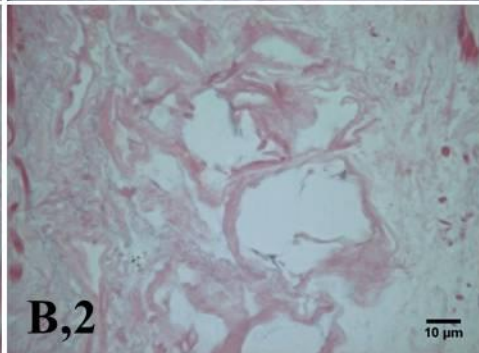
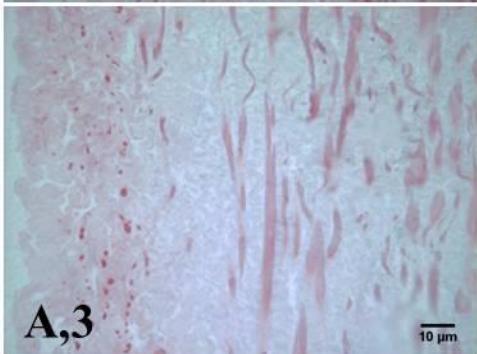
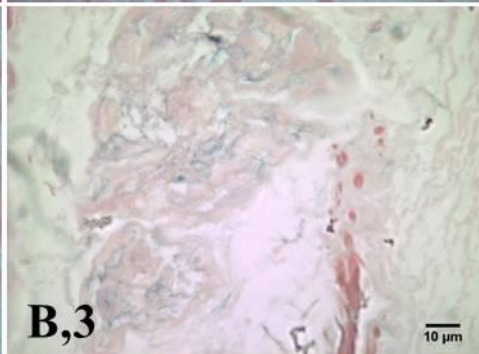


Figure 3.3: Histological staining by H&E of the trachea as native tissue (A) and after cycle 25 (B). Scale bar = 500 mm (Partington, Mordan et al. 2013).

	Epithelial Layer	Mucosal Gland
Native tissue	 A,0	 B,0
DEM scaffold: cycle 10	 A,1	 B,1
DEM scaffold: cycle 20	 A,2	 B,2
DEM scaffold: cycle 25	 A,3	 B,3

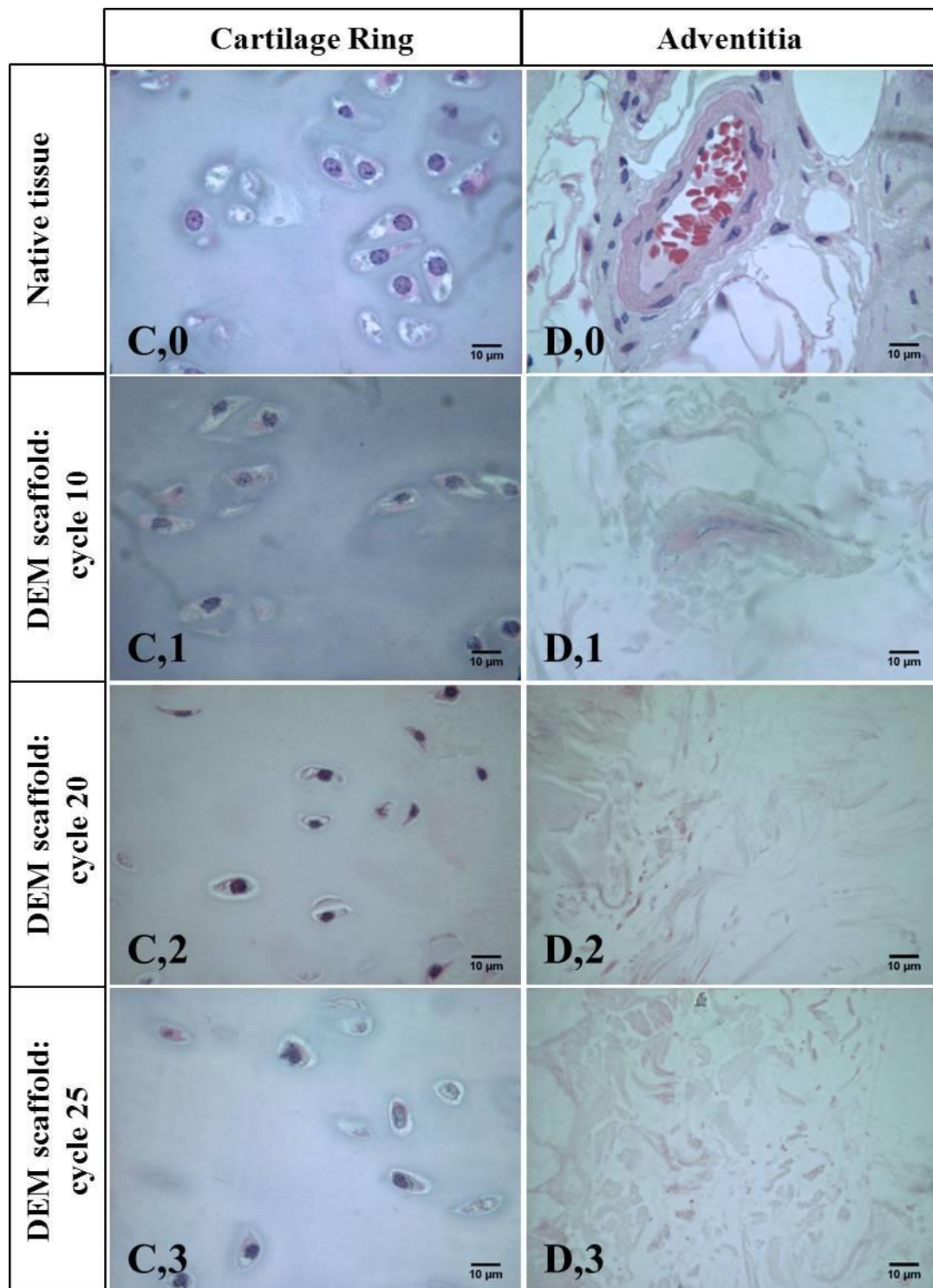


Figure 3.4: Histological staining by H&E of the tracheal epithelial layer (A), mucosal gland (B) cartilage ring (C) and adventitia (D) as native tissue (0), after cycle 10 (1), after cycle 20 (2) and after cycle 25 (3). Scale bar = 10 mm (Partington, Mordan et al. 2013). Permission to reproduce this figure has been granted by Elsevier.

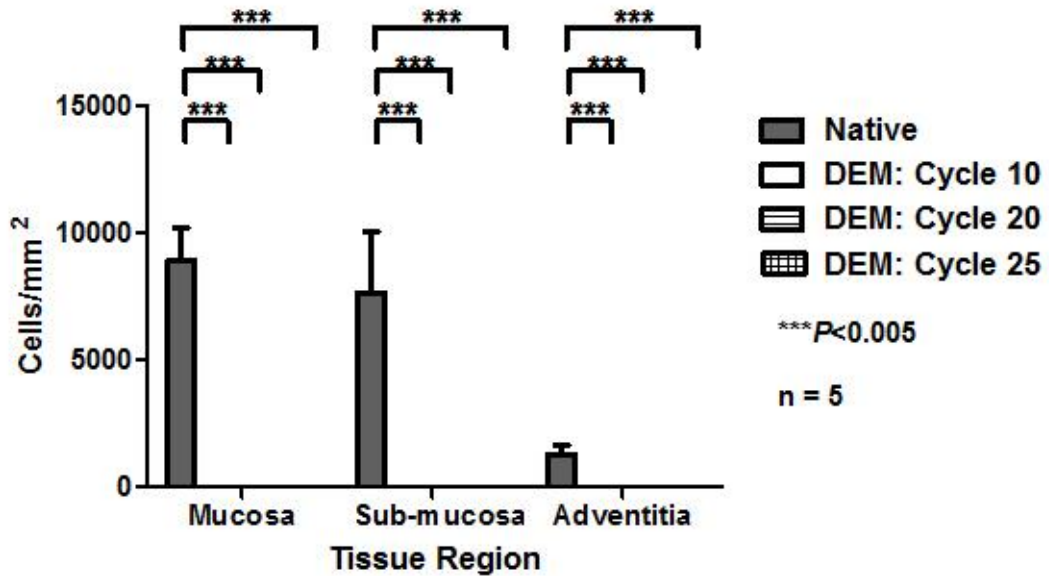


Figure 3.5: Cell clearance (by histological analysis of H&E) of the mucosa, sub-mucosa and adventitia sub-regions of the trachea as native tissue, after cycle 10, after cycle 20 and after cycle 25 (Partington, Mordan et al. 2013). Permission to reproduce this figure has been granted by Elsevier.

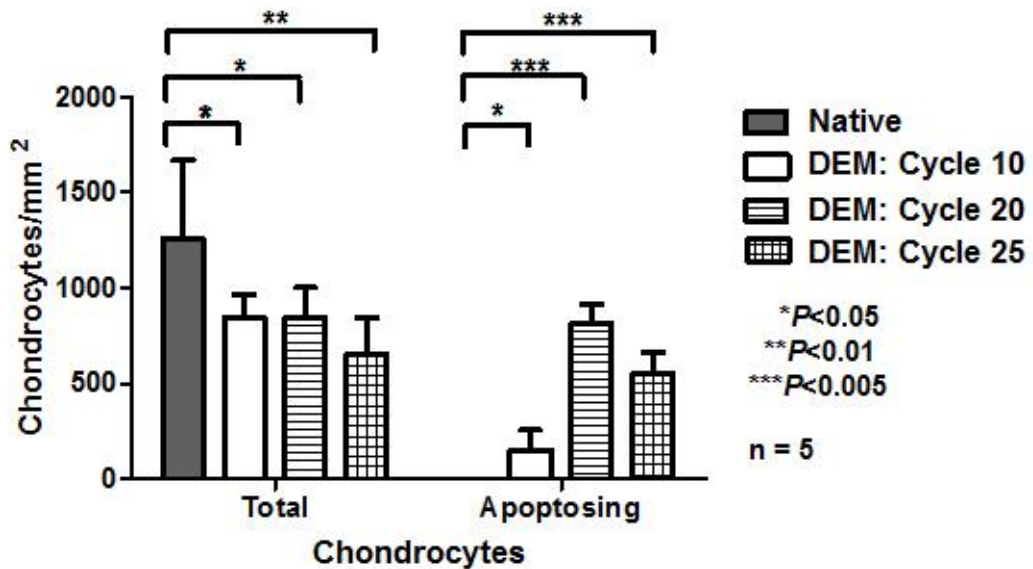


Figure 3.6: Chondrocyte clearance and apoptosis from the cartilage ring of the trachea as native tissue, after cycle 10, after cycle 20 and after cycle 25 (Partington, Mordan et al. 2013). Permission to reproduce this figure has been granted by Elsevier.

3.4.4 Analysis of DNA removal by detergent-enzymatic method of decellularisation

A statistically significant reduction in the concentration of DNA was observed throughout the DEM of decellularisation compared to native trachea. Following 10 cycles an increased amount of DNA had been removed due to the decellularisation process compared to the non-decellularised controls (DC: 274.96 ± 55.04 ng/mg, $P < 0.005$; NDC: 393.07 ± 118.04 ng/mg, $P < 0.01$) versus the native trachea (742.2 ± 236.6 ng/mg) (Figure 3.7). However, after 25 cycles of the DEM of decellularisation, the decellularised scaffold (264.66 ± 69.92 ng/mg, $P < 0.005$) and non-decellularised control (284.05 ± 37.74 ng/mg, $P < 0.005$) had achieved a similar reduction in DNA compared to the native tissue despite no DNase treatment in the non-decellularised control group (Figure 3.7) (Partington, Mordan et al. 2013).

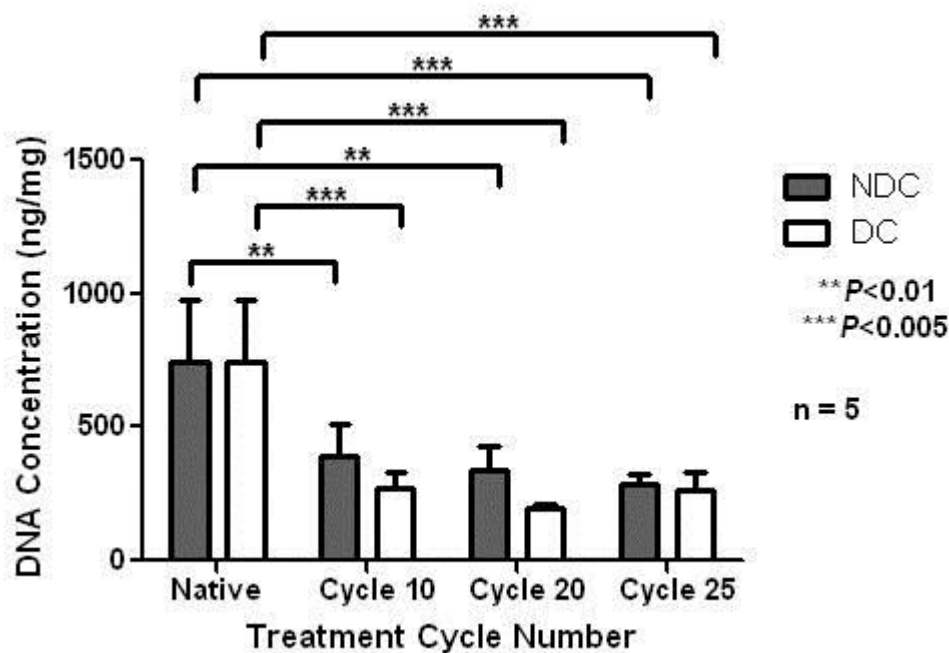


Figure 3.7: DNA quantification in tracheal tissue during decellularisation demonstrated a similar reduction in the decellularised ($P < 0.005$) and non-decellularised groups ($P < 0.005$) compared to the native trachea despite no DNase treatment in the non-decellularised group (Partington, Mordan et al. 2013). Permission to reproduce this figure has been granted by Elsevier.

DAPI staining revealed the locality of the remaining DNA in the decellularised group was predominantly in the lamina propria and the cartilage rings (Figure 3.8 A-D). It was clearly visible in the cartilage rings after 25 cycles of the DEM (Figure 3.8 D), as expected from the H&E staining. It was also possible to visualise DNA smeared over the ECM fibres in the lamina propria and particularly in the sub-mucosa gland regions after 25 cycles of DEM whereas in the native tissue the nuclear material is identifiably contained within the nuclei of the cells (Figure 3.8 A).

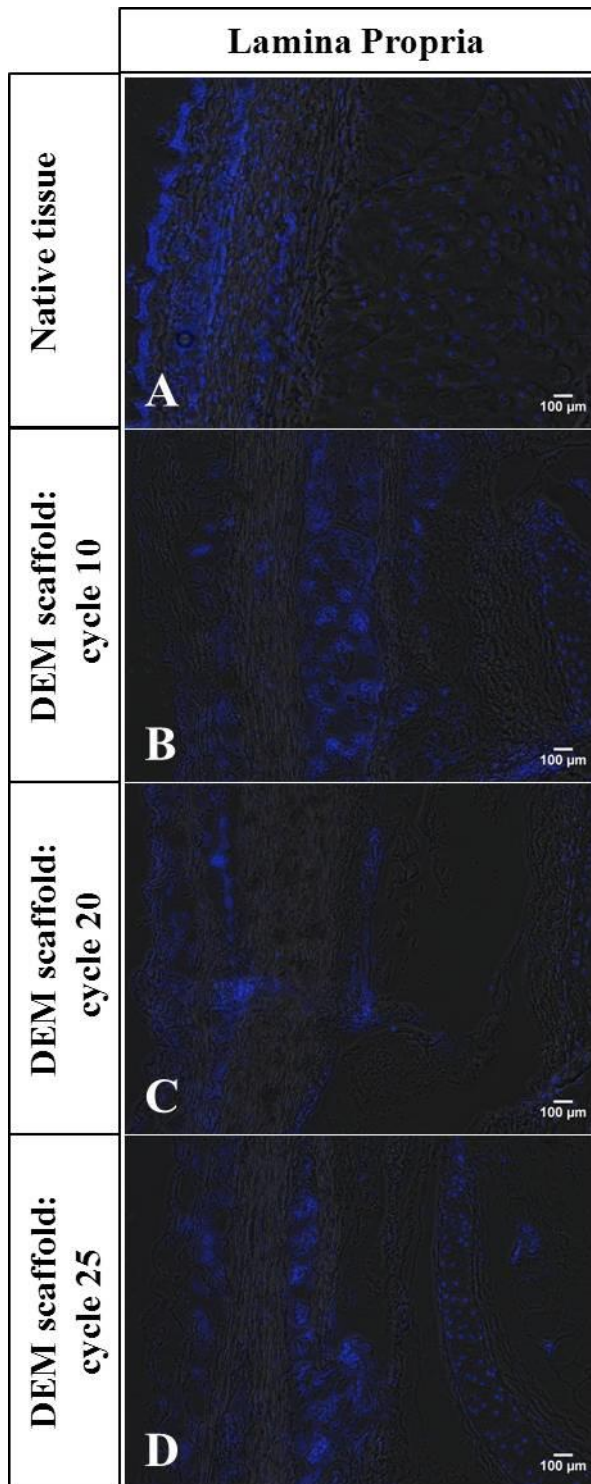


Figure 3.8: Fluorescent labeling of nuclear material with DAPI in the native trachea (A) and in scaffolds produced by DEM after cycle 10 (B), cycle 20 (C) and cycle 25 (D). Scale bar = 100 μm .

3.4.5 Analysis of protein concentration throughout and following the detergent-enzymatic method of decellularisation

Analysis of the protein concentration revealed that there was no significant change in the total protein concentration in the DEM scaffolds compared to the native trachea (Figure 3.9). The non-decellularised controls also retained similar total protein to the native trachea (Figure 3.9) (Partington, Mordan et al. 2013).

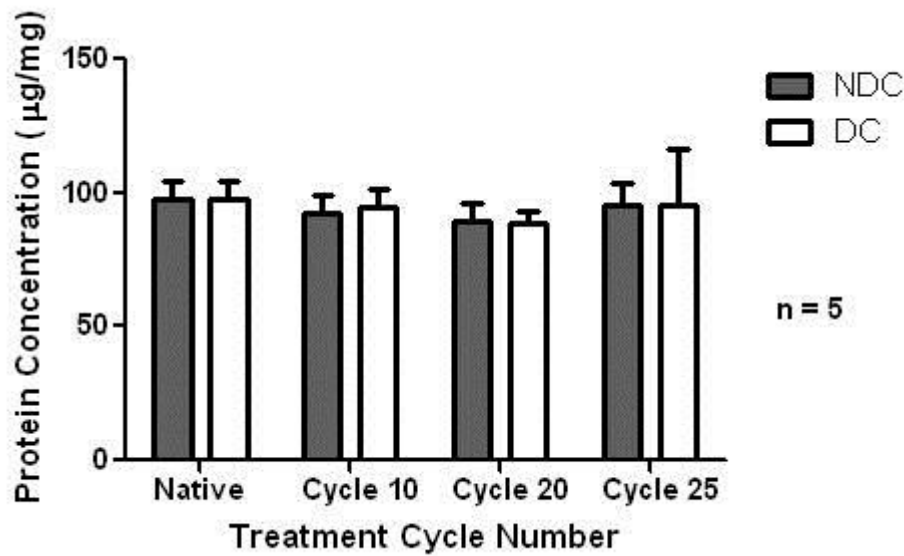


Figure 3.9: Protein quantification demonstrated no change in the decellularised (DC) and non-decellularised (NDC) groups, at any time point, compared to the native trachea (Partington, Mordan et al. 2013). Permission to reproduce this figure has been granted by Elsevier.

3.4.6 Analysis of key ECM proteins (laminin and fibronectin) throughout and following the detergent-enzymatic method of decellularisation

Although the overall total protein appeared not to be affected by the DEM, the effect of the DEM was investigated specifically on two key ECM proteins, laminin and fibronectin, due to their importance for recellularisation using immunofluorescence labelling. In the native trachea (Figure 3.10 A, B, and B'), laminin is shown with staining of the basement membrane, sub-mucosal glands and connective tissue in the lamina propria region. Laminin was clearly present in the same tissue sub-structures after 25 cycles of the DEM (Figure 3.10 C and C'). Labelling of the fibronectin protein in the native tissue demonstrated its presence throughout the trachea: in the basement membrane, sub-mucosal glands and connective tissue of the lamina propria

as well as the cartilage rings, the adventitia and the intra-cartilage rings connective tissue (Figure 3.10 D, E and E'). It was possible to observe similar levels of fluorescence labelling in the scaffolds that had undergone 25 cycles of the DEM (Partington, Mordan et al. 2013).

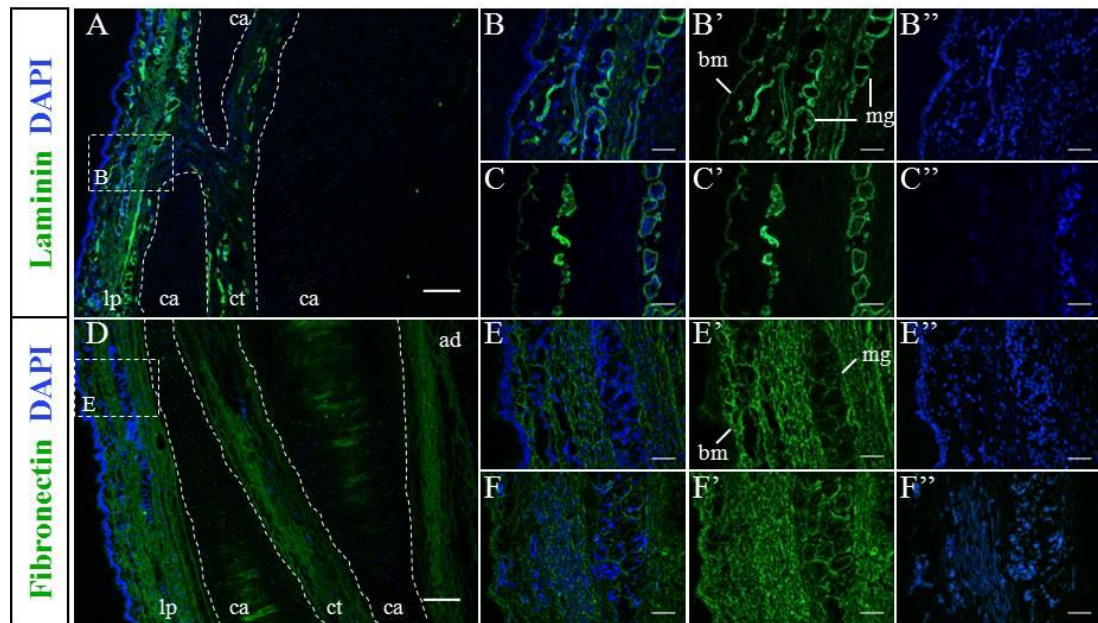
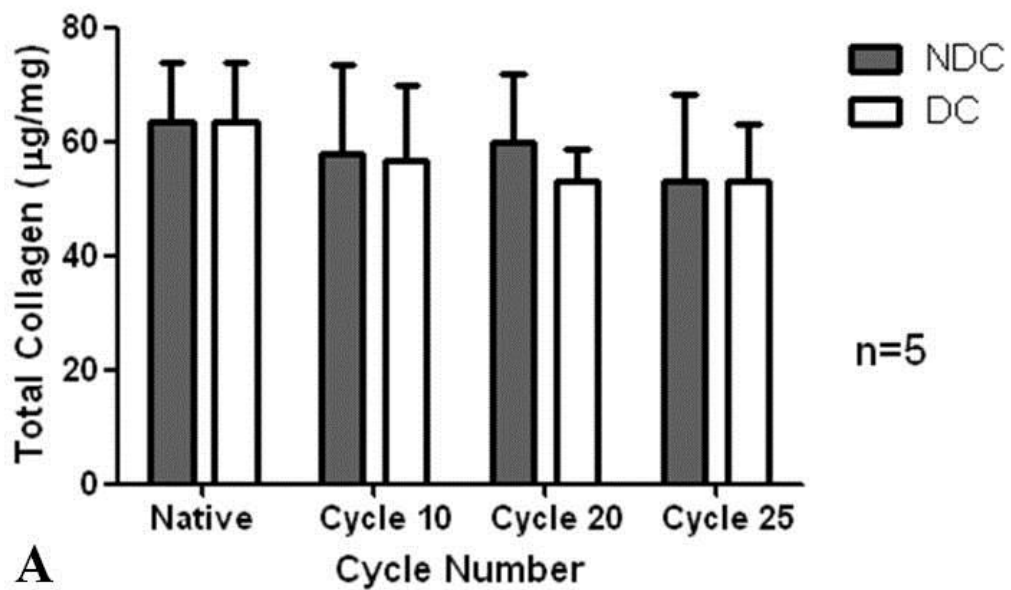


Figure 3.10: Immunofluorescence labelling of the two key ECM components laminin and fibronectin demonstrated they were conserved after the DEM decellularisation process. Laminin staining (A-C) in the native tracheae (A, B, B') demonstrated the staining to be localised to the lamina propria (lp), with the mucosal glands (mg) and basement membrane (bm) clearly stained, and connective tissue (ct). No laminin staining was observed in the cartilage (ca). In the DEM scaffold, the same structures were positively stained (C, C'). Fibronectin staining (D - F) in the native tracheae (D, E, E') and the DEM scaffold (F, F') demonstrated similar expression patterns and was present in the lamina propria (lp), connective tissue (ct), adventitia (ad) as well as at a low level in the cartilage (ca). Co-staining with DAPI indicated that genetic material remained post DEM decellularisation, mainly observed in mucosal glands (C'') or bound to matrix fibrils in the lamina propria (F''). Scale bar: (A and D) = 200 μ m; (B, C, E, F) = 50 μ m (Partington, Mordan et al. 2013). Permission to reproduce this figure has been granted by Elsevier.

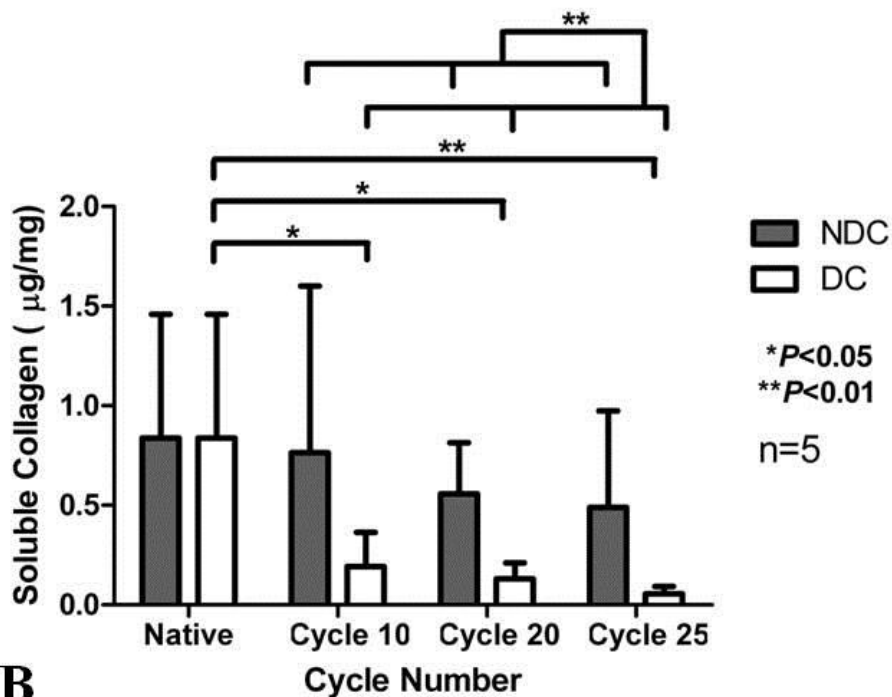
3.4.7 Analysis of collagen throughout and following the detergent-enzymatic method of decellularisation

Quantification of the total collagen indicated that there was no significant decrease in the total collagen content in the time-matched PBS stored tissue or the scaffolds that had undergone DEM decellularisation compared to the native tissue (Figure 3.11 A). There was, however, a comparable downward trend of collagen loss in both the time-matched PBS stored tissue and the DEM decellularised scaffolds at increasing time points compared to the native tissue (Figure 3.11 A) (Partington, Mordan et al. 2013). Quantification of the soluble collagen content indicated a loss of collagen in the decellularised scaffolds at cycles 10 ($P<0.05$), 20 ($P<0.05$) and 25 ($P<0.01$) compared to the native tissue (Figure 3.11 B). However in the time-matched PBS control, no significant decrease was observed compared to the native tissue, although similarly to the total collagen quantification assay, a decreasing trend of soluble collagen was noted in these controls (Figure 3.11 B). This indicated the significant decrease in soluble collagen in the DEM scaffolds was due to the decellularisation treatment ($P<0.01$). It should also be noted that the standard deviation of these data from this assay was greater than expected and therefore the value of these data must be considered carefully (Partington, Mordan et al. 2013).

The collagen content was further analysed by immunofluorescence labelling of the cartilage rings using both a monoclonal antibody (Figure 3.12 A-C) and a polyclonal antibody (Figure 3.12 D - F) specific to Type II collagen. The presence of Type II collagen is evident in the native trachea, the non-decellularised time matched PBS controls and the DEM decellularised samples after 25 cycles. In both the monoclonal and polyclonal antibody labelling there appears to be no discernible loss of collagen Type II in the NDC controls but a noticeable loss in the DEM samples. However, the results correlate well with the total collagen assay (Figure 3.11 A) as the overall decrease in collagen Type II in the cartilage rings appears to not be markedly different (Partington, Mordan et al. 2013).



A



B

Figure 3.11: Quantitative analysis of total collagen content indicated that decellularisation (DC) did not significantly alter the total collagen content (A). Quantitative analysis of soluble collagen content indicated that decellularisation (DC) reduced the amount of soluble collagen compared with time-matched PBS stored tissue (NDC) ($P < 0.01$) and native tissue ($P < 0.01$ and $P < 0.05$) (B). Values are mean \pm SD; $N = 5$ (Partington, Mordan et al. 2013). Permission to reproduce this figure has been granted by Elsevier.

Transmission electron microscopy was performed to investigate whether the DEM decellularisation had affected the ultrastructure of the cartilage matrix. These results indicated that the ultrastructure of the interlinking collagen bundles in the cartilage ring matrix appeared similar in the native trachea (Figure 3.13 A) and the tracheal scaffolds after 25 cycles of DEM decellularisation (Figure 3.13 B). This would suggest that no damage was caused to the collagen bundles by the decellularisation process (Partington, Mordan et al. 2013).

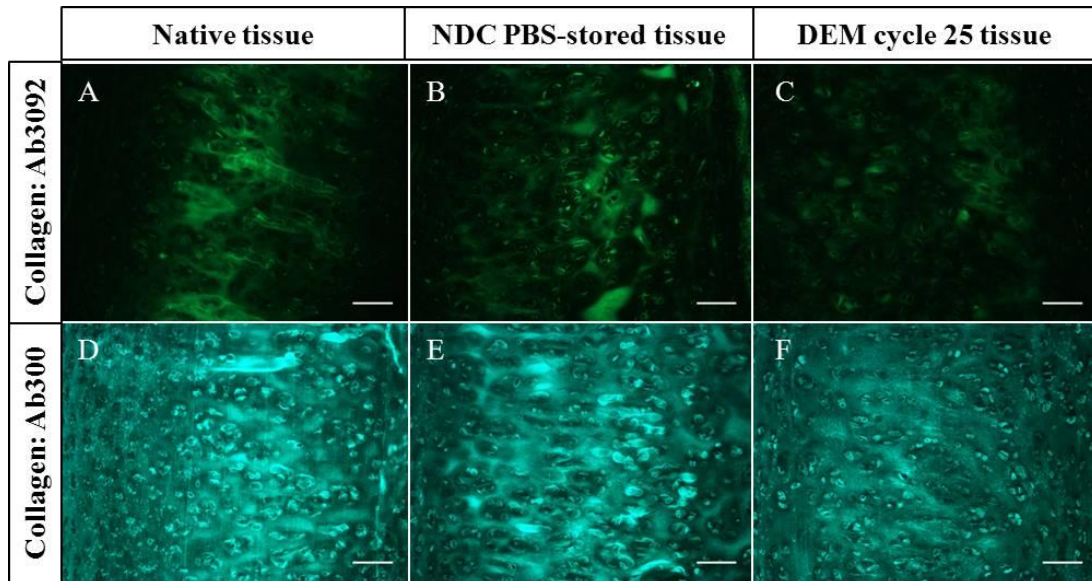


Figure 3.12: Immunofluorescence labelling of type II collagen within the cartilage matrix using two different antibodies (A–F) suggested that, compared with native trachea (A and D), the DEM scaffolds (C and F), but not PBS-stored trachea (NDC) (B and E), experienced a decline in collagen content. Scale bar for (A–F) = 100 μ m (Partington, Mordan et al. 2013). Permission to reproduce this figure has been granted by Elsevier.

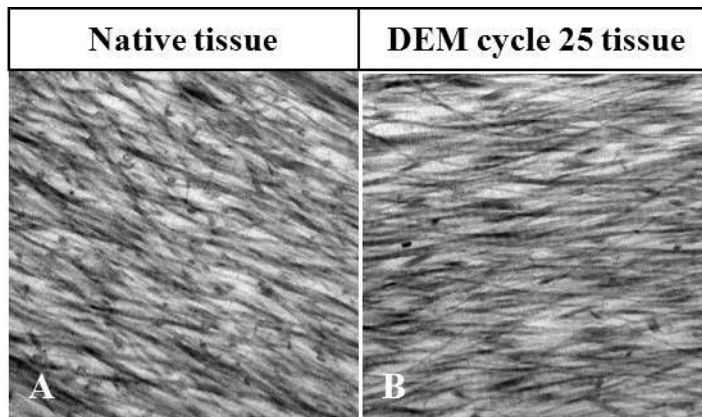


Figure 3.13: TEM images showed that the ultrastructure of the collagen bundles were similar in both the native trachea (A) and DEM-produced scaffolds (B), with parallel bundles of collagen fibres, of a similar diameter, appearing in both examples. Image at 40,000x magnification (Partington, Mordan et al. 2013). Permission to reproduce this figure has been granted by Elsevier.

3.4.8 Analysis of glycosaminoglycans throughout and following the detergent-enzymatic method of decellularisation

The level of sGAG was assessed in the native trachea, the time-matched PBS controls and the DEM decellularised scaffolds. The results indicate a time dependent incremental loss of sGAG ($P < 0.001$ at cycle 10 and $P < 0.005$ at cycles 20 and 25) in both the time-matched PBS controls and the DEM decellularised scaffolds compared with the native tracheae that is only slightly exacerbated by the DEM decellularisation process (Figure 3.14) (Partington, Mordan et al. 2013).

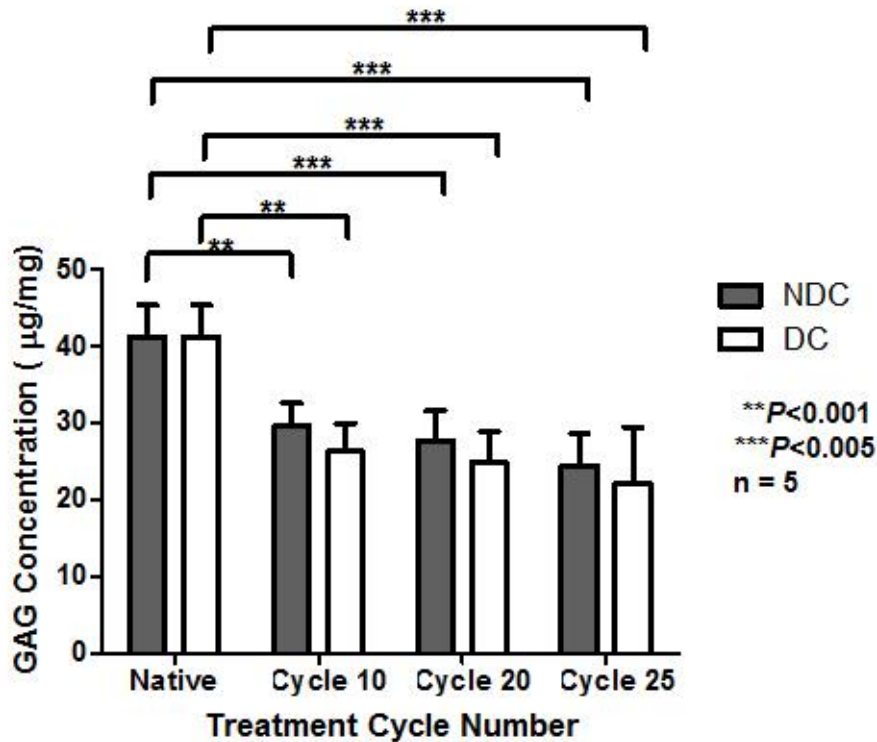


Figure 3.14 Quantitative sGAG analysis demonstrated a significant incremental loss of sGAG from both the time-matched PBS controls (NDC) and the DEM decellularised scaffolds (DC) compared with the native tissue, which appeared to only be slightly accelerated by the DEM treatment (Partington, Mordan et al. 2013). Permission to reproduce this figure has been granted by Elsevier.

Alcian blue staining was performed to assess whether the loss of GAG observed in the quantitative assay could be observed qualitatively. The results demonstrated an observable loss of GAG, stained blue, in both the time-matched PBS controls and in the DEM decellularised scaffolds compared with the native tracheae (Figure 3.15 A-F). However unlike in the quantitative assay, the loss of GAG from the DEM decellularised scaffolds was far more pronounced, with little alcian blue staining visible suggesting that little GAG remained (Figure 3.15 C, F). Considering that in the quantitative assay approximately 60% of the sGAG remained after 25 cycles of DEM decellularisation, this loss, although corroborating the quantitative assay, was unexpected. It is possible that the sGAG Blyscan Assay is more sensitive than the alcian blue assay and that, below a certain threshold level, alcian blue staining does not distinctly stain GAG, whereas the assay would still isolate and detect GAG below this level (Partington, Mordan et al. 2013).

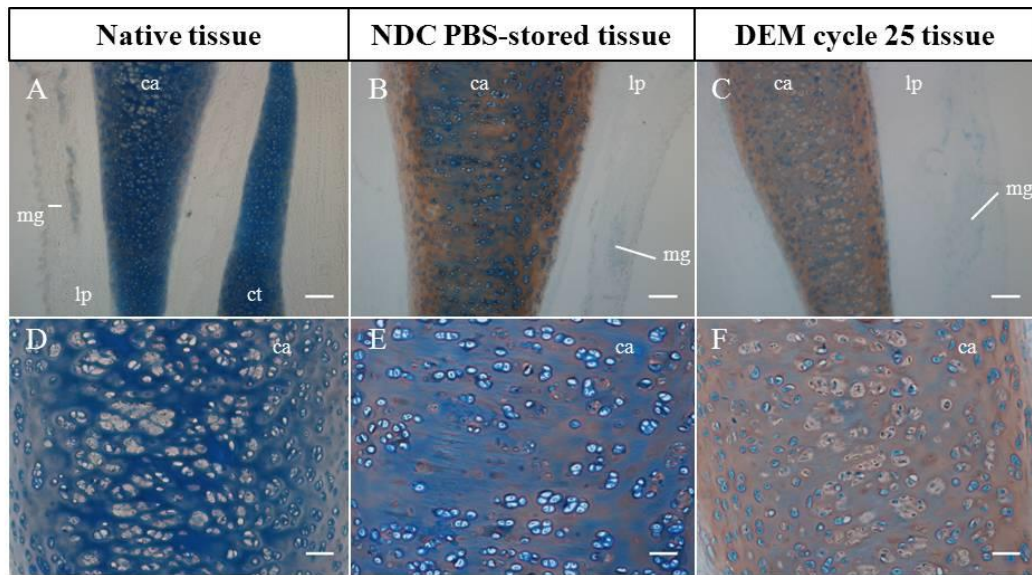


Figure 3.15: Alcian blue staining for qualitative GAG analysis demonstrated a significant loss of sGAG from the time-matched PBS controls (B, E) and the DEM decellularised scaffolds (C, F) compared with the native tissue (A, D), which appeared to be greatly accelerated by the DEM treatment (Partington, Mordan et al. 2013). Permission to reproduce this figure has been granted by Elsevier.

3.4.9 Tensile testing of scaffolds throughout and following the detergent-enzymatic method of decellularisation

Tensile testing was performed to assess the cartilage ring strength as a measure for retained strength and rigidity of the tracheae post-decellularisation treatment and therefore potentially as a predictor of collapsibility post-transplantation *in vivo*. The tests were performed on transverse (circumferential) sections of the tracheae. The Young's modulus was calculated for the tensile testing, termed here as tensile modulus, by determining the slope of the stress-strain curve. The results demonstrated no significant decrease in the stiffness in the time-matched PBS controls (NDC) compared with the native tracheae (Figure 3.16). However in the DEM decellularised scaffolds (DC), there was an observed incremental decrease in stiffness compared to the native tissue, which results in a significant loss of stiffness only after 25 cycle of DEM treatment ($P < 0.05$) compared to the native tracheae (Figure 3.16). Additionally, when comparing the DC with the NDC, the effect of the DEM decellularisation process was found to be significant ($P < 0.005$), resulting in a loss of stiffness to all treated samples (Figure 3.16) (Partington, Mordan et al. 2013).

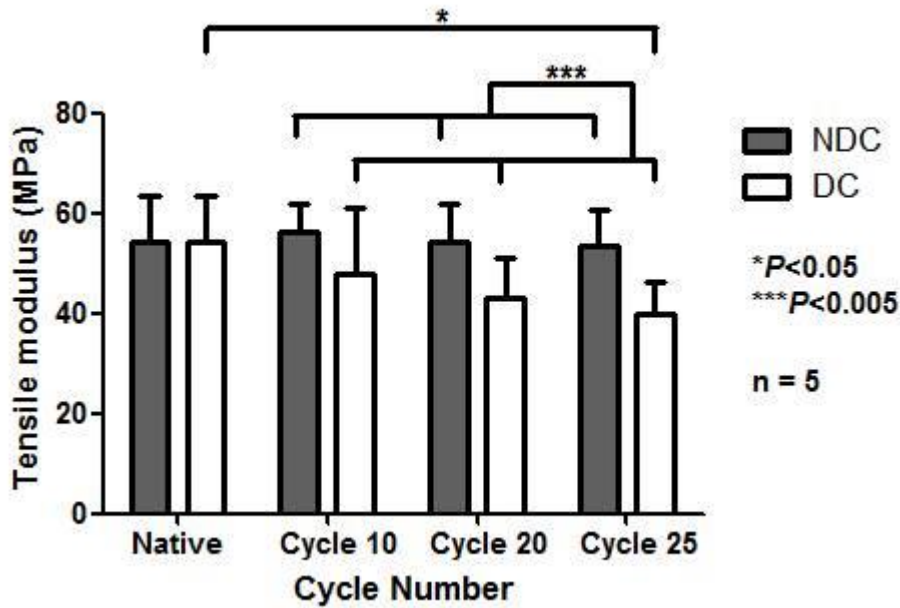


Figure 3.16: Young’s modulus of the tensile testing demonstrated a significant loss of stiffness in the DEM decellularised scaffolds (DC) only after 25 cycles ($P < 0.05$) compared to the native tracheae. However the effect of the DEM treatment overall had a significant effect, reducing the stiffness of the DEM scaffolds, compared to the time-matched PBS controls (NDC) ($P < 0.005$) (Partington, Mordan et al. 2013). Permission to reproduce this figure has been granted by Elsevier.

In addition to the Young’s modulus, the ultimate tensile stress and the ultimate tensile strain was also calculated from the tensile testing data. The ultimate tensile stress describes the maximum stress required to rupture the sample. These data correlate well with the Young’s modulus data and, similarly to the Young’s modulus data, demonstrate a loss of strength in the DEM scaffolds after 25 cycles of DEM decellularisation compared with the native tracheae ($P < 0.05$). They also demonstrate a loss in strength, due to the DEM process, in cycles 10 to 25 of the DEM scaffolds compared to the time-matched PBS controls ($p < 0.005$) (Figure 3.17). The ultimate tensile strain data, which describes the degree to which the sample is stretched before it ruptures, demonstrated no differences between the native tracheae, the time-matched PBS controls and the DEM scaffolds (Figure 3.18) (Partington, Mordan et al. 2013).

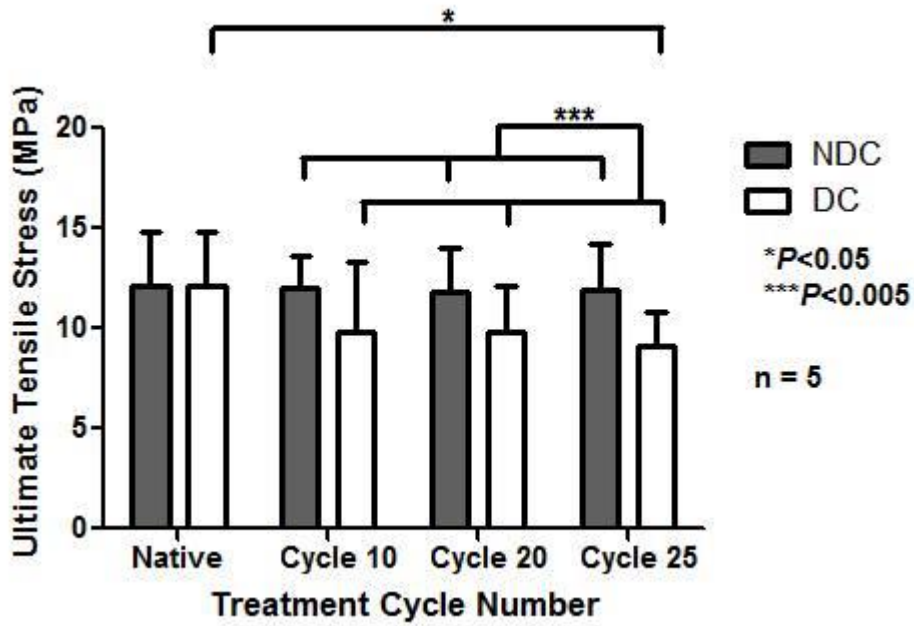


Figure 3.17: The ultimate tensile stress of the tensile testing demonstrated a significant loss of strength in the DEM decellularised scaffolds (DC) only after 25 cycles ($P < 0.05$) compared to the native tracheae. However the effect of the DEM treatment overall had a significant effect, reducing the strength of the DEM scaffolds, compared to the time-matched PBS controls (NDC) ($P < 0.005$) (Partington, Mordan et al. 2013). Permission to reproduce this figure has been granted by Elsevier.

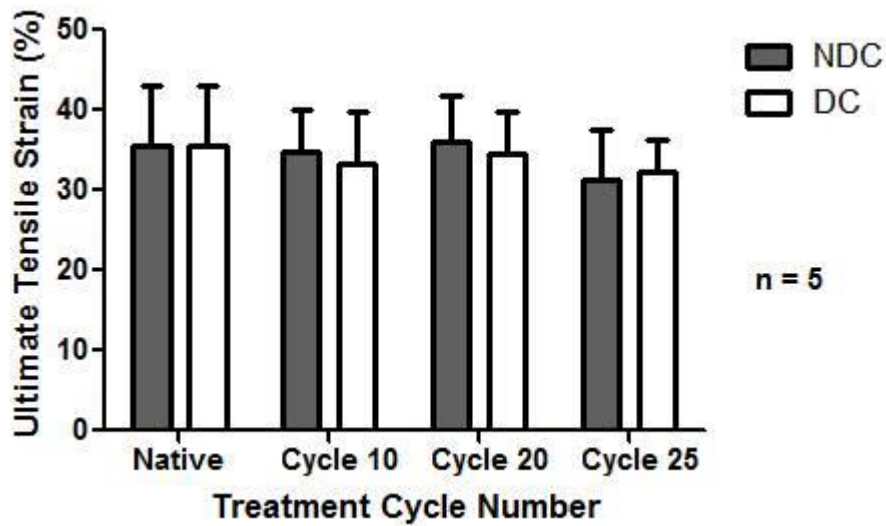


Figure 3.18: The ultimate tensile strain of the tensile testing demonstrated no significant differences between the native tracheae, the time-matched PBS controls (NDC) and the DEM scaffolds (DC) (Partington, Mordan et al. 2013). Permission to reproduce this figure has been granted by Elsevier.

3.4.10 DMA compression testing of scaffolds throughout and following the detergent-enzymatic method of decellularisation

DMA compression testing was performed to assess the stiffness and compressibility of the cartilage. The tests were performed on sections of the trachea cartilage ring. The Young's modulus was calculated for the compression testing, termed here as compressive modulus, by determining the slope of the initial linear proportion of the stress-strain curve. The results demonstrated no significant decrease in the stiffness in the time-matched PBS controls (NDC) or the DEM decellularised scaffolds (DC) compared with the native tracheae (Figure 3.19). The significant increase at cycle 10 in the time-matched PBS controls was identified to be due to a significant outlier in that dataset, as revealed by Grubb's test for outliers (Partington, Mordan et al. 2013).

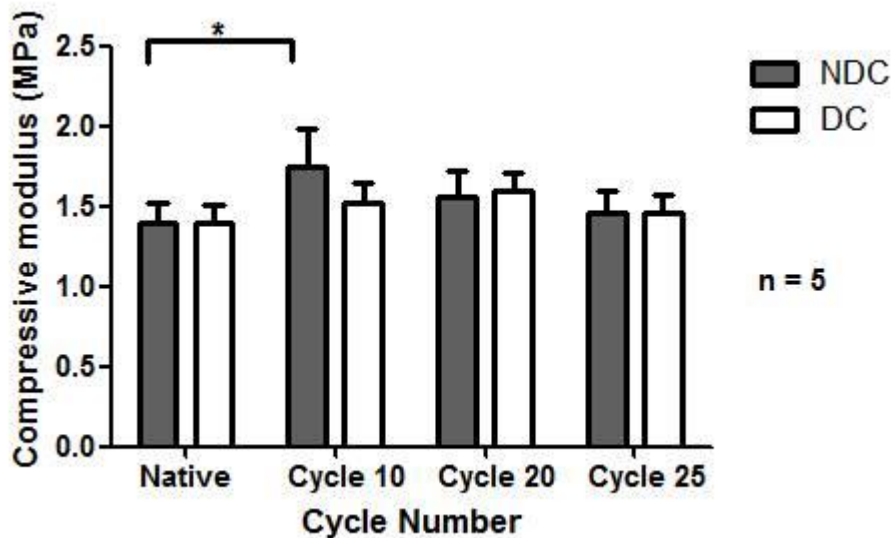


Figure 3.19: The compressive modulus of the DMA compression testing demonstrated no significant differences between the native tracheae, the time-matched PBS controls (NDC) and the DEM scaffolds (DC) (Partington, Mordan et al. 2013). Permission to reproduce this figure has been granted by Elsevier.

3.5 Discussion

The published methodologies of the original DEM (Conconi, De Coppi et al. 2005, Macchiarini, Jungebluth et al. 2008) and revised DEM (Jungebluth, Go et al. 2009, Go, Jungebluth et al. 2010) were ambiguous and despite personal communication with one of the published papers' authors to obtain clarity on the DEM (Jungebluth 2009), misinterpretation of the DEM occurred and resulted in an adapted DEM being used in this thesis. In a later paper published in 2012, Jungebluth described the process more clearly stating that a single treatment cycle involved a 48 hour water incubation step followed by cycles of a 4 hour detergent step and a 3 hour enzymatic step (Jungebluth, Bader et al. 2012). Unless the authors were operating the process on a 24 hour basis, there was a 16 hour overnight incubation/holding step that was not described nor included in the published methods. The adapted DEM method described here (Partington, Mordan et al. 2013) however, was very similar to a further revised DEM method published by Baiguera and colleagues in 2010 (Baiguera, Jungebluth et al. 2010), with overnight PBS hold/wash steps.

The preparation of the airway removed the larynx, the branches to the bronchi and the loose overlying fascia whereas the initial PBS and water washes removed the superficial blood. This resulted in reducing the superfluous surface area which allowed the focus of the decellularisation to be on the trachea.

In order to initially assess whether successful decellularisation had been achieved, histological analysis was performed on the native tracheal tissue to establish a baseline, as well as on DEM decellularised scaffolds at various points to establish if decellularisation had indeed occurred. Initially the native tracheae and DEM decellularised scaffolds were stained with toluidine blue where good staining was observed. However, the ability to distinguish the various regions of the trachea and the nuclei within those various regions of the trachea was difficult due to the overall similarity in stain colour and intensity. It was possible to crudely establish that decellularisation after 25 DEM cycles had occurred using toluidine blue, however a further aim of the histological analysis was to count the nuclei to quantify cell clearance. For this purpose toluidine blue was considered unsuitable because of the high likelihood of error due to the difficulty in distinguishing the individual nuclei clearly. The decision to use toluidine blue to stain trachea was due to the

inexperience of the researchers in preparing and analysing tracheal tissue. After some online research, it was decided that haematoxylin and eosin (H&E) would be a more appropriate stain, if a suitable method could be found to achieve good staining for hard resin embedded sections. The first tested method employed a twenty minute haematoxylin incubation followed by a three minute eosin incubation. However, it was determined that these incubations were not long enough to allow adequate stain penetration into the tissue and resulted in very weak staining of the tissue (data not shown). The second tested method (described in 3.3.3) with one hour incubations for both haematoxylin and eosin was tried and found to be suitable. The results from the histological analysis of H&E staining on the native tracheal tissue demonstrated typical H&E staining for the tracheal tissue, similar to that observed using paraffin, the more common embedding material. Given this satisfactory result, the DEM decellularised scaffolds were also stained with H&E to assess whether decellularisation had been achieved. The results demonstrated visible decellularisation of most regions of the tracheae, including the lamina propria, the epithelia layer and sub-mucosal glands as well as the adventitia layers. However, chondrocytes were observed in the cartilage rings even after 25 cycles of DEM decellularisation. These data agree with previously published data using the original and adapted DEM (Conconi, De Coppi et al. 2005, Jungebluth, Go et al. 2009) where chondrocytes were also still observed although the other regions of the trachea were cleared of cells.

Although the absolute numbers differ (Table 3.2), comparing the clearance of cells from the tracheae as a whole using this revised method with the previously published data (Conconi, De Coppi et al. 2005, Jungebluth, Go et al. 2009), a similar percentage reduction was observed after 20 DEM cycles compared with the native with approximately 5% of the cells remaining. Although, whereas all the cells were reportedly cleared after 22 cycles using the original DEM protocol (Conconi, De Coppi et al. 2005), cells still remained in the tracheal cartilage post- decellularisation after 25 cycles.

Cycle Number	Partington, 2013	Conconi, 2005	Jungebluth, 2009
	Cells/mm ² (%)	Cells/mm ² (%)	Cells/μm ² (%)
Native	19106 (100%)	3110 (100%)	29800000* (100%)
10	842 (4.4%)	-	15200000* (51%)
12	-	1230 (39.5%)	-
20	842 (4.4%)	-	1500000* (5%)
18	-	290 (9.3%)	-
22	-	0 (0%)	-
25	649 (3.4%)	-	-

Table 3.2: Cell clearance by DEM decellularisation literature comparison (Conconi, De Coppi et al. 2005, Jungebluth, Go et al. 2009, Partington, Mordan et al. 2013) *Likely to be a typographical error and actually 2980/mm², 1520/mm² and 150/mm² respectively.

The removal of donor nuclear material, predominately DNA, is important during the decellularisation process to ensure all immunogenic material from the donor is adequately removed prior to recellularisation and transplantation as it can otherwise potentially cause an immune response in the recipient (Zheng, Chen et al. 2005, Badylak and Gilbert 2008, Gilbert, Freund et al. 2009, Keane, Londono et al. 2012)}. DNA holds a particular challenge for decellularisation processes as it is sticky and has been shown to bind to the ECM upon release from the nucleus. It is because of this property that many decellularisation protocols incorporate DNase treatment steps ((Conconi, De Coppi et al. 2005); (Bolland, Korossis et al. 2007); (Keane, Londono et al. 2013)) or steps to mask residual DNA. The DNase treatment cleaves residual DNA strands independently at random sites to reduce the strand length and remove the DNA from the donor tissue. Analysis of the DEM scaffold quantitatively and qualitatively using DAPI staining indicated significantly reduced levels of DNA after 25 DEM cycles compared to the native tracheal tissue. However, levels were comparable to the non-decellularised time-matched PBS stored controls, which suggests that effective DNA removal was not occurring in the DEM decellularised scaffolds despite multiple DNase treatments. It could be possible that the original DEM protocol, which used ten times more DNase in the DNase step, would have been more effective with DNA removal. However, at the level of DNase used, an observable effect and a reduction over background levels would have been expected.

There are several reasons why the DNase treatments may not have further reduced the DNA content of the scaffolds. Firstly, the buffer used in the DNase step is 1M sodium chloride. It is widely accepted that DNase requires divalent metal cations to activate DNase I. Both Mg^{2+} and Ca^{2+} are required to activate DNase I effectively (Price 1972). A minimum concentration of Ca^{2+} is also required to stabilise DNase I against proteolytic digestion. It has also been demonstrated that ionic strength can affect the activity of DNase, and a high concentration of salts such as sodium chloride or potassium chloride above 5mM can have a strong inhibitory effect on DNase activity (Price 1972). The DEM DNase reaction buffer could therefore be deemed as unsuitable as it contained neither Mg^{2+} nor Ca^{2+} cations and contained a high concentration (1M) of sodium chloride, thereby limiting, or worse, inhibiting the activity of the DNase. Lastly, the DNase reaction was performed at room temperature, assumed to be 25°C. Although the activity of the DNase is measured at this temperature, it is widely acknowledged that the enzymatic activity at this temperature is limited and increasing the temperature to 37°C can improve DNA digestion.

Whether complete removal of DNA is required, or feasibly achievable, is currently unknown. Many commercially available products for regenerative medicine interventions have been demonstrated to have remnant DNA fragments present post-decellularisation (Badylak and Gilbert 2008, Gilbert, Freund et al. 2009), without adverse reactions in recipients. However the maximum level of DNA in the nine tested products was in Restore made from porcine small intestine (DePuy Orthopaedics) which had approximately 1.13 ± 0.03 ng DNA / mg of tissue (dry weight) and fragments sizes between 100 to 200 base pairs (bp) in size (Gilbert, Freund et al. 2009). The tracheal scaffolds from the DEM process had 264.66 ± 69.92 ng DNA / mg of tissue (wet weight) which, even accounting for differences in tissue type and wet vs. dry weight, is a much higher level of remaining DNA. It would therefore be prudent to investigate ways to optimize this step to improve DNA removal from the scaffolds and reduce the risk of an inflammatory response from the recipient or potential graft rejection (Partington, Mordan et al. 2013).

Tracheal function is dependent on its structure and the strength of that structure. The cells interact with the ECM via transmembrane receptors (Hynes 2009, Badylak, Weiss et al. 2012) and via these links play a role in the ECM homeostasis. Therefore

it cannot be precluded that removal of cells and therefore the loss of interaction of the cells with the ECM during a decellularisation process could in some way diminish the structural integrity of the ECM (Bader and Macchiarini 2010, Partington, Mordan et al. 2013). Although decellularisation is important to remove immunogenic material from the donor scaffold, it is a fine balance to not over-decellularise the scaffold and damage it or remove components that could be useful in the recipient. For example, a potentially key advantage of utilising a biological scaffold over a synthetic scaffold is the retention of key ECM proteins laid down by the donor's cells in the correct anatomical loci that will aid host recellularisation by directing cell adhesion, migration and differentiation. It has been shown that DEM decellularisation removes cells, MHC components and a significant amount of the DNA, however it has been reported that a core set of over 100+ polypeptides are retained which reportedly have roles beyond structural integrity, including epithelialisation and angiogenesis (Butler, Hsuan et al. 2011, Elliott, De Coppi et al. 2012), as well as specific proteins such as bFGF (Baiguera, Jungebluth et al. 2010). Retention of protein was observed in this investigation, where quantification revealed total protein levels were not diminished after 25 cycles of DEM decellularisation nor in the time-matched PBS-stored controls compared with the native tissue. Similarly, when certain key ECM proteins that are important for recellularisation and revascularisation, laminin and fibronectin, were examined in more detail, good retention and expression patterns were observed. These data would suggest that upon implantation of these biologically favourable scaffolds, recellularisation and revascularisation should occur and indeed this has been shown in several of the reported bioengineered tracheal transplants that utilise DEM decellularised scaffolds (Macchiarini, Jungebluth et al. 2008, Elliott, De Coppi et al. 2012).

ECM components, such as the collagens and the GAG which are involved in the structural integrity of the scaffold, are also critical to retain as these will impart the capacity for the graft to maintain an open airway upon transplantation. It is the role of the cartilage rings to maintain an open airway in the presence of intrathoracic pressure changes that occur through normal or laboured breathing, such as hyperpnea or tachypnea. Collagen type II and GAG are the main components of hyaline cartilage and the structural integrity of the cartilage rings in the trachea are due to the

functional coupling between the GAG-rich proteoglycans which creates a high osmotic pressure and the fibrillar collagen network which provides the tensile strength. The biomechanical properties of tracheal cartilage are non-linear (Teng, Ochoa et al. 2008), and so fairly complicated, however to take a holistic view, the circumferential strength of the cartilage rings which maintain the open airway are determined by their structural composition. Therefore, it is highly possible that the functional and structural properties of the hyaline cartilage rings would be affected if the ratio, quantities or arrangements of the cartilage matrix constituents were altered. Indeed, evidence from the literature has demonstrated that age-related loss of the proteoglycans content in cartilage can make the tissue stiffer. This was distinguished experimentally by observing an increase in the elastic modulus (Roberts, Rains et al. 1997).

In this particular study of the DEM decellularisation it was found that type II collagen, total and soluble collagen and GAG all undergo a decline. Although no differences were observed in the cartilage or collagen ultrastructure using TEM between the native trachea and the DEM decellularised scaffold, a decrease in collagen content was experimentally observed in the DEM decellularised scaffolds by IHC analysis and by quantification. These decreases were observed in non-decellularised time-matched controls which indicate the loss could be occurring through natural degradation of the tissue over time. For specific ECM components, collagen Type II and soluble collagen content, this natural loss appears to be accelerated by the DEM decellularisation process and that the effects increased gradually over time, whereas the overall total collagen content appeared not to be affected further by DEM decellularisation. It could be that the natural degradation of the cartilage over time allows deeper penetration of the decellularisation solutions into the cartilage matrix, further disrupting the cartilage matrix to allow even deeper penetration and potentially more degradation. It could be possible that reducing the length of the decellularisation process could moderate collagen loss. In addition to collagen loss, loss was also observed in the GAG content which also appears to be accelerated by the DEM decellularisation. A decrease in GAG was also observed in other published studies using the DEM decellularisation (Haykal, Soleas et al. 2012). Therefore, like with the collagen, shortening the length of the decellularisation protocol may moderate GAG loss. However, despite the loss of collagen and GAG,

the loss of total collagen was not significant and there was still an abundance of collagen and GAG after the decellularisation and the gross anatomical structure was still preserved in the DEM scaffolds after 25 cycles (Partington, Mordan et al. 2013).

The Biocolor Sircol soluble collagen assay kit uses an enzymatic process to solubilise the collagen in the sample. This, as the assay kit name suggests, results in only the soluble collagen being digested and therefore quantified. The mature collagen in the cartilage ring is insoluble and therefore remains undigested. In this study, the results from the soluble collagen are approximately 60 fold less than that achieved from the total collagen which could be accounted for by the amount of collagen that remained undigested. Several researchers in the field have used this assay to investigate collagen loss from trachea (Gray, Turner et al. 2012); (Lange, Greco et al. 2014), however due to the majority of the collagen in the tracheae and the scaffolds remaining undigested, it is probable that this assay is not suitable for this tissue type and therefore should not be used for the determination of collagen loss in this instance. For this reason, this assay will not be used to analyse the biochemical content trachea or tracheal scaffolds.

The ability to retain native-like biomechanical strength is currently a perceived necessary requisite or critical quality attribute in decellularised scaffolds, especially for scaffolds that will perform a specific structural role. In tracheal tissue engineering it is critical that an open airway is maintained and it is predominately the role of the cartilage rings to structurally support the airways and maintain an open airway. Failure for a tissue engineered trachea to maintain an open airway will likely result in the patient requiring a stent to prevent collapse. The prognosis of airway stenting commonly results in complications such as infection and damage to the lumen of the trachea. Therefore if a tissue engineered trachea required stenting then it could create future medical complications; rather than being the cure to the problem it could ultimately just start the illness cycle all over again. Current published biomechanical data of DEM has focused on uniaxial tensile testing in the longitudinal plane (Jungebluth, Go et al. 2009). Although this data will inform on the biomechanical strength and strain capacity of the ECM, it is limited to these parameters. It is unlikely that longitudinal uniaxial testing would inform on the potential for a decellularised and recellularised trachea to maintain an open airway *in vivo* post-transplantation in a patient, where *in vivo* airway collapse will be the

greatest risk if biomechanical stiffness and strength are lost due to decellularisation. Therefore, there was a need to develop a more relevant assay to predict *in vivo* collapsibility. A more relevant test was determined to be a tensile test on the cartilage rings to investigate the tensile modulus, the ultimate tensile stress and the ultimate tensile strain of the cartilage rings. Calculating the Young's modulus from tensile testing of the cartilage rings should predict the stiffness of the cartilage rings and therefore the ability of the cartilage rings to maintain an open airway.

The tracheae that were tested by the longitudinal uniaxial tensile testing maintained comparative strength to the native trachea until cycle 17 in porcine trachea (Jungebluth 2009) and cycle 25 in the human trachea (Baiguera, Birchall et al. 2010). In this study, where the cartilage rings were tested, it was determined that loss of the Young's modulus and the ultimate tensile stress was observed in DEM decellularised tracheae after just 10 cycles compared to time-matched PBS-stored controls. It could be possible that the loss of stiffness observed in the cartilage rings could be a consequence of the observed loss of GAG, soluble collagen and collagen type II. It is also possible that this loss of stiffness in the cartilage rings could potentially lead to *in vivo* tracheal collapse post-transplantation and it would certainly provide a plausible explanation for partial collapse in 3 out of 9 patients treated in an Italian cohort ((Badylak, Weiss et al. 2012)). In support of this argument are cases previously reported in the literature where significant loss of GAG-rich proteoglycan and type I collagen has been identified at fracture and stenosis sites in incidences of *in vivo* tracheal collapse (Mankarious, Adams et al. 2002) and incidences where GAG-rich proteoglycans loss followed by significant collagen loss are early indicators of osteoarthritis and a resulting decline in articular cartilage (Saarakkala, Julkunen et al. 2010). From this, one could conclude that adverse changes due to decellularisation in the ECM content or molecular arrangement could result in accelerated weakness and potentially an increased risk of collapse in a transplanted tissue engineered trachea. As the loss is observed at cycle 10 onwards, which relates to approximately 12 days of decellularisation processing, it could be possible that an optimized decellularisation process that could be completed in less cycles or time could negate loss of type II collagen and GAG and therefore potentially cartilage stiffness (Partington, Mordan et al. 2013).

However, it is also possible that observed failure in tissue engineered airways is not solely due to loss of structural rigidity of the airway due to ECM and cartilage ring damage during decellularisation, but could also be due to inadequate engraftment of seeded chondrocytes/chondrogenically-differentiated mesenchymal stromal cells or failure of chondrocytes or chondroblasts from adjacent healthy tissue to migrate, repopulate and undergo chondrogenesis and appropriate maturation in the tissue engineered sections of trachea. It is likely that re-establishment of the cartilage homeostasis by these means will be itself necessary to prevent future failure of these tissue engineered airway grafts (Partington, Mordan et al. 2013).

3.6 Conclusions

Although the gross macromolecular structure of the DEM decellularised trachea is preserved and so appears similar to native trachea, there is evidence to suggest that the decellularisation process results in the decline of the key structural components of the cartilage rings, GAG and collagen. These components are considered to determine the biomechanical strength of the cartilage rings, and therefore the scaffold, and the observed decline in GAG and collagen correlates well to the observed decline in the stiffness of the cartilage rings, which could ultimately result in collapse of a tissue engineered tracheae made using this decellularisation method, when transplanted *in vivo*. The DEM decellularisation also failed to remove residual DNA which could also provoke an immune response or result in graft rejection *in vivo* when transplanted in a patient. Aspects of the DEM decellularisation require optimisation to produce a method that better removes immunogenic material, such as DNA, within as short a time period as permissible to also achieve complete decellularisation, to better retain GAG and type II collagen and therefore theoretically biomechanical stiffness and strength, leading to increased biomechanical stability *in vivo*. The development of a rapid and fit-for-purpose method for decellularising tracheae for tissue engineering purposes, employing optimised decellularisation solutions, solution application and incubation temperatures would hopefully address the highlighted challenges and advance this field of research from cases performed on a compassionate basis to clinical studies and ultimately clinical practice (Partington, Mordan et al. 2013).

4 Design and engineering of a pressurised transmural bioreactor

4.1 Introduction

One of the conclusions drawn from decellularising tracheae with the detergent-enzymatic method (DEM) (section 3.6) (Conconi, De Coppi et al. 2005, Macchiarini, Jungebluth et al. 2008, Jungebluth, Go et al. 2009, Go, Jungebluth et al. 2010) was the method of application of the decellularisation solutions to the tissue needed to be optimised. The concept of a pressurised transmural flow method of decellularisation originated during a lecture discussing the concept of tangential flow filtration, where fluid is recirculated past a filter under pressure so that a percentage of the fluid is forced through the filter. The concept would involve the creation of a pressure gradient to actively flow the decellularisation solutions through the wall of the trachea, as opposed to the passive diffusion of the decellularisation solutions into the wall of the trachea that immersion generates, as used in the DEM of decellularisation. Theoretically application of the decellularisation solutions transmurally under pressure could make the decellularisation process more efficient and expedient.

The initial concept envisaged that the transmural flow of fluid would be from the external chamber to the internal chamber as the majority of the cells in the trachea are located on the luminal side and therefore less cell debris would be forced through the tracheal wall with flow in this single direction. It was also considered that turbulent flow could be advantageous over laminar flow as better mixing of the decellularisation solutions would be achieved.

In order to achieve pressurised transmural flow through the tracheae, a bioreactor would need to be designed and manufactured that could be used with the trachea to create a dual chamber system. After performing a literature search, it was realised that the concept of creating a pressurised transmural system had been applied to tissue engineering previously and that several bioreactors had been designed and manufactured that allowed for the creation of such dual chamber systems for hollow organ tissue engineering. The recellularisation of the trachea for clinical use in 2008 (Macchiarini, Jungebluth et al. 2008) utilised a dual chamber bioreactor (Asnaghi, Jungebluth et al. 2009) however the use of transmural pressure was not employed in this instance, the dual chamber system was solely used to deliver tailored media to

the different cells types seeded on either the lumen and abluminal sides of the trachea. Harvard Apparatus Regenerative Medicine has since purchased the rights to the bioreactor and have commercialised its sale as the InBreath Bioreactor for larger animal tissue and a smaller version, the MiniBreath Bioreactor, for small animal tissue (HARegenMed 2013). Harvard Apparatus Regenerative Medicine have also produced a bioreactor system (ORCA Bioreactor) which can be reportedly used for decellularisation and recellularisation. The ORCA decellularisation bioreactor chambers (HARegenMed 2013) appear to support either immersion of the tissue in a recirculating fluidic system or the perfusion of the decellularisation solutions through the an organ's blood vessel network reminiscent of a perfusion decellularisation methodology performed by other groups investigating decellularisation (Ott, Matthiesen et al. 2008, Price, Godin et al. 2015), but not transmural flow. Several examples did exist in the literature which detailed the use of pressurised transmural flow. One detailed where it had been used to improve the delivery of oxygen and nutrients into the walls of hollow tubular organs (tissue engineered arteries) to enable and encourage cell migration and growth in these regions (Bjork and Tranquillo 2009). More relevantly, a dual chamber bioreactor had also been designed to deliver pressurised transmural flow to decellularise blood vessels (umbilical veins) using a decellularisation solution of 20% acetone, 60% ethanol and 20% water (Montoya and McFetridge 2009). Another paper that described pressurised transmural decellularisation for the bladder did so by achieving a pressure gradient (internal to external) generated by distension of the bladder with decellularisation solutions, predominantly sodium dodecyl sulphate (SDS), followed by treatment with deoxyribonuclease I and ribonuclease A, rather than through attachment to a bioreactor (Bolland, Korossis et al. 2007).

Where bioreactors have been used they have typically been designed by academic groups, manufactured by local/academic engineering workshops and, apart from those commercialised by Harvard Apparatus Regenerative Medicine, were not available commercially. Also, depending on the ultimate application, whether decellularisation or recellularisation, and the specific hollow organs in question, which were typically blood vessels (decellularisation and recellularisation) or trachea (recellularisation), the bioreactor would need to be tailored for the organ and application it was to be used for. It was realised that an off-the-shelf bioreactor

would not be available for purchase and would need to be bespoke designed for the specific application for decellularising trachea and that the bioreactor needed to be designed and manufactured in-house.

To be able to generate transmural flow through a trachea, a bioreactor system that created separate internal and external chambers to allow independent access to the lumen and abluminal side of the trachea would be necessary. Additionally, other requirements were deemed to be critical in the design of the bioreactor. The bioreactor would require inlet and outlet ports for both the internal and external chambers. The ports would need to be machined so that suitable ancillary parts could be affixed to enable fluid flow. It would need to be able to withstand low pressure concurrent with transmural flow pressures of up to 10 psi. It would need to be easily and cost effectively sterilised by autoclaving without deflection over multiple sterilisation cycles. In addition to the bioreactor itself, ancillary parts would be required in the form of connectors, tubing, pumps and clamps/valves to enable and create the fluid flow path and pressure gauges/pressure transducers and temperature probes to monitor the fluid flow parameters.

Ultimately the bioreactor should aid progression of the decellularisation process, despite its inherent heterogeneity due to the starting donor material, towards the principles of precision manufacturing by providing the basis for a process that is controllable and repeatable with minimal user intervention and, with development, automatable (Williams, Thomas et al. 2012).

4.2 Aims and hypotheses

Aims

- To design a bioreactor large enough to house porcine and human trachea and enable transmural flow through the wall of the trachea.
- To optimise a bioreactor system that enables and supports a controllable and reliable transmural decellularisation process for tracheal decellularisation.

Hypotheses

- Through the creation of a dual chamber bioreactor system, independent fluid flows can be created, measured and controlled.
- By using decellularisation solutions and creating a back pressure in one of the chambers of the bioreactor, stable transmural flow will be achieved through the luminal wall of the trachea.

4.3 Materials, methods and results

As this chapter focused on the development of a novel decellularisation bioreactor and the design of the ancillary parts of the bioreactor, the materials, methods and results were combined into a single section.

4.3.1 Pressurised transmural bioreactor design v1.0

One of the potential issues with the DEM of decellularisation (Conconi, De Coppi et al. 2005) was that the method relied on immersion of the tracheae in the decellularisation solutions which resulted in 18 to 25 cycles of the detergent and enzymatic treatments being required. The proposed solution to this challenge was to design a decellularisation process which relied upon transmural flow through the tracheal wall to reduce the number of treatments required. Therefore it was anticipated that a dual chamber bioreactor with separately controllable fluid flows would be required to achieve a transmural flow process. The bioreactor concept and initial design was discussed with UCL Biochemical Engineering faculty staff members; Martina Michelletti, a senior lecturer with expertise in fluid dynamics in reactors and Alan Craig, an engineer in the Biochemical Engineering workshop, on how best to achieve the transmural flow in such a bioreactor system.

The concept of initial bioreactor design v1.0 was to enable attachment of a porcine trachea to create a dual chamber bioreactor with separate recirculation of an external fluid, the decellularisation solution, and an internal fluid, a wash solution. The conceptual design allowed for the decellularisation solutions to be pumped into the external chamber (EC), the abluminal side, of a fixed trachea with the pressure controlled using pre and post chamber valves and monitored using pre and post chamber pressure gauges. The wash solutions would be pumped through the internal chamber (IC), the luminal side, of the tracheal with pre and post chamber valves to control pressure and pre and post pressure gauges to monitor the pressure. The pressure of the external decellularisation solution would be greater than the internal wash solution causing abluminal to luminal transmural flow of the decellularised solution which is then removed, with cell debris, from the luminal side of the trachea by the wash solution. A downstream filter would, if necessary, be fitted to remove cell debris before the decellularisation solution is returned to the solution reservoir. A pulse dampener would also be considered on the internal and external circuits, if

necessary, to reduce the pulsatile effect of the peristaltic pump. From these discussions, drawings were produced in PowerPoint (Figure 4.1) and presented to the EngD supervisors for approval to allow the bioreactor to be built.

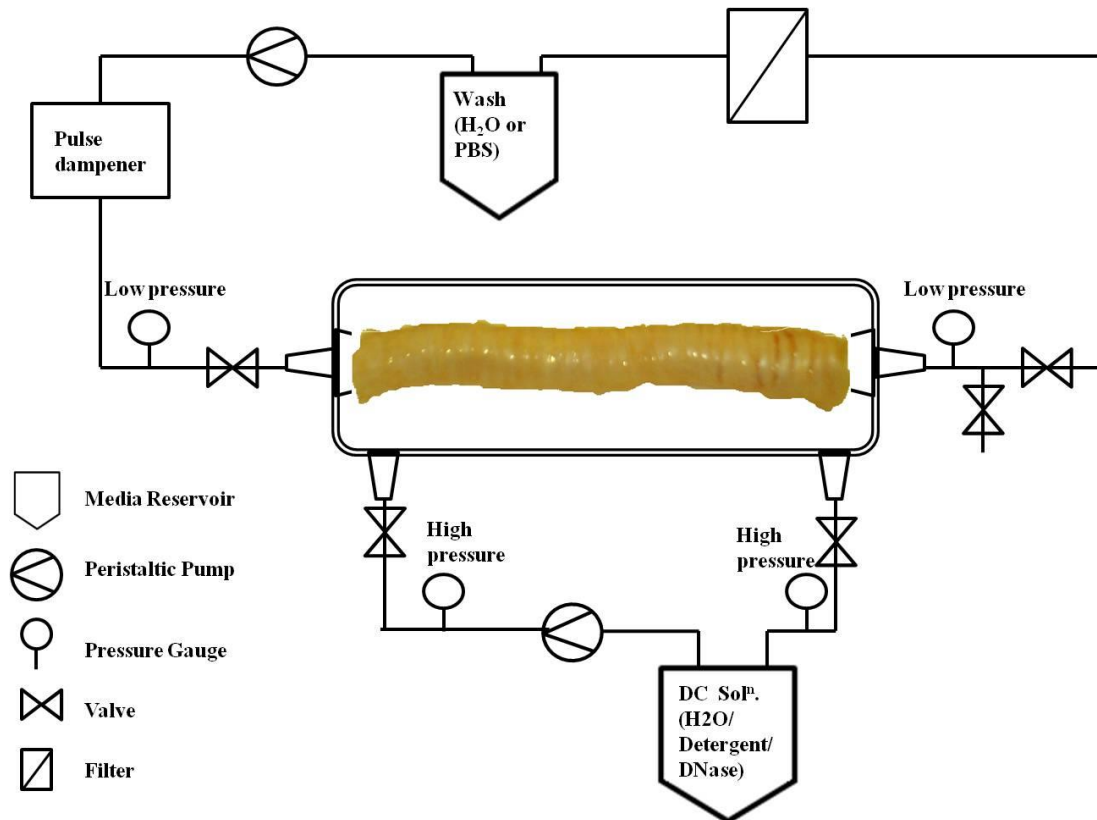


Figure 4.1 Schematic of the initial dual chambered pressurised transmurular decellularisation bioreactor design v1.0. The concept envisaged the decellularisation solution to be pumped under pressure into the external chamber of the tracheal bioreactor and whilst pumping wash solution through the internal chamber of the tracheal bioreactor. The pressure differential would permit transmural flow of the decellularisation through the tracheal wall which decellularises the trachea over the course of the flow. The aim was to achieve abluminal to luminal transmural flow due to the larger density of cells on the luminal side of the trachea in the lamina propria.

4.3.2 Manufacture of the pressurised transmurular bioreactor v1.0

Having gained approval of the pressurised transmurular pressure bioreactor design v1.0, the design was presented to the UCL Biochemical Engineering workshop for production and, in collaboration with engineer Alan Craig, the bioreactor design was finalised. Prototype bioreactor parts (Figure 4.2) produced by Alan Craig were tested, in particular the bioreactor length, internal diameter and the size adjustable

connectors (SACs) external diameter on the trachea attachment side, to ensure the bioreactor would be fit for purpose.

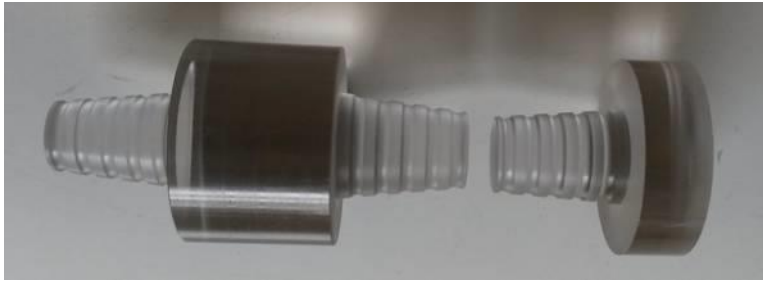


Figure 4.2: Prototype parts of the SAC connectors to ensure the SACs were suitable for the attachment of porcine trachea.

Once the prototype testing was complete, the pressurised transmural bioreactor was manufactured and leaked tested by Alan Craig in the Biochemical Engineering Workshop. The outer bioreactor tube (200 mm (L) x 36 mm (ID)) was made from 2 mm thick polycarbonate to allow for sterilisation by autoclaving and good visibility of the internal components of the bioreactor as well as the trachea when *in situ*. The length of the bioreactor tube and the position of the external ports on the bioreactor were designed to accommodate tracheas of 85 to 120 mm in length (Figure 4.3 A and B). The SACs were designed to accommodate tracheas of 16 to 21 mm in internal diameter with grooves machined into the hollow organ attachment side of the SAC to facilitate securement of the organ with wire/sutures (Figure 4.3 A and Figure 4.4 A and B). To assist with the attachment of the trachea to the SAC, a SAC was clamped to a laboratory support stand with the trachea positioned onto the SAC (Figure 4.4 A). The second SAC can be inserted into the top end of the trachea and also clamped to hold the trachea and SACs in position before securing the trachea to the SAC with appropriate material (Figure 4.4 A and B, Figure 4.5 A). The design of the lip on the SACs allows for the assembly of an O-ring (Figure 4.5 B) and an O-ring compressor (Figure 4.5 C) to be held in place and the O-ring to be compressed and create a seal against the bioreactor tube as the SAC fastener is tightened (Figure 4.5 D). As the SAC assemblies are not fixed inside the bioreactor they allow for the trachea to be attached and the SAC assemblies to be assembled before being passed through into the bioreactor tube (Figure 4.6 A). The addition of a screw allows one of the SAC assemblies to be easily tightened. The other SAC assembly had to be slightly angled to create resistance between the SAC, O-ring and O-ring compressor

and the bioreactor tube to allow the SAC fastener to be tightened without twisting the trachea/hollow organ (Figure 4.6 B). Assembly of the bioreactor with and without the trachea *in situ* demonstrated that the bioreactor did not leak and was fit-for-purpose.

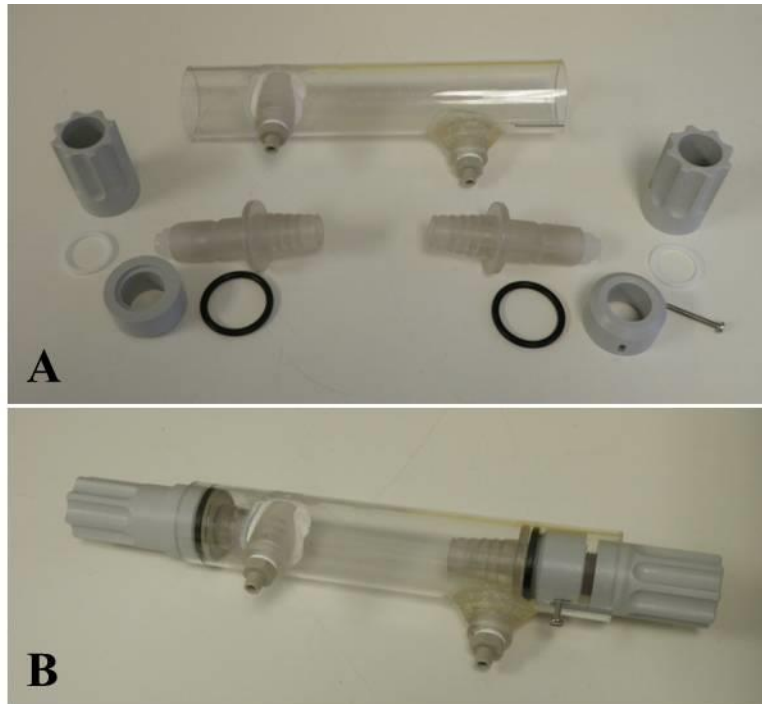


Figure 4.3: Images of bioreactor components and assembly. Manufactured from polycarbonate, the bioreactor can be sterilised by autoclaving. The internal and external ports were machined to produce BSP $\frac{1}{8}$ or G $\frac{1}{8}$ female threads allowing a range of adapters to be fitted. The trachea was secured to the size adjustable connectors (SACs) using sutures outside of the bioreactor. The O-ring and the O-ring compressor were slotted onto the SAC and the SAC fastener was threaded onto the SAC but not tightened. The internal assembly was then passed into the bioreactor tube. The external chamber of the bioreactor was sealed through compression of the O-ring by the O-ring compressor as the SAC fastener was tightened. One SAC assembly was prevented from rotating inside the bioreactor tube whilst tightened by the addition of a screw. The other SAC assembly was prevented from rotating by slightly angling the SAC assembly as tightened. This allowed the bioreactor to be assembled and sealed without twisting the trachea *in situ*.



Figure 4.4: Attachment of the trachea to the SAC using sutures was aided by utilisation of a laboratory support stand (A) and clamps to hold the SAC and trachea in position (B).

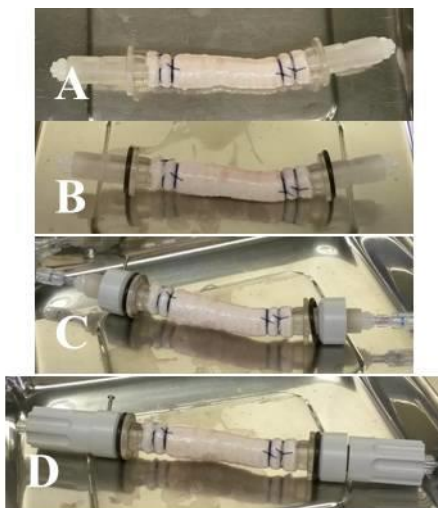


Figure 4.5: Sequential assembly of the SACs with the trachea in position. After attachment of the trachea to both SACs (A) the O-rings were positioned onto the SACs (B), then the O-ring compressor, with the screw in position on the left-hand side (C), and finally the SAC fasteners (D).

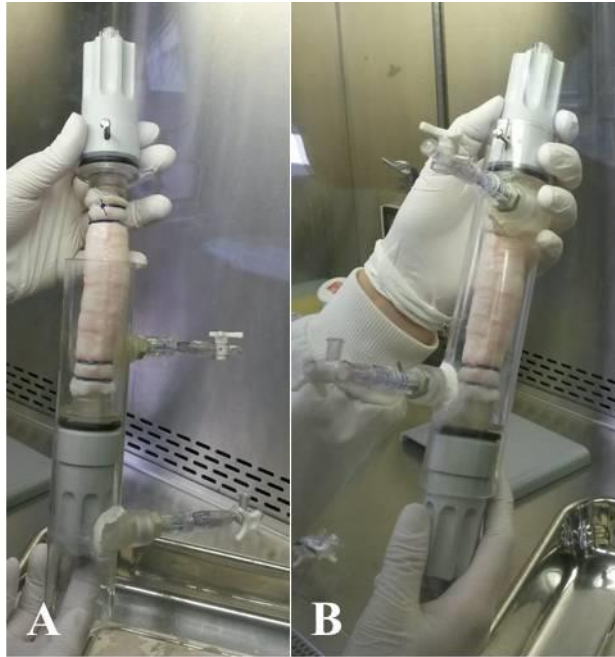


Figure 4.6: The assembled SACs, with the trachea in position, was passed through the bioreactor (A). The screw was slotted into a slit in the bioreactor wall and assisted with the tightening of the top SAC. The bottom SAC was then tightened, taking care not to twist the trachea (B).

4.3.3 Visual analysis of the mixing of internal and external flows in the pressurised transmural bioreactor v1.0

With the manufacture of the pressurised transmural bioreactor v1.0 complete, it was prudent to assess the fluid flow in the internal and external chambers (IC and EC) to see if laminar or turbulent flow type was prevalent and if the fluid flow mixed enough to create a homogenous solution and the time-frame required to achieve a homogenous solution. To visualise the fluid flow in the IC and EC, trypan blue (Sigma Aldrich, Poole, UK) was injected into water that was being pumped into the IC or EC of the bioreactor using a peristaltic pump. The bioreactor was assembled with 6 mm hose barb to G $\frac{1}{8}$ male thread connectors attached to each of the SAC connectors on the internal chamber side. Onto these hose barbs, a section of clear PVC tubing, sized to mimic rabbit trachea, with an ID of 6.4 mm was fixed to create separate internal and external chambers. Onto the two external chamber and two internal chamber ports, 6 mm hose barb to G $\frac{1}{8}$ male thread connectors were attached with 6.4 mm ID silicone tubing (FB56473, Fisher Scientific) attached to the hose barbs, connected to peristaltic pumps (503U and 505S, Watson Marlow, Falmouth,

UK) and placed into solutions reservoirs. The solutions were pumped using peristaltic pumps into either the external or internal chamber. The external chamber pump speeds tested were 10, 20 and 40 rpm. The internal chamber pump speeds tested were 2 and 3 rpm. To assess flow and mixing, the pump was operated at the rpm rate described with water being pumped to either one of the chambers. After continuous flow had been established with no air bubbles visible, trypan blue was injected into the water flow in the tubing and mixing in the bioreactor recorded as video footage (Medical Illustrations, Royal Free Hospital, London, UK). Analysis of the video footage allowed the type of flow and the time taken for mixing to achieve a homogenous solution to be determined.

From the video footage it was possible to determine that in the internal chamber, with a small diameter trachea mimic, predominately laminar flow was achieved with both 2 and 3 rpm pump speeds (Figure 4.7 A-E; 2 rpm data not shown). The pulsatile effect of the peristaltic pump potentially aided achievement of a degree of non-laminar flow with complete mixing observed in the internal chamber after 18 seconds at a pump speed of 3 rpm. However, there was an observable region of unmixed fluid directly adjacent to the inlet port, where the tubing was wider than the port inlet, due to the laminar flow not enabling backward mixing. This region however was minimal and should not have affected the wash effect of the internal flow and could even be mitigated by the transmural flow from the external chamber. Video footage of the mixing in the external chamber, at a pump speeds of 10, 20 and 40rpm (Figure 4.7 F – J and F' to J'; 10 and 40 rpm data not shown), demonstrated turbulent flow with eddies being created by the pulsatile flow and the angle of entrance of the fluid from the inlet port to the bioreactor external chamber (EC). This turbulent flow meant that there were no observable regions of unmixed fluid in the external chamber and complete mixing was observed in the external chamber after 35 seconds at a pump speed of 40 rpm, 70 seconds at a pump speed of 20 rpm and 2 minutes 23 seconds at a pump speed of 10 rpm (Figure 4.8:Figure 4.8). This suggested a linear relationship between mixing time and pump speed in the EC. The fluid flow experiments demonstrated that independent flow with complete mixing of the solutions could be achieved in both the internal and the external chambers.

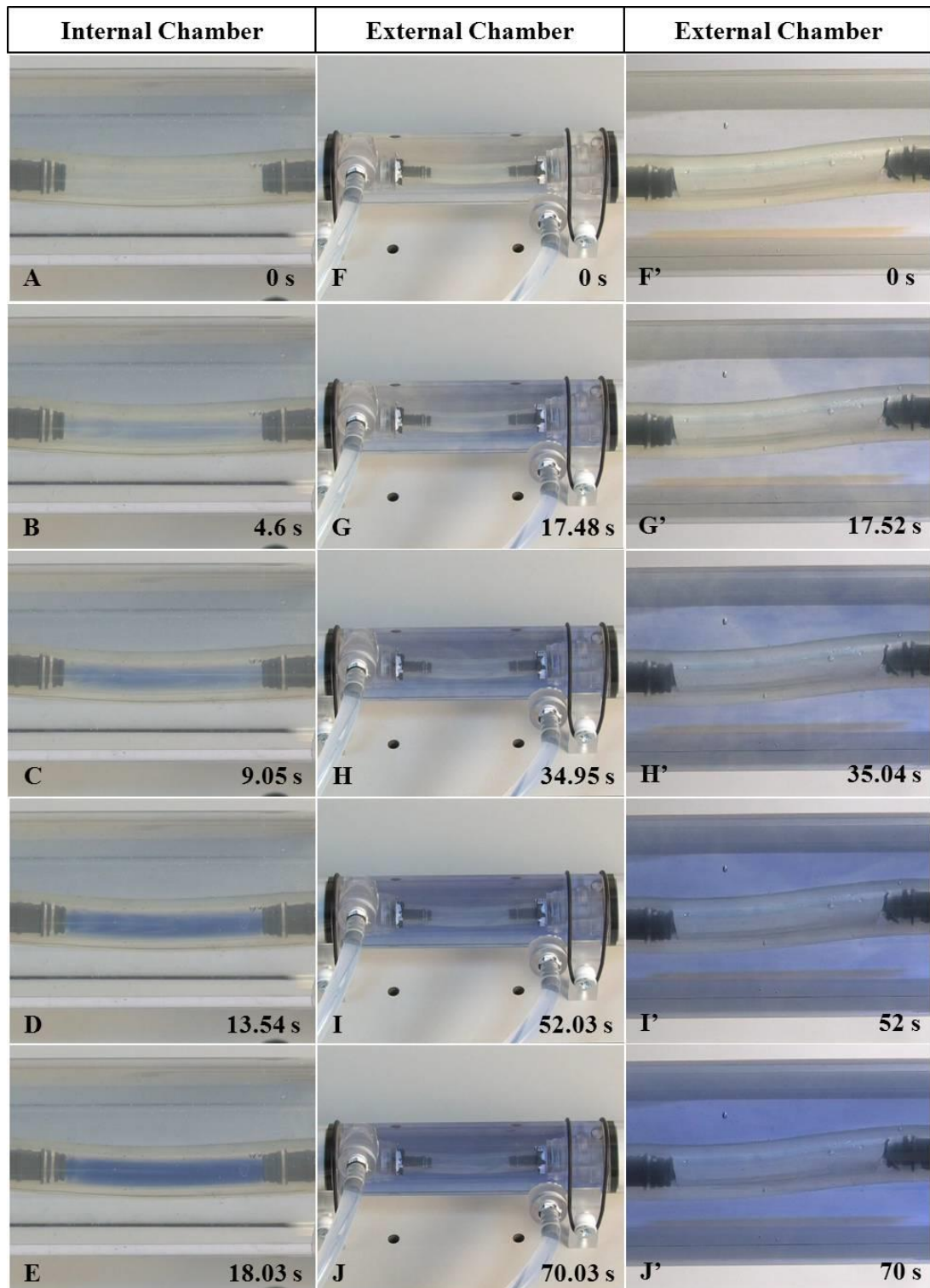


Figure 4.7: Stills were captured from mixing experiments on the internal and external chamber. The internal chamber experiment demonstrated laminar flow that took 18.03 seconds to fully mix post injection of the dye at a pump speed of 3 rpm (A – E). The external chamber experiment demonstrated turbulent flow that took 70

seconds to fully mix post injection of the dye at a pump speed of 20 rpm (F – J and F’- J’).

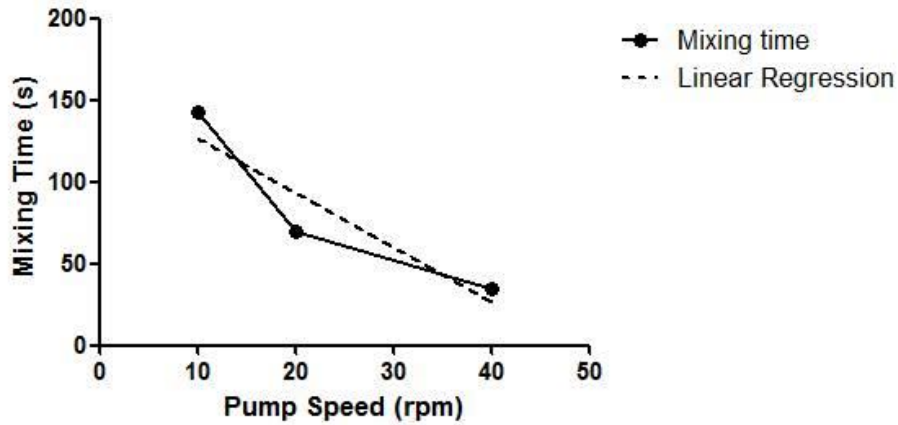


Figure 4.8: The mixing time for the specified pump speeds tested indicated there was a linear relationship between the two factors. N = 1.

4.3.4 Transmural flow testing in bioreactor design v1.0

Having established that independent flow could be achieved, the bioreactor design v1.0 was set up to determine if transmural flow from the EC to the IC could be achieved. This would be tested by pumping a blue coloured solution through the EC at a higher pressure than a clear solution pumped through IC and observing if any blue dye had transmurally flowed into the IC. This involved setting up the bioreactor as described in section 4.3.2 with a porcine trachea *in situ* securely attached between the internal parts of the two SACs using thin copper wire stripped from electrical cable. Once the trachea had been securely attached, male G $\frac{1}{8}$ to 6 mm hose barbs connectors (795-102, RS Components, Corby, UK) were attached to the SAC ports and to the bioreactor side ports with the addition of polytetrafluoroethylene (PTFE) tape (RS components, Corby, UK) in the threaded joints to ensure a good seal would be maintained under pressure. Silicone tubing, with an ID of 6.4 mm, was attached the hose barbs at all four bioreactor ports. Ratchet tubing clamps (Sigma Aldrich, Poole, UK) were attached to tubing within close proximity of the four ports. Online analogue pressure gauges which could measure 0-6 bar (2435919 RS components, Corby, UK) were connected upstream and downstream of the internal and external chambers using 3-way metal female G $\frac{1}{4}$

T-connectors (3675922, RS components, Corby, UK) and G¹/₄ to 6 mm hose barbs (795-118, RS components). Upstream of the bioreactor for the internal and external chambers, the tubing was placed into two peristaltic pumps (Marlow Watson, Falmouth, UK) to allow for independent control of fluid flow into the separate chambers. The internal chamber tubing upstream of the internal chamber pump was placed into a solution reservoir containing Hank's Balanced Salt Solution (HBSS) (Gibco) with the corresponding return tubing, downstream of the internal chamber, placed into the same reservoir. The external chamber tubing upstream of the external chamber pump was placed into a solution reservoir containing HBSS and 0.4% trypan blue (Sigma Aldrich, Poole, UK) to give the solution a blue colour, with the corresponding return tubing, downstream of the external chamber, placed into the same reservoir. To attempt transmural flow of solution from the external chamber to the internal chamber, the internal and external chamber pumps were run to fill both chambers and remove any air bubbles then run the pumps for the IC and the EC at varying speeds to see if transmural flow could be achieved. Additionally, in case varying pump speeds did not create enough of a pressure differential between the IC and the EC to create transmural flow then the ratchet clamp downstream of the external chamber would be semi-closed to varying levels to create a back pressure in the external chamber and force transmural flow.

The set-up of the trachea in the pressurised transmural bioreactor v1.0 was accomplished successfully and fluid flow was achieved through the internal and external chamber as expected (Table 4.1 and Figure 4.9 A). However transmural flow was not discernibly achieved. Decreasing the speed of the internal chamber pump and increasing the speed of external chamber should have increased the external chamber pressure relative to the internal chamber pressure, however no transmural flow was observed. The additional use of back pressure in the external chamber had no observable effect on the transmural flow either though an interesting effect was noted. As the external pressure increased relative to the internal pressure, the trachealis muscle of the trachea was pushed into the luminal area of the trachea (Figure 4.9 B). Reciprocally, if the internal pressure was increased relative to the external pressure using the downstream clamp on the internal chamber, the trachea swelled, again predominantly at the trachealis muscle (Figure 4.9 C). This indicated that the trachealis muscle region of the trachea was, unsurprisingly, the weakest

region of the trachea in terms of pressure and therefore if pressure is to be applied externally then a steady pressure would need to be maintained to avoid internal collapse of the trachea which would hinder or prevent internal fluid flow at the least and cause structural damage to the trachealis muscle at worst. If pressure is applied internally then over-pressurising could damage or even rupture the trachea in the trachealis muscle region. The results from these transmural flow experiments indicated that achieving transmural flow from the EC (abluminal side) of the trachea to the IC (luminal side) of the trachea would be problematic, due to the collapsible nature of the trachealis muscle and therefore future transmural decellularisation experiments would focus on IC to EC (luminal to abluminal) transmural flow.

Internal chamber pump speed (rpm)	External chamber pump speed (rpm)	Post-EC clamp closure	Time (min)	Effect
3	20	-	15	None
1	20	-	10	None
1	40	-	10	None
1	40	1 notch	10	None
1	40	2 notches	10	Tracheal collapse at back wall.

Table 4.1: Experimental detail and results from the initial attempts to achieve transmural flow. For post-EC clamp closure, the number of notches related to the extent of closure of the ratchet clamp. Incrementally increasing the notch the clamp was closed to, increased the level of closure.



Figure 4.9: Stills from the initial transmural experiments demonstrate the trachea in position (A), the effect of external over-pressurisation (B) causing internal collapse of the trachealis muscle and the effect of internal over-pressurisation (C) causing external strain of the trachealis muscle.

4.3.5 Pressurised transmural bioreactor design v1.1

Hose barbs had been used in pressurised transmural bioreactor design v1.1 and had provided secure attachment of the silicone tubing with a wide range of connector types. However the ability to connect the ancillary parts of the bioreactor design together was limited due to the connectors requiring a short section of silicone tubing between each other. This meant the design required structural support in several areas of the set up. It was proposed that the hose barbs connectors would be changed to luer connectors. Luer connectors can be directly connected to each other without the need for additional tubing and although the connectors have limited load bearing, the luer connectors would create a rigid structure. Luer connectors are also available in an extremely wide variety of connectors therefore changing to luer connectors would allow for easy modification and future adaptation of the bioreactor's ancillary parts. Luer connections are also widely used for medical and clinical applications and therefore provided a semi-closed system more suitable for GMP translation.

The hose barbs (Figure 4.10 A & B and Figure 4.12 A) were replaced by luer lock connectors (Figure 4.11 A - G and Figure 4.12 B & C) to create an entire luer connector based system. The luer connectors produce a semi-closed system which allowed media changes to be performed at a lower risk of contamination in an open laboratory environment. For research purposes, this was advantageous as it meant the bioreactor system was no longer dependent on being run in or transferred into a class II microbiological safety cabinet when performing media changes. With regard to future translation to a GMP process, luer connectors can be produced to GMP required standards and be sterilised using a GMP validated procedure by the Royal Free London NHS Foundation Trust Central Sterile Services Department (CSSD). Luer connectors are also commonly used to dock sterile single-use monitoring devices such as temperature probes and pressure transducers. Establishing a luer based connection system enabled an easy system for setting up and connecting the bioreactor with the ancillary parts and the wide variety of connection options future-proofed the system to allow easy integration of temperature probes and pressure transducers.

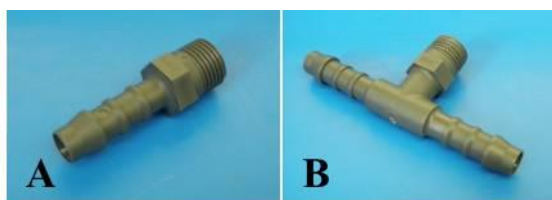


Figure 4.10: 6 mm hose barb to G¹/₄ male thread (A) and T-connector with 6 mm hose barbs to G¹/₈ male thread (B).

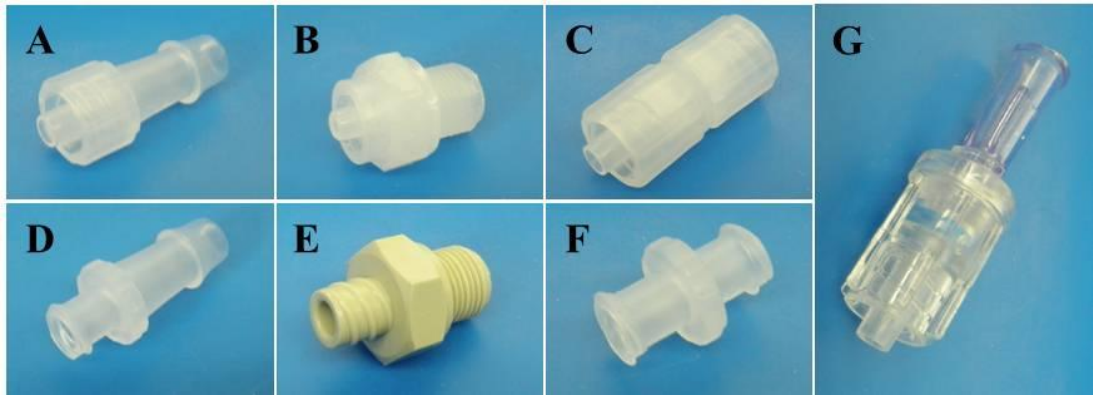


Figure 4.11: 6.4 mm hose barb to male luer (A), male luer to G $\frac{1}{8}$ male thread (B), male luer to male luer (C), 6.4 mm hose barb to female luer (D), female luer to G $\frac{1}{8}$ male thread (E), female luer to female luer (F), male luer to female luer rotating connector (G).

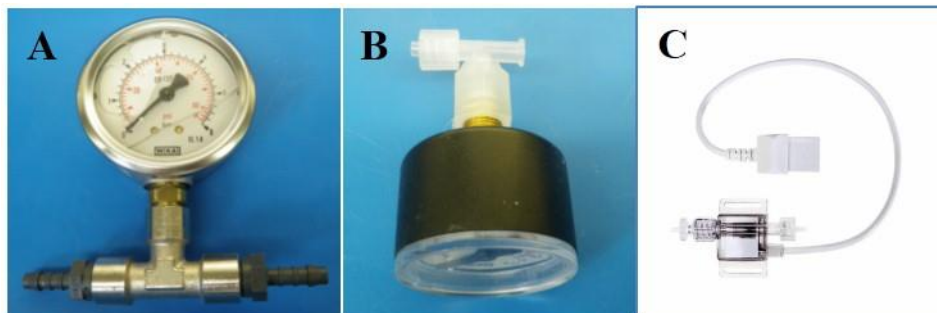


Figure 4.12: 0 - 6 bar pressure gauge connected to a 3 way t-connector (3 G $\frac{1}{4}$ female threads) and G $\frac{1}{4}$ male thread to 6 mm hose barbs (A). 0 -1.6 bar pressure gauge connected to a G $\frac{1}{8}$ female thread to male luer and a 3 way t-connector (2 female and 1 male luer) (B). A male luer to female luer pressure transducer (C).

4.3.6 Pressurised transmural bioreactor design v1.2

Watson Marlow peristaltic pumps 503U and 505S were used in the early process development stages of transmural decellularisation. Both pumps utilised a pump head type with two sprung rollers (Figure 4.13 A). The tubing used was Fisherbrand peristaltic pump grade silicone (FB56473, Fisher Scientific) which was Food and Drug Administration (FDA) approved and certified to USP XXII class 6 and commonly used in the field of medicine (Figure 4.13 A). During the course of early experiments, which could last up to 10 days or 240 hours, tube creep of the silicone

tubing would commonly occur, mostly with devastating consequences. The tubing, after a certain amount of creep, would ultimately form a loose section that would be caught by the pump head, become entangled around the pump head, which would rip the tubing, causing loss of the decellularisation solution and prevent the pump head from spinning (Figure 4.13 B and B'). Experiments where this occurred resulted in the experiments having to be discontinued as it commonly occurred overnight. Consultation with various experts in the field recommended replacement of both the pump type and tubing type. The replacement pump that was selected was the Watson Marlow 323Dz which featured top tube loading head with a four cartridge roller (Figure 4.13 C). The replacement tube type that was selected was Bioprene tubing (933.0064.016, Watson Marlow) which was certified to USP Class VI, FDA compliant and suitable for biopharmaceutical applications (Figure 4.13 C). This replacement tubing was rated to have a pump life of approximately 10,000 hours continuous usage in a peristaltic pump and should therefore add extra process security by greatly reducing the likelihood of the tube splitting.

Replacement of the pump to the top-loading head type with Bioprene tubing instantly increased the reliability of the bioreactor system and allowed multiday decellularisation protocols to be completed without incidents and therefore allowed the development of the decellularisation process. Further development of the pressurised transmural decellularisation (PTD) system incorporated a top-loading pump (Figure 4.13 D) from Harvard Apparatus (Harvard Apparatus, Holliston, USA) which was controlled and the pump speed recorded by the Bio_1 software (Harvard Apparatus, Holliston, USA). The Harvard Apparatus pump developed a fault and therefore was only used for a few experiments. The Marlow Watson D323Z was then reinstalled into the system and used in subsequent experiments.

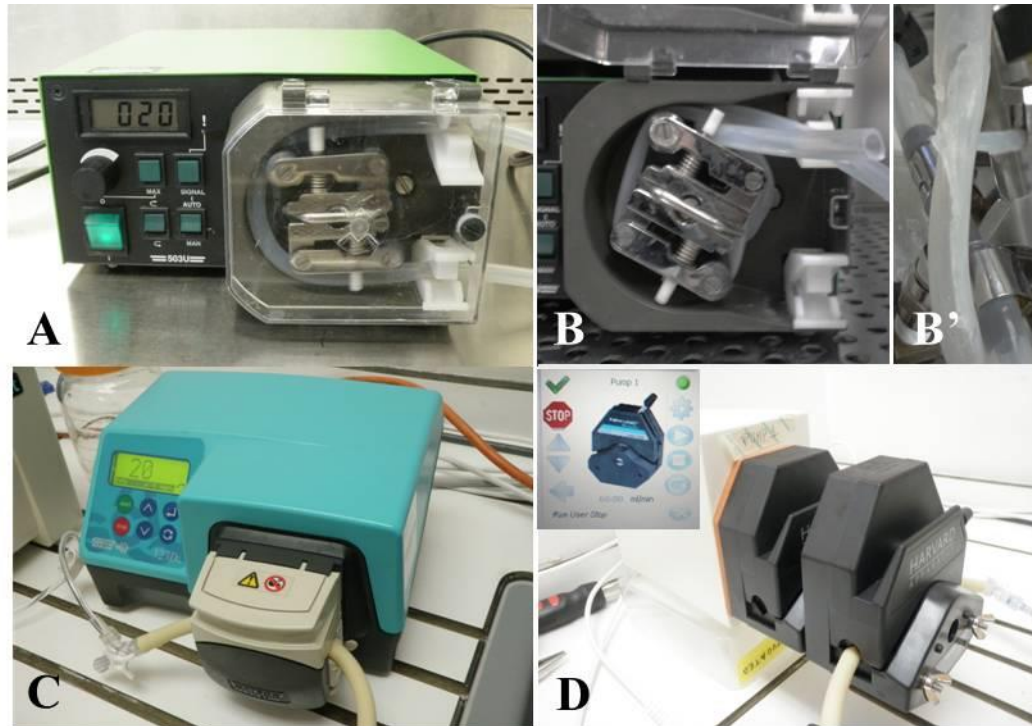


Figure 4.13: The pumps used in early experiments were the Watson Marlow 503U (A) and 505S (not shown) peristaltic pumps which both utilized a two sprung rollers pump-head. The tubing was 6.4 mm ID silicone tubing. Due to tubing creep, common with the two sprung roller type of pump-head over long experiments, the tubing frequently became entangled in the pump head (B) and in doing so shredded the tubing (B') causing leakage of the decellularisation solution. As this tended to occur overnight, it meant the experiment frequently had to be abandoned. Another style of peristaltic pump with top tube loading and a four cartridge roller (C) along with 6.4 mm ID Bioprene tubing was adopted which mitigated tube creep and established reliability to the pump system which allowed the development of the bioreactor system to progress. After development of the pressurised transmural method, the system was transferred to the Harvard Apparatus OCRA controller and so the use of their peristaltic pump (D) was briefly used which was controlled via the Bio_1 software (D inset).

4.3.7 Pressurised transmural bioreactor design v1.3

Initially ratchet tubing clamps (Figure 4.14 A) were used to create a back pressure in the internal bioreactor chamber but they were not suitable as they were not sensitive enough for fine adjustment required to stably create the required pressure, which

would result in either under-pressurisation or over-pressurisation. This would either not create enough pressure to achieve transmural flow or damage the tracheae respectively for the subtle tube clamping required to create a stable pressure in the internal chamber of the trachea for decellularisation. Due to this the ratchet tubing clamps were replaced by Hoffman clamps (Figure 4.14 B) which could be finely adjusted to clamp the tubing and create the desired back pressure in the bioreactor chamber, which was measured using an analogue pressure gauge. However as the pressure was created by clamping the tubing, attaining the required pressure was a tedious process which required multiple fine re-adjustments over several hours. Even when the pressure appeared to have stabilised, any creep or slight movement of the tubing or clamp could cause a slow increase or decrease in the pressure in the chamber resulting in either damage or rupture to the tracheae or a lack of transmural flow due to insufficient pressure. Due to the unreliability of the Hoffman clamps, the early pressurised transmural decellularisation experiments were often prone to failure and there was a need to improve the mechanism for attaining stable pressure within the IC of the bioreactor.

The proposed solution was to use luer one way check valves (Smart Products, Morgan Hill, USA) which were purchased customised to open or crack at a specified pressure (Figure 4.14 C). The check valve after the internal chamber was set to 4.82 psi. This check valve set the pressure in the internal chamber so that only once this pressure had been achieved in the internal chamber did the check valve open and allow flow of the decellularisation solution. The concept was to have a check valve before and after the internal chamber. This would isolate the internal chamber of the bioreactor because the check valves also had a high back pressure capacity of approximately 60 psi, so the back pressure would not affect the pump or solution reservoir.

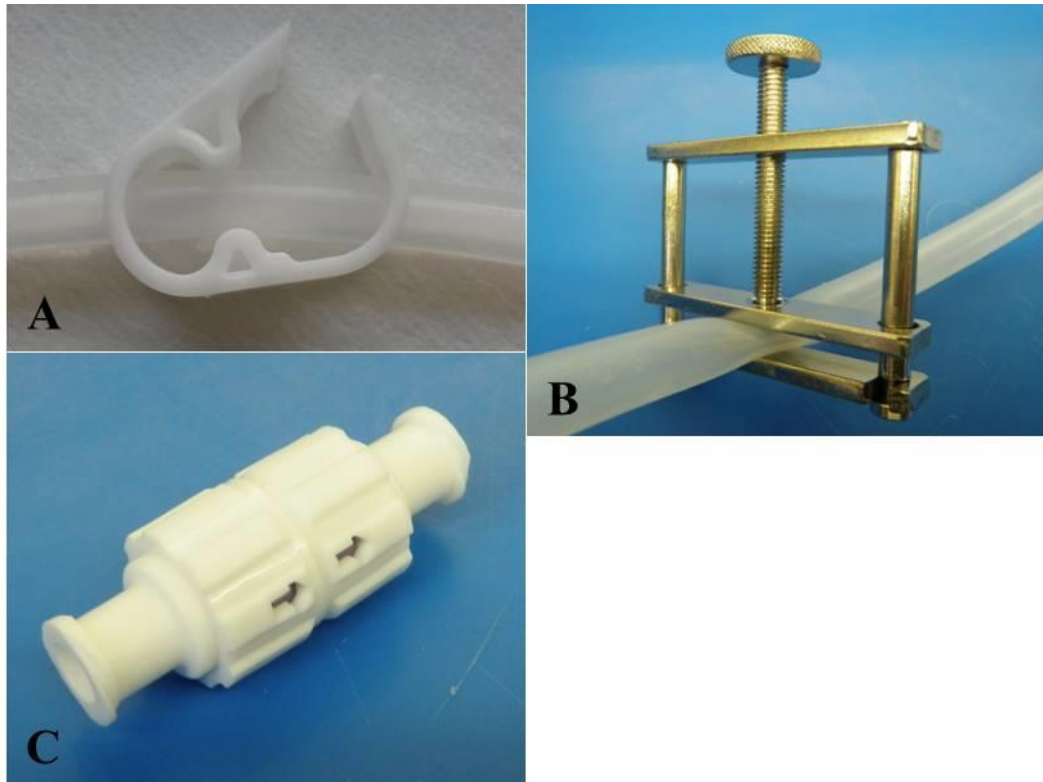


Figure 4.14: The use of ratchet tubing clamps (A) did not allow for fine enough control when creating a back pressure to achieve transmural flow. Replacement with the Hoffman clamps (B) allowed for fine control to transmural flow via back pressure but did not provide long-term stable pressure over multiple days of use. Replacement by one-way check valves (C) set at manufacture to the desired cracking pressure allowed for long term stable transmural flow over multiple days without the need for user intervention.

After testing samples of one-way check valves at various set pressures (0.09, 4.82, 7.5, 13.24, 16.56 psi), two one-way check valves were incorporated into the system with both check valves set at 4.82 psi (0.33 bar). The first check valve was placed upstream of the internal chamber of the transmural bioreactor and monitoring instrumentation. The second check valve was placed downstream of the transmural bioreactor and monitoring instrumentation. The incorporation of the one-way check valves was a major process development breakthrough in maintenance of a stable pressure within the IC (Figure 4.15) to create transmural flow without appearing to damage or rupture the tracheae. Along with the simultaneous replacement of the pump and tubing, the check valves created a reliable decellularisation system which

could run without issues over multiple days, which allowed pressurised transmural decellularisation methodologies to be evaluated.

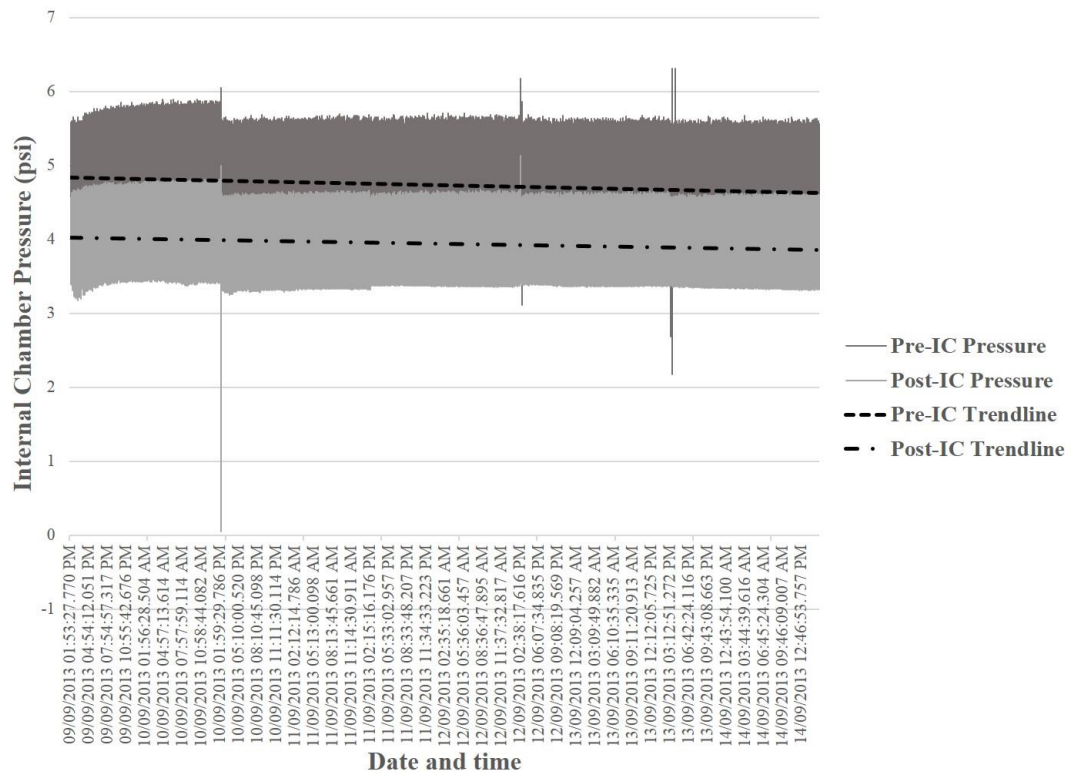


Figure 4.15: Readings from the ORCA controller from the pressure transducers positioned pre and post the internal chamber (IC), or tracheal lumen, demonstrated the average pre-IC pressure was 4.79 ± 0.17 psi and the average post-IC pressure was 4.00 ± 0.16 psi with an average difference of 0.79 psi between the two pressure transducers.

4.3.8 Pressurised transmural bioreactor design v1.4

One of the conclusions from chapter 3.6 stated that performing certain decellularisation steps at 37°C could be beneficial and therefore methods to warm the decellularisation solutions and bioreactor were explored. The early attempts at decellularisation solutions and bioreactor were explored. The early attempts at decellularisation were initially carried out in a 37°C , 5% CO_2 , humidified cell culture incubators to warm the decellularisation solutions and the internal and external chambers to 37°C (Figure 4.16 A). Any leaks from the bioreactor system required the cleaning and decontamination of the entire incubator, rendering it unuseable for several days. Peristaltic pumps are also not best suited to the heated and humidified environment and can fail as a result. Additionally, if the pump started

to overheat then this had a subsequent effect of preventing the incubator from maintaining its set temperature. An ideal solution would be to have access to a non-humidified incubator/oven capable of maintaining 37°C to prevent corrosion of the internal components of the pump. Also to prevent the pump from overheating it would be preferable to position the pump outside of the 37°C incubator whilst fitting the media reservoir and bioreactor inside the incubator and running the tubing through an access port. However exclusive access to a non-humidified 37°C was not feasible and the tubing and access requirements to house the pump outside of the current incubator made doing so prohibitive. The alternative solution to achieve running the process at 37°C was to set up a water bath (Grant Instruments, Shepreth, UK) adjacent to the peristaltic pump for the solution reservoir to be heated to 37°C before the solutions were pumped through the bioreactor (Figure 4.16 B). The bioreactor, and the ancillary parts of the bioreactor, were also set up in a sink drainage area so any leaks could be easily contained and cleaned up (Figure 4.16 B). Because the decellularisation process was to be performed on the laboratory bench, it became essential to monitor the temperature of the internal chamber. Online temperature monitoring using temperature probes, (TC-02 Biorep, Miami, USA or PIT-6 Physitemp Instruments Inc, Clifton, USA) with tuohy borst adapters (Biorep, Miamo, USA (80409 Qosina, Edgewood, USA)) to allow connection to the bioreactor, were set up to monitor the temperature of the solutions pre-entry to and post-exit from the internal chamber to determine any temperature difference across the chamber (Figure 4.16 C and D). The temperature was displayed using either the Mon-a-therm 6510 (Mallinckrodt Medical, St. Louis, USA) (Figure 4.16 B), which was only capable of measuring the current temperature at the two sites, or the ORCA Bioreactor system (Harvard Apparatus, Holliston), which could measure and digitally record the temperatures.

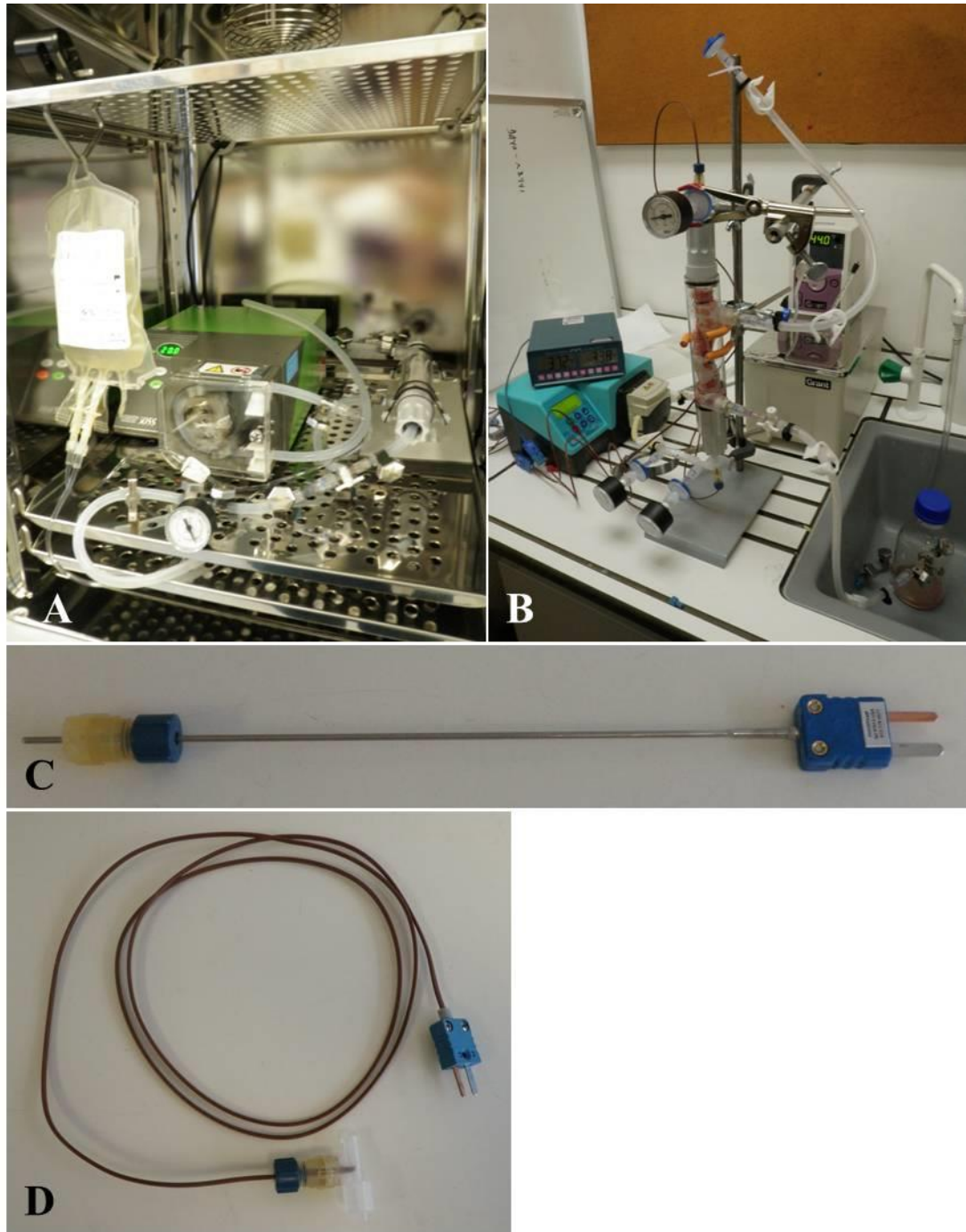


Figure 4.16: Early experiments were performed in a 37°C CO₂ to maintain the experiment at 37°C (A). This potentially caused instrument failure of the incubator. Therefore the experiment was moved to a laboratory bench where a water bath was used to heat the decellularisation solution (B). Temperature probes from Harvard Apparatus (C) and Biorep (D) were used to monitor the solution temperature in the internal chamber.

As expected, the addition of a water bath to warm the decellularisation solutions allowed the bioreactor system to be positioned on a laboratory bench (Figure 4.16 B) and nullified the dependency on a 37°C incubator (Figure 4.16 A). Additionally, by setting the system up on a laboratory bench, it should reduce the incidence of pump or incubator failure. Integration of temperature probes positioned immediately upstream and immediately downstream of the internal bioreactor chamber allowed for monitoring of the solution temperature across the chamber. However, relying solely on a water bath to provide a heated environment did have its limitations. Most predominately there was a temperature drop of 9.31°C of the solution temperature from the solution reservoir in the water bath to the temperature probe positioned upstream of the internal chamber, due to the exposure of the tubing to a room temperature environment. In addition there was a temperature loss of 0.84°C detected between the upstream and downstream temperature probes. To compensate for this, the water bath was set to 42.9°C, however due to the extent of temperature loss and the desire to not overheat or potentially denature the enzymes in the decellularisation solutions, this resulted in an average internal chamber temperature of 33.35°C over the course of decellularisation process instead of the required temperature of 37°C (Figure 4.17). Employment of a pump that was suited to use in a 37°C incubator and performing the decellularisation in a 37°C incubator could have resolved this issue. Alternatively, sourcing a heat jacket with an integrated solution heating or cooling device with an online feedback mechanism to achieve the desired temperature of 37°C in the luminal and abluminal chambers, as commonly utilised in stirred tank bioreactor systems, would provide an ideal resolution to this issue. After use in several PTD experiments, the Biorep temperature probe (Figure 4.16 D) was deemed unsuitable for the pressurised transmural decellularisation process as the application of pressure caused the passage of the decellularisation solution inside the temperature probe casing, which would then leak out at T-type connector on the temperature probe. As this was a safety concern, this temperature probe was replaced by a solid metal temperature probe (Figure 4.16 C) which had no such issues.

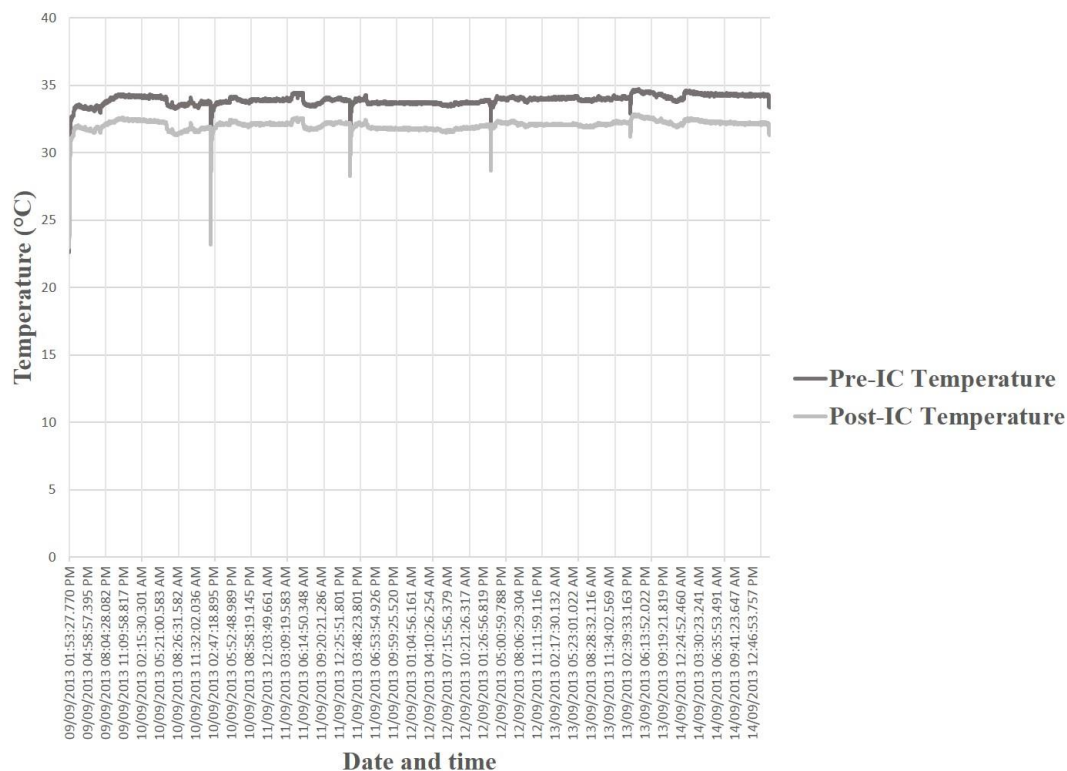


Figure 4.17: Readings from the ORCA controller from the temperature probes positioned pre and post the internal chamber (IC), or tracheal lumen, demonstrated the average pre-IC temperature was $33.59 \pm 0.66^{\circ}\text{C}$ and the average post-IC temperature was $33.10 \pm 1.31^{\circ}\text{C}$ with an average difference of 0.84°C between the two temperatures probes.

4.3.9 Pressurised transmural bioreactor design v1.5

The bioreactor was initially set up horizontally on a stand (Figure 4.18 A) manufactured by Alan Craig (Biochemical Engineering Workshop, UCL). It was realised that in this orientation it was difficult to completely fill the lumen of the trachea (the internal chamber) as an air pocket would form inside the trachea above the level of the inlet and outlet ports. Removal of this air pocket required raising the outlet port until it was vertically above the inlet port until no more air bubbles could be seen in the outlet tubing. However, air would commonly build back up over the long periods of the decellularisation process. The proposed solution to prevent this air pocket during initial set up and from forming during the decellularisation process was to change the orientation of the bioreactor so that the inlet port was vertically below the outlet port (Figure 4.18 B).

Modifying the bioreactor orientation from horizontal to vertical (Figure 4.18 B) eliminated any build-up of air within the internal chamber.

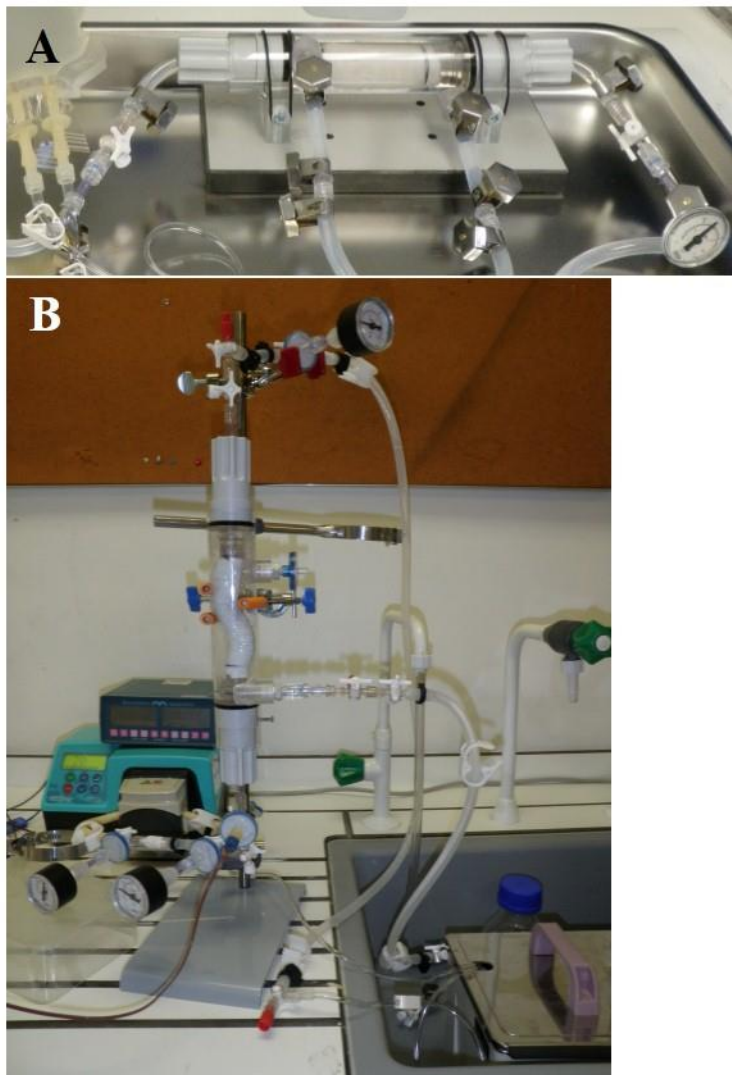


Figure 4.18: Horizontal orientation (A) of the pressurised transmural bioreactor resulted in a build-up of air above the port inlet and outlets. Rotation of the pressurised transmural bioreactor to a vertical orientation (B) prevented any such build-up and allowed total transmural flow through all areas the tracheae.

4.3.10 Pressurised transmural bioreactor design v1.6

When the trachea was attached to the SAC and placed under internal pressure, the trachea would deform due to the pressure and leave the trachea twisted. To prevent this deformation, a GMP-grade wire mesh (Figure 4.19 A) (Biorep, Miami, USA) was rolled and crafted into a stent (Figure 4.19 B) to internally support the trachea *in*

vitro in the bioreactor whilst still allowing unimpeded flow of the decellularisation solutions (Figure 4.19 C).

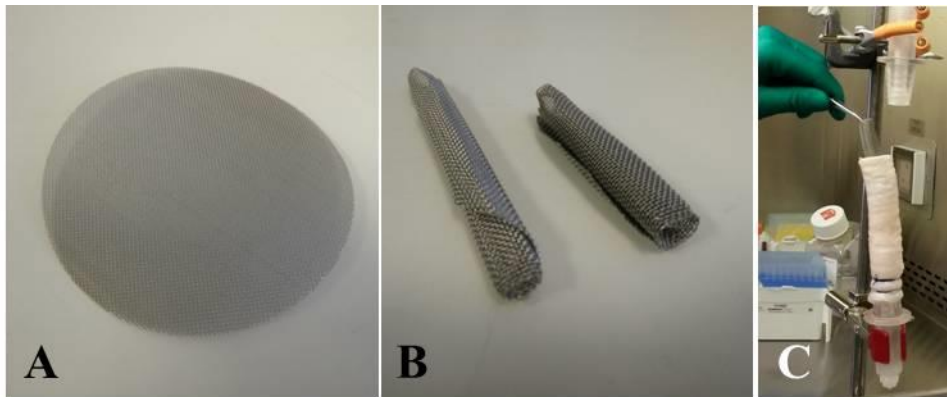


Figure 4.19: GMP grade wire mesh (A) was rolled and trimmed, as appropriate, to produce stents (B) which were then inserted into the lumen of the trachea during tracheal attachment to the SACs (C) as part of the bioreactor assembly.

The addition of the internal stent (Figure 4.19 B) into the lumen of the trachea enabled pressurised transmural decellularisation to be achieved without deformation the trachea (Figure 4.20 A & B). This prevented undue strain being placed onto the tracheae throughout the decellularisation process and could result in an overall stronger scaffold.

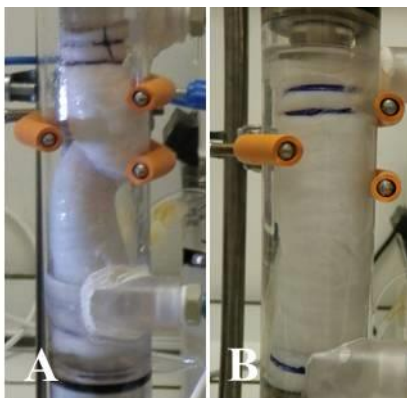


Figure 4.20: Pressurised transmural decellularisation without a stent would cause the trachea to twist and kink (A) which could weaken the tracheal scaffold at that pressure point. The addition of a stent prevented such contortion (B).

4.4 Discussion

Although the initial design, development and manufacture of the actual transmural bioreactor was successfully accomplished and was fit-for purpose without the need to alter the design after the prototype development, the bioreactor is only a small part of a system required to successfully achieve pressurised transmural flow. The ancillary parts of the system required to generate flow and pressure as well as maintain the desired temperature are equally critical to the development of the system. If any one part of the overall bioreactor system did not function correctly then the system failed as a whole, as happened on numerous occasions during the bioreactor development. Initial early experiments that investigated the possibility of creating transmural flow in the system highlighted the issue of luminal obstruction by trachealis muscle collapse when trying to obtain abluminal to luminal transmural flow, therefore the original concept of abluminal to luminal transmural flow was changed to luminal to abluminal flow. Even though this would mean that cell debris from the more populous luminal side could be forced through the wall of the trachea, if the decellularisation protocol was adequate, then full decellularisation should still be achievable. It was also likely that, as the luminal epithelium was very quickly removed during the DEM of decellularisation, that it could be equally rapidly removed by the intra-luminal flow of decellularisation solutions in the PTD method.

Due to the multiple failures of the ancillary parts of the bioreactor system, the initial major issue with the bioreactor system was its stability and reliability in allowing an experiment to be run without failure over the course of several days. The alteration of the system to incorporate a pump with top-loading pump-head, Bioprene tubing and one-way check valves had the most overall dramatic impact on the stability of the bioreactor system. The new pump in collaboration with the Bioprene tubing produced an ancillary fluidic system that did not wear or fail. The new check valves enabled a stable pressure to be created and maintained within the internal chamber of the bioreactor system. The combination of these three changes radically improved the stability and reliability of the bioreactor system and enabled pressurised transmural flow to be achieved continuously over the duration of the experiment. This reliability allowed the focus to shift from optimizing the bioreactor system to developing a decellularisation methodology that could fully decellularise a trachea in a rapid time period in the pressurised transmural bioreactor system. Optimisation of

other aspects of the bioreactor system improved the ease of usability, controllability and reproducibility of the system. The incorporation of the luer connectors allowed for easy set up and commencement of the decellularisation process in the bioreactor system. The luer connectors furthermore allowed for easy adaptation of the bioreactor system set-up and integration of new components such as the check valves and the monitoring instrumentation. The online analogue pressure gauges and online digital temperature probes initially used were limited to solely measuring the pressure and temperature. Therefore only snapshots of the bioreactor system could be recorded. By revising this part of the system to integrate online digital temperature probes and pressure transducers that simultaneously measured and recorded the temperature and pressure every 15 seconds, it provided the ability to analyse the bioreactor's robustness over multiple runs of the system, which would be a necessary step towards validating the decellularisation methodology if it were to be translated to GMP and/or commercialised. Future experimentation could take this further to incorporate feedback loops for both the temperature and pressure from the online measurements to build into the system's automated controls and cascade systems. This was attempted with regard to the pressure control using the ORCA controller (Harvard Apparatus) but not realised due to time constraints and software issues; but would be possible with development. Similarly, with a more sophisticated software package and controller, a solution reservoir with a heat jacket and a heat jacket for the decellularisation bioreactor, feedback loops could also be used to control the solution temperature accurately at 37°C in the decellularisation bioreactor. The use of the stent prevented the tracheae from over-deformation whilst under pressure which could have resulted in superfluous damage to the decellularised scaffolds. The amendment of the bioreactor orientation to vertical prevented any build-up of air pockets which would have impeded the ability to deliver the decellularisation solutions to, and affected the decellularisation potential of, those regions of the trachea.

The only aspect of the system that was not improved by the system amendments was the implementation of the water bath to allow the decellularisation to be performed on the laboratory bench. Although the temperature had not been monitored whilst the decellularisations were attempted in the humidified 5% CO₂ incubator, it was assumed that the solution reservoir and the decellularisation bioreactor chambers

were reliably heated and maintained at 37°C as the surrounding air temperature was maintained at 37°C by the incubator. However the problems caused by installing the bioreactor system inside the incubator made doing so impractical resulting in the water-bath alternative being the only solution. Performing the decellularisation on the laboratory bench at room temperature with sole reliance of heating the entire bioreactor system using the heating of the solution reservoir in a water bath was always likely to be problematic. The desired internal chamber of 37°C was never achieved due to temperature loss from the tubing between the solution reservoir and the bioreactor. To compensate, the temperature of the decellularisation solution reservoir in the water bath was raised above 37°C, however the temperature loss was too substantial to overcome without potentially impacting the stability of the decellularisation solutions. Although the average recorded temperature in the internal chamber was less than the desired temperature, it was still considered an improvement over performing the decellularisation at room temperature and therefore an acceptable compromise. Future experimentation would be well advised to investigate the use of a heated jacket system to additionally warm the decellularisation bioreactor to 37°C to further lessen the impact of heat lost from the tubing.

4.5 Conclusion

The dual chamber bioreactor designed for this project proved itself fit for purpose. It allowed tracheae to be attached and separate luminal and abluminal flow to be achieved. The ancillary parts of the bioreactor system proved to be the challenging aspect of the bioreactor system design and were the common point of failure in the attempt to achieve a pressurised system and transmural flow. The sites of failure were most frequently associated with the peristaltic pump, the tubing and the clamping of the tubing downstream of the internal chamber to achieve the desired backpressure. Optimisation of these ancillary parts and the introduction of two one-way check valves produced a reliable, stable and manually controllable bioreactor system which would allow tracheal decellularisations to be carried out over the multiple days which, from historical evidence, was presumed to be necessary to produce a fully decellularised trachea. Further system improvements could be incorporated in the future such as temperature and pressure control with feedback loops to automatically control the desired temperature and pressure of the decellularisation from predetermined set points and automatically control the filling and drainage of the decellularisation and wash solutions to and from the IC and EC chambers.

5 Pressurised transmural decellularisation

5.1 Introduction

Limitations associated with the scalability and automatability of the DEM of decellularisation process, which took approximately 28 working days to complete, and the quality of the scaffold product derived using the passive DEM of decellularisation for the trachea (Conconi, De Coppi et al. 2005)) drove the need to develop an alternative method for decellularisation. Specific quality issues related to the loss of biomechanical strength of the resulting scaffold and the inadequate removal of DNA from the ECM of the scaffold (Partington, Mordan et al. 2013) meant that an innovative approach was necessary to develop an alternative method of decellularisation. Therefore, whilst building on prior experience and success in the field of tissue engineered tracheae, the composition of the applied decellularisation solutions, the temperature of the applied decellularisation solutions and the method of application of the decellularisation solutions were to be investigated. Ideally a quality by design (QbD) approach would be taken in the development of the new method and design of experiments (DoE) used to understand which are the important factors in the decellularisation process and are there any interactions between these factors. However, on the advice of DoE experts, due to the biological variability of the starting material in the porcine model and even more so with cadaveric human tracheae, it would be difficult to create the strict reproducibility required to obtain a design space or window of operation for optimal decellularisation parameters using DoE and QbD. Therefore the more traditional approach of method development where one factor at a time was changed was undertaken.

The composition of the decellularisation solutions utilised in decellularisation can vary greatly from one decellularisation process to another depending on the type of tissue to be decellularised. Due to clinical success using the DEM of decellularisation, detergent and enzymatic solutions were chosen as the basis of the decellularisation solutions for the method to be developed. With regard to detergent selection for tracheal decellularisation, it was preferable to choose a detergent that had shown to achieve good cell clearance whilst causing little disruption to the ECM and cartilage and minimal removal of GAGs from the ECM and cartilage. Sodium deoxycholate had been well documented as a detergent used for tracheal

decellularisation and was commonly prepared as a 4% solution in water ((Conconi, De Coppi et al. 2005, Macchiarini, Jungebluth et al. 2008)). Although sodium deoxycholate was assumed to be more disruptive to the ECM than sodium dodecyl sulphate (SDS) ((Gilbert, Sellaro et al. 2006)), SDS has been reported to damage collagen and remove GAGs ((Gilbert, Sellaro et al. 2006)). Triton X-100 has also been used for tracheal decellularisations in conjunction with sodium deoxycholate prepared in Hank's Balanced Salt Solution (HBSS) in tracheal decellularisation (Lange, Greco et al. 2015) and therefore was incorporated. For the enzymatic selection, DNase is commonly used for DNA degradation and clearance and also RNase is often included to aid with RNA degradation and could be considered beneficial (Bolland, Korossis et al. 2007, Lange, Greco et al. 2015). However RNA is unstable and could degrade easily without the need for RNase, so the addition of RNase should be investigated to minimise the CoG. As previously discussed, the DNase is commonly dissolved in sodium chloride (NaCl), Phosphate Buffered Saline (PBS) or HBSS, however these buffers contain high levels of sodium chloride and potassium chloride which can inhibit or diminish the efficiency of the DNase enzyme. Therefore a DNase buffer which is specifically designed for maximum DNase efficiency such as has been developed for DNA digestion in RNA samples prior to PCR, for example Tris buffer with set concentrations of MgCl₂ and CaCl₂, would be an alternative possible buffer. Tris buffer has been used as a buffer for decellularisation solutions and therefore could possibly be used as the buffer for the detergent, DNase and wash solutions (Bolland, Korossis et al. 2007).

The temperature of applied decellularisation solutions varied greatly in the published literature. In the DEM method, as described in chapter 3, the detergent and enzymatic steps are performed at room temperature and the main wash step was performed overnight at 4°C. This meant that the enzymatic step, which utilises DNase to non-specifically cleave DNA to reduce the length of the DNA strands, was performed at room temperature. DNase is often used to remove DNA from RNA for reverse transcriptase - polymerase chain reaction (RT-PCR). Although some DNase treatment protocols recommend that the DNase treatment can be performed at this temperature, it is widely acknowledged that DNase treatment will often be incomplete at this temperature and remnant DNA will still persist and that DNase is more effective and efficient when incubated at 37°C. It is also worth considering, for

steps performed at “room temperature” that the temperature is not a set temperature and for scientific work is assumed to be between 20°C and 26°C but is often described as 25°C. However, in the UK in the winter, room temperature could be as cool as 16°C - 18°C, which could further reduce the efficiency of DNase if the incubations are performed in a cool environment. Ideally, if processes such as DNase treatment were to be performed at room temperature, they would be controlled and ultimately validated by performing the processes in a temperature-controlled incubator set for example at 25°C which would at least reduce the spatial and temporal fluctuations of performing the lengthy processes on the bench.

As mentioned in section 4.1, the concept of transmural flow for tracheal decellularisation was formed from the comparative technical applicability of tangential flow in tangential flow filtration (TFF). If a positively pressurised solution is passed through a separated internal chamber of a tubular structure and the tubular structure is permeable to the solution, then, as the solution is recirculated, a proportion of the solution will be forced through the wall of the tubular structure. In TFF this application can be used to concentrate solutions or harvest permeate. If it were to be applied to decellularisation, the application can be used to gently force decellularisation solutions transmurally through the trachea and in doing so penetrate the entire thickness of the wall of the trachea rapidly with the decellularisation solutions.

Very few decellularisation methods have employed the use of transmural flow or convective flow as it has also been termed. In one example, bladder decellularisation using distension is described ((Bolland, Korossis et al. 2007)) with the use of detergent and nuclease enzymatic steps, in a similar manner as the DEM. A difference between the solutions used in the two methods is in the base buffer used in decellularisations. For the bladder decellularisation, a Tris buffer was used as the base and wash buffer instead of the water or sodium chloride based buffers that were used in the DEM. Another difference in the bladder decellularisation method was that the detergent used was sodium dodecyl sulphate (SDS) in a Tris buffer. The nuclease step also utilised ribonuclease A as well as deoxyribonuclease I in a Tris buffer (Bolland, Korossis et al. 2007).

In another example, transmural decellularisation of blood vessels, or more specifically human umbilical vein (HUV), was achieved by generating a positive internal pressure gradient using a peristaltic pump upstream of a dual chamber bioreactor and a single one-way check valve downstream of the bioreactor. The decellularisation involved a single solvent-alcohol based solution (acetone and ethanol in water) to lyse the cells through dehydration and as well as solubilisation and removal of the lipids (Montoya and McFetridge 2009, Crapo, Gilbert et al. 2011). This method of solution application demonstrated that internal transmural pressure was able to decellularise these hollow organs more efficiently than simply immersing the organs into a decellularisation solution (Montoya and McFetridge 2009) This method was also submitted and described in the Patent Grant US 7775965 B2 (McFetridge 2010).

Examples detailing the application of transmural flow decellularisation to tracheal decellularisation were not found in the literature indicating that this could be the first example of transmural flow decellularisation in a tracheal model.

5.2 Aims and hypotheses

Aims:

- To develop and optimise a pressurised transmural decellularisation (PTD) protocol that fully decellularises porcine trachea to produce a scaffold that retains important biochemical and biomechanical properties to a comparative level as native trachea.

Hypotheses:

- The dual chamber transmural flow bioreactor will significantly reduce processing time and make the decellularisation process more amenable to scale-out/scale-up and automation.
- Transmural flow produces an active flow of decellularisation solutions through the wall of the trachea which will breakdown and remove cell and cell debris in a continuous flow. Therefore it will achieve full decellularisation of porcine trachea more rapidly than methods such as DEM that rely solely on immersion in and passive diffusion of decellularisation solutions.
- Decreasing the time taken to fully decellularise the trachea and therefore the scaffold exposure to decellularisation solutions will result in better retention of GAG, collagen and biomechanical strength.
- Optimisation of nuclease buffer and the temperature of the nuclease incubation steps will increase the removal and degradation of observable and detectable DNA and nucleic acids.

5.3 Materials and methods

5.3.1 Preparation of the pressurised transmural decellularisation (PTD) decellularisation solution and waste reservoirs

The decellularisation solution reservoirs were prepared as described below for the specific bioreactor versions. For bioreactor version 2.0 there were separate solution and waste reservoirs. The solution reservoir set-up was prepared (Figure 5.1) by inserting two spike to male luer connectors with a 10 cm length of tubing and a pinch clamp (S-M10, Origen Biomedical, Austin, USA) into the two ports on a 600 mL transfer bag.

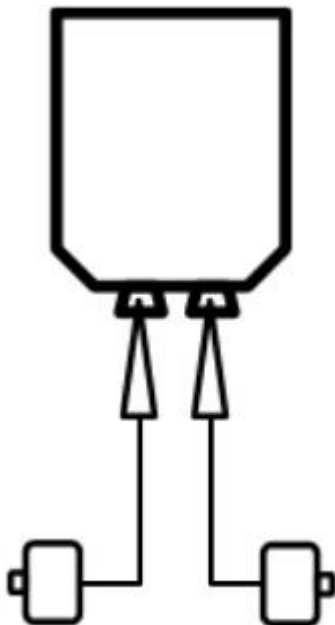


Figure 5.1: Solution reservoir set-up for bioreactor version 2.0 which comprised a 600 mL transfer bag with two male luer lock (MLL) port to spike lines.

The waste reservoir set-up was prepared (Figure 5.2) by inserting 6.4 mm hose barb to female luer lock (FLL) connector into 6.4 mm ID silicone tubing and attaching this to the bottom port of a modified 500 mL Duran that had two 6.4 mm hose barbs added by a UCL glassmaker.

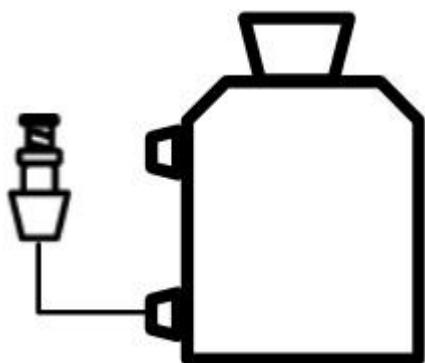


Figure 5.2: Waste reservoir set-up for bioreactor version 2.0 which comprised an adapted 500 mL Duran bottle with two added glass 6.4 mm hose barbs ports. Silicone tubing with the other end connected to a hose barb to female luer lock (FLL) were added to the bottom served as the waste line.

For the bioreactor versions 2.1, 2.2 and 2.3 the solution reservoir set-up was amended and therefore prepared (Figure 5.3) by inserting a spike to two port connector (2P-S16, Origen Biomedical, Austin, USA) into a port of a 600 mL transfer bag (Fenwal, Basingstoke, UK). Into the remaining port on the 600 mL transfer bag and the two ports of the 2 port to one spike, three spike to male luer lock (MLL) connectors with a 10 cm length of tubing and a pinch clamp (S-M10, Origen Biomedical, Austin, USA) were attached.

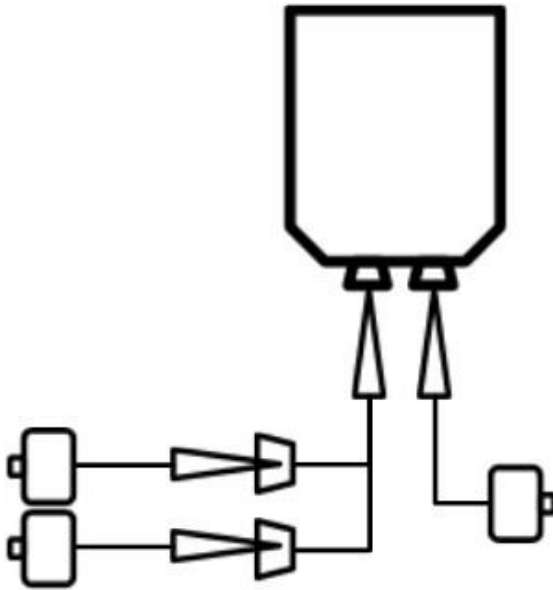


Figure 5.3: Solution reservoir set-up for the bioreactor versions 2.1, 2.2 and 2.3 which comprised a 600 mL transfer bag with a spike to two spike ports adapter and three MLL port to spike lines.

To transfer the media into the solution reservoir, a spike to needle injection site was spiked into a haematology pump segment set at one end. At the other end, the spike of the haematology pump segment was sterilely placed into a 500 mL Duran containing the appropriately prepared and sterilised decellularisation solution. The needle injection site was then removed to reveal a FLL. This was connected to the MLL connector of the inlet spike to solution reservoir and the decellularisation solution pumped (Watson-Marlow, Falmouth, UK) into the transfer bag making sure the appropriate pinch clamps were either open or shut. Once filled, any excess air in the bag was released and the pinch clamps closed.

To drain the decellularisation/waste solution from the transfer bags, all of the ports were opened and the waste drained into a collection vessel where it was then treated with Virkon (VWR, Lutterworth, UK).

5.3.2 Preparation of the pressurised transmural decellularisation (PTD) decellularisation solutions

The decellularisation solutions were investigated to optimise: the type of the solutions used (primarily the buffer/wash used); the concentration of the detergent

solution; the order of application of the decellularisation solutions and the frequency and length of the application.

The decellularisation solutions used are listed below. With regard to the preparation and for the application of the solutions in the PTD experiments refer to Table 5.1.

- The detergent solution (I) consisted of either: a buffer of 1 x HBSS with 2% sodium deoxycholate and 0.3% Triton X-100 mixed until fully dissolved containing 100 units/mL of penicillin, 100 µg/mL of streptomycin, and 250 ng/mL of amphotericin B solution added immediately before use; or a buffer of 50 mM Trizma - HCl (pH 7.2 buffered with Trizma - base) into which between 0.3% to 2.25% sodium deoxycholate and between 0.125% to 0.3% Triton X-100 were mixed until fully dissolved. Details for the exact concentration used are listed in Table 5.1. The detergent solutions were autoclaved and 100 units/mL of penicillin, 100 µg/mL of streptomycin, and 250 ng/mL of amphotericin B solution was added immediately before use.
- The nuclease solutions (I/II) consisted of a buffer of 50 mM Trizma - HCl (pH 7.2 buffered with Trizma - base) with 5.2 mM MgCl₂ and 130 µM CaCl₂. The buffer was autoclaved and to this buffer 2 Kunitz units/mL of DNase (D4263, Sigma Aldrich, Poole, UK), 4U/mL RNase (AM2295, Life Technologies, Paisley, UK) and 100 units/mL of penicillin, 100 µg/mL of streptomycin, and 250 ng/mL of amphotericin B solution were added immediately before use.
- The wash buffers (I/II) consisted of either: a buffer of de-ionised water with 100 units/mL of penicillin, 100 µg/mL of streptomycin, and 250 ng/mL of amphotericin B solution added immediately before use; or a buffer of 50 mM Trizma - HCl (pH 7.2 buffered with Trizma - base), details of the exact buffers used are listed in Table 5.1. The wash buffers were autoclaved and 100 units/mL of penicillin, 100 µg/mL of streptomycin, and 250 ng/mL of amphotericin B solution was added immediately before use.

5.3.3 Bioreactor versions for pressurised transmural decellularisation

5.3.3.1 Bioreactor version 2.0

The bioreactor system was set up as detailed in Figure 5.4 and Figure 5.5. The predominant feature of this version being that the transmural flow was sent to waste and not re-circulated through the system. Briefly, the solution reservoir was positioned into the water bath. Connected to the solution reservoir was the spike to MLL line which connected to a three way stopcock. The stopcock was positioned to allow the inlet to change and air to be pumped through the bioreactor system to clear the lines of decellularisation solution. An optional connection of a 0.22 µm filter would allow the air to be filtered and sterile upon entry. The stopcock connected to a 30 cm section of Bioprene tubing, with MLL to hose barb connectors at each end, with the pump positioned approximately 5 - 10 cm down the pump tubing line to pump the decellularisation solutions through the bioreactor system and internal chamber of the bioreactor. Downstream of the pump tubing was the first FLL to FLL one-way check valve, set at 7.5 psi, to contain the pressurisation to within the next section of the bioreactor system by being capable of holding a back pressure of up to 60 psi. Pressure gauges capable of measuring 0 - 25 psi (1.6 bar) were placed either side of the check valve using luer tee connectors, rotating MLL to FLL and MLL to G1/8 female connectors with a 0.22 µm filter between the pressure gauge and the bioreactor system as the pressure gauges were not sterile. A luer tee connector followed to allow the attachment of the first temperature probe via a MLL to tuohy borst adapter. Between the t-connectors and the bioreactor itself, rotating MLL to FLL connector attached to the lower FLL to male G1/8 port of the bioreactor to allow easy assembly of the periphery lines. The decellularisation solution then passed through the lumen of the trachea which was also described as the internal chamber of the bioreactor. Downstream of the upper FLL to male G1/8 port of the internal chamber another rotating MLL to FLL and a luer tee connector allowed for the attachment of the second temperature probe via a MLL to tuohy borst connector. A third pressure gauge attached via a tee connector, a rotating MLL to FLL, a 0.22 µm filter and a MLL to G1/8 adaptor was positioned just upstream of the second FLL to FLL one-way check valve, set at 4.82 psi, which along with the first one-way check valve created the pressurisation of ~ 4.82 psi within the internal chamber of the bioreactor. After a 3-way stopcock, the solution then returned to the solution

reservoir via the MLL to spike line to allow continuous flow of decellularisation solution within the internal chamber of the bioreactor. Additionally to this, at the start of each decellularisation step, after ensuring no leakage from the internal chamber when the trachea is under pressure, the lower male G1/8 to FLL port of the external chamber was connected to a rotating MLL to FLL, a 3-way stopcock and a MLL to hose barb, to connect to a section of sterile silicone tubing to a MLL to hose barb, a rotating MLL to FLL and a FLL to hose barb and finally a short section of sterile silicone tubing to attach the external chamber to the waste reservoir. The line on the 3-way stopcock was opened to allow drainage of the transmural waste. To the upper male G1/8 to FLL port of the external chamber a sterile silicone tubing line with MLL to hose barb connectors at each end was connected, and a sterile 0.22 μm filter attached, to allow sterile venting of the external chamber and allow the transmural waste to drain to the waste reservoir.

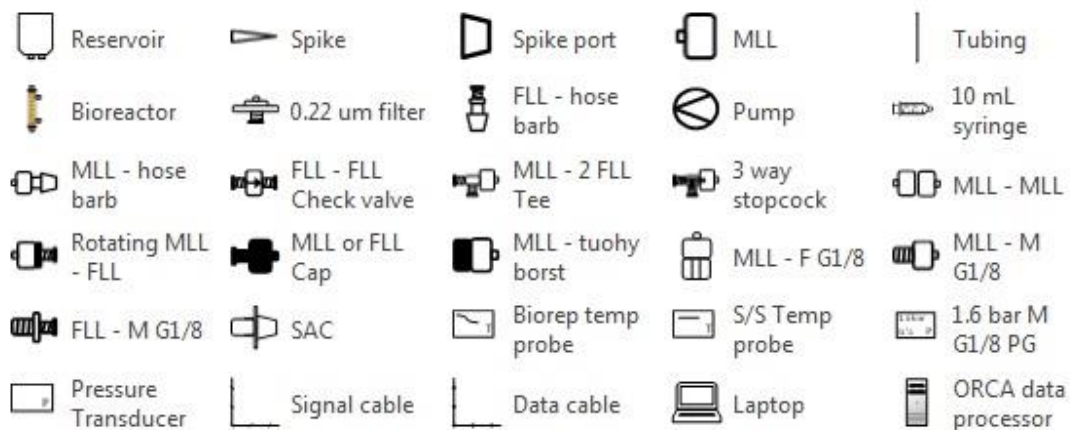


Figure 5.4: Bioreactor system assembly components for bioreactor version 2.0 to 2.3.

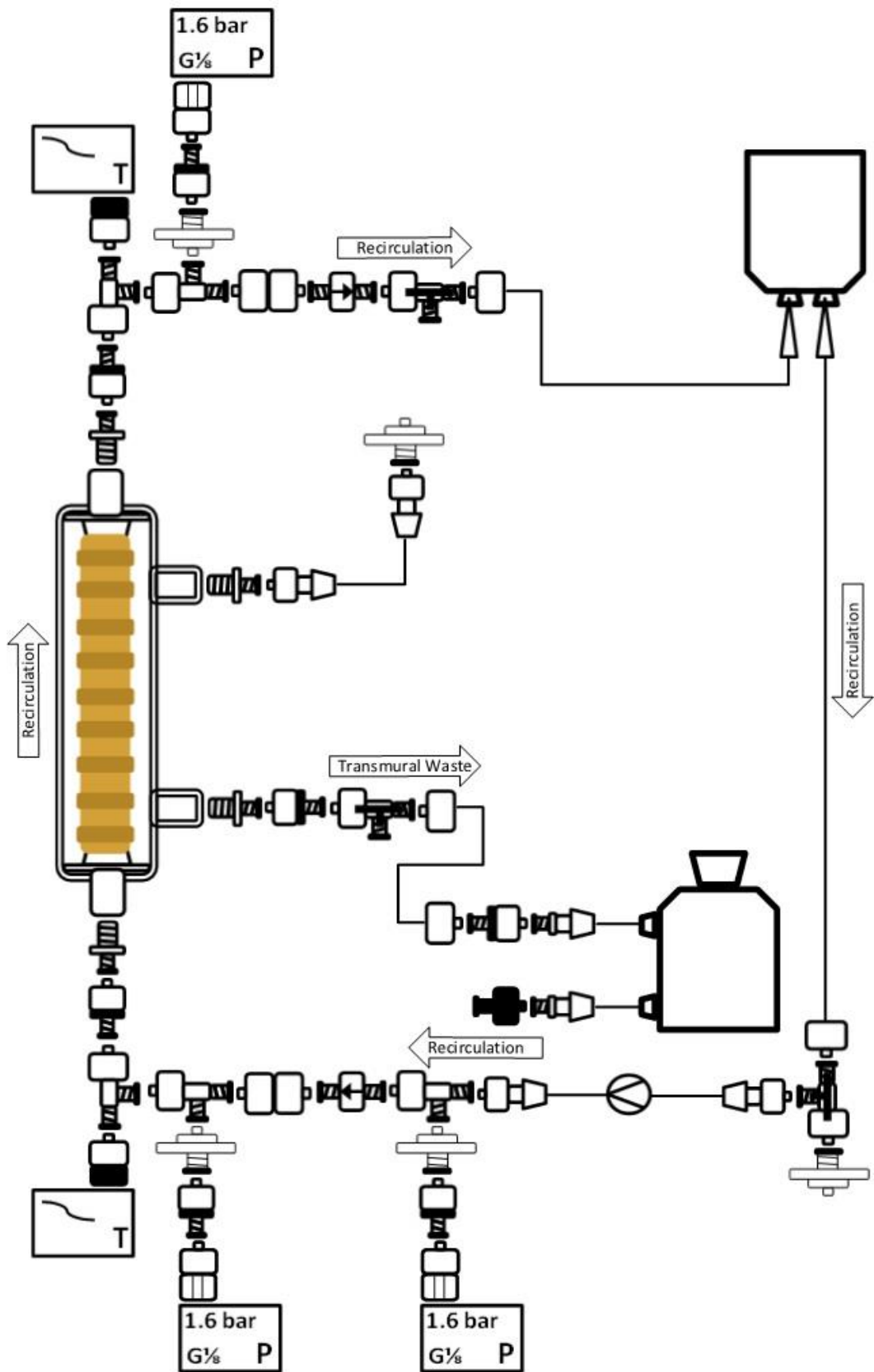


Figure 5.5: Bioreactor version 2.0. With this version the decellularisation solution was recirculated through the internal chamber/lumen of the trachea and the transmural flow was collected in the waste reservoir.

5.3.3.2 Bioreactor version 2.1

The bioreactor system was set up as detailed in Figure 5.4 and Figure 5.6. The main changes from the PTD version 2.0 bioreactor were:

- The pressure gauges were removed from bioreactor v2.1 as evaluation of the pressures from PTD 1-3 experiments in bioreactor v2.0 had demonstrated the check valves reliably produced a pressure in the internal chamber of 4 - 5.5 psi.
- The transmural “waste” line from the outer chamber of the bioreactor was re-positioned so the decellularisation solution was re-circulated back to the solution reservoir as a return line. Therefore there was no transmural waste line.
- The transmural return line from the outer chamber of the bioreactor was relocated to the top port of the bioreactor so the outer chamber would be filled before the solution returned to the solution reservoir to allow the outer surface of the trachea to be immersed in the decellularisation solution.
- For PTD 5 the bioreactor set-up was as described below and for PTD 6 and 7 the bioreactor set-up had the below set-up with the following amendment; the external ports for the internal chamber were changed from a G¹/₈ -female luer to a G¹/₈ -male luer which omitted the need to have male to male adapters before and after the internal chamber.

Briefly, the solution reservoir was positioned into the water bath. Connected to the solution reservoir was the inlet spike to MLL line which was connected to a three way stopcock sandwiched between two rotating MLL to FLL connectors. The stopcock was positioned to allow air to be pumped through the bioreactor system to clear the lines of decellularisation solution. An optional connection of a 0.22 µm filter would allow the air to be filtered and sterile upon entry. The stopcock connected to a 30 cm section of Bioprene tubing, with MLL to hose barb connectors at each end, with the pump positioned approximately 5 - 10 cm down the pump tubing line to pump the decellularisation solutions through the bioreactor system and internal chamber of the bioreactor. Downstream of the pump tubing was a rotating MLL to FLL to aid connection, the first FLL to FLL one-way check valve, set at

4.82 psi, to contain the pressurisation to within the next section of the bioreactor system by being capable of holding a back pressure of up to 60 psi. Next, another rotating MLL to FLL connector connected to a luer tee connector to allow the attachment of the first temperature probe, connected using a MLL to tuohy borst adapter, and a MLL to MLL adapter*. Downstream of the MLL to MLL adapter* there was another rotating MLL to FLL connector which attached to the lower male G1/8 to FLL or a male G1/8 to MLL port of the internal chamber of the bioreactor to allow easy assembly of the periphery lines. The decellularisation solution then passed through the lumen of the trachea which served as the internal chamber of the bioreactor. Downstream of the internal chamber from the upper male G1/8 to FLL port or a male G1/8 to MLL there was a rotating MLL to FLL, connected to MLL to MLL adapter*, another rotating FLL to MLL adapter*, then a luer tee connector which allowed attachment of the second temperature probe via a MLL to tuohy borst adapter. Downstream there was another rotating FLL to MLL connector, the second one-way FLL to FLL check valve, set at 4.82 psi, which along with the first one-way check valve created the pressurisation within the internal chamber of the bioreactor, and finally a 3-way stopcock. The solution was then returned to the solution reservoir via a MLL to spike return line to allow continuous flow of decellularisation solution within the internal chamber of the bioreactor. Connections on the external chamber ports were as follows: the lower male G1/8 to FLL port was closed using a MLL cap; downstream of the upper male G1/8 to FLL port was a rotating MLL to FLL then a 3-way stopcock before connecting to the MLL to spike return line to the decellularisation solution reservoir.

*Due to the change of the internal chamber ports from G1/8 to FLL port to a male G1/8 to MLL, these connectors were not required for PTD 6 and 7.

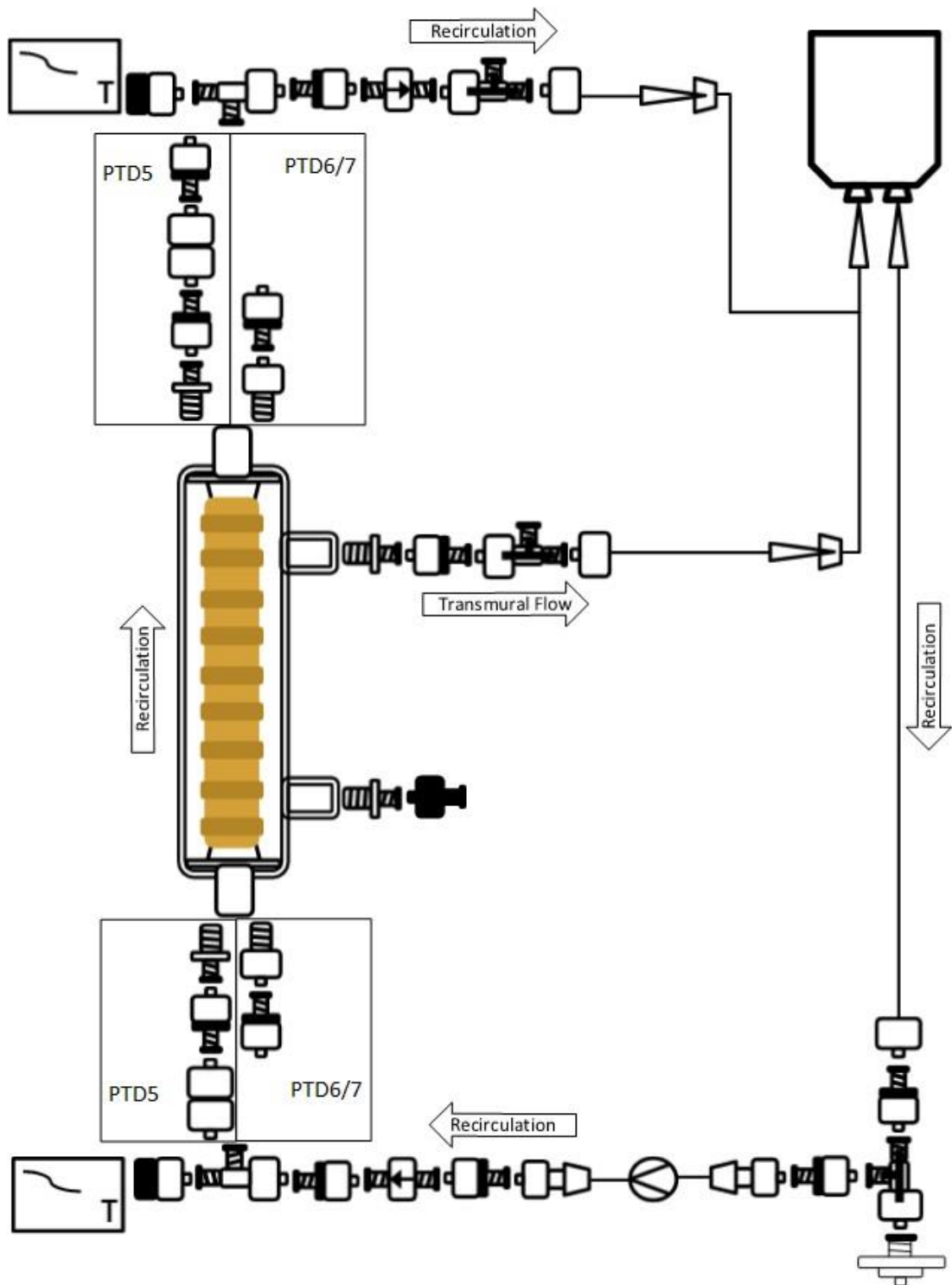


Figure 5.6: Bioreactor version 2.1 with the two differing set-ups from the size adjustable connectors (SACs) for PTD 5 or PTD 6 and 7. With these set-ups the decellularisation solution was recirculated through the internal chamber/lumen of the trachea and the transmural flow was collected in the same reservoir and recirculated.

5.3.3.3 Preparation of porcine tracheal scaffolds by transmural decellularisation version 2.2

The bioreactor system was set up as detailed in Figure 5.4 and Figure 5.7. The main changes from the PTD version 2.1 bioreactor were:

- Three pressure transducers were incorporated to measure digitally the pressure before and after the internal chamber and outside of the external chamber by the upper port.
- The temperature probes were changed from the flexible Biorep temperature probes to Physitemp stainless steel shaft probes (Physitemp, Clifton, NJ, USA) which allowed for an improved seal to be created by the tuohy borst adapter.
- The set-up incorporated the ORCA Controller with the Bio_1 software from Harvard Apparatus Regenerative Technology (Harvard Apparatus, Holliston, USA) to digitally record online the temperature output from the two temperature probes and the pressure output from the three pressure probes. In the previous bioreactor systems this information had been measured via analogue systems and recorded manually.
- Incorporation of a Dino-lite white light digital microscope (IDCP, Naarden, Netherlands) to automate imaging the trachea as it underwent decellularisation and enable remote viewing through live video capture.
- Use of Harvard Apparatus pumps for some of the PTD experiments was incorporated, however after use in a couple of PTD experiments they emitted a strange sound, as if they were on the verge of breaking, and therefore the Watson-Marlow pump was reinstalled.

The bioreactor was as follows. Briefly, the solution reservoir was positioned into the water bath. Connected to the solution reservoir spike port was a spike to MLL line which was connected to a three way stopcock. The stopcock was positioned to allow air to be pumped through the bioreactor system to clear the lines of decellularisation solution. An optional connection of a 0.22 µm filter would allow the air to be filtered and sterile upon entry. The stopcock connected to a 30 cm section of Bioprene

tubing, with MLL to hose barb connectors at each end, with the pump positioned approximately 5 - 10 cm down the pump tubing line to pump the decellularisation solutions through the bioreactor system and internal chamber of the bioreactor. Downstream of the pump tubing was a rotating FLL to MLL to aid connection, the first one-way FLL to FLL check valve, set at 4.82 psi, to contain the pressurisation to within the next section of the bioreactor system by being capable of holding a back pressure of up to 60 psi, a luer tee connector to allow the attachment of the first pressure transducer with a 3-way stopcock and 10 mL syringe and then a second luer tee connector to allow attachment of the first temperature probe, connected using a MLL to tuohy borst adapter. Downstream there was a rotating MLL to FLL connector which attached to the lower male G1/8 to MLL port of the internal chamber of the bioreactor to allow easy assembly of the periphery lines. The decellularisation solution then passed through the lumen of the trachea which served as the internal chamber of the bioreactor. Downstream of the upper male G1/8 to MLL port of the internal chamber, there was a rotating FLL to MLL then a tee connector which allowed attachment of the second temperature probe via a MLL to tuohy borst adapter. Downstream there was another luer tee connector to allow for attachment of the second pressure transducer with a 3-way stopcock and 10 mL syringe. Downstream of the tee connector there was the second FLL to FLL check valve, set at 4.82 psi, which along with the first one-way check valve created the pressurisation within the internal chamber of the bioreactor, a 3-way stopcock and finally a rotating MLL to FLL connector to allow easy connection of the periphery line. The solution was then returned to the solution reservoir via a MLL to spike return line to allow continuous flow of decellularisation solution within the internal chamber of the bioreactor. Connections on the external chamber ports were as follows: downstream of the lower male G1/8 BSPP to FLL port was closed using a MLL cap or a 3-way stopcock; downstream of the upper male G1/8 BSPP to FLL port was a rotating MLL to FLL, then a luer t-connector connector to allow for attachment of the third pressure transducer with a 3-way stopcock and 10 mL syringe then a 3-way stopcock before connecting to the MLL to spike return line to the decellularisation solution reservoir. The 3-way stopcocks and 10 mL syringes downstream of each of the pressure transducers were required to allow the decellularisation solution to be drawn over the pressure transducers to enable the pressure to be accurately measured.

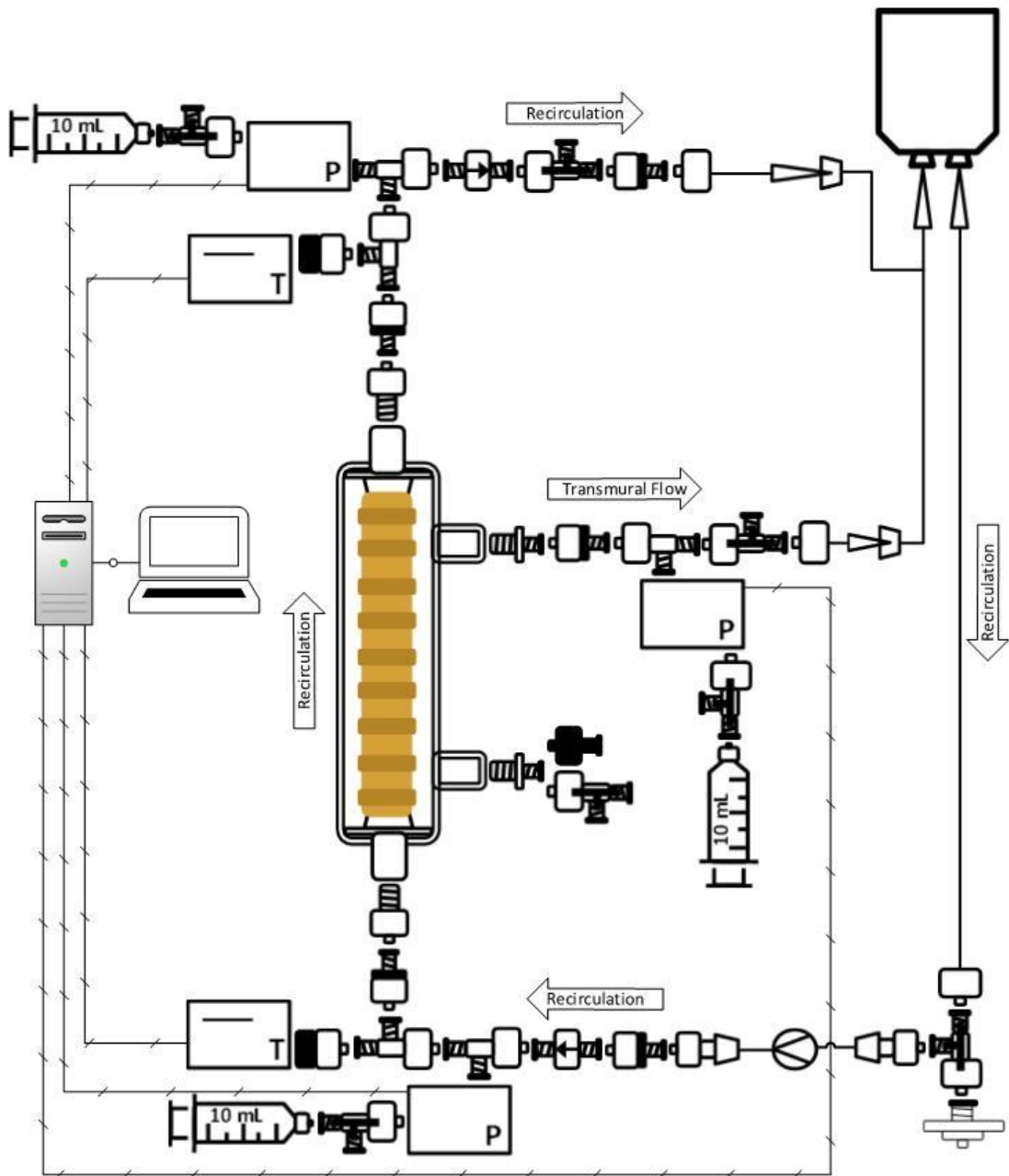


Figure 5.7: Bioreactor version 2.2. With this set-up the decellularisation solution was recirculated through the internal chamber/lumen of the trachea and the transmural flow was collected in the same reservoir and recirculated. The pressure and temperature was measured and recorded online.

5.3.3.4 Preparation of porcine tracheal scaffolds by pressurised transmural decellularisation version 2.3

The bioreactor system was set up as detailed in Figure 5.4 and Figure 5.8. The changes from the PTD version 2.2 bioreactor were:

- Three additional 3-way stopcocks were added. The first was between the luer tee connector and the first pressure transducer, the second was between the luer tee connector and the second pressure transducer and the third was on the lower port of the external chamber after the rotating MLL to FLL. The addition of these three 3-way stopcocks allowed the inner and outer chambers to be emptied of the decellularisation solutions with minimal manipulation of the bioreactor chamber. Prior to the addition of these three stopcocks it was necessary to invert the bioreactor chamber to drain the solution from both chambers. Optional sterile 0.22 µm filters could be added to the upper 3-way stopcocks to ensure the air entering the internal and external chamber of the bioreactor was sterile when draining the internal and external chambers of the bioreactor.
- The removal of the third pressure transducer from the upper port of the external chamber as it was deemed unnecessary.

The bioreactor was as follows. Briefly, the solution reservoir was positioned into the water bath. Connected to the solution reservoir spike port was a spike to MLL line which was connected to a three way stopcock. The stopcock was positioned to allow air to be pumped through the bioreactor system to clear the lines of decellularisation solution. An optional connection of a 0.22 µm filter would allow the air to be filtered and sterile upon entry. The stopcock connected to a 30 cm section of Bioprene tubing, with MLL to hose barb connectors at each end, with the pump positioned approximately 5 - 10 cm down the pump tubing line to pump the decellularisation solutions through the bioreactor system and internal chamber of the bioreactor. Downstream of the pump tubing was the first one-way FLL to FLL check valve, set at 4.82 psi, to contain the pressurisation to within the next section of the bioreactor system by being capable of holding a back pressure of up to 60 psi, a luer tee connector to allow the attachment of the first pressure transducer with an preceding 3-way stopcock to allow easy drainage of the internal bioreactor chamber and a

succeeding 3 way stopcock and a 10 mL syringe. Downstream there was a second luer tee connector to allow attachment of the first temperature probe, connected using a MLL to tuohy borst adapter. Downstream there was a rotating MLL to FLL connector which attached to the lower male G1/8 to MLL port of the internal chamber of the bioreactor to allow easy assembly of the periphery lines. The decellularisation solution then passed through the lumen of the trachea which served as the internal chamber of the bioreactor. Downstream of the upper male G1/8 to MLL port of the internal chamber, there was a rotating FLL to MLL then a tee connector which allowed attachment of the second temperature probe via a MLL to tuohy borst adapter. Downstream there was another luer tee connector to allow for attachment of the second pressure transducer with a preceding 3-way stopcock to aid drainage of the internal chamber and a succeeding 3-way stopcock and 10 mL syringe. Downstream of the tee connector there was the second FLL to FLL check valve, set at 4.82 psi, which along with the first one-way check valve created the pressurisation within the internal chamber of the bioreactor. The solution was then returned to the solution reservoir via a MLL to spike return line to allow continuous flow of decellularisation solution within the internal chamber of the bioreactor. Connections on the external chamber ports were as follows: downstream of the lower male G1/8 BSPP to FLL port was a rotating FLL to MLL and a 3-way stopcock to allow for easy drainage of the external bioreactor chamber; downstream of the upper male G1/8 BSPP to FLL port was a rotating MLL to FLL, then a 3-way stopcock, to allow for easy drainage of the external bioreactor chamber, before connecting to the MLL to spike return line to the decellularisation solution reservoir. The 3-way stopcocks and 10 mL syringes downstream of each of the pressure transducers were required to allow the decellularisation solution to be drawn over the pressure transducers to enable the pressure to be accurately measured.

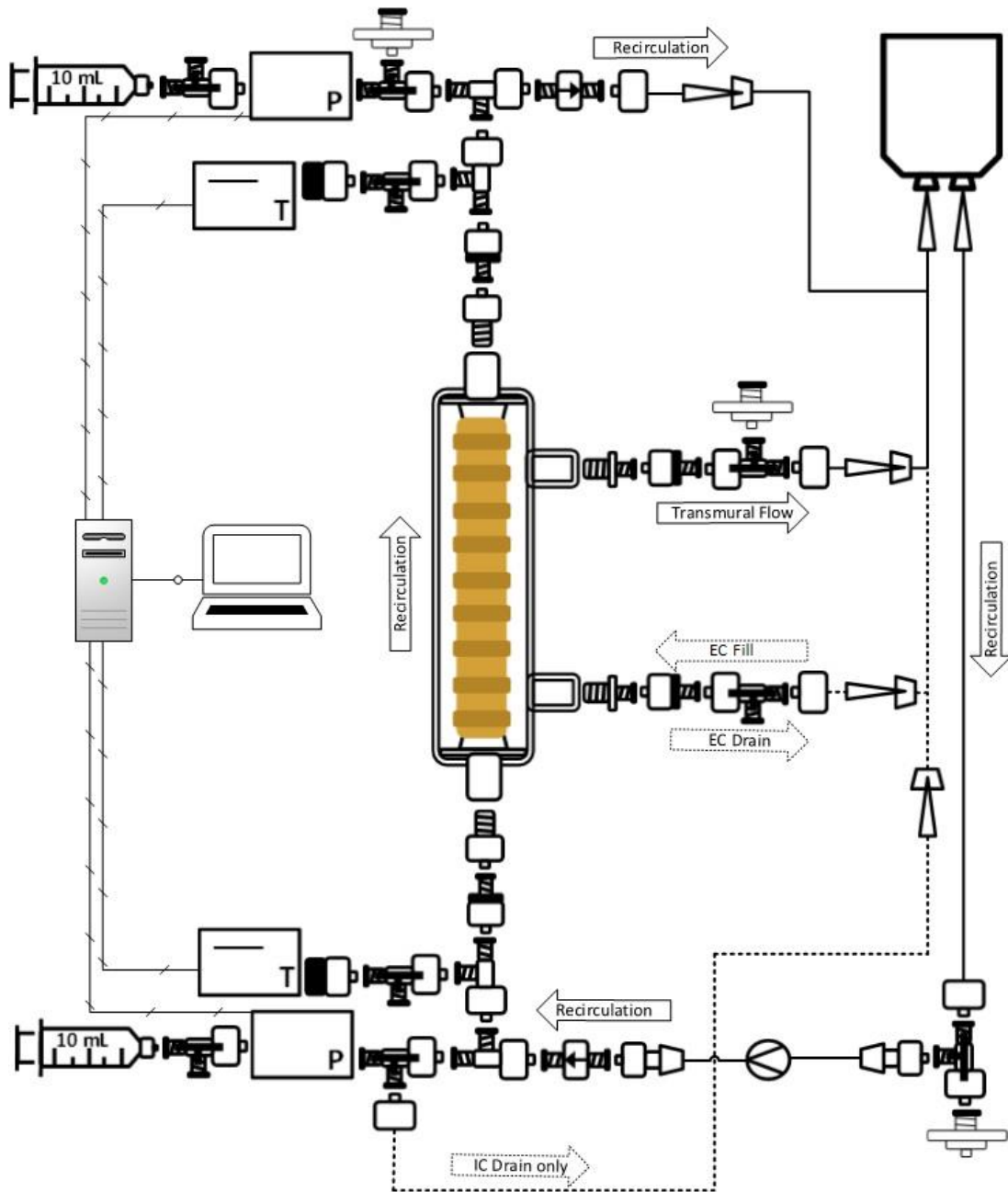


Figure 5.8: Bioreactor version 2.3. With this set-up the decellularisation solution was recirculated through the internal chamber/lumen of the trachea and the transmural flow was collected in the same reservoir and recirculated. The external chamber was pre-filled and minimal manipulation was required to drain the internal and external chambers. The pressure and temperature was measured and recorded online.

5.3.4 Preparation of porcine tracheal scaffolds by pressurised transmural decellularisation

5.3.4.1 Pressurised transmural decellularisation experiments 1, 2 and 3

After the tracheae had been prepared following procurement from Cheale Meats (refer to section 2.1), they were stored frozen, to incorporate a freeze-thaw step, in Viaspan (Bristol-Myers Squibb, Uxbridge, UK) in a falcon tube at -80°C (PTD 1 and PTD 2) and dry at -20°C (PTD 3). The tracheae were used in the decellularisation process within 1 month of freezing or discarded. A frozen trachea was thawed overnight at 4°C . When defrosted the trachea was attached to the bioreactor using a 1 PDS (polydioxanone) absorbable suture (Ethicon, Livingston, UK) and the bioreactor assembled according to bioreactor version 2.0 (see section 4.3 and 5.3.3.1). The decellularisation protocol involved the application of the following decellularisation solutions, 500 mL of each, for up to 24 hours each at 37°C in the following order; detergent I, wash I, nuclease I and wash II for PTD 1 and nuclease I, detergent I, nuclease II and wash I for PTD 2 and 3. For exact details of the solutions used refer to Table 5.1.

At the start of each decellularisation step the internal chamber was checked to ensure no leakage from the trachea when pressurised. The decellularisation solution was pumped through the bioreactor system and the internal chamber at 20 rpm which equated to 60 mL/min. Decellularisation solution exchange was performed between the decellularisation solutions by clamping the solution reservoir and switching the 3-way stopcock to pump air to clear the tubing of solution. The bioreactor chamber was inverted to ensure all the solution was removed from the internal chamber and the tubing. The spent solution reservoir was removed and the fresh solution reservoir was attached. The transmural decellularisation solution was pumped to waste from the lower port of the external chamber, therefore following brief manipulation of the bioreactor to ensure the external chamber and the waste tubing was clear. The spent waste bottle was exchanged for a fresh waste bottle. The spent solution and waste were treated with Virkon (VWR, Lutterworth, UK) prior to disposal.

PTD #	Bioreactor set-up	Trachea Storage	Decellularisation Process Timings					Decellularisation Solutions						Outer chamber pre-filled	
			Nuclease I	Detergent I	Wash I	Nuclease II	Wash II	Detergent Solution		Nuclease Solution		Wash Solution			
								[Sodium Deoxycholate] (%)	[Triton X-100] (%)	[DNase] (kU/mL)	[Rnase] (U/mL)	Wash I	Wash II		
1	v2.0	-80oC UW	-	24h @37°C	24h @37°C	20h @37°C	8h @37°C	2 in water	0.3 in water	2	4	Water	Water	No	
2	v2.0	-80oC UW	24h @37°C	22h @37°C	-	17h @37°C	7.5h @37°C	0.3 in Tris	0.3 in Tris	2	4		Tris	No	
3	v2.0	-20oC dry	20.5h @37°C	15.5h @37°C	-	3.2h @37°C	3.8h @37°C	0.3 in Tris	0.3 in Tris	2	4		Tris	No	
4	v2.0	-80oC UW	Hole in TM area - experiment abandoned												
5	v2.1	-80oC UW	24h @37°C	24h @37°C	-	24h @37°C	24h @37°C	0.3 in Tris	0.3 in Tris	2	4		Tris	No	
6	v2.1	-80oC UW	24h @37°C	24h @37°C	-	24h @37°C	24h @37°C	0.3 in Tris	0.3 in Tris	2	4		Tris	No	
7	v2.1	-80oC UW	24h @37°C	24h @37°C	-	24h @37°C	24h @37°C	2 in Tris	0.25 in Tris	2	4		Tris	No	
8	v2.2	-80oC UW	24h @37°C	24h @37°C	-	24h @37°C	24h @37°C	2.25 in Tris	0.25 in Tris	2	4		Tris	No	
9	v2.2	-80oC UW	24h @37°C	24h @37°C	24h @37°C	24h @37°C	24h @37°C	1.125 in Tris	0.125 in Tris	2	4	Tris	HBSS	No	
10	v2.2	-80oC UW	24h @37°C	24h @37°C	24h @37°C	24h @37°C	24h @37°C	0.5 in Tris	0.25 in Tris	2	4	Tris	HBSS	No	
11	v2.2	Fresh	24h @37°C	24h @37°C	24h @37°C	24h @37°C	24h @37°C	2.25 in Tris	0.25 in Tris	2	4	Tris	HBSS	No	
12	v2.2	-80oC UW	Hole in TM area - experiment abandoned												
13	v2.2	-80oC UW	24h @37°C	24h @37°C	3h @ 4°C	21 h @ 37oC	24 h @ 4°C	1.125 in Tris	0.125 in Tris	2	4	HBSS	HBSS	No	
14	v2.3	-80oC HBSS	24h @37°C	24h @ RT	3h @ 4°C	21 h @ 37°C	24 h @ 4°C	1.125 in Tris	0.125 in Tris	2	4	Tris	HBSS	Yes	
15	v2.3	-80oC UW	24h @37°C	24h @37°C	3h @ 4°C	21 h @ 37°C	24 h @ 4°C	1.125 in Tris	0.125 in Tris	2	4	Tris	HBSS	Yes	
16	v2.3	Fresh	Leaked at attachment point - experiment abandoned												
17	v2.3	Fresh	Leaked at G1/8 SAC connector join - experiment abandoned												
18	v2.3	Fresh	24 h @ 37°C	24 h @ 37°C	24 h @ 37°C	24 h @ 37°C	24 h @ 37°C	2.25 in Tris	0.25 in Tris	2	4	Tris	HBSS	Yes	
19	v2.3	Fresh	Valve issue and trachea split - experiment abandoned												
20	v2.3	Fresh	24 h @ 37°C	24 h @ 37°C	24 h @ 37°C	24 h @ 37°C	24 h @ 37°C	2.25 in Tris	0.25 in Tris	2	4	Tris	HBSS	Yes	

Table 5.1: Summary of the experiments for the pressurised transmural decellularisation.

5.3.4.2 Pressurised transmural decellularisation experiments 5, 6, 7 and 8

After the tracheae had been prepared following procurement from Cheale Meats (see section 2.1), the tracheae were frozen to -80°C in Viaspan. The tracheae were used in the decellularisation process within 1 month of freezing or discarded. For use in the decellularisation process a frozen trachea was defrosted overnight at 4°C before use. When defrosted the trachea was attached to the bioreactor using a 1 PDS (polydioxanone) absorbable suture and the bioreactor assembled according to bioreactor v2.1 (see section 4.3 and 5.3.3.2) for PTD 5, 6, and 7 and according to bioreactor version 2.2 (see section 4.3 and 5.3.3.3) for PTD 8. The decellularisation protocol involved the application of the following decellularisation solutions, 500 mL of each, for 24 hours at 37°C in the following order; nuclease I, detergent I, nuclease II and wash II. For exact details of the solutions used refer to Table 5.1. At the start of each decellularisation step the internal chamber was checked to ensure no leakage from the trachea when pressurised. The decellularisation solution was pumped through the bioreactor system and the internal chamber at 20 rpm which equated to 60 mL/min. Decellularisation solution exchange was performed between the decellularisation solutions by clamping the solution reservoir and switching the 3-way stopcock to pump air to clear the tubing of solution. The bioreactor chamber was inverted to ensure all the solution was removed from the internal and external chambers and the internal and external chamber tubing. The spent solution reservoir was removed and the fresh solution reservoir was attached. The spent solution was treated with Virkon prior to disposal.

5.3.4.3 Pressurised transmural decellularisation experiments 9 and 10

After the tracheae had been prepared following procurement from Cheale Meats (see section 2.1), the tracheae were frozen to -80°C in Viaspan. The tracheae were used in the decellularisation process within 1 month of freezing or discarded. For use in the decellularisation process a frozen trachea was defrosted overnight at 4°C before use. When defrosted the trachea was attached to the bioreactor using a 1 PDS (polydioxanone) absorbable suture and the bioreactor assembled according to bioreactor version 2.2 (see section 4.3 and 5.3.3.3). The decellularisation protocol involved the application of the following decellularisation solutions, 500 mL of each, for 24 hours at 37°C in the following order; nuclease I, detergent I, wash I, nuclease

II and wash II. For exact details of the solutions used refer to Table 5.1. At the start of each decellularisation step the internal chamber was checked to ensure no leakage from the trachea when pressurised. The decellularisation solution was pumped through the bioreactor system and the internal chamber at 20 rpm which equated to 60 mL/min. Decellularisation solution exchange was performed between the decellularisation solutions by clamping the solution reservoir and switching the 3-way stopcock to pump air to clear the tubing of solution. The bioreactor chamber was inverted to ensure all the solution was removed from the internal and external chambers and the internal and external chamber tubing. The spent solution reservoir was removed and the fresh solution reservoir was attached. The waste was treated with Virkon prior to disposal.

5.3.4.4 Pressurised transmural decellularisation experiments 13, 14 and 15

After the tracheae had been prepared following procurement from Cheale Meats (see section 2.1), the tracheae were frozen to -80°C in Viaspan for PTD 13 and 15 and to -80°C in HBSS for PTD 14. The tracheae were used in the decellularisation process within 1 month of freezing or discarded. For use in the decellularisation process a frozen trachea was defrosted overnight at 4°C before use. When defrosted the trachea was attached to the bioreactor using a 1 PDS (polydioxanone) absorbable suture and the bioreactor assembled according to bioreactor version 2.2 (see section 4.3 and 5.3.3.3) for PTD 13 or according to bioreactor version 2.3 (see section 4.3 and 5.3.3.4) for PTD 14 and 15. The decellularisation protocol involved the application of the following decellularisation solutions, 500 mL of each, for either 3, 21 or 24 hours at 4°C, 37°C or room temperature in the following order; nuclease I, detergent I, wash I, nuclease II and wash II. For exact details of the solutions, timings and temperatures used refer to Table 5.1. At the start of each decellularisation step the internal chamber was checked to ensure no leakage from the trachea when pressurised. Additionally for PTD 14 and 15, at the start of each decellularisation step, after ensuring no leakage from the internal chamber when the trachea was under pressure, the external chamber was filled with decellularisation solution by attaching the MLL line from the reservoir to the 3-way stopcock on the lower external port, opening the upper external port to air (an optional 0.22 µm filter can be attached) and filling the external chamber by gently applying pressure to the solution reservoir until the chamber was filled. The lower port was closed using the 3-way

stopcock and the MLL line from the reservoir was attached to the upper port and the line opened. The decellularisation solution was pumped through the bioreactor system and the internal chamber at 20 rpm which equated to 60 mL/min. Decellularisation solution exchange for the bioreactor version 2.2 was performed between the decellularisation solutions by clamping the solution reservoir and switching the 3-way stopcock to pump air to clear the tubing of solution. The bioreactor chamber was inverted to ensure all the solution was removed from the internal and external chambers and the internal and external chamber tubing. The spent solution reservoir was removed and the fresh solution reservoir was attached. The waste was treated with Virkon prior to disposal. Decellularisation solution exchange for the bioreactor version 2.3 was performed between the decellularisation solutions by clamping the solution reservoir and switching the 3-way stopcock to pump air to clear the tubing of solution. The solution reservoir tubing was then attached to the lower drainage 3-way stopcock and the lines opened to allow the solution in the internal chamber to drain into the reservoir. The top 3-way drainage stopcock was opened after the lower stopcock was opened to allow the solution to fully drain. When the internal chamber was fully drained these lines were then closed and the reservoir attached to the 3-way stopcock on the lower port of the external chamber and the lines opened to allow the external chamber to drain. The 3-way stopcock on the upper port of the external chamber was opened and the bioreactor manipulated slightly to allow the solution to fully drain. The lines were then closed and the spent solution reservoir was removed and the fresh solution reservoir was attached. The waste was treated with Virkon prior to disposal.

5.3.4.5 Pressurised transmural decellularisation experiments 11, 18 and 20

After the tracheae had been prepared following procurement from Cheale Meats (see section 2.1), the tracheae were used fresh (no freezing) in the decellularisation process. The trachea was attached to the bioreactor using a 1 PDS (polydioxanone) absorbable suture and the bioreactor assembled according to bioreactor v2.2 (see section 4.3 and 5.3.3.3) for PTD 11 or according to bioreactor v2.3 (see section 4.3 and 5.3.3.4) for PTD 18 and 20.

The decellularisation protocol involved the application of the following decellularisation solutions, 500 mL of each, for 24 hours at 37°C in the following

order; nuclease I, detergent I, wash I, nuclease II and wash II. For exact details of the solutions, timings and temperatures used refer to Table 5.1. At the start of each decellularisation step the internal chamber was checked to ensure no leakage from the trachea when was pressurised. Additionally for PTD 18 and 20, at the start of each decellularisation step, after ensuring no leakage from the internal chamber when the trachea was under pressure, the external chamber was filled with decellularisation solution by attaching the MLL line from the reservoir to the 3-way stopcock on the lower external port, opening the upper external port to air (an optional 0.22 µm filter can be attached) and filling the external chamber by gently applying pressure to the solution reservoir until the chamber was filled. The lower port was closed using the 3-way stopcock and the MLL line from the reservoir was attached to the upper port and the line opened.

The decellularisation solution was pumped through the bioreactor system and the internal chamber at 20 rpm which equated to 60 mL/min. Decellularisation solution exchange for the bioreactor version 2.2 was performed between the decellularisation solutions by clamping the solution reservoir and switching the 3-way stopcock to pump air to clear the tubing of solution. The bioreactor chamber was inverted to ensure all the solution was removed from the internal and external chambers and the internal and external chamber tubing. The spent solution reservoir was removed and the fresh solution reservoir was attached. The waste was treated with Virkon prior to disposal. Decellularisation solution exchange for the bioreactor version 2.3 was performed between the decellularisation solutions by clamping the solution reservoir and switching the 3-way stopcock to pump air to clear the tubing of solution. The solution reservoir tubing was then attached to the lower drainage 3-way stopcock and the lines opened to allow the solution in the internal chamber to drain into the reservoir. The top 3-way drainage stopcock was opened after the lower stopcock was opened to allow the solution to fully drain. When the internal chamber was fully drained these lines were then closed and the reservoir attached to the 3-way stopcock on the lower port of the external chamber and the lines opened to allow the external chamber to drain. The 3-way stopcock on the upper port of the external chamber was opened and the bioreactor manipulated slightly to allow the solution to fully drain. The lines were then closed and the spent solution reservoir was removed and the

fresh solution reservoir was attached. The waste was treated with Virkon prior to disposal.

5.3.5 Pressurised transmural decellularisation experiment failures

5.3.5.1 Pressurised transmural decellularisation 4:

This PTD was set up using a trachea that had been frozen for 32 days at -80°C in Viaspan. The experiment would have been performed as described for PTD 3 except the pressure gauge between the pump and the first check valve was omitted as it was deemed unnecessary and both pre and post IC check valves had a cracking pressure of 4.82 psi. A day after starting the experiment a leak was detected due to a small perforation in the trachealis muscle. This leak meant transmural flow would not be achieved and the experiment was abandoned and the tissue discarded.

5.3.5.2 Pressurised transmural decellularisation 12:

This PTD was set up using a trachea that had been frozen for 6 days at -80°C in Viaspan. The trachea was defrosted overnight at 4°C. The experiment would have been performed as described for PTD 9 with the same detergent concentrations and incubation times. Four hours into the second wash step, the final step of the decellularisation process, a leak was detected due to a small perforation in the trachealis muscle. This leak meant transmural flow would not be achieved for the final wash step and the experiment was abandoned and the tissue discarded.

5.3.5.3 Pressurised transmural decellularisation 16:

This PTD was set up using a fresh trachea that had been harvested that morning. The experiment would have been performed as described for PTD 11 with the same detergent concentrations and incubation times. As with PTD 15 the outer chamber was also pre-filled to ensure the outer surface of the trachea was submerged and immersed in the decellularisation solution from the start of each of the experiment steps. Shortly after commencing the first DNase/RNase step, the first step of the decellularisation process, a leak was detected at the point where the trachea was attached to the upper port of the bioreactor. This leak meant transmural flow would not be achieved and the experiment was abandoned and the tissue discarded.

5.3.5.4 Pressurised transmural decellularisation 17:

This PTD was set up using a fresh trachea that had been stored at 4°C for 2 days in Viaspan. The experiment would have been performed as described for PTD 11 with the same detergent concentrations and incubation times. As with PTD 15 the outer chamber was also pre-filled to ensure the outer surface of the trachea was submerged and immersed in the decellularisation solution from the start of each of the experiment steps. Shortly after commencing the first DNase/RNase step, the first step of the decellularisation process, a leak was detected from the bioreactor and in trying to fix that leak, one of the male G¹/₈ to MLL connectors broke and started to leak. This was not easily fixable so the bioreactor was disassembled, the experiment abandoned and the tissue discarded.

5.3.5.5 Pressurised transmural decellularisation 19:

This PTD was set up using a fresh trachea that had been harvested that morning. The experiment would have been performed as described for PTD 11 and 18 with the same detergent concentrations and incubation times. As with PTD 15 the outer chamber was also pre-filled to ensure the outer surface of the trachea was submerged and immersed in the decellularisation solution from the start of each of the experiment steps. Whilst changing the decellularisation solution for the first wash step, the third step of the decellularisation process, a three way stopcock valve on the IC return line to the solution reservoir was accidentally not opened causing the pressure to rise in the internal chamber of the bioreactor (the inside of the trachea). This caused a perforation in the trachealis muscle. This leak meant transmural flow would not be achieved and the experiment was abandoned and the tissue discarded.

5.3.6 Cost comparison of the DEM and PTD methods

The cost of the reagents only were calculated for the DEM and PTD methods to create a basic cost of goods (CoG) analysis by calculating the cost of each reagent multiplied by the percentage of reagent used per step and by the number of steps in which it was used in the total process. This was summed to give an overall CoG.

5.4 Results

5.4.1 Pressurised transmural decellularisation 1 to 3 (PTD 1 - 3)

Following the setting up of the bioreactor system v2.0 (Figure 5.5 and Figure 5.9), it was noted that the bioreactor system worked well in that: no bubbles were trapped in the system; the desired pressure was maintained; and transmural flow was achieved. The first three pressurised transmural decellularisations (PTD 1 – 3) were defined primarily by the transmural flow going directly to a waste reservoir from the bottom port of the external chamber. There were however issues due to the fact the transmural waste was sent to a directly to a waste reservoir which meant the external chamber never filled and therefore the abluminal side of the trachea was never submerged in decellularisation solution. This resulted in what appeared to be patches of tissue which were decellularised and patches of tissue where the decellularisation solution had not come through transmurally and therefore not decellularised as well. This was more evident in the PTD 3 which had been frozen dry and therefore not washed or immersed in solution previously. This was confirmed when DNA analysis of the less or “non decellularised” (NDC) regions (334.49 ± 10.01 ng/mg) had five times more DNA remaining in samples than the “decellularised” (DC) regions (66.94 ± 12.77 ng/mg) (Figure 5.10).

Another issue with the transmural solution being sent to a waste reservoir was that if the transmural flow was high then all of the decellularisation solution would flow through the trachea in less than the desired 24 h. At the highest flow rate of 156 mL/h, the 500 mL of decellularisation solution flowed transmurally through the trachea in 3 hours 10 min (Table 5.2). At this rate a minimum of 3.79 L of decellularisation solution would be required to decellularise the trachea with transmural flow for the full 24 h which would greatly increase the cost of the process in terms of raw materials. It was therefore decided that it would be cost effective to investigate the effect of recycling the transmural solution to the solution reservoir to allow a full 24 hours of PTD by returning the transmural flow to the solution reservoir via the upper port of the external chamber to allow the abluminal side of the trachea to also be immersed in the decellularisation solution.

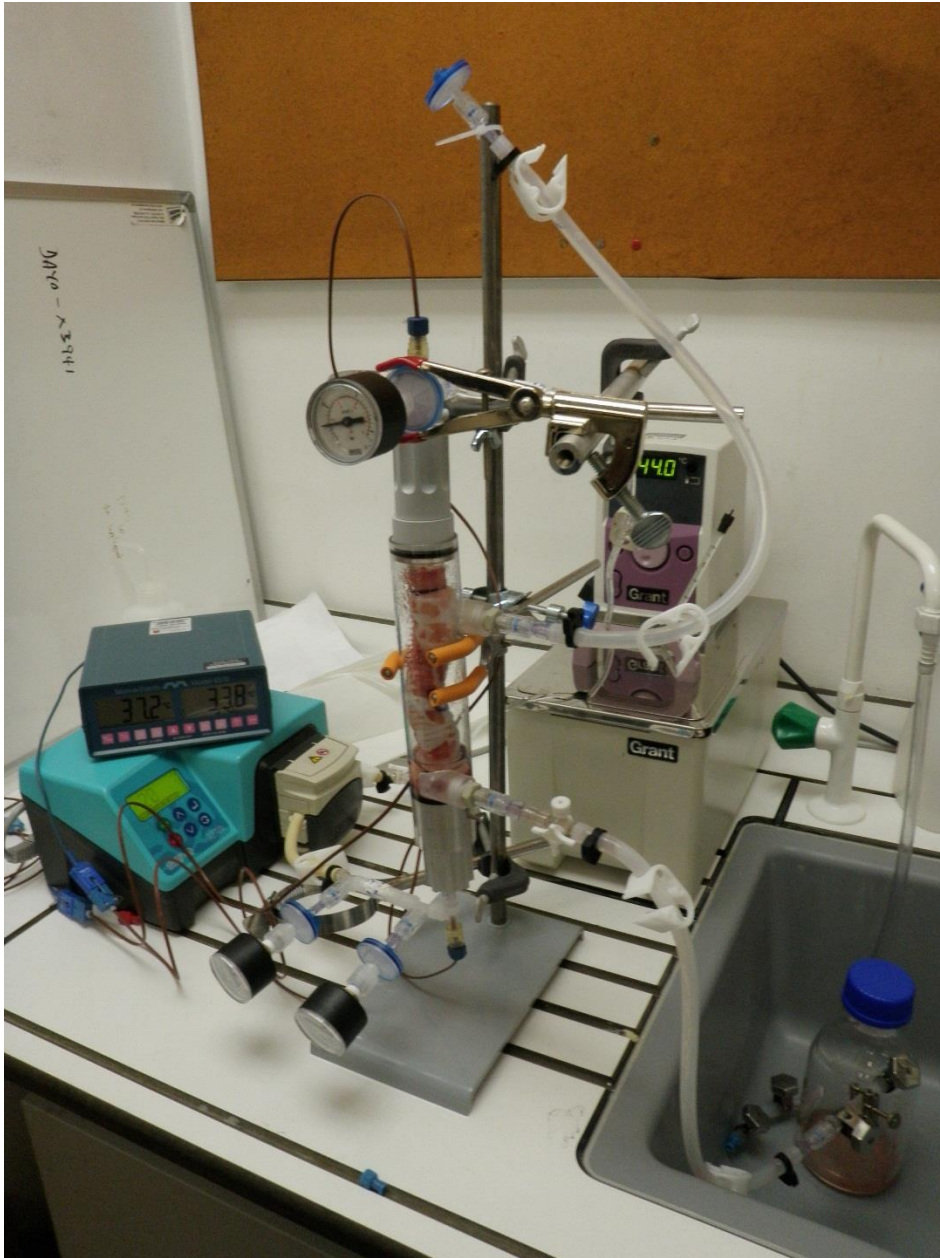


Figure 5.9: Bioreactor version 2.0 in use with the PTD 3.

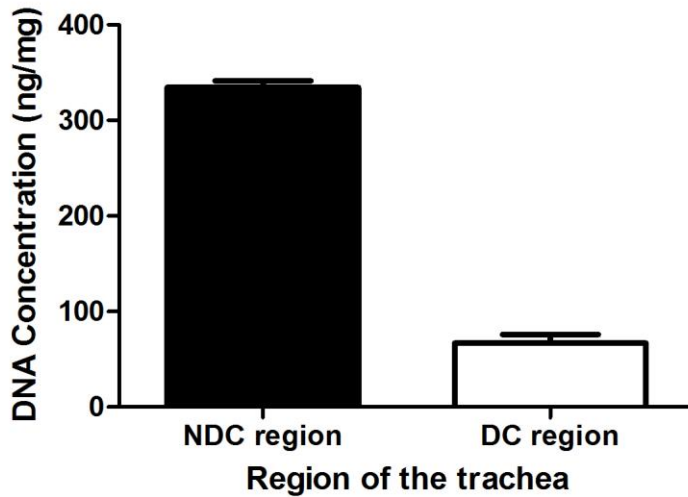


Figure 5.10: Differences in remaining DNA in the “decellularised” (DC) regions of the trachea compared to the “non-decellularised” (NDC) regions of the trachea due to uneven transmural flow.

Several other parameters of the decellularisation were investigated. The tracheae were either freeze-thawed at -80°C in Viaspan (PTD 1 and 2) or at -20°C dry (PTD 3) to identify whether this had an effect on the decellularisation. Freezing at -20°C dry appeared to greatly increase the rate of transmural flow (Table 5.2) which could indicate greater ECM disruption during the freeze-thaw process, which was not desirable so freezing was subsequently performed in Viaspan to -80°C .

PTD #	Trachea Storage	Transmural Flow Rates (mL/h)				
		Nuclease I	Detergent I	Wash I	Nuclease II	Wash II
1	-80°C UW	-	20.83333333	20.833333	25	62.5
2	-80°C UW	20.83333333	22.72727273	-	29.4117647	66.6666667
3	-20°C dry	24.3902439	32.25806452	-	156.25	131.578947

Table 5.2: Transmural flow rates of the decellularisation solutions for PTD 1-3.

Different decellularisation regimes were also tested; a detergent, wash, nuclease and wash regime, which is similar to the DEM regime, was initially tested for PTD 1. It was noted that debris and viscous material had collected in the external chamber during the detergent and wash steps which was removed by the nuclease step. Given that the freeze-thawing of the trachea would cause cell lysis and release of nuclear material it was theorised that the viscous material could be nuclear material

(Meezan, Hjelle et al. 1975). Therefore it was decided to perform a nuclease step at the start of the process for the next PTD experiments with a nuclease, detergent, nuclease and wash regime. The latter regime achieved an increased transmural flow rate earlier in the process, but in the final wash a similar flow rate was achieved for both regimes in these instances. However there was a no build-up of viscous material, which implied it was released nuclear material, and therefore the nuclease, detergent, nuclease and wash regime was adopted for the future PTD experiments.

A noted issue was, in order to heat the decellularisation solution to the temperature of 37°C upon entry to the internal chamber, it was necessary to set the water bath to 44°C. However, according to a thermometer the water bath was actually at 41°C. The first temperature probe measured the decellularisation solution just before the internal chamber as being 36.9°C indicating a loss of 4.1°C in the tubing between the water bath and the entry to the bioreactor. The second temperature probe measured the decellularisation solution just after the internal chamber as being 34°C indicating a loss of 2.9°C in the internal chamber of the bioreactor.

Observations were also made to assess the effectiveness of the check valves at maintaining the pressure within the internal chamber (Figure 5.11) The measured pressure was consistently lower after the internal chamber (pressure gauge 3), average 4.17 psi \pm 0.3 psi, than before the internal chamber (pressure gauge 2), average 5.21 psi \pm 0.43 psi, and had an average between the two pressure gauges of 4.67 psi \pm 0.31 psi. The pressure measured by the first pressure gauge between the first check valve and the peristaltic pump varied greatly and fluctuated between approximately 4 and 13 psi for each turn of the pump due to the peristaltic pumping mechanism.

Histological analysis of the trachea indicated that regions remained undecellularised and nuclei were visible after PTD 1 -3 (black arrows, Figure 5.12 A and B) in not only the cartilage rings, as had also been observed in the DEM of decellularisation, but also in the mucous glands indicating the protocol for the PTD 1 - 3 was inadequate and required amendment.

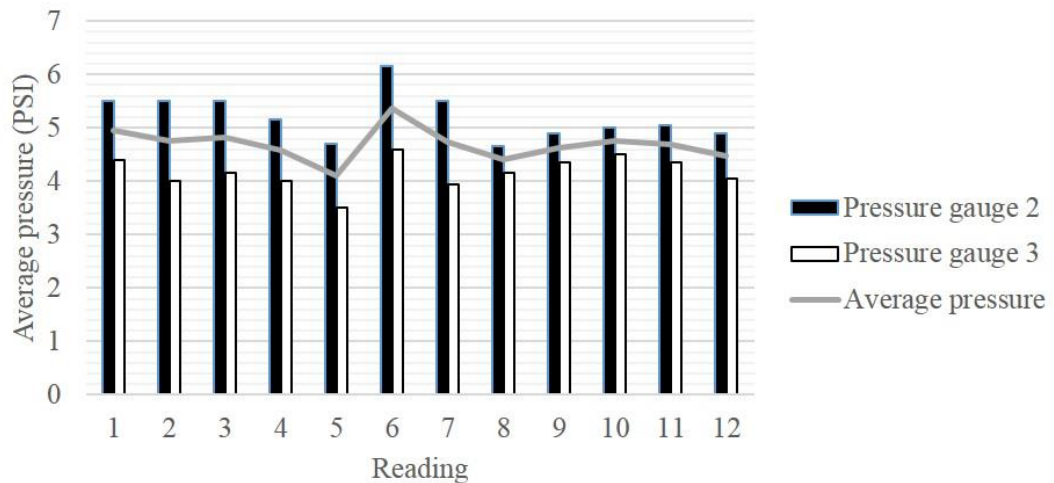


Figure 5.11: Readings from the pressure gauges before (PG2) the and after (PG3) the internal chamber.

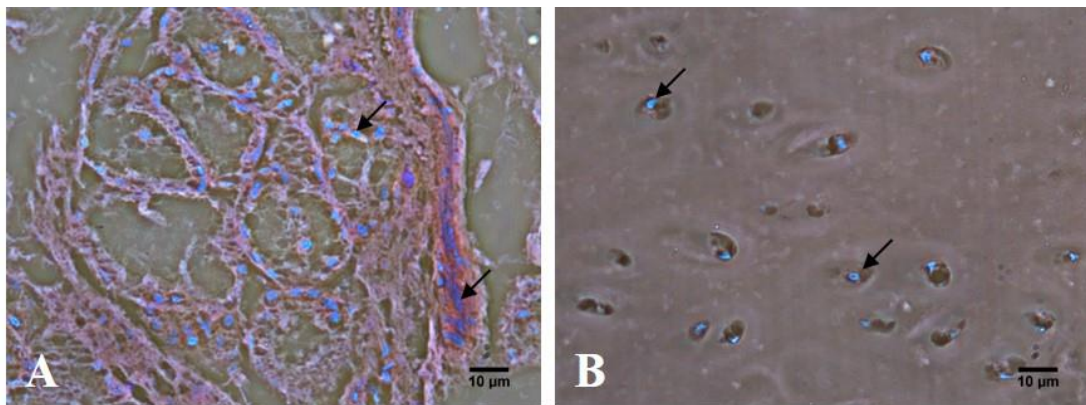


Figure 5.12: Histological analysis of the mucous glands (A) and cartilage rings (B) of the trachea (PTD 2 results shown) stained with H&E revealed the presence of nuclei in both regions indicating these regions were not adequately decellularised.

5.4.2 Pressurised transmurial decellularisation 5 to 8 (PTD 5 - 8)

The decellularisation experiments PTD 5 to 8 were characterised by all having undergone a freeze-thaw step at the start, then a DNase step, a detergent step (at three different detergent concentrations), followed by the second DNase step and finally a wash step. The bioreactor set-up was amended so that, after filling the external chamber of the bioreactor, the transmural flow would be recirculated to the solution reservoir and be available for recirculation through the lumen and available for further transmural flow (Figure 5.6 and Figure 5.13). The result was that the solution reservoir was not depleted by the transmural flow being sent to waste and

the solution recirculated continuously and with transmural flow for the full 24 hours for each step. Again the bioreactor worked well with the transmural flow, pressure and the temperature being maintained throughout the entire decellularisation process.

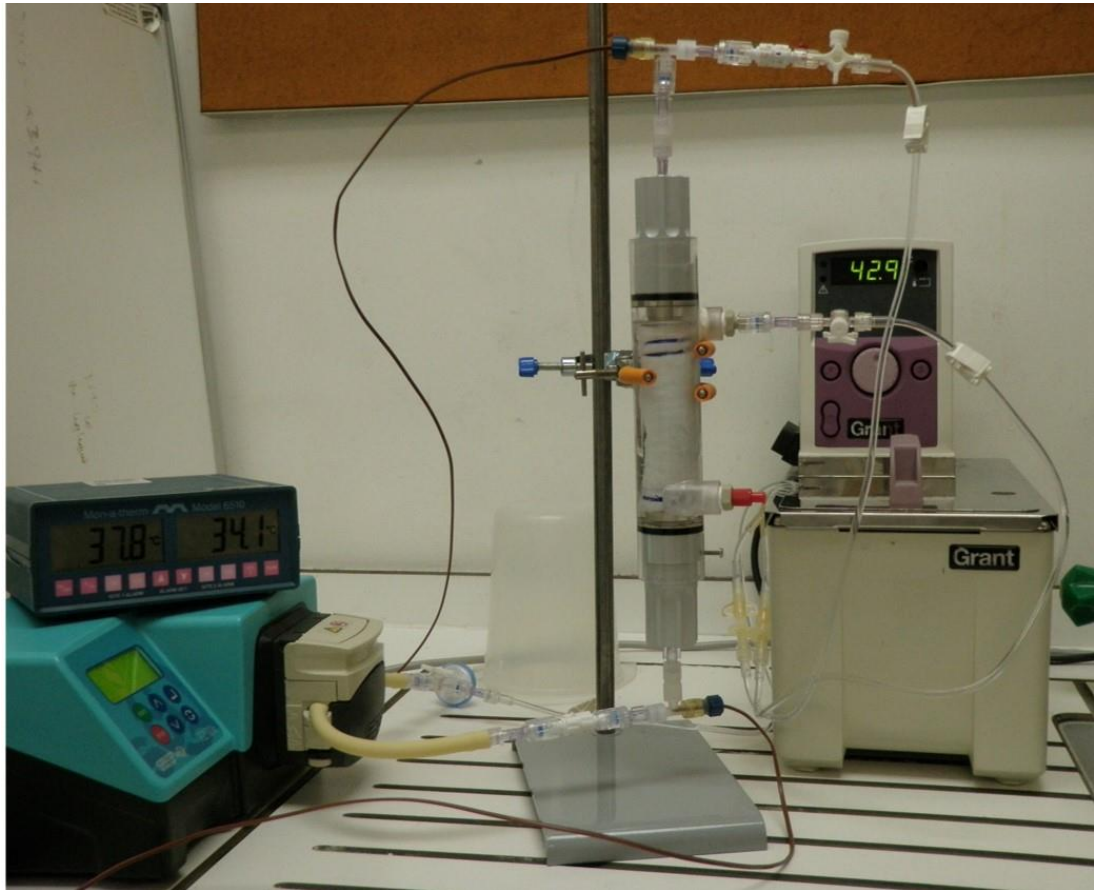


Figure 5.13: Bioreactor version 2.1 in use with the PTD 5.

Histological analysis using H&E staining indicated total decellularisation had not been achieved in the trachealis muscle and mucous gland regions of the trachea for the PTD 5 and 6 experiments where lower concentrations of detergent had been used (Figure 5.14). The PTD 7 and 8 experiments incorporated an increased concentration of detergent and the resulting effect was complete cell clearance within the different regions of the tracheal scaffold with the occasional nuclei remaining in the cartilage ring region (Figure 5.14), as observed with the DEM of decellularisation.

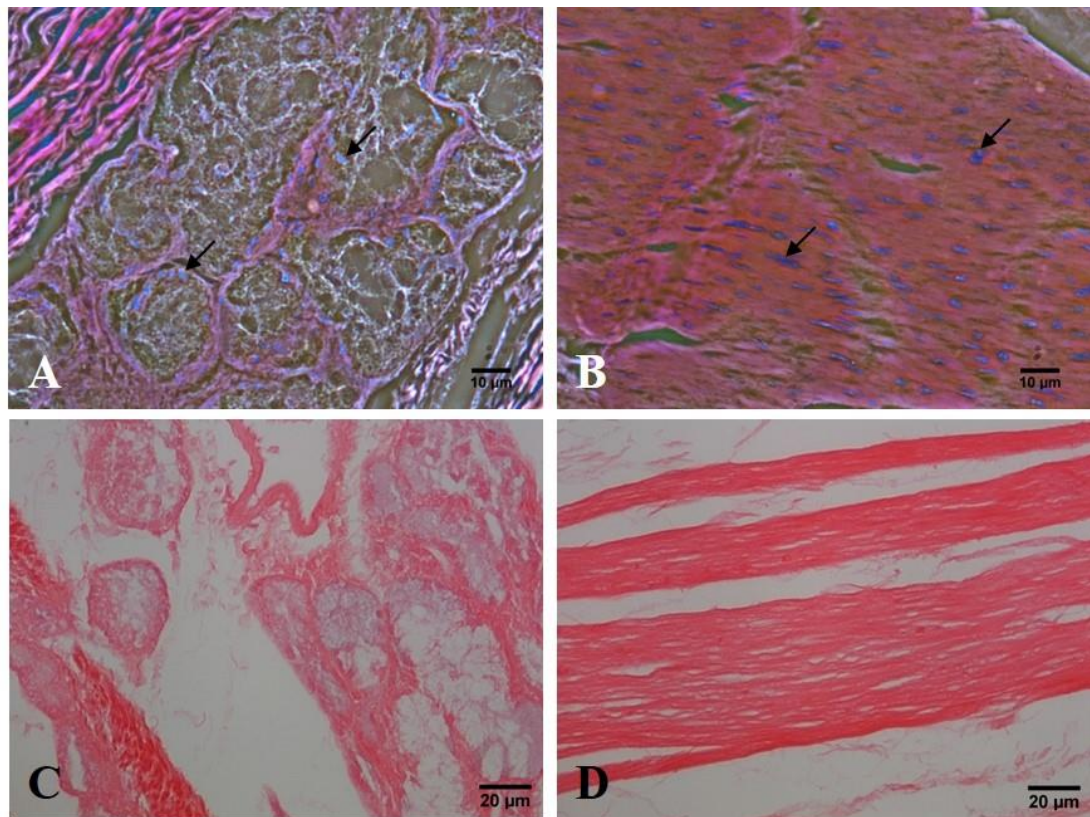


Figure 5.14: Histological analysis of the mucous glands (A) and trachealis muscle (B) of experiment PTD 6 stained with H&E revealed the presence of nuclei in these regions indicating an inadequate level of cell clearance compared to the analysis of the mucous glands (C) and trachealis muscle (D) of experiment PTD 8 which indicated a good level of cell clearance.

The method of compression testing of the trachea and the decellularised scaffolds was introduced from experiment PTD 5 and was considered to be a more representative test for tracheal cartilage ring resistance to mimic compression and collapse *in vivo*. Results from this compression testing indicated that for PTD 5 and 6 the tracheal resistance to collapse under load was approximately 50% (2.04 ± 0.19 N) of that of native tissue (4.23 ± 0.89 N) and approximately equivalent to that observed in tracheae that had undergone a freeze thaw process, either -80°C in UW (1.99 ± 0.75 N) or -80°C in HBSS (2.40 ± 1.02 N) or -20°C dry (2.29 ± 0.56 N) (Figure 5.15). This indicated that the decellularisation process at this concentration of detergent was not detrimental to the mechanical strength of the scaffold. However, as shown, it also did not achieve complete decellularisation by cell clearance. The PTD 7 & 8 experiments at increased concentration of detergent

achieved cell clearance in the non-cartilaginous regions of the scaffolds. However, the compression testing indicated in increased weakening of the PTD 7 and the PTD 8 scaffolds to approximately 13% of the native tissue (0.56 ± 0.09 N) (Figure 5.15).

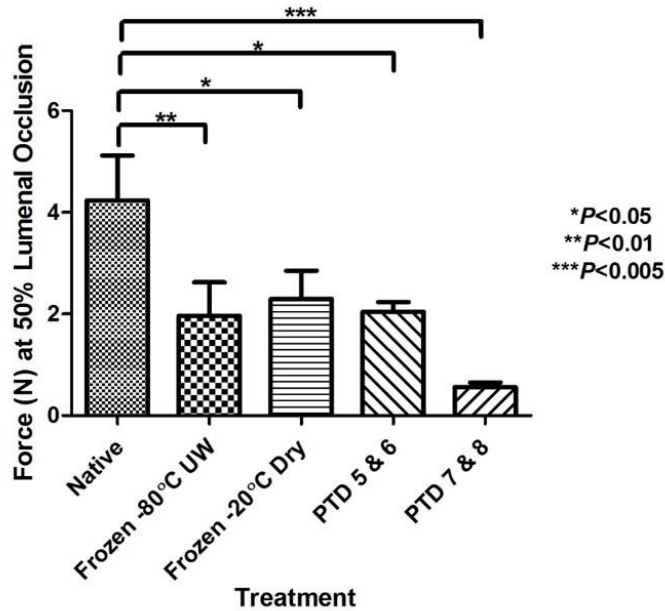


Figure 5.15: Compression testing in the PTD 5 - 8 experiments indicated weakened scaffolds comparable to tracheae that had undergone a freeze-thaw step for PTD 5 and 6 when a lower detergent concentration was used and increased weakening in the scaffold beyond that observed in freeze-thawed tracheae for PTD 7 and 8 when a higher detergent concentration was used.

The inclusion of the Dinocapture microscope to monitor the decellularisation during experiment PTD 8 also highlighted another potential issue of increasing the detergent concentration. From two hours after the start of the second DNase step there was the formation of salt crystals on the abluminal side of the tracheal scaffold (Figure 5.16) that dissolved back into solution during the wash step. It was hypothesised that this could be due to the sodium from the detergent reacting with the chloride ions from either the Trizma-HCl, $MgCl_2$ or $CaCl_2$ in the DNase buffer. For future PTD experiments, a wash step was incorporated between the detergent step and the second DNase in order to remove the remnant detergent from the scaffold before the DNase step commenced.



Figure 5.16: Formation of salt crystals on the ablumen of the tracheae during the second DNase step of PTD8.

5.4.3 Pressurised transmural decellularisation 9 and 10 (PTD 9 & 10)

The decellularisation experiments PTD 9 and 10 were characterised by all having undergone a freeze-thaw step at the start, then a DNase step, a detergent step (at two differing detergent concentrations), then a wash step followed by the second DNase step and finally a second wash step in the bioreactor v2.2 set up (Figure 5.17).

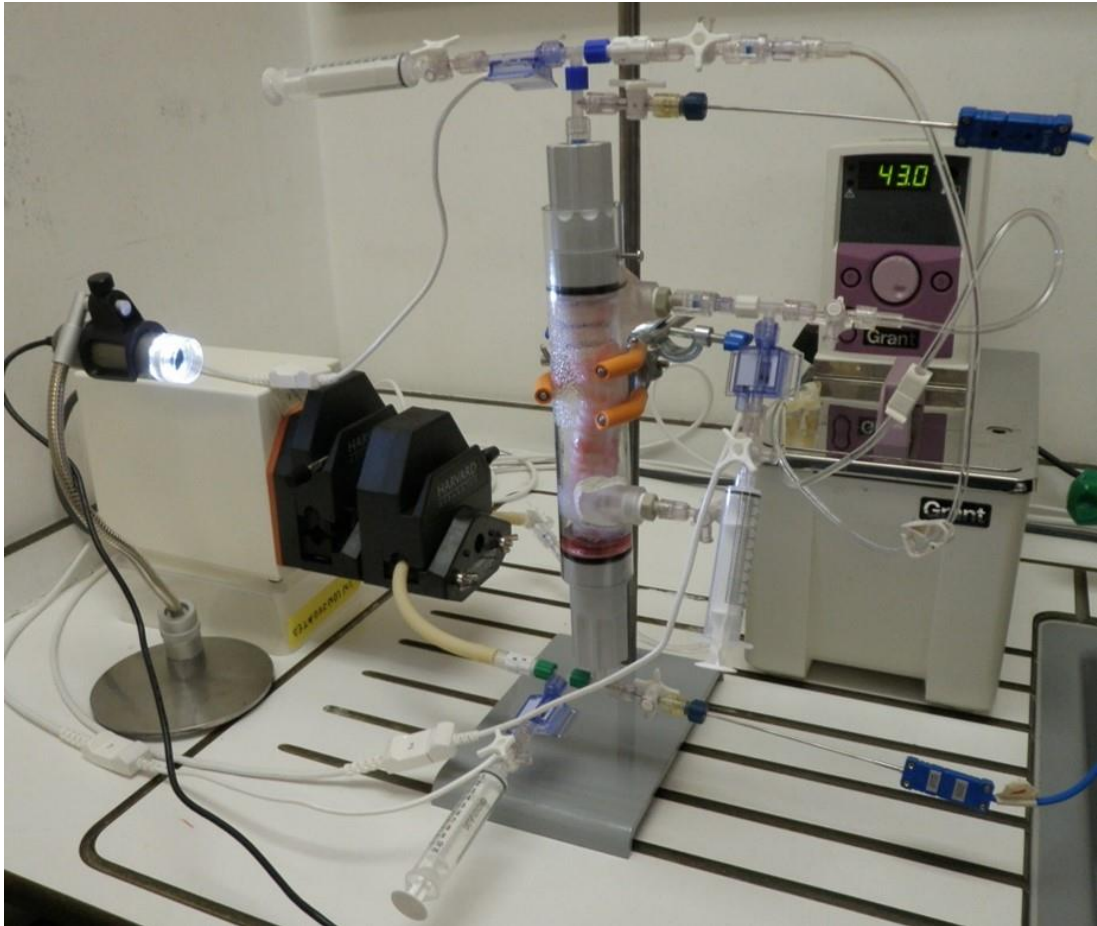


Figure 5.17: Bioreactor v2.2 whilst performing experiment PTD 10.

The additional 24 hour wash step between the detergent step and the second DNase step was added to ensure the detergent had been cleared from the bioreactor system before proceeding with the DNase step. Images confirmed that the introduction of this wash step achieved its purpose as no salt crystals were observed. Two different detergent concentrations were also investigated under these conditions PTD9 at a total of 1.25% detergent and PTD 10 at 0.75% detergent. Histological observation demonstrated that good cell clearance was observed for PTD 9 at the higher detergent concentration with all of the non-cartilaginous regions of the trachea being successfully cleared of cells (Figure 5.18). However at the lower detergent concentration the cell clearance was not adequate with cells being observed in the mucous glands and the trachealis muscle regions as well as the cartilage rings (Figure 5.18).

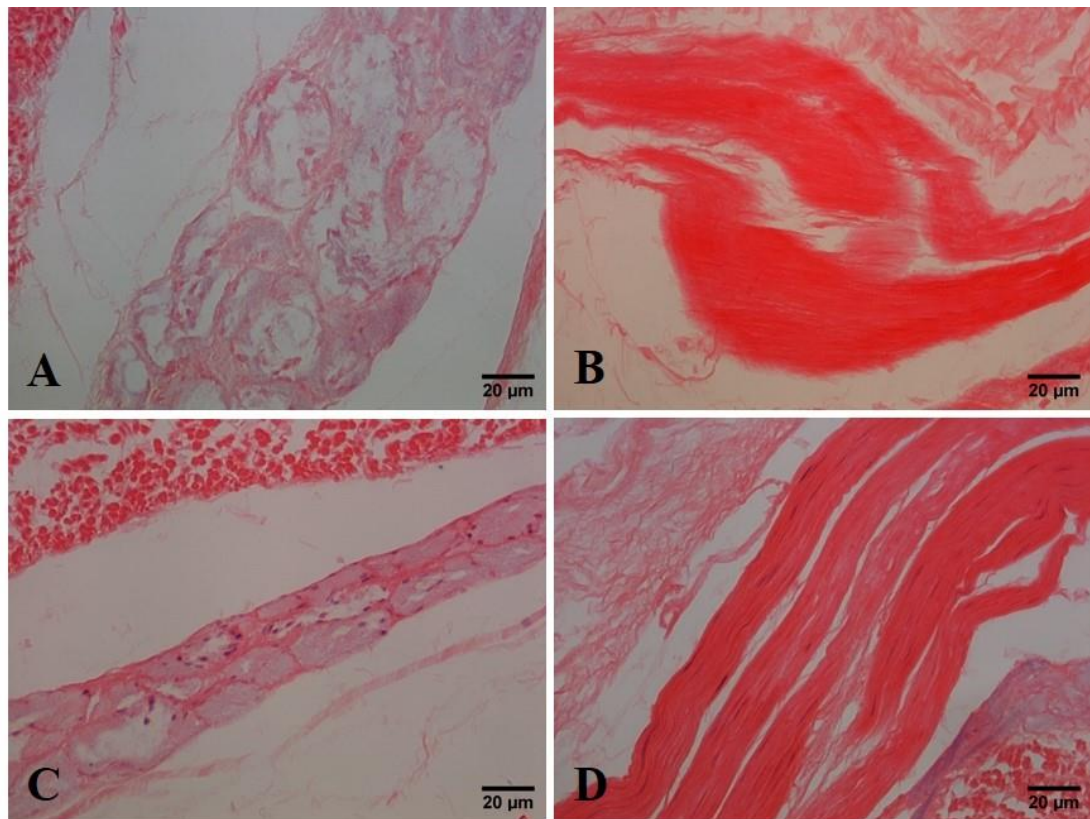


Figure 5.18: Histological analysis of the cell clearance in PTD 9 revealed good removal of cells from the trachea by the decellularisation process in all regions of the trachea, for example the mucous glands (A) and the trachealis muscle (B) with a few nuclei remaining in the cartilage rings. However for PTD 10 cells were observed to be present after decellularisation in the mucous glands (C) and the trachealis muscle (D) as well as the cartilage rings.

With regard to the effect of the additional wash step on the biomechanical strength, the compression testing indicated that the PTD 9 and 10 scaffolds (0.75 ± 0.34 N) were comparable in compressive resistance to the PTD 7 and 8 scaffolds at approximately 17% of the strength of the native tracheal tissue (4.23 ± 0.89 N) (Figure 5.19). This indicated that, even at the lower concentration of detergent, the additional 24 hours of processing was deleterious to the scaffolds beyond the freeze-thaw step.

It was therefore decided to investigate shortening the wash step between the detergent step and the second DNase step and to perform the wash step at 4°C as this also may help maintain the biomechanical strength in the scaffolds.

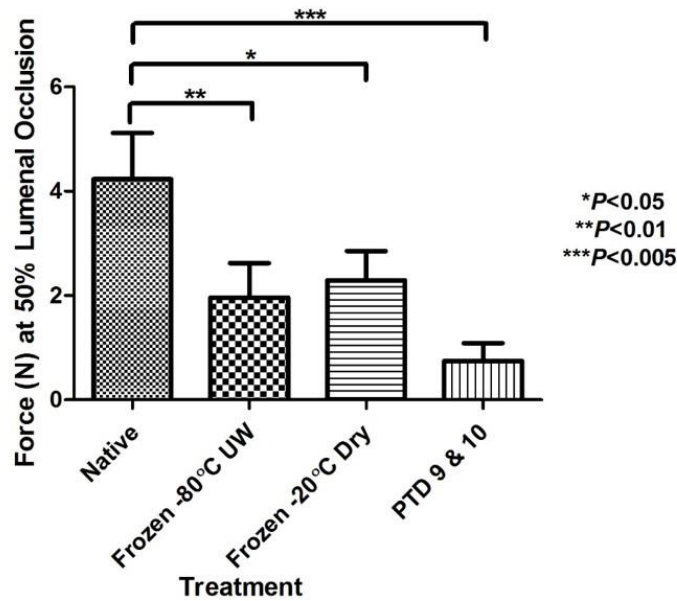


Figure 5.19: Compression testing in the PTD 9 & 10 experiments indicated weakened scaffolds beyond the tracheae that had undergone a freeze-thaw step.

Pressurised transmural decellularisation 13 to 15 (PTD 13 - 15)

The decellularisation experiments PTD 13 to 15 were characterised by all having undergone a freeze-thaw step at the start, then a DNase step, a detergent step (all at a total of 1.25% detergent), then a 3 hour wash step at 4°C followed by a second 21 hour DNase step and finally a 24 hour wash step at 4°C. Bioreactor v2.2 was used for PTD 13 and bioreactor v2.3 was used for PTD 14 and 15 (Figure 5.20).



Figure 5.20: Bioreactor v2.3 which had extra ports included to allow for easy fill and drain of the decellularisation solutions.

Histological analysis of the tracheal scaffolds indicated good cell clearance from most regions of the trachea including the mucous glands and the trachealis muscle as shown for PTD 14 (Figure 5.21). However there were some apoptotic cells visible in the cartilage rings and nuclei visible in the lamina propria as shown for PTD 14 (Figure 5.21).

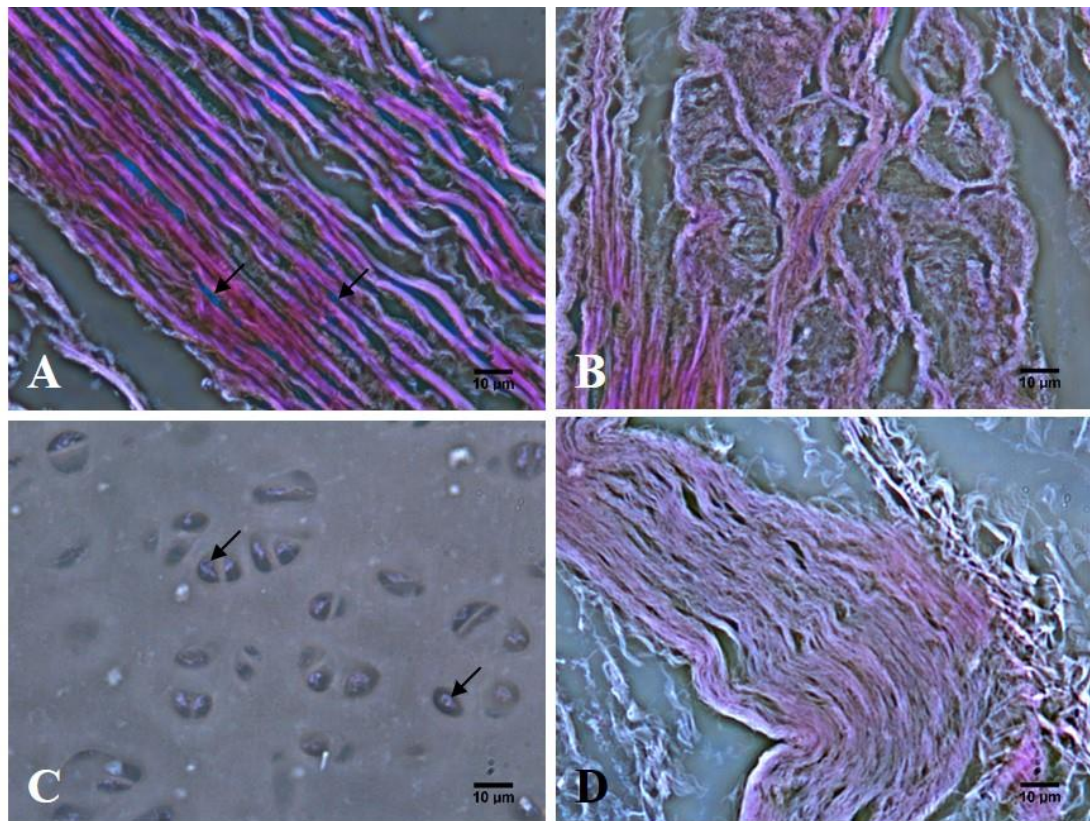


Figure 5.21: Histological analysis of PTD 14 indicated removal of cells from the mucous gland (A) and the trachealis muscle (D) however there were some remaining nuclei in the lamina propria (B) and some apoptotic cells visible in the cartilage rings (C).

The compression testing indicated that compressive resistance for PTD 13 to 15 (1.98 ± 1.20 N) were similar to tracheae that had been freeze-thawed (2.00 ± 0.75 N) and therefore just under 50% the strength of native tracheal tissue (4.23 ± 0.89 N) (Figure 5.22). This indicated that there was a benefit to shortening the first wash step and perhaps by performing the wash steps at 4°C. However the scaffolds still only retained 50% compressive strength of the native tissue which appeared to be caused by the initial freeze thaw step performed at the commencement of the decellularisation process. It was therefore decided to perform the pressurised transmural decellularisation on trachea that had not been freeze-thawed to ascertain if decellularisation could be achieved whilst the biomechanical strength retained. Due to the anticipated increased retention in compressive strength due to the starting decellularisation material being fresh, longer washes and the higher levels of

detergent were used to increase the probability of good cell clearance also being achieved.

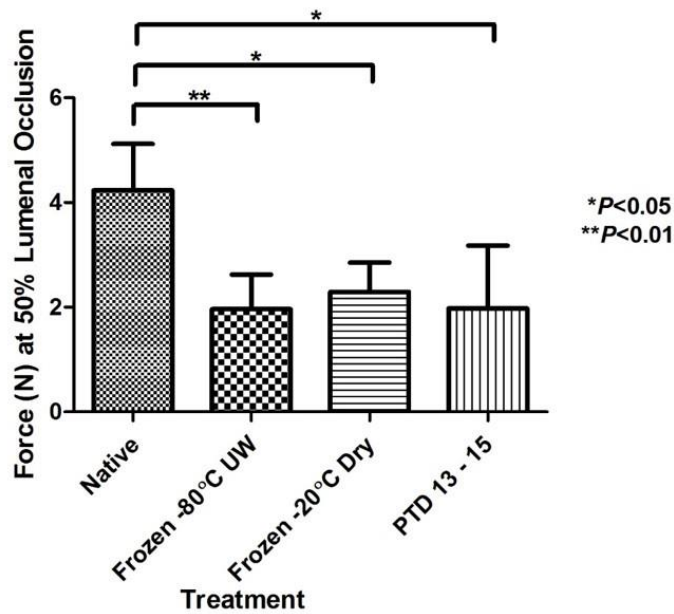


Figure 5.22: Compression testing of PTD 13 – 15 indicated a comparable loss in strength in the decellularised scaffolds as tracheae that had undergone a freeze-thaw step and approximately 50% of the compressive strength of native tracheae.

5.4.4 Pressurised transmural decellularisation (PTD 11, 18 and 20)

The decellularisation experiments PTD 11, 18 and 20 were characterised by being performed on fresh trachea with a nuclease step, a detergent step (all at a total of 2.5% detergent), then a wash step followed by a second nuclease step and then a final wash step. All steps were 24 hours in length and performed at 37°C. Bioreactor v2.2 was used for PTD 11 and bioreactor v2.3 was used for PTD 18 and 20 (Figure 5.20). The inclusion of the ORCA bioreactor allowed certain process parameters, temperature and pressure, to be monitored and recorded online. The average pre-internal chamber (pre-IC) temperature was $33.59 \pm 0.66^\circ\text{C}$ and the average post-internal chamber (post-IC) temperature was $33.10 \pm 1.31^\circ\text{C}$ (Figure 5.23). The average pre-internal chamber (pre-IC) pressure was 4.79 ± 0.17 psi and the average post-internal chamber (post-IC) pressure was 4.00 ± 0.16 psi (Figure 5.24).

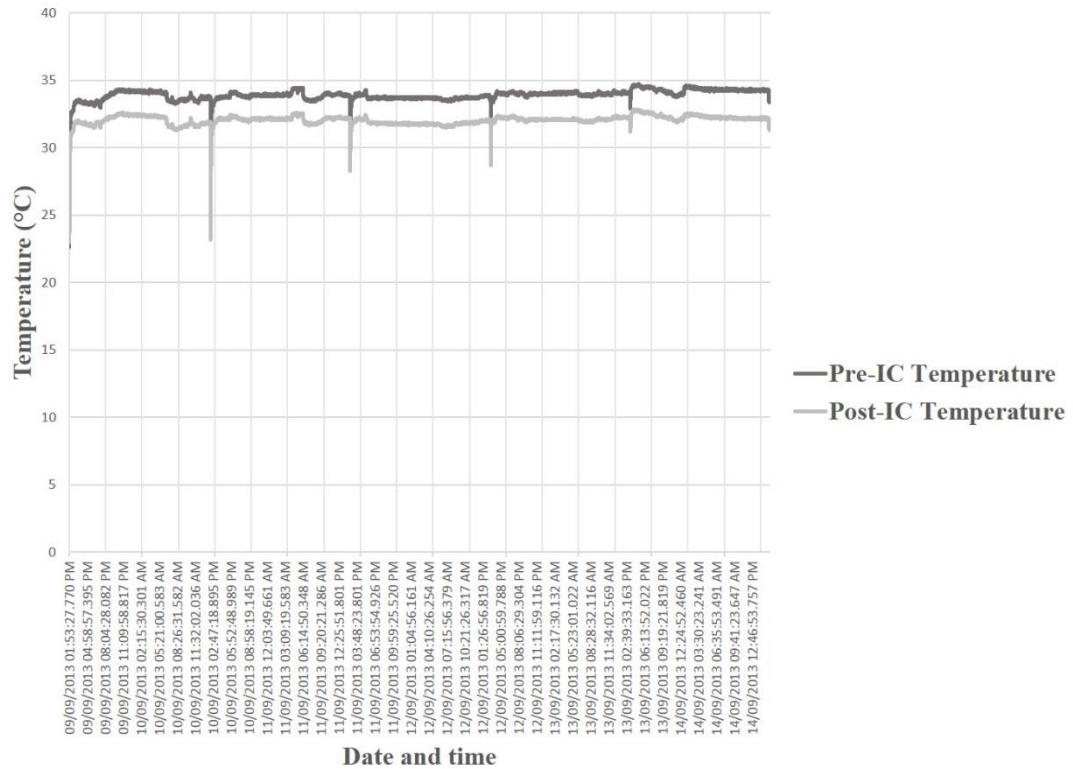


Figure 5.23: The ORCA controller was able to record the online temperature of the decellularisation solutions from the readings off the temperature probes positioned before and after (pre and post) the internal chamber (IC) or tracheal lumen. Both temperatures were stably maintained over the course of the decellularisation with an average difference of 0.84°C detected across the lumen with the solution cooling as it travelled down the fluidic path from the solution reservoir.

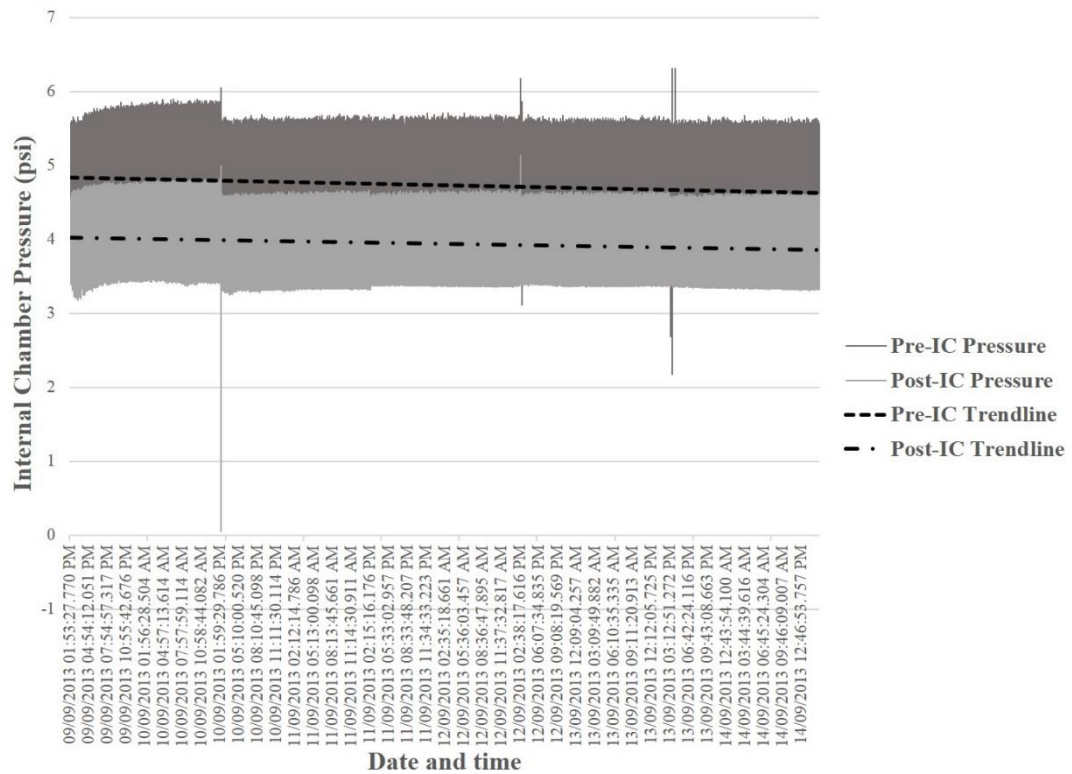


Figure 5.24: The ORCA controller was able to record the online pressure of the decellularisation solutions from the readings from the pressure transducers positioned before and after (pre and post) the internal chamber (IC) or tracheal lumen. Both pressures were stably maintained over the course of the decellularisation with an average difference of 0.79 psi detected across the lumen with the pressure of the solution diminishing as it travelled further down the fluidic path from the peristaltic pump.

5.4.4.1 Macroscopic overview of the native trachea and PTD scaffolds

The porcine tracheal scaffolds produced using PTD (PTD 20 shown) appeared denuded, compared to the native porcine trachea, as was expected of a decellularised organ. The overall morphological structure was retained, notably with the cartilage rings maintaining the open structure of the hollow organ (Figure 5.25). The rings also resisted collapse under light pressure. The epithelial lining of the lumen was also intact and denuded, as would be expected.

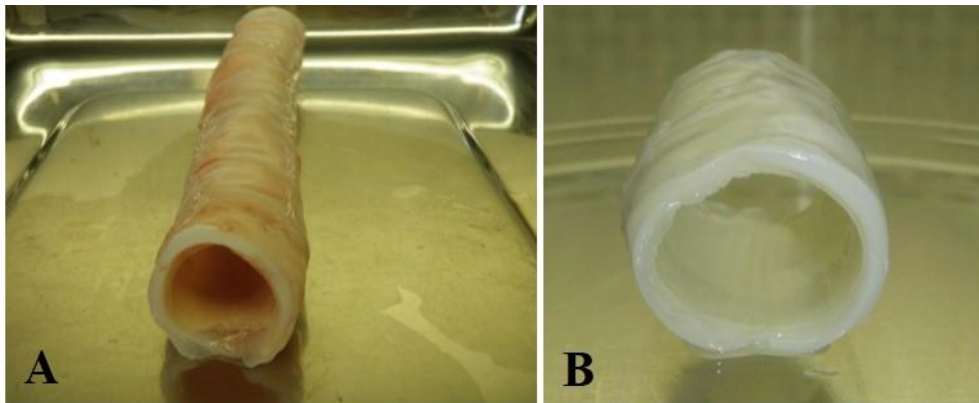


Figure 5.25. Comparing the native trachea (A) with the PTD 20 tracheal scaffold (B), the gross morphological appearance of the scaffold is retained appearing denuded with the cartilage rings maintaining an open structure and a visible epithelial layer lining the lumen.

5.4.4.2 Histological analysis of PTD scaffolds by H&E staining

H&E staining of native tracheae and decellularised scaffolds (PTD 11, 18 and 20) demonstrated that under microscopic observation the structure of the trachea and the structure of the tracheal sub-regions were retained after pressurised transmural decellularisation (Figure 5.26). Histological analysis by H&E staining also demonstrated excellent cell and nuclei removal from the majority of the decellularised scaffolds. Histological analysis was categorised into the major sub-regions of the trachea to cover the mucosa region of the lamina propria, the sub-mucosal gland region of the lamina propria, the cartilage rings and the adventitia. It was extended to also include the trachealis muscle region, having observed some inadequate removal of cells from this region in previous versions of the PTD method. Analysis of these sub-regions demonstrated that in the mucosa (epithelial and sub-epithelial) region (Figure 5.27), the sub-mucosal region (Figure 5.27), the

adventitia (Figure 5.28) and the trachealis muscle (Figure 5.29) complete clearance of the cells and the nuclei was achieved in the decellularised scaffolds. In the cartilage ring, as with the DEM, chondrocytes were observed after the decellularisation process in the scaffolds (Figure 5.28). For the PTD 18 and 20, histological analysis also revealed potential damage could have occurred to the trachealis muscle as the amount of visible smooth muscle appears to have decreased (Figure 5.29).

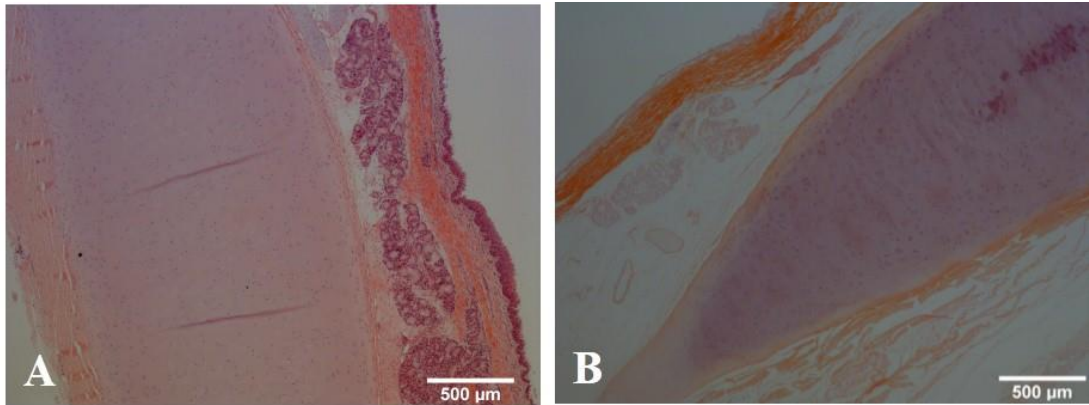


Figure 5.26: Low power (x4) microscopic evaluation of native trachea (A) and PTD demonstrated overall retention of the microscopic structure of the tracheae in the decellularised scaffold and overall clearance of cells.

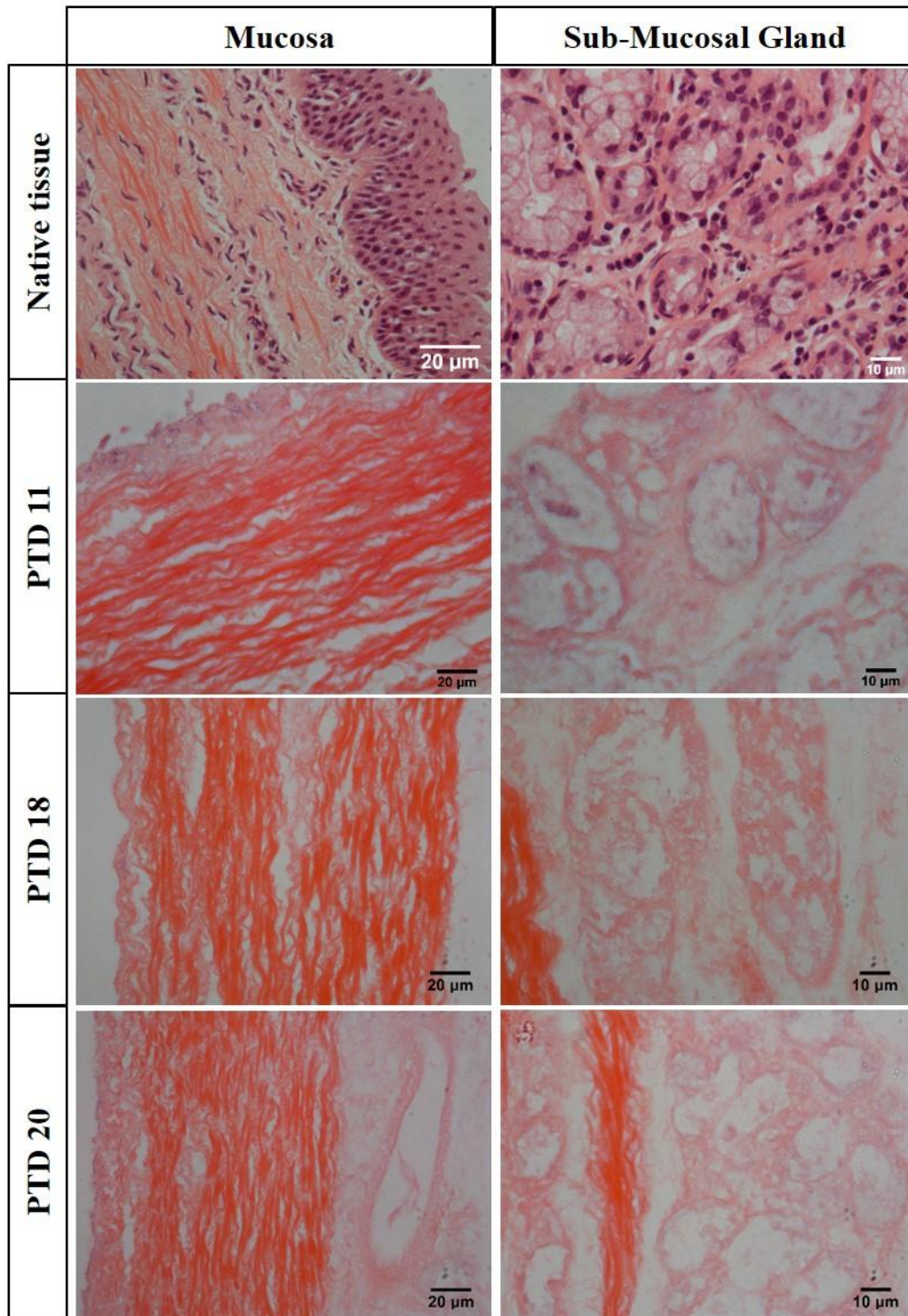


Figure 5.27: High power (x60) microscopic evaluation comparing native trachea and PTD 11, PTD 18 and PTD 20 demonstrated retention of the microscopic structure of the tracheae in the decellularised scaffold and total clearance of cells in the mucosa and mucosal glands regions of the decellularised scaffold.

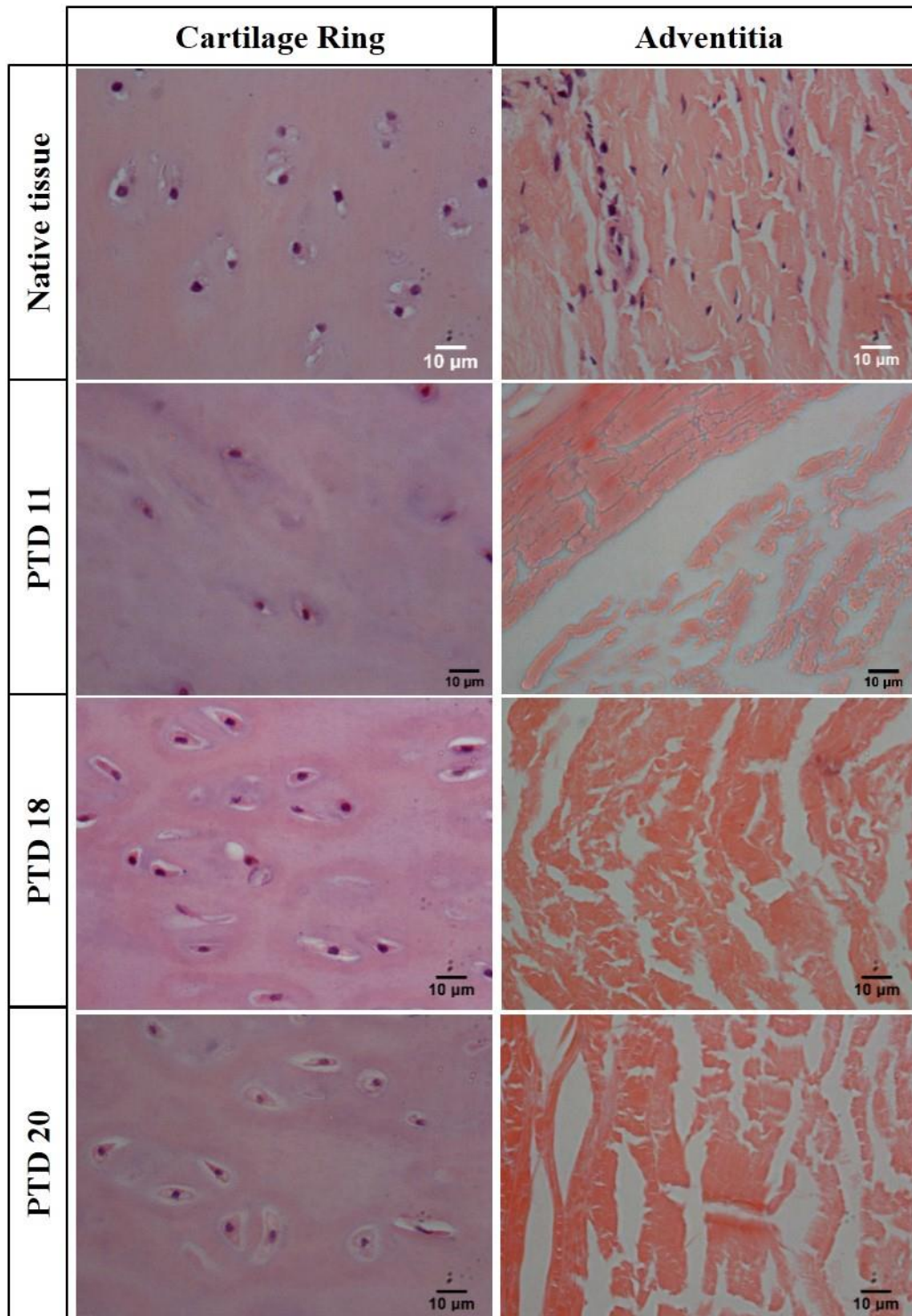


Figure 5.28: High power (x60) microscopic evaluation comparing native trachea and PTD 11, PTD 18 and PTD 20 demonstrated retention of the microscopic structure of the tracheae in the decellularised scaffold and total clearance of cells in the adventitia region of the decellularised scaffold. However chondrocytes were observed in the cartilage rings of the decellularised scaffold.

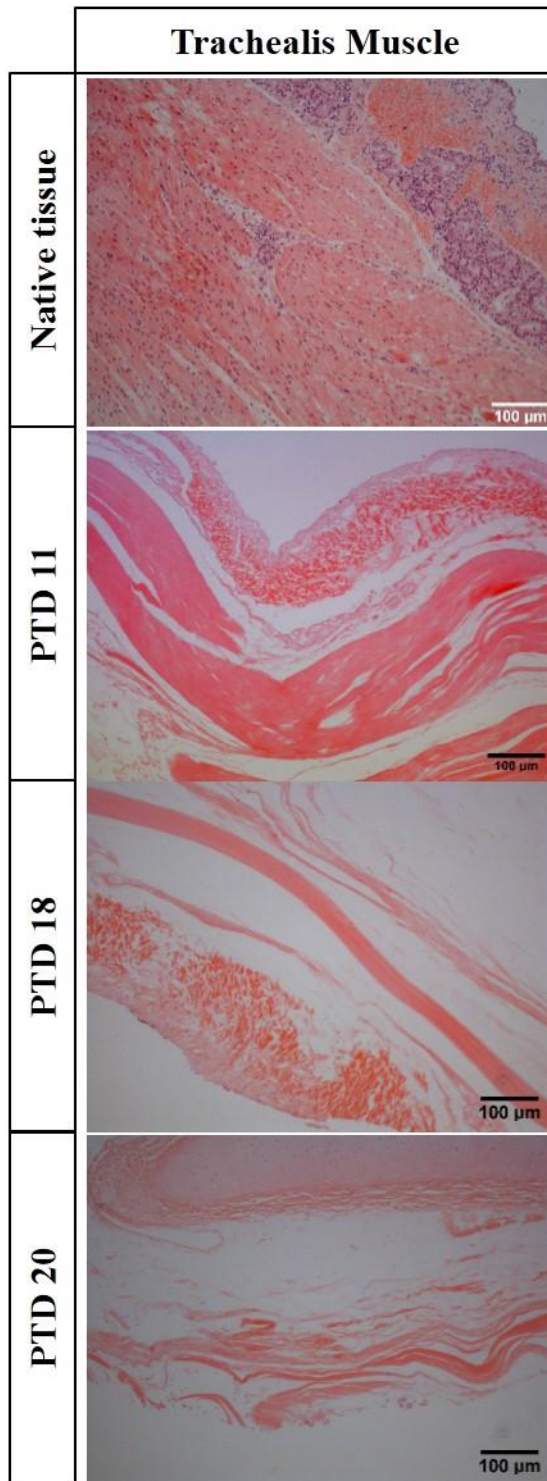


Figure 5.29: Low power (x10) microscopic evaluation comparing native trachea and PTD 11, PTD 18 and PTD 20 demonstrated retention of the microscopic structure of the tracheae in the decellularised scaffold and total clearance of cells in the trachealis muscle region of the decellularised scaffold.

Image analysis was performed to quantify the cell clearance from the various regions of the tracheae. In native trachea the number of cells observed were 8910 ± 1280 cells/mm² in the mucosa, 7639 ± 2418 cells/mm² in the sub-mucosa, 1298 ± 346 cells/mm² in the adventitia, 6917 ± 372 cells/mm² in the trachealis muscle and 1257 ± 412 cells/mm² in the cartilage. In the PTD treated scaffolds no cells were observed in the mucosa, sub-mucosa, adventitia and trachealis muscle regions (Figure 5.30). In the cartilage regions 1302 ± 412 cells/mm² were observed in the PTD treated scaffolds which indicated no cell clearance from the cartilage rings, however of these 759 ± 599 cells/mm² were observed to have undergone apoptosis (Figure 5.31).

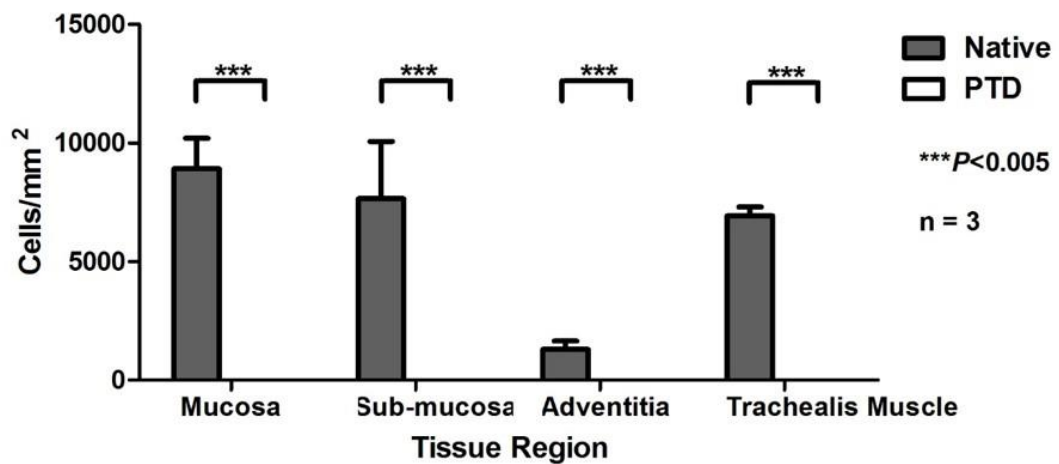


Figure 5.30: Quantification of the cell clearance observed in the mucosa, sub-mucosa, adventitia and trachealis muscle regions of the trachea demonstrated total cell clearance was achieved in these non-cartilaginous regions.

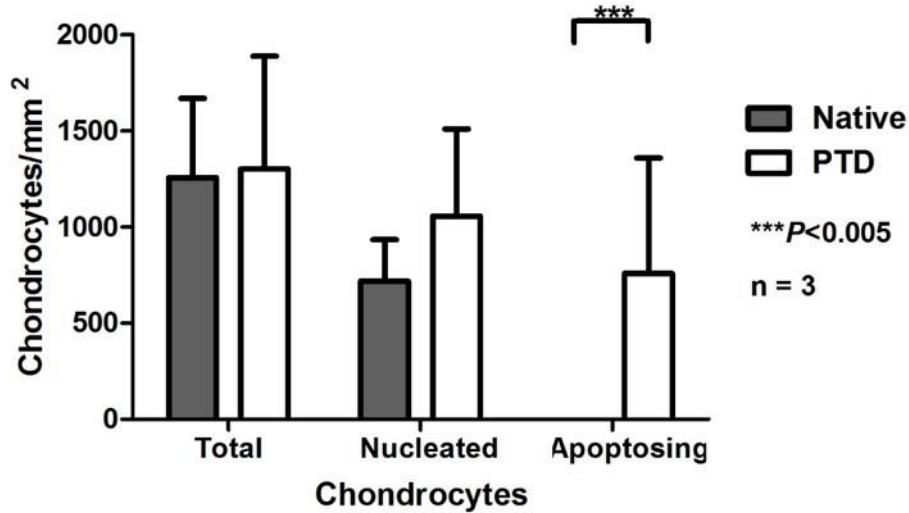


Figure 5.31: Quantification of the cell clearance observed in the cartilage rings regions of the trachea demonstrated no cell clearance was achieved however over 50% of the cells appeared to have undergone apoptosis.

5.4.4.3 Analysis of DNA removal in PTD scaffolds

Quantitative analysis of residual DNA to determine the effectiveness of DNA removal by the PTD method demonstrated statistically significant improved removal of DNA compared with the DEM of decellularisation. After PTD, 38.53 ± 9.84 ng/mg of DNA remained compared to 264.7 ± 69.92 ng/mg ($P < 0.05$) in the DEM (Figure 5.32). This represented a 6.7 fold increase in DNA removal using the new PTD method compared to the DEM. However both of the methods demonstrated significant removal ($P < 0.005$) of DNA when compared to the levels of DNA (695.87 ± 159.02 ng/mg) observed in native tissue (Figure 5.32).

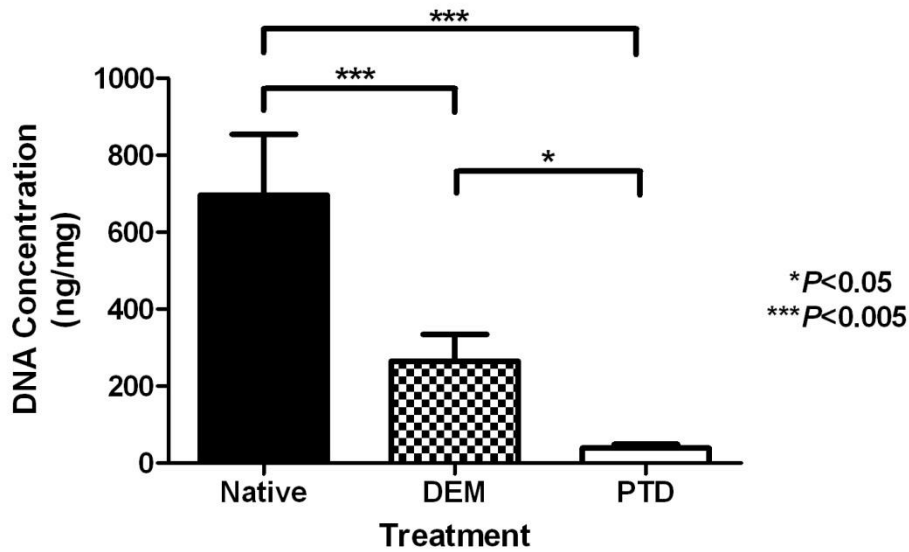


Figure 5.32: Quantitative DNA analysis demonstrated a significant decrease in the DNA concentration in the PTD scaffold (38.53 ± 9.84 ng/mg) compared to native trachea (695.87 ± 159.02 ng/mg) and scaffolds produced with the DEM of decellularisation (264.7 ± 69.92 ng/mg).

5.4.4.4 Analysis of collagen in PTD scaffolds

Quantitative analysis of total collagen following PTD revealed comparable levels of retained collagen in the PTD scaffolds (379.29 ± 14.36 μ g/mg) as in the native tissue (387.16 ± 22.44 μ g/mg) (Figure 5.33). When collagen levels from the PTD method were compared to the DEM (298.07 ± 39.66 μ g/mg), statistically significant increased levels of collagen ($P < 0.005$) were retained by the PTD method (Figure 5.33).

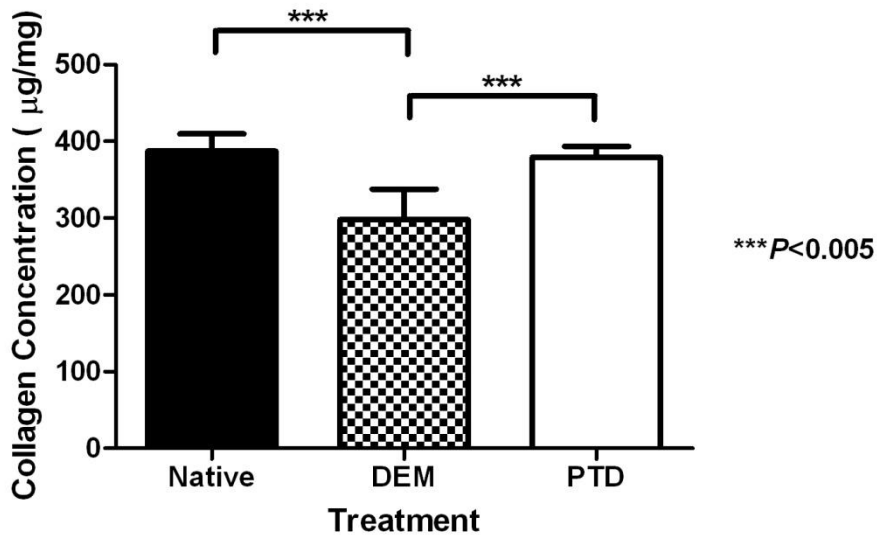


Figure 5.33: Quantitative analysis of the total collagen content of the native tissue versus DEM and PTD scaffolds indicated native levels of collagen were retained in the PTD scaffolds (97.97% retained) whereas loss of collagen content was identified in the DEM scaffolds (76.99% retained) ($P<0.005$).

5.4.4.5 Analysis of glycosaminoglycans in PTD scaffolds

Quantitative analysis of GAGs following PTD revealed slightly decreased but comparable levels of retained GAG in the PTD scaffolds ($34.55 \pm 2.98 \mu\text{g/mg}$) compared to native tissue ($39.67 \pm 5.82 \mu\text{g/mg}$) (Figure 5.34). When GAG levels from the PTD method were compared to the DEM ($22.12 \pm 7.32 \mu\text{g/mg}$), statistically significant increased levels of GAG ($P<0.001$) were retained by the PTD method (Figure 5.34).

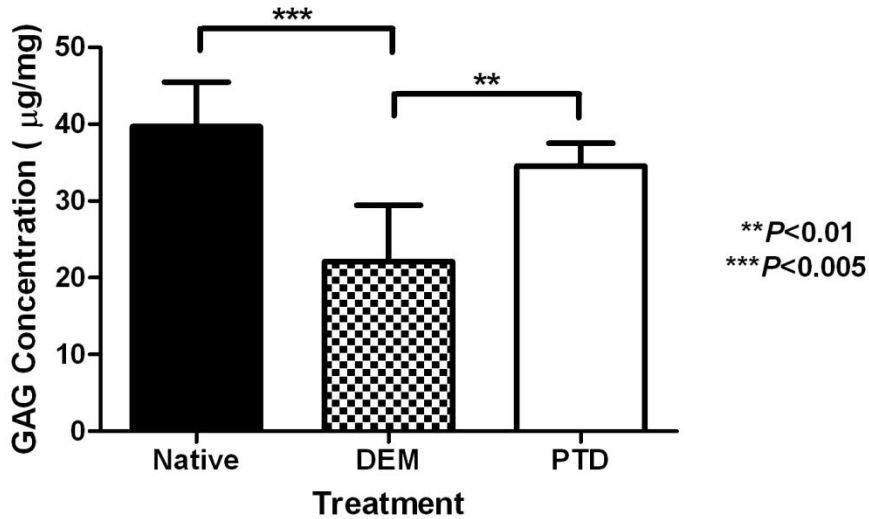


Figure 5.34: Quantitative analysis of the GAG content of the native tissue versus DEM and PTD scaffolds indicated comparable levels of GAGs were retained in the PTD scaffolds (87.09% retained) whereas loss of GAGs were identified in the DEM scaffolds (55.76% retained) ($P<0.005$).

5.4.4.6 Tensile testing of PTD scaffolds

Tensile testing was performed on the decellularised scaffolds to determine the biomechanical strength of the PTD scaffolds compared to native tracheal tissue and DEM decellularised scaffolds. When analysing the tensile modulus of the PTD scaffolds, there was no statistical change in modulus of the PTD scaffolds (49.41 ± 11.39 MPa) when compared to the native trachea (54.07 ± 9.42 MPa) (Figure 5.35). This was in contrast to scaffolds produced by the DEM of decellularisation (39.86 ± 6.54 MPa) where there was statistically significant decrease ($P<0.05$) observed in the tensile modulus (Figure 5.35).

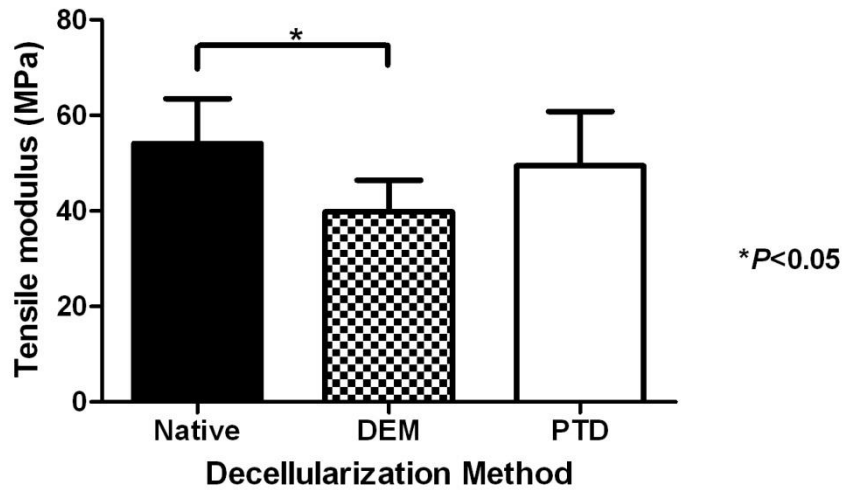


Figure 5.35: Measurement of the tensile modulus indicated comparable tensile modulus was retained between the native tracheae and the PTD scaffolds (91.39%) however tensile modulus decreased in the DEM scaffolds (73.71%) compared to native tracheae ($P < 0.05$).

From the tensile testing, the ultimate tensile strength could also be determined. These data showed that a statistically significant loss of ultimate tensile strength was observed in both the scaffolds produced by DEM (9.12 ± 1.73 MPa) ($P < 0.05$) and the PTD (7.79 ± 2.8) ($P < 0.01$) compared to the native tracheal tissue (12.13 ± 2.71) (Figure 5.36).

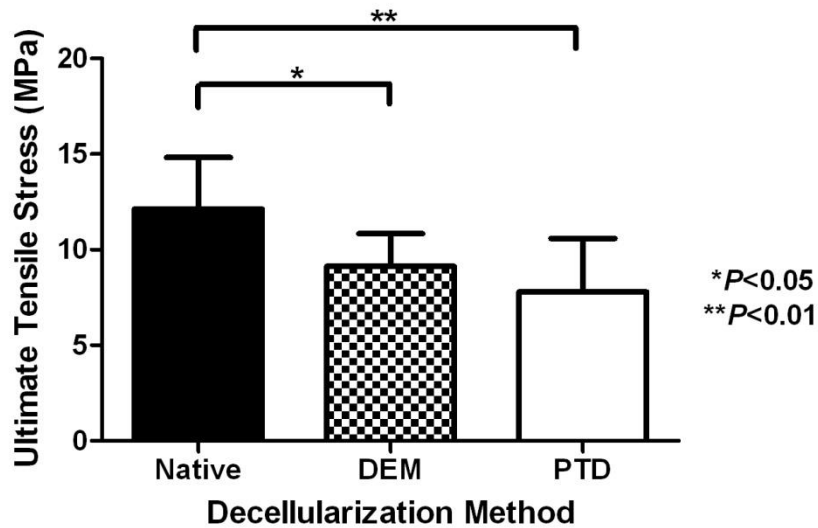


Figure 5.36: Measurement of the ultimate tensile stress indicated a loss of the ultimate tensile stress capacity of the PTD scaffolds (64.25%) ($P<0.05$) and the DEM scaffolds (75.19%) ($P<0.01$) compared to native tracheae.

From the tensile testing the ultimate tensile strain could also be determined. The PTD scaffolds ($20.21 \pm 5.4\%$) demonstrated a statistically significant decrease in ultimate tensile strain from both the native tissue ($35.56 \pm 7.57\%$) ($P<0.005$) and the DEM produced scaffolds ($32.22 \pm 4.03\%$) ($P<0.005$) (Figure 5.37).

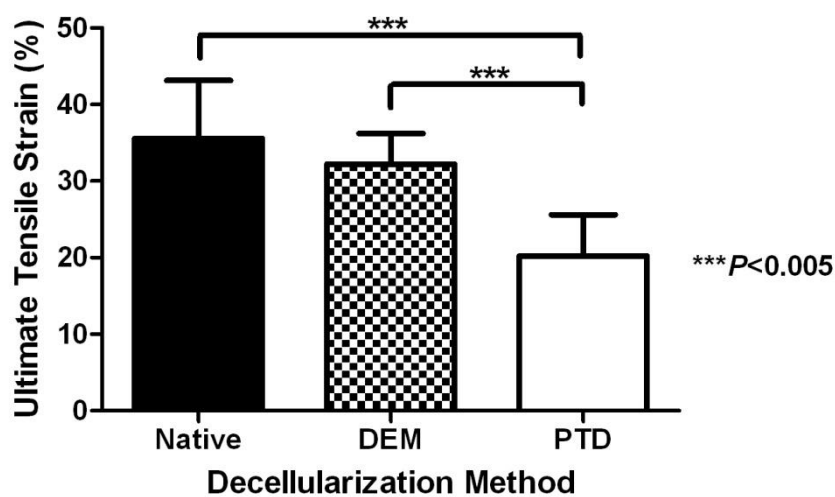


Figure 5.37: Measurement of the ultimate tensile strain indicated a loss of the ultimate tensile strain capacity of in the PTD scaffolds (56.85%) ($P<0.005$)

compared to native tracheae whilst comparative strain was observed in the DEM scaffolds (90.61%).

5.4.4.7 Compression testing of PTD scaffolds

Compression testing of complete sections of trachea was performed to assess the collapse resistance of the trachea and decellularised scaffolds to 50% occlusion. It was anticipated that this test should better represent biomechanical resistance to *in vivo* collapse post-transplantation. The greater the force required to occlude the trachea/scaffolds to 50% occlusion the stronger the trachea/scaffold. Tests on the PTD decellularised scaffolds (3.61 ± 1.67 N) demonstrated a noticeable but non-statistically significant decrease (14.54%) in the force required to occlude the scaffold to 50% compared to the native tissue (4.23 ± 0.89 N), demonstrating that the scaffolds produced by PTD were comparable to native trachea in this test (Figure 5.38).

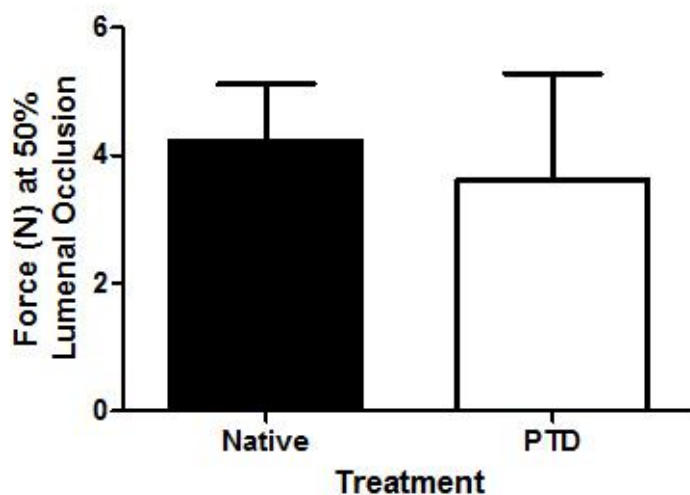


Figure 5.38: Measurement of the compression testing indicated the force required to occlude the lumen to 50% was statistically comparable between the native tracheae and the PTD scaffolds (85.45%).

5.4.5 Pressurised transmural decellularisation experiment failures

5.4.5.1 Pressurised transmural decellularisation 4:

The experiment was abandoned after only 24 hours of decellularisation so no meaningful results were obtained from this experiment.

5.4.5.2 Pressurised transmural decellularisation 12:

The experiment was abandoned only 20 hours prior to the completion of the decellularisation due to a perforation in the trachealis muscle. Therefore the trachea was not submitted to the range of analytical tests due to the failure of the experiment. However, it was observed that the trachea felt weakened, indicating degradation to the cartilage rings due to the decellularisation process.

5.4.5.3 Pressurised transmural decellularisation 16:

The experiment was abandoned shortly after commencing the initial decellularisation step so no meaningful results were obtained from this experiment.

5.4.5.4 Pressurised transmural decellularisation 17:

The experiment was abandoned shortly after commencing the decellularisation due to a failure in the bioreactor integrity so no meaningful results were obtained from this experiment.

5.4.5.5 Pressurised transmural decellularisation 19:

The experiment was abandoned during commencement of the third process step of the decellularisation so no meaningful results were obtained from this experiment.

5.4.6 Cost comparison of the DEM and PTD methods

The cost of the reagents only were calculated for the DEM and PTD methods to create a basic cost of goods (CoG) analysis. The reagent CoG for the DEM totalled £733.18 and the reagent CoG for the PTD totalled £71.37 (Figure 5.39). This indicated a greater than 10 fold reduction in the CoG could be achieved on the reagent costs alone by using the PTD methodology.

Reagent	DEM	PTD
Sodium deoxycholate	£253.88	£7.14
Protein Solubilizer X-100		£1.63
Hanks' Balanced Salt Solution	£374.60	£14.98
Trizma-HCL		£4.12
Pulmozyme (DNase) (2kU/mL)	£79.43	£7.94
RNase		£29.79
Water	£6.34	£1.22
Antibiotic-Antimycotic	£18.93	£4.55
	£733.18	£71.37

Figure 5.39: Reagent CoG for the DEM and PTD methods indicated a >10 fold reduction in the CoG for the PTD compared to the DEM.

5.5 Discussion

The bioreactor version 2.0 demonstrated successful containment of the pressure within the internal chamber using a two check valve system and achieved recirculation of the decellularisation solution along with transmural flow. The use of two check valves were instrumental to the set-up and with the bioreactor system in use demonstrated that the first check valve, along with containing the pressurisation in the internal chamber, also served to protect the lumen of the trachea from the fluctuating effect of pressure caused by the peristaltic pump. The reliability of the bioreactor system, based on the improvements described in chapter 4, enabled decellularisations utilising pressurised transmural flow to be performed on tracheae in a reproducible manner. The first three experiments did however highlight issues with the bioreactor set-up with regard to the transmural flow being sent to a separate waste reservoir. This design element appeared to cause insufficient decellularisation of the tracheae, with cells and nuclei being observed in the apparently decellularised tissue and higher levels of DNA remaining in regions judged to be less decellularised. Another issue was the level of transmural flow was higher than originally anticipated and as a result an increased volume of decellularisation solution would be required to run the steps of the decellularisation, particularly the latter steps, as the porosity of the scaffold increased with decellularisation. However for these experiments the volume was restricted to a set limit of 500 mL for cost reasons and therefore some of the latter process steps were completed in a matter of hours. This would also have decreased the time exposure of the tissue to the decellularisation solutions which have reduced the decellularisation potential.

These early experiments did answer some questions though. The lower flow rates observed in the tracheae that had undergone the freeze-thaw step to -80°C in Viaspan (or UW solution) had final flow rates of approximately half that of the final flow rates of the trachea that had undergone the freeze-thaw step to -20°C dry. This evidence suggests an increased final porosity in the tracheae that had been frozen to -20°C dry and therefore a more open final ECM. This could also be interpreted as an increase in the level of damage and therefore it was decided to not use the -20°C dry frozen method as a way of storing the tracheae post-harvest until use in the decellularisation method. It also resolved the process step order in that the first step should be a DNase step. When detergent was introduced as the first step in the

decellularisation process, as employed by the DEM of decellularisation, a build-up of viscous material was observed, which was only cleared by the subsequent DNase step. By considering what that buildup of viscous material was, it was realised that mucous produced by the mucous glands and ducts coat the trachea and through the ducts it permeates the lamina propria and sub-mucosal regions at the start of the decellularisation process. It is also well documented that mucous contains DNA and DNase-based medicine (Pulmozyme) and is used by Cystic Fibrosis patients to help breakdown the DNA in the mucous to loosen the mucous and aid expectoration. With the addition of the freeze thaw step that will have caused cell lysis and release of nuclear material, it was no surprise that the buildup of a viscous material, likely to have been nuclear material, occurred. By amending the order of the process steps and starting the decellularisation steps with a nuclease step it was surmised that the first nuclease step would break down the residual mucous allowing increased access to the lamina propria and the sub-mucosal regions and additionally breakdown the nuclear material that had been released through cell lysis. The change in the order of the process steps was affirmed when the buildup of viscous/nuclear material was avoided for the entire process and therefore taken forward into future experiments as the optimal order for the process steps.

With the changes to the bioreactor amended to incorporate the recirculation of the transmural flow and the order of the process steps resolved, it was possible to focus the next set of experiments on the investigation of different detergent concentrations. It was hypothesised that the detergent concentration would be key to obtaining the required level of cell clearance and maintaining the desired level of biomechanical strength. Therefore the lower and higher extremes of the detergent concentration were investigated. The results demonstrated clearly that if the detergent concentration was too low then cell clearance would not be adequately achieved although biomechanical strength would be retained to a comparable level of a trachea undergoing a freeze-thaw step. Conversely, if the detergent concentration was too high then cell clearance would be obtained but with the compromise of biomechanical strength being lost. It was realised that a fine balance of detergent concentration would be required to obtain adequate cell clearance whilst retaining biomechanical strength. Another discovery from this set of experiments was that at higher concentrations of detergent salt crystals precipitated out of solution in the

second nuclease step. Given that salt crystals were likely sodium chloride, this could reduce the efficacy of the DNase as sodium chloride inhibits DNase activity. Therefore to prevent salt precipitation in the second nuclease step, a wash step was introduced to remove the residual detergent from the bioreactor and the scaffold, which was shown to resolve the issue.

The next two experiments investigated the effect of the additional wash step at two new detergent concentrations that were in-between the previously employed higher and lower detergent concentrations. Adequate cell clearance was only achieved in the experiment that employed the higher detergent concentration of the two but both scaffolds suffered from a reduction in biomechanical strength which indicated that increased exposure of the tracheal scaffold to the bioreactor to five days and the additional wash was not optimal for the scaffold strength.

The next set of three experiments focused on the successful detergent concentration from the previous two experiments which had obtained good cell clearance, but shortened the five days of processing back to four days by greatly reducing the wash step between the detergent step and the second nuclease step from 24 hours to 3 hours and slightly reducing the second nuclease step from 24 hours to approximately 21 hours. Both wash steps were also performed at 4°C. Adequate cell clearance was mostly achieved at this detergent concentration, however donor to donor variability of the tracheae demonstrated that at this concentration, the efficacy of the cell clearance was at its limit, as in one of the scaffolds, nuclei were still visible in the lamina propria. The reduction in processing time and perhaps the reduction in the wash step temperature did have the desired effect though as the biomechanical strength was not reduced beyond that observed from freeze-thawing the scaffold.

The inability to store decellularised tracheal scaffolds without deterioration of the scaffold is a known issue (Bauguera, Del Gaudio et al. 2012). Therefore the use of a freeze-thaw step prior to decellularisation to aid both the decellularisation of the trachea and add flexibility to the commencement of the decellularisation process, by allowing storage of the trachea for up to one month was considered favourably. The step had been introduced to the concept of PTD decellularisation after recommendation of the use of the freeze-thaw step from the decellularisation team at the Department of Surgical Research at Northwick Park Institute for Medical

Research (NPIMR). Although the freeze-thaw step was clearly beneficial from a flexibility point of view and could be aiding the decellularisation, it was clear from the compression testing results that the freeze-thaw step was detrimental and caused a 50% reduction to the biomechanical strength of the scaffold. It was therefore decided to investigate if the PTD decellularisation could be successfully performed on fresh trachea that had not undergone any freeze-thaw steps.

The initial impressions of the tracheal scaffolds post PTD 11, 18 and 20 were of scaffolds that appeared fully denuded by the decellularisation process but still retained the overall structure and biomechanical strength. Histological staining gave the first insight into how successful the PTD decellularisation had been on fresh trachea. Microscopic observation using the 4x objective demonstrated that the microscopic structure of the tracheae had been preserved with the various sub-regions of the trachea remaining distinct and intact. Under increased magnification, microscopic observation demonstrated total cell clearance from all non-cartilaginous regions of the tracheae. In the cartilage rings, as with the DEM of decellularisation, chondrocytes and nuclei were still observed in the cartilage matrix. Clearly, cartilage restricts the movement of solution through the tissue due to retaining its own turgid state. The impermeability of cartilage might in itself explain why retained chondrocytes does not cause an immunologic reaction in patients who have already received engineered airways.

Further analysis of the effect of PTD on the biochemical state of the tracheal scaffolds revealed the PTD achieved a significant improvement in the removal of residual DNA from the scaffold compared to the DEM of decellularisation. Approximately 6.7 times more DNA was removed by the PTD method compared with the DEM. This is achieved even though only two nuclease steps (48 hours in total) are performed using the PTD method compared to the twenty-five DNase steps (75 hours in total) that are performed by the DEM. It is probable that this improvement in DNA removal is due to the optimisation of the nuclease buffer and the performance of the nuclease steps at near 37°C as well as possibly the inclusion of RNase to the nuclease step. It has been suggested that the quantitative criteria for DNA removal in tissues to be used for transplantation purposes is to reduce the DNA concentration to less than 50 ng/mg (dry weight) of dsDNA ((Badylak, Weiss et al.

2012)) which the PTD method is likely to achieve based on current results. Other biochemical tests looked at the total collagen concentration and the GAG concentration in the PTD scaffolds compared to native tracheal tissue and DEM scaffold tissue. Again the results suggested a significant improvement in the retention of collagen and GAG in the PTD scaffolds compared to the DEM scaffolds, with the PTD scaffolds retaining a similar level of collagen and GAG to that observed in the native tissue whilst significant amounts of collagen and GAG are lost when the tracheae is decellularised using the DEM. This could be due to the reduction in the process time for decellularisation of the scaffolds. The DEM takes 28 days to complete whilst the PTD is 7 fold faster, taking 5 days to complete. This suggests that even though the PTD scaffolds are subject to a more intense decellularisation regime where the decellularisation solution is forced through the scaffold, the overall reduction in the length of exposure is beneficial to the retention of these key ECM proteins.

As discussed in section 3.5, the ability for the tracheal scaffolds to maintain an open airway would be a CQA in a tracheal scaffold. Therefore biomechanical testing was performed using two different methods, tensile testing which had been reported on previously with the DEM scaffolds and a new method of compression testing, which was anticipated to be more representative. The tensile testing informed on the tensile modulus, the ultimate tensile stress and the ultimate tensile strain of the scaffolds. The tensile modulus of the PTD scaffolds were comparable to the native scaffold whereas for the DEM scaffolds there was a significant reduction in the tensile modulus. This corresponded well with the PTD scaffold biochemical results where the levels of collagen and GAGs were retained and were comparable to the native trachea. This would suggest, as hypothesised, that retaining key ECM components known to contribute to the biomechanical properties of the cartilage would enable the scaffolds to retain their biomechanical strength and therefore tensile modulus. Whereas, in the DEM scaffolds, the reduction observed in the collagen and GAG levels resulted in a reduced tensile modulus. The ultimate tensile stress and ultimate tensile strain results for the PTD scaffolds, which were the raw outputs from the tensile testing, were confusing at first. Statistically significant decreases were observed for both ultimate tensile stress and ultimate tensile strain which suggested, in contrast to the tensile modulus, that the PTD scaffolds had lost biomechanical

strength compared the native tissue and the DEM scaffolds. Young's modulus is a measure of the stiffness of the material being tested and the stiffness of the cartilage rings was considered an important factor in the ability of the cartilage rings to maintain an open airway. When interrogating the ultimate tensile stress and ultimate tensile strain results, the cartilage rings from the DEM scaffolds stretched the same amount as those from the native trachea with an equivalent ultimate tensile strain, however they ruptured under significantly less ultimate tensile stress than those from the native trachea which resulted in the cartilage rings from the DEM scaffolds being significantly weaker and more flaccid than those from the native trachea. With the ultimate tensile stress and ultimate tensile strain results from the cartilage rings of the PTD scaffolds, whilst the cartilage rings stretched significantly less they also rupture under significantly less stress than those from the native trachea. Because both the ultimate tensile stress and ultimate tensile strain were reduced proportionally by a comparable amount then ultimately the stiffness of the cartilage rings in the PTD scaffolds had been maintained and shown to be comparable to the cartilage rings from the native tracheal tissue. If the stiffness of the PTD scaffolds was truly maintained to that of the native trachea then it would be expected that comparable level of external force would be required to compress sections of those scaffolds. Therefore these data from the tensile testing experiments were corroborated by the compression testing results where the force required to occlude the lumen of the PTD scaffolds was shown to be equivalent to the force required to occlude the lumen of the native trachea.

Although, if time allowed, more experimental parameters would have been explored and a wider range of characterising assays employed to investigate PTD produced scaffolds using fresh trachea, the data obtained so far was encouraging and appeared to have built upon upon prior experimental knowledge and hypotheses to develop a potentially improved scaffold for tracheal tissue engineering. Although the development of the decellularisation scaffold is only a single piece of the work that must be achieved to manufacture a tissue engineered trachea, by manufacturing a scaffold that retains biomechanical strength whilst being immunologically inert, it is providing the recellularisation part of the process with what would currently be considered the best starting point. The ability of these PTD scaffolds to engraft with the host tissue, recellularise and enable the re-establishment of cartilage homeostasis

would need to be investigated in representative models before they are employed for tissue engineering purposes.

The bioreactor overall proved successful however there was a 25% failure rate which was unacceptably high. Three of the failures were due to a rupture in the trachealis muscle of the trachea, due to that region not being able to withstand the pressure administered. Two of these failures were due to the tissue itself being naturally weaker due to donor to donor variability. In order to prevent trachealis muscle failure it would be pragmatic to investigate if using lower pressures in the internal chamber could achieve comparable decellularisation whilst lowering the risk of failure. However, the donor to donor variability of the starting material is noted to be problematic when attempting to scale-up and automate reproducible manufacturing strategies for regenerative medicine (Brindley, Wall et al. 2013). The other scaffold failure was due to a user error causing a pressure build-up. In any highly-manual non-automated process, potential user errors are a high risk (Brindley, Wall et al. 2013). The rupture due to user error could be avoided by employment of thorough SOPs, quality manufacturing principles, operator training as well as simplification and automation of the bioreactor (Williams, Thomas et al. 2012). Of the other two failures, one was due to the attachment of the trachea to the bioreactor not being sufficiently sealed and one was due to the bioreactor leaking due to repetitive autoclave fatigue. These could both be avoided by an improved bioreactor design. Machining the entire bioreactor body out of a single piece of autoclavable material would be necessary to prevent this issue reoccurring. Implementing these improvements would hopefully reduce the failure rate and improve the reliability of the bioreactor system.

By reducing the number of process steps and reagent quantities, there was a significant ten-fold reduction in the reagent CoG. The CoG will be critical to reduce when scaling-up the process to achieve affordable commercialisation of the process.

5.6 Conclusion

A prototype bioreactor system was successfully built and improved upon enabling process development of the PTD method and in-process monitoring of the decellularisation process. Over the course of 15 successful decellularisation process runs, a series of product-informed improvements were implemented. Histological analysis along with biochemical and biomechanical assays indicated that the PTD method described for PTD 11, 18 and 20 using fresh tracheae as the starting material produced porcine scaffolds that have the potential to fulfill the CQA required for tissue engineering. The method improvements included the introduction of a pressurised transmural flow as a way to decellularise tissue, the optimisation of the decellularisation buffers used, a change in the order of application of the decellularisation solutions and an increase in the temperature the decellularisation was performed at. These improvements enabled a reduction in the processing time from 28 days to 5 days and a ten-fold reduction in the reagent CoG. The resulting scaffold from this PTD method had absolute cell clearance from the non-cartilaginous regions of the trachea, remnant DNA levels that were below the recommended DNA levels for decellularised products to be used in advanced therapy medicinal products (ATMPs), retained the key ECM components of collagen and GAG to a level comparable to native trachea and retained biomechanical strength and stiffness to a level comparable to native trachea. This suggests that, the final PTD method is a rapid and fit-for purpose method that has the potential to manufacture tracheal scaffolds for tissue engineering purposes in a reproducible process and advance this area of clinical study.

6 Discussion

6.1 Current process

6.1.1 Unmet clinical need

The driving force behind the need to translate tissue engineered trachea from the research lab to clinic is the current unmet clinical need to treat patients suffering from congenital tracheal atresia or stenosis and tracheal injury or disease in both children and adults. Currently, methodology has relied upon on producing bespoke tissue engineered trachea or tracheal scaffolds for named patients on a compassionate basis under the UK “Specials” scheme which allows for the manufacture and release of Advanced Therapeutic Medicinal Products (ATMPs) without clinical trials or marketing authorisation (MA) (Macchiarini, Jungebluth et al. 2008, Elliott, De Coppi et al. 2012, Gonfiotti, Jaus et al. 2014). If current medical need is to be met then this production of bespoke tissue-engineered tracheae needs to be translated into an ability to manufacture the quantities required, estimated to be two hundred per year (Boseley 2008), to meet current UK demand. The guiding principles that should be employed to achieve this aim are those currently employed for precision manufacturing where process knowledge and validation of the process leads to the principle of the “process is the product” (Williams, Thomas et al. 2012, Brindley, Wall et al. 2013). This means knowing your process is knowing your product, but the complexity of regenerative medicine and tissue engineering products can make achieving these principles particularly challenging (Brindley, Wall et al. 2013).

This thesis addressed this challenge by firstly investigating the current gold standard methodology, the detergent-enzymatic method (DEM) for decellularisation of the tracheae (Conconi, De Coppi et al. 2005, Macchiarini, Jungebluth et al. 2008), which had been used in the first in man studies on a named compassionate basis. Despite the reported clinical successes, in some of the cases partial collapse and/or stenosis were observed and it was acknowledged that further development of the decellularisation process was required (Badylak, Weiss et al. 2012, Gonfiotti, Jaus et al. 2014). In-house studies indicated the DEM had many limitations including: the loss of observed biochemical and biomechanical properties of the decellularised scaffold (Partington, Mordan et al. 2013); the process taking 28 days to complete;

the process requiring multiple operator managed wash/decellularisation solution exchanges per day or cycle; and the process requiring 25 detergent-enzymatic cycles. Additional to this, the need to repeat the detergent-enzymatic cycle 25 times drove up the cost of goods (CoG) and some aspects of the methodology appeared counterintuitive to achieving an optimal product. One of the principle investigators of this research co-authored a paper which suggested changes which could be implemented to overcome potential issues with the product including: additional DEM cycles or a freeze-thaw step if adequate decellularisation had not been achieved; or reducing the number of DEM cycles if a loss of structural integrity was observed in the tissue (Bader and Macchiarini 2010). Although these could be solutions to the challenges observed, a radical rethink of the decellularisation process as a whole could present a more elegant solution.

6.1.2 Process developments

Whilst changes to the length of the incubations, the temperature the incubations are performed at and the decellularised solutions used could improve the decellularised scaffold, these are minor changes. This thesis focused on a major rethink of how the decellularisation solutions were applied to the tissue with the use of pressure and transmural flow to force the decellularisation solutions through the tissue being considered a radical change from the passive diffusion into the tissue via immersion of the tissue in the decellularisation solutions as currently employed by the DEM. The first challenge in creating a decellularisation system with pressurised transmural flow was to design, make and validate a bioreactor system capable of creating and maintaining a stable transmural flow. The second challenge was to optimise the ancillary parts of the bioreactor system, such as the pump, the pump tubing and the clamps/check valves required to create the appropriate level of back pressure for stable transmural flow to be achieved. The latter challenge proved to be the most problematic aspect of the bioreactor system design. These issues were however overcome and a stable bioreactor system was achieved which allowed for the methodology of pressurised transmural decellularisation (PTD) process, using the bioreactor system, to be optimised.

The development and implementation of an automatable and controllable bioreactor system will ultimately be critical in the need to reduce the failure rate, standardise

the manufacturing process and the commercialisation of decellularised tracheal scaffolds and therefore tissue-engineering tracheae to ensure consistency in final product and enable cross-site comparability in the manufacturing process. The improvement to the manufacturing process should impact on and result in both process and product improvements such as reduced processing time, a reduction in the CoG, a lower risk of contamination and ultimately a final product of reproducible high quality (Williams, Thomas et al. 2012, Brindley, Wall et al. 2013).

The basis of the PTD method was drawn from both the DEM (Conconi, De Coppi et al. 2005, Macchiarini, Jungebluth et al. 2008) and vacuum assisted decellularisation (VAD) (Ansari 2011, Lange, Greco et al. 2014) methodologies due to the clinical application of these methods, with commonality in the detergent and enzymatic steps being applied. Additionally, a freeze-thaw step was added at the start of the process, with a presumed beneficial effect due its inclusion in the VAD method as well as other decellularisation methods and the possible necessity of the freeze-thaw step to achieve complete decellularisation due to the anticipated reduction in the number of process steps required in the PTD method. The methodology development of the PTD method focused primarily on varying the detergent concentration whilst the nuclease step stayed constant. It was apparent from the initial PTD experiments performed, which incorporated the freeze-thaw step, that higher concentrations of detergent resulted in an acellular but weakened scaffold and lower concentrations of detergent resulted in a stronger scaffold but regions of scaffold remained undecellularised. Further biomechanical tests on scaffolds part way through the decellularisation process revealed that the freeze-thaw step alone, whether performed to -80°C in Viaspan solution or to -20°C with the trachea kept dry, resulted in approximately a 50% reduction in scaffold strength. It was therefore decided to attempt a 5 day PTD process without the initial freeze-thaw step, which was considered then to be detrimental to the biomechanical strength of the scaffold. The resulting scaffolds retained biomechanical strength, along with native levels of GAG and collagen whilst being acellular in the non-cartilaginous regions with approximately 95% of the DNA removed. This success supported the hypothesis that PTD could be a rapid decellularisation method that produced tracheal scaffolds that met the required critical quality attributes. The reduction in the number of process steps and days required to achieve the appropriate decellularisation also resulted in a

ten-fold reduction in the basic CoG, which would benefit commercialisation of the process.

6.1.3 Limitations of the current process

There were however limitations and restrictions on what was or could be achieved within the time limit. Overcoming these limitations could be a body of work which would progress the PTD system towards clinical use. One of the most limiting factors was the source and variation of the starting material, a tracheae from a human cadaver (Brindley, Wall et al. 2013). In the porcine model this variation was not as discernible due to pigs of a set age, sex and weight from a single abattoir being the sole tissue source. However with a human source from the National Health Service Blood and Transplant (NHSBT), the availability of organ donors was in general limited. This was amplified when trying to source tracheae as they are an uncommon organ to donate. However, as the physique of the donors varies greatly, so did the dimensions of the donated tracheae. This meant that, when sourcing a trachea for a patient, the choice of trachea would be extremely limited and therefore a degree of compromise was required to obtain a trachea that would be suitable for the patient. Potentially the optimal method of mitigating this variation would be to investigate a storage method either pre or post decellularisation to enable a stock of tracheae to be available for matching the most suitable trachea available to the patient (Baiguera, Del Gaudio et al. 2012) An example of large scale tissue storage is the Euro Tissue Bank which utilises glycerol to store donated skin for up to two years for use in allografts or tissue engineering (Euro_Tissue_Bank 2015).

Other limiting factors of the PTD bioreactor system were the manual tasks required to attach the trachea to the bioreactor and assemble the bioreactor, which was composed of many pieces and required diligence during assembly. These highly manual tasks posed as risks for the introduction of contamination or errors (Brindley, Wall et al. 2013). Future work could simplify the bioreactor set up by amending the bioreactor design with new ports to enable direct attachment of pressure transducer and temperature probes. Daily interaction was also required to drain the spent decellularisation solution and refill the bioreactor with the next decellularisation solution. With the use of manifolds, automated pinch valves and programmable pump systems the solutions could be automatically drained from the bioreactor

chambers to a large waste bag and filled from sterile bags that are prepared in advance. However, due to the limited stability of the DNase and RNase, the addition of these components and solutions would need to be prepared fresh on the day of the use. The use of sterile weldable tubing to attach and seal bags or manifold sets to and from the system as required would also fully close the bioreactor system and allow processing to be achieved to a GMP compliant standard in a grade D background laboratory.

In addition to the work to simplify the bioreactor system set up, the main body of the bioreactor would also require redesigning. The ports on the external chambers were machined and then glued onto the main cylindrical body of the bioreactor. When the bioreactor was autoclaved tiny air pockets in the glue expanded in between the joints and with multiple autoclaving resulted in the joints leaking. This was temporarily solved with a sealant around the exterior of the joint but meant that latter PTD experiments could not be performed in a sterile manner as the bioreactor could not be autoclaved. Therefore before embarking on any further work, the bioreactor would need to be redesigned to ensure that it was either machinable from a single piece of plastic or built from multiple parts clamped together and sealed with O-rings. Additionally, the use of a biocompatible and autoclavable thermoplastic polymer, such the polyetheretherketone (PEEK) polymer Ketron® Peek-Classix™ LSG would be recommended as it is approved for contact or implantation in human tissue for up to 30 days. Another manufacturing option could be injection moulding. The bioreactor could be reusable and autoclavable if using a thermoplastic such as Ultem™ resin (polyetherimide) as used by Biorep for their reusable Ricordi Chambers. Alternatively, if CoG allow, the bioreactor could be disposable if using a DuraStar™ polymer as used by Biorep for their disposable Ricordi Chambers. By manufacturing from a single piece of plastic, it should remove the need for glue to be used between joints which could potentially fail. It also means the entire bioreactor could be manufactured using a single validated material which would reduce the need for additional validation of extractables and leachables when translating into GMP.

6.1.4 Future work

In addition to development of the bioreactor system, further development of the PTD methodology would be recommended prior to GMP translation and implementation into a manufacturing process. The final PTD decellularisation process described in this thesis using fresh (non-freeze-thaw treated) tracheae had only been performed using one condition after it was realised that using fresh trachea was a critical criteria for obtaining a product that could potentially attain the assumed critical quality attributes of the decellularised scaffold product. Further process development of the decellularisation process could involve titrating the detergent and DNase solutions to determine the lowest possible concentrations that could be used whilst ensuring the critical quality attributes of the scaffold are still achieved. Also, several experimental failures were caused due to the pressurisation of the internal chamber causing perforation of the trachealis muscle. Therefore it would be prudent to investigate alternative pressure levels below 4.82 psi to investigate if transmural flow and decellularisation can be achieved with equivalent efficiency at a lower internal pressure level whilst reducing the number of scaffold failures. It would be preferable if these experiments could be performed using a DoE approach to gain insight into the importance of and the interactions between the different decellularisation solutions and pressure level but due to the variability of the starting material, this may not be achievable.

An interesting output from the PTD experiments 11, 18 and 20 (section 5.4.4.6) was the result from tensile testing which suggested the scaffold appeared to lose tensile strength and strain, which suggests the scaffold was weaker and stiffer, whilst also appearing to retain proportionally equivalent elasticity from the Young's modulus result, when compared to the native tissue. As biomechanical strength is assumed to be critical to the decellularisation scaffold, it would be necessary to further investigate this result and to fully understand the impact of the decellularisation on the biomechanical properties as well as investigating and understanding the methodology of biomechanical testing to ensure the biomechanical testing being performed is relevant and informative.

Additional to this, once sterile decellularisation is again possible and implemented, further work investigating contaminants in the decellularised scaffold product would

need to be investigated. This would likely be a three pronged approach looking at chemical contaminants such as leachables from the bioreactor system components and residual contaminants from the decellularisation solutions which would, for example, inform if further wash steps were required. It would also investigate microbial, mycobial and viral contamination that where either still present from the starting material or had been introduced during the process and would inform on the level of decontamination, using irradiation or other methods, required prior to storage or recellularisation. Once these contaminant issues, if necessary, had been resolved then the immunogenicity of the scaffold would need to be established in an animal model, e.g. sub-cutaneous implantation in a rat, to ensure the scaffold was suitable for implantation and not induce graft vs. host disease, tissue rejection or failure.

6.2 Future projects

Future project work that would need to be investigated to ultimately progress this project to regular clinical use would include; the length of the shelf life of the decellularised scaffold, the optimal storage conditions, the impact of storage on the scaffold and the incorporation of irradiation/sterilisation protocols prior to storage to increase preservation of the scaffold (Baiguera, Del Gaudio et al. 2012). Prior to clinical trials, non-clinical trials would be required with the scaffolds implanted sub-cutaneously to determine the host immune response and graft remodelling. The recellularisation of the scaffold would be necessary (Go, Jungebluth et al. 2010) both for the replacement of mesenchymal stem cells directly into the decellularised tracheal scaffold and the luminal epithelial layer which could be delivered onto the decellularised tracheal scaffold or produced as a cell sheet on a decellularised skin/membrane scaffold (Bhargava, Chapple et al. 2004, Richters, Pirayesh et al. 2008) and added to the tracheal scaffold after the trachea has been revascularised *in vivo* as well as validated assays to determine adequate cell seeding had been achieved (Jungebluth, Haag et al. 2013). If such a surgical strategy were used, pre-clinical studies would then be required to ensure that hetero-transplantation *in vivo* resulted in vascularisation of the tracheal scaffold and survival of the mesenchymal stem cells, and subsequent ortho-transplantation and incorporation of the recellularised epithelial cell sheet allowed for continued survival without a debilitating immune response. For clinical delivery of the final recellularised tracheal

product, a comprehensive recellularisation strategy with process development will be required as well as incorporating the logistics of product delivery to the clinical site and clinician training for hetero- and ortho- transplantation into the patient, post-operative care and patient follow-up following release from clinical care. The project presented in the thesis has helped inform subsequent ongoing projects that are currently involved in pre-clinical studies with pig models to address epithelialisation and vascular integration as well as ensuring immunological inertness of the scaffold.

From the use of the Harvard Apparatus ORCA controller and Bio_1 software it was realised that online pressure transducers could be used to create a feedback loop to control and maintain a stable internal chamber pressure using two peristaltic pumps by controlling the fluid flow into the internal chamber (pump 1) with the fluid flow out of the internal chamber (pump 2). Using two peristaltic pumps in this manner would mitigate the need for one-way check valves and easily allow different pressure levels to be tested or changed throughout the decellularisation process. It is likely that the OCRA controller and the Bio_1 software is currently not sophisticated enough to achieve this set up but using a more sophisticated controller and software system e.g. the Finesse G3Lab Bioreactor Controller with TruBio software, would allow the set points to be achieved by controlling cascade mechanisms on the two pumps.

The methodology of the mechanical testing requires further improvement to representatively mimic *in situ* stresses. The introduction of the compression testing, as described in chapter 2 and 5, to measure the force required to occlude the lumen of tracheae and compare to decellularised scaffolds, resulted in a perceived improvement to method of biomechanical testing of the tracheae compared to the methods originally reported in the literature ((Baiguera, Jungebluth et al. 2010, Go, Jungebluth et al. 2010)) and the tensile testing described in chapter 2 and 3. Further improvements could however be made to build a more representative assay. For example, a luminal occlusion assay which, utilising Bose or Instron instrumentation, oscillated between set representative pressures over a period of time, for example 24 hours, whilst the trachea or scaffold was maintained in a sterile PBS bath. This would be a representative mimic of an observed *in vivo* condition in a patient where the trachea was compressed between the oesophagus and the aortic loop. Due to the pulsatile effect of the blood pumping through the aorta, the compression of the

trachea was pulsatile and the external pressure on the trachea oscillated. This *in vitro* assay set up would hopefully inform the scaffold's ability to withstand over time any oscillating external pressure without weakening.

Once a suitable manufacturing process for both the bioreactor system and the scaffold have been established, proven to demonstrate reproducibility and been validated to achieve the required critical quality attributes through the manufacture of a representative number of decellularised tracheal scaffolds to account for any variability in the starting material, then it can be assumed that the process is the product. Therefore the final product manufactured for patients should not need to be tested to the same degree and release criteria assays, which are selected critical quality attributes that can be measured within the product shelf-life pre-implantation, can be determined and implemented. This process and product knowledge, based on the principles of quality manufacturing, should aid GMP translation of the decellularised scaffold product and market authorisation of a recellularised scaffold as an ATMP for clinical use.

7 Conclusions

This thesis investigated the decellularisation of tracheae for tissue-engineering purposes and sought to investigate if an improved method of decellularisation that would aid scale-up and commercialisation of the process could be developed. The current clinically-used decellularisation method, the detergent-enzymatic method (DEM), was assessed and deemed unsuitable as a scalable method due to the length of the process, the difficulty in automating the numerous process steps and the potentially detrimental effect of the process on the resulting scaffold. A new method of decellularisation was proposed that would investigate if pressurised transmural flow could be used to decellularise trachea. A novel bioreactor system, which incorporated a solution reservoir, a pump and a dual chamber bioreactor, was developed which could permit flow through either the internal chamber, the external chamber or both chambers. Added online probes enabled measurement of certain process parameters, temperature and pressure, to validate the decellularisation process. The development of the bioreactor system enabled pressurised transmural decellularisation (PTD) to be explored. Various PTD conditions were tested and a successful method developed which achieved in the decellularised scaffold: the requisite removal of donor cells; an acceptable reduction of donor nuclear material; the retention of key ECM components, GAGs and collagen, comparable to native tracheae; and retained overall biomechanical strength comparable to native tracheae. This scaffold improvement was achieved alongside a process improvement of: a reduction in the number of process steps from 76 to 5 steps; a reduction in the process time from 28 to 5 days; and a ten-fold reduction in the basic cost of goods. With further process development the bioreactor system could be simplified, controlled by the online feedback from the process parameters and automated using software programming to enable minimal operator interaction. By accomplishing this, the PTD could achieve the principles of quality manufacturing and progress the process of biological scaffold manufacture and ultimately tracheal tissue engineering towards routine clinical use.

References

- Ansari, T. (2011). Method for the Vacuum-Assisted Decellularisation of Porcine and Human Trachea, Northwick Park Institute of Medical Research: 2.
- Asnaghi, M. A., P. Jungebluth, M. T. Raimondi, S. C. Dickinson, L. E. Rees, T. Go, T. A. Cogan, A. Dodson, P. P. Parnigotto, A. P. Hollander, M. A. Birchall, M. T. Conconi, P. Macchiarini and S. Mantero (2009). "A double-chamber rotating bioreactor for the development of tissue-engineered hollow organs: from concept to clinical trial." Biomaterials **30**(29): 5260-5269.
- Bader, A. and P. Macchiarini (2010). "Moving towards in situ tracheal regeneration: the bionic tissue engineered transplantation approach." Journal of Cellular and Molecular Medicine **14**(7): 1877-1889.
- Badylak, S. F. and T. W. Gilbert (2008). "Immune response to biologic scaffold materials." Seminars in Immunology **20**(2): 109-116.
- Badylak, S. F., D. J. Weiss, A. Caplan and P. Macchiarini (2012). "Engineered whole organs and complex tissues." The Lancet **379**(9819): 943-952.
- Baiguera, S., M. A. Birchall and P. Macchiarini (2010). "Tissue-Engineered Tracheal Transplantation." Transplantation.
- Baiguera, S., C. Del Gaudio, M. O. Jaus, L. Polizzi, A. Gonfiotti, C. E. Comin, A. Bianco, D. Ribatti, D. A. Taylor and P. Macchiarini (2012). "Long-term changes to in vitro preserved bioengineered human trachea and their implications for decellularized tissues." Biomaterials **33**(14): 3662-3672.
- Baiguera, S., P. Jungebluth, A. Burns, C. Mavilia, J. Haag, P. De Coppi and P. Macchiarini (2010). "Tissue engineered human tracheas for in vivo implantation." Biomaterials **31**(34): 8931-8938.
- Balasundari, R., R. Gupta, V. Sivasubramanian, R. Chandrasekaran, S. Arumugam, K. Cherian and S. Guhathakurta (2007). "Complete microbe free processed porcine xenograft for clinical use." Indian Journal of Thoracic and Cardiovascular Surgery **23**(4): 240-245.
- Bhargava, S., C. R. Chapple, A. J. Bullock, C. Layton and S. Macneil (2004). "Tissue-engineered buccal mucosa for substitution urethroplasty." BJU International **93**(6): 807-811.
- Birchall, M. and P. Macchiarini (2008). "Airway transplantation: a debate worth having?" Transplantation **85**(8): 1075-1080.
- Bjork, J. W. and R. T. Tranquillo (2009). "Transmural flow bioreactor for vascular tissue engineering." Biotechnology and Bioengineering **104**(6): 1197-1206.
- Bolland, F., S. Korossis, S. P. Wilshaw, E. Ingham, J. Fisher, J. N. Kearney and J. Southgate (2007). "Development and characterisation of a full-thickness acellular porcine bladder matrix for tissue engineering." Biomaterials **28**(6): 1061-1070.
- Boseley, s. (2008). Transplant first a giant leap for surgery. The Guardian. London.
- Brindley, D. A., I. B. Wall and K. E. Bure (2013). "Automation of cell therapy biomanufacturing." BioProcess International **11**(SUPPL. 3): 18-25.
- Bristol_University. (2008, 19 November 2008). "Adult stem cell breakthrough " News from the University - Press releases Retrieved Feb 26, 2010 from <http://www.bristol.ac.uk/news/2008/6010.html>.
- Butler, C., J. Hsuan, N. Beaumont, S. Janes, T. Ansari and M. Birchall (2011). "Proteomic Analysis of Decellularized Tissue Engineered Laryngeal-Tracheal Scaffolds." Otolaryngology -- Head and Neck Surgery **145**(2 suppl): P82.
- Caceci, D. T. (2008). "VM8054 Veterinary Histology, Respiratory System I: Mammals." VM8054: Veterinary Histology Version 5.2. Retrieved 7th December

2009, from <http://education.vetmed.vt.edu/curriculum/vm8054/labs/Lab25/lab25.htm>.

Cameron, P. D. P., B. M. (1999). Oxford Textbook of Critical Care. Oxford, Oxford University Press.

Canadian_Lung_Association. (2015, 08 April 2015). "The Respiratory System." Retrieved 08 April 2015, 2015, from <http://www.lung.ca/lung-health/lung-info/respiratory-system>.

Caprio, M. (2005, 09/29/05). "Studying Tissue Slides." Retrieved 10 December, 2009, from <http://iweb.tntech.edu/mcaprio/>.

Chute, R. M. (2008, 4/22/2008). "Trachea Cross Section." Retrieved 10 December, 2009, from <http://nhscience.lonestar.edu/bioL/respiratory/trachea.htm>.

Conconi, M. T., P. De Coppi, R. Di Liddo, S. Vigolo, G. F. Zanon, P. P. Parnigotto and G. G. Nussdorfer (2005). "Tracheal matrices, obtained by a detergent-enzymatic method, support in vitro the adhesion of chondrocytes and tracheal epithelial cells." Transplant International **18**(6): 727-734.

Crapo, P. M., T. W. Gilbert and S. F. Badylak (2011). "An overview of tissue and whole organ decellularization processes." Biomaterials **32**(12): 3233-3243.

Daley, B. J. R., L. L. (2009, 4 June 2009). "Tracheal Tumors." Retrieved 4th January 2010, 2010, from <http://emedicine.medscape.com/article/425904-overview>.

Daniels, J. T. (2010). Adult Stem Cells: Delivery of Stem Cell Therapy in the Cornea. Stem Cell and Regenerative Medicine Bioprocessing. London, UCL.

Delaere, P. (2009, 14 Dec 2009). "Doctors at K.U.Leuven perform world's first vascularized tracheal allotransplantation." Press Release Retrieved Feb 26, 2010, from <http://www.kuleuven.be/cltr/en/allo/pressrelease.html>.

Delaere, P., J. Vranckx, G. Verleden, P. De Leyn and D. Van Raemdonck (2010). "Tracheal allotransplantation after withdrawal of immunosuppressive therapy." N Engl J Med **362**(2): 138-145.

Delaere, P. R., J. J. Vranckx and M. D. Hondt (2014). "Tracheal allograft after withdrawal of immunosuppressive therapy." New England Journal of Medicine **370**(16): 1568-1570.

Elder, B. D., S. V. Eleswarapu and K. A. Athanasiou (2009). "Extraction techniques for the decellularization of tissue engineered articular cartilage constructs." Biomaterials **30**(22): 3749-3756.

Elliott, M. J., P. De Coppi, S. Speggorin, D. Roebuck, C. R. Butler, E. Samuel, C. Crowley, C. McLaren, A. Fierens, D. Vondryns, L. Cochrane, C. Jephson, S. Janes, N. J. Beaumont, T. Cogan, A. Bader, A. M. Seifalian, J. J. Hsuan, M. W. Lowdell and M. A. Birchall (2012). "Stem-cell-based, tissue engineered tracheal replacement in a child: A 2-year follow-up study." The Lancet **380**(9846): 994-1000.

Engelhardt, J. F., H. Schlossberg, J. R. Yankaskas and L. Dudus (1995). "Progenitor cells of the adult human airway involved in submucosal gland development." Development **121**(7): 2031-2046.

Euro_Tissue_Bank. (2015). "Euro Tissue Bank." Retrieved 11/4/2015, 2015, from <http://www.eurotissuebank.nl/euro-tissue-bank-en-GB/>.

Ford, J. L., D. E. Robinson and B. E. Scammell (2003). "The fate of soft callus chondrocytes during long bone fracture repair." Journal of Orthopaedic Research **21**(1): 54-61.

Funamoto, S., K. Nam, T. Kimura, A. Murakoshi, Y. Hashimoto, K. Niwaya, S. Kitamura, T. Fujisato and A. Kishida (2010). "The use of high-hydrostatic pressure treatment to decellularize blood vessels." Biomaterials **31**(13): 3590-3595.

Gilbert, T. W., J. M. Freund and S. F. Badylak (2009). "Quantification of DNA in Biologic Scaffold Materials." Journal of Surgical Research **152**(1): 135-139.

Gilbert, T. W., T. L. Sellaro and S. F. Badylak (2006). "Decellularization of tissues and organs." Biomaterials **27**(19): 3675-3683.

Go, T., P. Jungebluth, S. Baiguero, A. Asnagli, J. Martorell, H. Ostertag, S. Mantero, M. Birchall, A. Bader and P. Macchiarini (2010). "Both epithelial cells and mesenchymal stem cell-derived chondrocytes contribute to the survival of tissue-engineered airway transplants in pigs." The Journal of Thoracic and Cardiovascular Surgery **139**(2): 437-443.

Gonfiotti, A., M. O. Jaus, D. Barale, S. Baiguera, C. Comin, F. Lavorini, G. Fontana, O. Sibila, G. Rombolà, P. Jungebluth and P. Macchiarini (2014). "The first tissue-engineered airway transplantation: 5-year follow-up results." The Lancet **383**(9913): 238-244.

Gratzer, P. F., R. D. Harrison and T. Woods (2006). "Matrix Alteration and Not Residual Sodium Dodecyl Sulfate Cytotoxicity Affects the Cellular Repopulation of a Decellularized Matrix." Tissue Engineering **12**(10): 2975-2983.

Gray, F. L., C. G. Turner, A. Ahmed, C. E. Calvert, D. Zurakowski and D. O. Fauza (2012). "Prenatal tracheal reconstruction with a hybrid amniotic mesenchymal stem cells-engineered construct derived from decellularized airway." Journal of Pediatric Surgery **47**(6): 1072-1079.

Green, W. T., Jr. (1977). "Articular cartilage repair. Behavior of rabbit chondrocytes during tissue culture and subsequent allografting." Clin Orthop Relat Res(124): 237-250.

Grillo, H. C. (2002). "Tracheal replacement: a critical review." Ann Thorac Surg **73**(6): 1995-2004.

HARegenMed, H. A. R. M.-. (2013). "Hollow Organ Bioreactors." Regenerative Medicine from Research to Clinical, 2014, from <http://www.harvardapparatusregen.com/media/pdf/Hollow%20Organ%20Brx.pdf>.

HARegenMed, H. A. R. M.-. (2013). "ORCA Bioreactors." Regenerative Medicine from Research to Clinical, 2014, from <http://www.harvardapparatusregen.com/media/pdf/ORCA%20Bioreactor%20Brochure.pdf>.

Hashimoto, Y., S. Funamoto, S. Sasaki, T. Honda, S. Hattori, K. Nam, T. Kimura, M. Mochizuki, T. Fujisato, H. Kobayashi and A. Kishida (2010). "Preparation and characterization of decellularized cornea using high-hydrostatic pressurization for corneal tissue engineering." Biomaterials.

Hathaway, D., R. Winsett, M. Prendergast and I. Subaiya (2003). "The first report from the patient outcomes registry for transplant effects on life (PORTEL): differences in side-effects and quality of life by organ type, time since transplant and immunosuppressive regimens." Clinical Transplantation **17**(3): 183-194.

Haykal, S., J. P. Soleas, M. Salna, S. O. P. Hofer and T. K. Waddell (2012). "Evaluation of the structural integrity and extracellular matrix components of tracheal allografts following cyclical decellularization techniques: Comparison of three protocols." Tissue Engineering - Part C: Methods **18**(8): 614-623.

Herberhold, C., B. Franz and W. Breipohl (1980). "Chemical-conservated human trachea as prosthesis in covering tracheal defects - First experiences." CHEMISCH-KONSERVIERTE MENSCHLICHE TRACHEA ALS PROTHESENATERIAL ZUR DECKUNG TRACHEALER DEFEKTE. ERSTE ERFAHRUNGEN **59**(8): 453-457.

Highfield, R. (2008, 19 Nov 2008). "Transplant of windpipe grown from stem cells heralds new era in medicine." Telegraph.co.uk Retrieved Feb 26, 2010, from <http://www.telegraph.co.uk/science/science-news/3486000/Transplant-of-windpipe-grown-from-stem-cells-heralds-new-era-in-medicine.html>.

Hollister, S. J. (2009). "Scaffold Design and Manufacturing: From Concept to Clinic." Advanced Materials **21**(32-33): 3330-3342.

Hutmacher, D. W. (2000). "Scaffolds in tissue engineering bone and cartilage." Biomaterials **21**(24): 2529-2543.

Hynes, R. O. (2009). "The extracellular matrix: Not just pretty fibrils." Science **326**(5957): 1216-1219.

Ivanov. (2007, 18 June 2007). "Trachea Diseases." CTSNet Wiki Notes, from <http://wiki.ctsnet.org/index.php?n=Main.TrachealDiseases>.

Jones, M. C., F. A. Rueggeberg, A. J. Cunningham, H. A. Faircloth, T. Jana, D. Mettenburg, J. L. Waller, G. N. Postma and P. M. Weinberger (2014). "Biomechanical changes from long-term freezer storage and cellular reduction of tracheal scaffoldings." The Laryngoscope: n/a-n/a.

Jungebluth, P. (2009). Re: Trachea decellularisation method needed. L. Partington. email.

Jungebluth, P., E. Alici, S. Baiguera, K. L. Blanc, P. Blomberg, B. Bozóky, C. Crowley, O. Einarsson, K. H. Grinnemo, T. Gudbjartsson, S. L. Guyader, G. Henriksson, O. Hermanson, J. E. Juto, B. Leidner, T. Lilja, J. Liska, T. Luedde, V. Lundin, G. Moll, B. Nilsson, C. Roderburg, S. Strömblad, T. Sutlu, A. I. Teixeira, E. Watz, A. Seifalian and P. MacChiarini (2011). "Tracheobronchial transplantation with a stem-cell-seeded bioartificial nanocomposite: A proof-of-concept study." The Lancet **378**(9808): 1997-2004.

Jungebluth, P., A. Bader, S. Baiguera, S. Möller, M. Jaus, M. L. Lim, K. Fried, K. R. Kjartansdóttir, T. Go, H. Nave, W. Harringer, V. Lundin, A. I. Teixeira and P. Macchiarini (2012). "The concept of in vivo airway tissue engineering." Biomaterials **33**(17): 4319-4326.

Jungebluth, P., T. Go, A. Asnaghi, S. Bellini, J. Martorell, C. Calore, L. Urbani, H. Ostertag, S. Mantero, M. T. Conconi and P. Macchiarini (2009). "Structural and morphologic evaluation of a novel detergent-enzymatic tissue-engineered tracheal tubular matrix." Journal of Thoracic & Cardiovascular Surgery **138**(3): 586-593; discussion 592-583.

Jungebluth, P., J. C. Haag, M. L. Lim, G. Lemon, S. Sjöqvist, Y. Gustafsson, F. Ajallouelian, I. Gilevich, O. E. Simonson, K. H. Grinnemo, M. Corbascio, S. Baiguera, C. Del Gaudio, S. Strömblad and P. Macchiarini (2013). "Verification of cell viability in bioengineered tissues and organs before clinical transplantation." Biomaterials **34**(16): 4057-4067.

Kahan, B. D., P. Keown, G. A. Levy and A. Johnston (2002). "Therapeutic drug monitoring of immunosuppressant drugs in clinical practice." Clinical Therapeutics **24**(3): 330-350.

Kapickis, M., P. Sassu and S. M. Thirkannad (2009). "Evaluation of Two Types of Vascular Bundles for Revascularization of Avascular Tissue." Journal of Hand Surgery **34**(8): 1461-1466.

Kay, D. J. G., A. J. (2007, 13 November 2007). "Congenital Malformations, Trachea." Congenital Malformations of the Head & Neck Retrieved 5 January, 2009, from <http://emedicine.medscape.com/article/837827-overview>.

Keane, T. J., R. Londono, R. M. Carey, C. A. Carruthers, J. E. Reing, C. L. Dearth, A. D'Amore, C. J. Medberry and S. F. Badylak (2013). "Preparation and

characterization of a biologic scaffold from esophageal mucosa." Biomaterials **34**(28): 6729-6737.

Keane, T. J., R. Londono, N. J. Turner and S. F. Badylak (2012). "Consequences of ineffective decellularization of biologic scaffolds on the host response." Biomaterials **33**(6): 1771-1781.

Kemp, P. (2010). Developing Scalable Commercial Products. Stem Cell and Regenerative Medicine Bioprocessing. London, UCL: 58-69.

Kolchanov, N. A., E. V. Ignatieva, E. A. Ananko, O. A. Podkolodnaya, I. L. Stepanenko, T. I. Merkulova, M. A. Pozdnyakov, N. L. Podkolodny, A. N. Naumochkin and A. G. Romashchenko. (2002). "Trachea." Transcription Regulatory Regions Database (TRRD): its status in 2002 Retrieved 18 February 2010, 2010, from <http://www.mgs.bionet.nsc.ru/mgs/gnw/trrd/thesaurus/Re/trachea.html>.

Lange, P., K. Greco, L. Partington, C. Carvalho, S. Oliani, M. A. Birchall, P. D. Sibbons, M. W. Lowdell and T. Ansari (2014). Pilot study of a novel vacuum-assisted method for decellularization of tracheae for clinical Tissue Engineering applications. Manuscript submitted for publication. N. Department of Surgical Research, Watford Rd, Harrow, HA1 3UJ, UK Manuscript submitted for publication.

Lange, P., K. Greco, L. Partington, C. Carvalho, S. Oliani, M. A. Birchall, P. D. Sibbons, M. W. Lowdell and T. Ansari (2015). "Pilot study of a novel vacuum-assisted method for decellularization of tracheae for clinical tissue engineering applications." Journal of Tissue Engineering and Regenerative Medicine: n/a-n/a.

Langer, R. and J. P. Vacanti (1993). "Tissue engineering." Science **260**(5110): 920-926.

Legasto, A. C., J. O. Haller and R. J. Giusti (2004). "Tracheal web." Pediatr Radiol **34**(3): 256-258.

Macchiarini, P., P. Jungebluth, T. Go, M. A. Asnaghi, L. E. Rees, T. A. Cogan, A. Dodson, J. Martorell, S. Bellini, P. P. Parnigotto, S. C. Dickinson, A. P. Hollander, S. Mantero, M. T. Conconi and M. A. Birchall (2008). "Clinical transplantation of a tissue-engineered airway." Lancet **372**(9655): 2023-2030.

Mankarious, L. A., A. B. Adams and V. L. Pires (2002). "Patterns of Cartilage Structural Protein Loss in Human Tracheal Stenosis." The Laryngoscope **112**(6): 1025-1030.

Marom, E. M., P. C. Goodman and H. P. McAdams (2001). "Diffuse abnormalities of the trachea and main bronchi." AJR Am J Roentgenol **176**(3): 713-717.

Martin, D. E. (1988). Respiratory anatomy and physiology. St. Louis, Mosby.

McFetridge, P. S. (2010). Decellularized grafts from umbilical cord vessels and process for preparing and using same, Google Patents.

Meezan, E., J. T. Hjelle, K. Brendel and E. C. Carlson (1975). "A simple, versatile, nondisruptive method for the isolation of morphologically and chemically pure basement membranes from several tissues." Life Sciences **17**(11): 1721-1732.

Meyer-Blaser, U., J. Handschel, T. Meyer, H. P. Wiesmann and SpringerLink (Online service) (2009). Fundamentals of Tissue Engineering and Regenerative Medicine. Berlin, Heidelberg, Springer Berlin Heidelberg.

Moioli, E. K., P. A. Clark, M. Chen, J. E. Dennis, H. P. Erickson, S. L. Gerson and J. J. Mao (2008). "Synergistic actions of hematopoietic and mesenchymal stem/progenitor cells in vascularizing bioengineered tissues." PLoS One **3**(12).

Montoya, C. V. and P. S. McFetridge (2009). "Preparation of ex vivo based biomaterials using convective flow decellularization." Tissue Engineering - Part C: Methods **15**(2): 191-200.

Morrison, W. A. (2009). "Progress in tissue engineering of soft tissue and organs." Surgery **145**(2): 127-130.

Neville, W. E., P. J. P. Bolanowski and G. G. Kotia (1990). "Clinical experience with the silicone tracheal prosthesis." Journal of Thoracic and Cardiovascular Surgery **99**(4): 604-613.

NHSBT. (2009, October 2009). "Statistics - Transplants save lives." Organ Donation Retrieved 4 March, 2010, from <http://www.organdonation.nhs.uk/ukt/statistics/statistics.jsp>.

Ott, H. C., T. S. Matthiesen, S. K. Goh, L. D. Black, S. M. Kren, T. I. Netoff and D. A. Taylor (2008). "Perfusion-decellularized matrix: using nature's platform to engineer a bioartificial heart." Nature Medicine **14**(2): 213-221.

Ott, H. T., D (2009). DECELLULARIZATION AND RECELLULARIZATION OF ORGANS AND TISSUES U. P. a. T. Office. US, REGENTS OF THE UNIVERSITY OF MINNESOTA. **A1**: 1 of 1.

Panthagani, I. D., M. C. Santos and C. T. D'Angio (2009). "Use of computed tomography to categorize the type of tracheal agenesis." Journal of Pediatric Surgery **44**(5): 1044-1046.

Partington, L., N. J. Mordan, C. Mason, J. C. Knowles, H. W. Kim, M. W. Lowdell, M. A. Birchall and I. B. Wall (2013). "Biochemical changes caused by decellularization may compromise mechanical integrity of tracheal scaffolds." Acta Biomaterialia **9**(2): 5251-5261.

Phipps, L. M., J. A. Raymond and T. M. Angeletti (2006). "Congenital tracheal stenosis." Crit Care Nurse **26**(3): 60-69.

Price, A. P., L. M. Godin, A. Domek, T. Cotter, J. D'Cunha, D. A. Taylor and A. Panoskaltis-Mortari (2015). "Automated Decellularization of Intact, Human-Sized Lungs for Tissue Engineering." Tissue Engineering. Part C, Methods **21**(1): 94-103.

Price, P. A. (1972). "Characterization of Ca⁺⁺ and Mg⁺⁺ Binding to Bovine Pancreatic Deoxyribonuclease A." Journal of Biological Chemistry **247**(9): 2895-2899.

Richters, C. D., A. Pirayesh, H. Hoeksema, E. W. A. Kamperdijk, R. W. Kreis, R. P. Dutrieux, S. Monstrey and M. J. Hoekstra (2008). "Development of a dermal matrix from glycerol preserved allogeneic skin." Cell and Tissue Banking **9**(4): 309-315.

Rinker, B. (2009). "Cryopreservation and the age of the allotransplant." Organogenesis **5**(3): 85-89.

Roach, H. I., T. Aigner and J. B. Kouri (2004). "Chondroptosis: a variant of apoptotic cell death in chondrocytes?" Apoptosis **9**(3): 265-277.

Roberts, C. R., J. K. Rains, P. D. Paré, D. C. Walker, B. Wiggs and J. L. Bert (1997). "Ultrastructure and tensile properties of human tracheal cartilage." Journal of biomechanics **31**(1): 81-86.

Rock, J. R., S. H. Randell and B. L. M. Hogan (2010). "Airway basal stem cells: a perspective on their roles in epithelial homeostasis and remodeling." Disease Models & Mechanisms **3**(9-10): 545-556.

Saarakkala, S., P. Julkunen, P. Kiviranta, J. Mäkitalo, J. S. Jurvelin and R. K. Korhonen (2010). "Depth-wise progression of osteoarthritis in human articular cartilage: investigation of composition, structure and biomechanics." Osteoarthritis and cartilage / OARS, Osteoarthritis Research Society **18**(1): 73-81.

Sasaki, S., S. Funamoto, Y. Hashimoto, T. Kimura, T. Honda, S. Hattori, H. Kobayashi, A. Kishida and M. Mochizuki (2009). "In vivo evaluation of a novel scaffold for artificial corneas prepared by using ultrahigh hydrostatic pressure to decellularize porcine corneas." Molecular Vision **15**: 2022-2028.

Simpson, D. G. and G. L. Bowlin (2006). "Tissue-engineering scaffolds: can we re-engineer mother nature?" Expert Review of Medical Devices **3**(1): 9-15.

Slomianka, L. (2009, 6 August 2009). "Blue Histology - Notes " Retrieved 15 June, 2010, from <http://www.lab.anhb.uwa.edu.au/mb140/>.

Soh, H., H. Kawahawa, K. Imura, M. Yagi, A. Yoneda, A. Kubota and A. Okada (1999). "Tracheal agenesis in a child who survived for 6 years." J Pediatr Surg **34**(10): 1541-1543.

Takahama, T., K. Onishi, F. Kanai, M. Hiraishi, Z. Yamazaki, A. Furuse and T. Yoshitake (1989). "A new improved biodegradable tracheal prosthesis using hydroxy apatite and carbon fiber." ASAIO Transactions **35**(3): 291-293.

Tan, Q., R. Steiner, S. P. Hoerstrup and W. Weder (2006). "Tissue-engineered trachea: History, problems and the future." European Journal of Cardio-Thoracic Surgery **30**(5): 782-786.

Tan, Q., R. Steiner, L. Yang, M. Welti, P. Neuenschwander, S. Hillinger and W. Weder (2007). "Accelerated angiogenesis by continuous medium flow with vascular endothelial growth factor inside tissue-engineered trachea." European Journal of Cardio-thoracic Surgery **31**(5): 807-812.

Teng, Z., I. Ochoa, Z. Li, Y. Lin, J. F. Rodriguez, J. A. Bea and M. Doblare (2008). "Nonlinear mechanical property of tracheal cartilage: A theoretical and experimental study." Journal of Biomechanics **41**(9): 1995-2002.

Visosky, A. M. (2004, 29 March 2006). "Tracheal Neoplasms." Retrieved 6th January, 2010 from http://www.bcm.edu/oto/grand/11_04_04.htm.

Williams, D. J., R. J. Thomas, P. C. Hourd, A. Chandra, E. Ratcliffe, Y. Liu, E. A. Rayment and J. R. Archer (2012). "Precision manufacturing for clinical-quality regenerative medicines." Philosophical Transactions of the Royal Society A: Mathematical, Physical and Engineering Sciences **370**(1973): 3924-3949.

Zheng, M. H., J. Chen, Y. Kirilak, C. Willers, J. Xu and D. Wood (2005). "Porcine small intestine submucosa (SIS) is not an acellular collagenous matrix and contains porcine DNA: Possible implications in human implantation." Journal of Biomedical Materials Research Part B: Applied Biomaterials **73B**(1): 61-67.